IAEA-TECDOC-910

Manual on mathematical models in isotope hydrogeology

INTERNATIONAL ATOMIC ENERGY AGENCY IAEA

October 1996

The IAEA does not normally maintain stocks of reports in this series. However, microfiche copies of these reports can be obtained from

INIS Clearinghouse
International Atomic Energy Agency
Wagramerstrasse 5
P.O. Box 100
A-1400 Vienna, Austria

Orders should be accompanied by prepayment of Austrian Schillings 100,– in the form of a cheque or in the form of IAEA microfiche service coupons which may be ordered separately from the INIS Clearinghouse.

IAEA-TECDOC-910

Manual on mathematical models in isotope hydrogeology

INTERNATIONAL ATOMIC ENERGY AGENCY IAEA

The originating Section of this publication in the IAEA was:

Isotope Hydrology Section
International Atomic Energy Agency
Wagramerstrasse 5
P.O. Box 100
A-1400 Vienna, Austria

MANUAL ON MATHEMATICAL MODELS IN ISOTOPE HYDROGEOLOGY
IAEA, VIENNA, 1996
IAEA-TECDOC-910
ISSN 1011–4289

Printed by the IAEA in Austria
October 1996

FOREWORD

Methodologies based on the use of naturally occurring isotopes are, at present, an integral part of studies being undertaken for water resources assessment and management. Applications of isotope methods aim at providing an improved understanding of the overall hydrological system as well as estimating physical parameters of the system related to flow dynamics. Quantitative evaluations based on the temporal and/or spatial distribution of different isotopic species in hydrological systems require conceptual mathematical formulations. Different types of model can be employed depending on the nature of the hydrological system under investigation, the amount and type of data available, and the required accuracy of the parameter to be estimated.

Water resources assessment and management requires a multidisciplinary approach involving chemists, physicists, hydrologists and geologists. Existing modelling procedures for quantitative interpretation of isotope data are not readily available to practitioners from diverse professional backgrounds. Recognizing the need for guidance on the use of different modelling procedures relevant to specific isotope and/or hydrological systems, the IAEA has undertaken the preparation of a publication for this purpose. This manual provides an overview of the basic concepts of existing modelling approaches, procedures for their application to different hydrological systems, their limitations and data requirements. Guidance in their practical applications, illustrative case studies and information on existing PC software are also included. While the subject matter of isotope transport modelling and improved quantitative evaluations through natural isotopes in water sciences is still at the development stage, this manual summarizes the methodologies available at present, to assist the practitioner in the proper use within the framework of ongoing isotope hydrological field studies.

In view of the widespread use of isotope methods in groundwater hydrology, the methodologies covered in the manual are directed towards hydrogeological applications, although most of the conceptual formulations presented would generally be valid.

Y. Yurtsever, Division of Physical and Chemical Sciences, was the IAEA technical officer responsible for the final compilation of this report.

It is expected that the manual will be a useful guidance to scientists and practitioners involved in isotope hydrological applications, particularly in quantitative evaluation of isotope data in groundwater systems.

EDITORIAL NOTE

In preparing this publication for press, staff of the IAEA have made up the pages from the original manuscripts as submitted by the authors. The views expressed do not necessarily reflect those of the governments of the nominating Member States or of the nominating organizations.

Throughout the text names of Member States are retained as they were when the text was compiled.

The use of particular designations of countries or territories does not imply any judgement by the publisher, the IAEA, as to the legal status of such countries or territories, of their authorities and institutions or of the delimitation of their boundaries.

The mention of names of specific companies or products (whether or not indicated as registered) does not imply any intention to infringe proprietary rights, nor should it be construed as an endorsement or recommendation on the part of the IAEA.

The authors are responsible for having obtained the necessary permission for the IAEA to reproduce, translate or use material from sources already protected by copyrights.

CONTENTS

SUMMARY 7

Lumped parameter models for interpretation of environmental tracer data 9
P. Maloszewski, A. Zuber

Numerical models of groundwater flow for transport 59
L.F. Konikow

Quantitative evaluation of flow systems, groundwater recharge and transmissivities using environmental traces 113
E.M. Adar

Basic concepts and formulations for isotope geochemical modelling of groundwater systems 155
R.M. Kalin

List of related IAEA publications 207

SUMMARY

The IAEA has, during the last decade, been actively involved in providing support to development and field verification of the various modelling approaches in order to improve the capabilities of modelling for reliable quantitative estimates of hydrological parameters related to the dynamics of the hydrological system. A Co-ordinated Research Programme (CRP) on Mathematical Models for Quantitative Evaluation of Isotope Data in Hydrology was implemented during 1990-1994. The results of this CRP were published as IAEA-TECDOC-777, in which the present state-of-the-art in modelling concepts and procedures with results obtained from applied field research are summarized. The present publication is a follow-up to the earlier work and can be considered to be a supplement to TECDOC-777.

Methodologies based on the use of environmental (naturally occurring) isotopes are being routinely employed in the field of water resources and related environmental investigations. Temporal and/or spatial variations of commonly used natural isotopes (i.e. stable isotopes of hydrogen, oxygen and carbon; radioactive isotopes of hydrogen and carbon) in hydrological systems are often employed for two main purposes:

(i) improved understanding of the system boundaries, origin (genesis) of water, hydraulic interconnections between different sub-systems, confirmation (or rejection) of boundary conditions postulated as a result of conventional hydrological investigations;

(ii) quantitative estimation of dynamic parameters related to water movement such as travel time of water and its distribution in the hydrological system, mixing ratios of waters originating from different sources and dispersion characteristics of mass transport within the system.

Methodologies of isotope data evaluations (as in i) above) are essentially based on statistical analyses of the data (either in the time or the space domain) which would contribute to the qualitative understanding of the processes involved in the occurrence and circulation of water, while the quantitative evaluations, as in (ii) above, would require proper conceptual mathematical models to be used for establishing the link between the isotopic properties with those of the system parameters.

The general modelling approaches developed so far and verified through field applications for quantitative interpretations of isotope data in hydrology cover the following general formulations:

- Lumped parameter models, that are based on the isotope input-output relationships (transfer function models) in the time domain,

- Distributed parameter numerical flow and transport models for natural systems with complex geometries and boundary conditions,

- Compartmental models (mixing cell models), as quasi-physical flow and transport of isotopes in hydrological systems,

- Models for geochemical speciation of water and transport of isotopes with coupled geochemical reactions.

While the modelling approaches cited above are still at a stage of progressive development and refinement, the IAEA has taken the initiative for the preparation of guidance material on the use of existing modelling approaches in isotope hydrology. The need for such a manual on the basic formulations of existing modelling approaches and their practical use for isotope data obtained from field studies was recognized during the deliberations of the earlier CRP mentioned above. Other relevant IAEA publications available in this field are listed at the end of this publication.

Use of specific models included in each of the available general methodologies, and data requirements for their proper use will be dictated by many factors, mainly related to the type of hydrological system under consideration, availability of basic knowledge and scale of the system. Groundwater systems are often much more complex in this regard, and use of isotopes is much more widespread for a large spectrum of hydrological problems associated with proper assessment and management of groundwater resources. Therefore, this manual, providing guidance on the modelling approaches for isotope data evaluations, is limited to hydrogeological applications.

Further developments required in this field include the following specific areas:

- use of isotopes for calibration of continuum and mixing-cell models,
- incorporation of geochemical processes during isotope transport, particularly for kinetic controlled reactions,
- improved modelling of isotope transport in the unsaturated zone and models coupling unsaturated and saturated flow,
- stochastic modelling approaches for isotope transport and their field verification for different types of aquifers (porous, fractured).

The IAEA is presently implementing a new CRP entitled "Use of Isotopes for Analyses of Flow and Transport Dynamics in Groundwater Systems", which addresses some of the above required developments in this field. Results of this CRP will be compiled upon its completion in 1998.

While the aim for the preparation of the manual was mainly to provide practical guidance on the existing modelling applications in isotope data interpretations for water resources systems, and particularly for groundwater systems, the methodologies presented will also be relevant to environmental studies in hydro-ecological systems dealing with pollutant transport and assessment of waste sites (toxic or radioactive).

LUMPED PARAMETER MODELS FOR THE INTERPRETATION OF ENVIRONMENTAL TRACER DATA

P. MALOSZEWSKI
GSF-Institute for Hydrology
Oberschleissheim,
Germany

A. ZUBER
Institute of Nuclear Physics,
Cracow, Poland

Abstract

Principles of the lumped-parameter approach to the interpretation of environmental tracer data are given. The following models are considered: the piston flow model (PFM), exponential flow model (EM), linear model (LM), combined piston flow and exponential flow model (EPM), combined linear flow and piston flow model (LPM), and dispersion model (DM). The applicability of these models for the interpretation of different tracer data is discussed for a steady state flow approximation. Case studies are given to exemplify the applicability of the lumped-parameter approach. Description of a user-friendly computer program is given.

1. Introduction

1.1. Scope and history of the lumped-parameter approach

This manual deals with the lumped-parameter approach to the interpretation of environmental tracer data in aquifers. In a *lumped-parameter model* or a *black-box model*, the system is treated as a whole and the flow pattern is assumed to be constant. Lumped-parameter models are the simplest and best applicable to systems containing young water with modern tracers of variable input concentrations, e.g., tritium, Kr-85 and freons, or seasonably variable ^{18}O and ^{2}H. The concentration records at the recharge area must be known or estimated, and for measured concentrations at outflows (e.g. springs and abstraction wells), the global parameters of the investigated system are found by a trial-and-error procedure. Several simple models commonly applied to large systems with a constant tracer input (e.g. the piston flow model usually applied to the interpretation of radiocarbon data) also belong to the category of the lumped-parameter approach and are derivable from the general formula.

The manual contains basic definitions related to the tracer method, outline of the lumped-parameter approach, discussion of different types of flow models represented by system response functions, definitions and discussion of the parameters of the response functions, and selected case studies. The case studies are given to demonstrate the following problems: difficulties in obtaining a unique calibration, relation of tracer ages to flow and rock parameters in granular and fissured systems, application of different tracers to some complex systems. Appendix A contains examples of response functions for different injection-detection modes. Appendix B contains an example of differences between the water age, the conservative

tracer age, and the radioisotope age for a fissured aquifer. Appendix C contains user's guide to the FLOW - a computer program for the interpretation of environmental tracer data in aquifers by the lumped-parameter approach, which is supplied on a diskette. [*]

The interpretation of tracer data by the lumped-parameter approach is particularly well developed in chemical engineering. The earliest quantitative interpretations of environmental tracer data for groundwater systems were based on the simplest models, i.e., either the piston flow model or the exponential model (mathematically equivalent to the well-mixed cell model), which are characterized by a single parameter [1]. A little more sophisticated two-parameter model, represented by binomial distribution was introduced in late 1960s [2]. Other two-parameter models, i.e, the dispersion model characterized by a uni-dimensional solution to the dispersion equation, and the piston flow model combined with the exponential model, were shown to yield better fits to the experimental results [3]. All these models have appeared to be useful for solving a number of practical problems, as it will be discussed in sections devoted to case studies. Recent progress in numerical methods and multi-level samplers focused the attention of modellers on two- and three-dimensional solutions to the dispersion equation. However, the lumped-parameter approach still remains to be a useful tool for solving a number of practical problems. Unfortunately, this approach is often ignored by some investigators. For instance, in a recent review [4] a general description of the lumped-parameter approach was completely omitted, though the piston flow and well-mixed cell models were given. The knowledge of the lumped-parameter approach and the transport of tracer in the simplest flow system is essential for a proper understanding of the tracer method and possible differences between flow and tracer ages. Therefore, even those who are not interested in the lumped-parameter approach are advised to get acquainted with the following text and particularly with the definitions given below, especially as some of these definitions are also directly or indirectly applicable to other approaches.

1.2. Useful definitions

In this manual we shall follow definitions taken from several recent publications [5, 6, 7, 8, 9] with slight modifications. However, it must be remembered that these definitions are not generally accepted and a number of authors apply different definitions, particularly in respect to such terms as model verification and model validation. Therefore, caution is needed, and, in the case of possible misunderstandings, the definitions applied should be either given or referred to an easily available paper. As far as verification and validation are concerned the reader is also referred to authors who are very critical about these terms used in their common meaning and who are of a opinion that they should be rejected as being highly misleading [10, 11].

The *tracer method* is a technique for obtaining information about a system or some part of a system by observing the behaviour of a specified substance, the tracer, that has been added to the system. Environmental tracers are added (injected) to the system by natural processes, whereas their production is either natural or results from the global activity of man.

[*] User Guide and diskette are available free of charge from Isotope Hydrology Section, IAEA, Vienna, upon request.

An *ideal tracer* is a substance that behaves in the system exactly as the traced material as far as the sought parameters are concerned, and which has one property that distinguishes it from the traced material. This definition means that for an ideal tracer there should be neither sources nor sinks in the system other than those adherent to the sought parameters. In practice we shall treat as a good tracer even a substance which has other sources or sinks if they can be properly accounted for, or if their influence is negligible within the required accuracy.

A *conceptual model is* a qualitative description of a system and its representation (e.g. geometry, parameters, initial and boundary conditions) relevant to the intended use of the model.

A *mathematical model* is a mathematical representation of a conceptual model for a physical, chemical, and/or biological system by expressions designed to aid in understanding and/or predicting the behaviour of the system under specified conditions.

Verification of a mathematical model, or its computer code, is obtained when it is shown that the model behaves as intended, i.e. that it is a proper mathematical representation of the conceptual model and that the equations are correctly encoded and solved. A model should be verified prior to calibration.

Model calibration is a process in which the mathematical model assumptions and parameters are varied to fit the model to observations. Usually, calibration is carried out by a trial-and-error procedure. The calibration process can be quantitatively described by the goodness of fit.

Model calibration is a process in which the inverse problem is solved, i.e. from known input-output relations the values of parameters are determined by fitting the model results to experimental data. The direct problem is solved if for known or assumed parameters the output results are calculated (model prediction). Testing of hypotheses is performed by comparison of model predictions with experimental data.

Validation is a process of obtaining assurance that a model is a correct representation of the process or system for which it is intended. Ideally, validation is obtained if the predictions derived from a calibrated model agree with new observations, preferably for other conditions than those used for calibration. Contrary to calibration, the validation process is a qualitative one based on the modeller's judgment.

The term "a correct representation" may perhaps be misleading and too much promising. Therefore, a somewhat changed definition can be proposed: *Validation* is a process of obtaining assurance that a model satisfies the modeller's needs for the process or system for which it is intended, within an assumed or requested accuracy [9]. A model which was validated for some purposes and at a given stage of investigations, may appear invalidated by new data and further studies. However, this neither means that the validation process should not be attempted, nor that the model was useless.

Partial validation can be defined as validation performed with respect to some properties of a model [7, 8]. For instance, models represented by solutions to the transport equation yield proper solute velocities (i.e. can be validated in that respect - a partial validation), but usually do not yield proper dispersivities for predictions at larger scales.

In the case of the tracer method the validation is often performed by comparison of the values of parameters obtained from the models with those obtainable independently (e.g. flow velocity obtained from a model fitted to tracer data is shown to agree with that calculated from the hydraulic gradient and conductivity known from conventional observations [7, 8, 12, 13]. When results yielded by a model agree with results obtained independently, a number of authors state that the model *is confirmed*, e.g. [11], which is equivalent to the definition of validation applied within this manual.

The *direct problem* consists in finding the output concentration curve(s) for known or assumed input concentration, and for known or assumed

model type and its parameter(s). Solutions to the direct problem are useful for estimating the potential abilities of the method, for planning the frequency of sampling, and sometimes for preliminary interpretation of data, as explained below.

The *inverse problem* consists in searching for the model of a given system for which the input and output concentrations are known. Of course, for this purpose the graphs representing the solutions to the direct problem can be very helpful. In such a case the graph which can be identified with the experimental data will represent the solution to the inverse problem. A more proper way is realized by searching for the best fit model (calibration). Of course, a good fit is a necessary condition but not a sufficient one to consider the model to be validated (confirmed). The fitting procedure has to be used together with the geological knowledge, logic and intuition of the modeller [14]. This means that all the available information should be used in selecting a proper type of the model prior to the fitting. If the selection is not possible prior to the fitting, and if more than one model give equally good fit but with different values of parameters, the selection has to be performed after the fitting, as a part of the validation process. It is a common sin of modellers to be satisfied with the fit obtained without checking if other equally good fits are not available.

In dispersive dynamic systems, as aquifers, it is necessary to distinguish between different ways in which solute (tracer) concentration can be measured. The *resident concentration* (C_R) expresses the mass of solute (Δm) per unit volume of fluid (ΔV) contained in a given element of the system at a given instant, t:

$$C_R(t) = \Delta m(t)/\Delta V \tag{1}$$

The *flux concentration* (C_F) expresses the ratio of the solute flux ($\Delta m/\Delta t$) to the volumetric fluid flow ($Q = \Delta V/\Delta t$) passing through a given cross-section:

$$C_F = \frac{\Delta m(t)/\Delta t}{\Delta V/\Delta t} = \frac{\Delta m(t)}{Q\Delta(t)} \tag{2}$$

The resident concentration can be regarded as the mean concentration obtained by weighting over a given cross-section of the system, whereas the flux concentration is the mean concentration obtained by weighting by the volumetric flow rates of flow lines through a given cross-section of the system. The differences between two types of concentration were shown either theoretically or experimentally by a number of authors [15, 16, 17, 18]. However, numerical differences between both types of concentration are of importance only for laminar flow in capillaries and for highly dispersive systems [18, 19] (see Appendix A).

The *turnover time* or *age of water leaving the system* (t_w) is defined as:

$$t_w = V_m/Q \tag{3a}$$

where V_m is the volume of mobile water in the system. For systems which can be approximated by unidimensional flow, Eq. 3 reads:

$$t_w = V_m/Q = \frac{Sn_e x}{Sn_e v_w} = \frac{x}{v_w} \tag{3b}$$

where x is the length of the system measured along the streamlines, v_w is the mean velocity of water, n_e is the space fraction occupied by the mobile water (effective porosity), and S is the cross-section area normal to flow. According to Eq. 3b, the *mean water velocity* is defined as:

$$v_w = Q/(n_e S) = v_f/n_e \tag{4}$$

where v_f is *Darcy's velocity* defined as Q/S.

2. Immobile systems

Discussion of immobile systems is beyond the scope of this manual, but for the consistency of the age definitions they are briefly discussed below. For old groundwaters, a distinction should be made between mobile and immobile systems, especially in respect to the definition of age. A radioisotope tracer, which has no other source and sink than the radioactive decay, represents the age of water in an immobile system, if the system is separated from recharge and the mass transfer with adjacent systems by molecular diffusion is negligible. Then the *radioisotope age* (t_a), understood as the time span since the separation event, is defined by the well known formula of the radioactive decay, and it should be the same in the whole system:

$$C/C(0) = \exp(-\lambda t_a) \tag{5}$$

where C and C(0) are the actual and initial radioisotope concentrations, and λ is the radioactive decay constant.

Unfortunately, ideal radioisotope tracers are not available for dating of old immobile water systems. Therefore, we shall mention that the accumulation of some tracers is a more convenient tool, if the accumulation rate can be estimated from the *in situ* production and the crust or mantle flux as it is in the case of ^4He and ^{40}Ar dating for both mobile and immobile systems. Similarly, the dependence of ^2H and ^{18}O contents in water molecules on the climatic conditions of recharge during different geological periods as well as noble gas concentrations expressed in terms of the temperature at the recharge area (noble gas temperatures) may also serve for reliable tracing of immobile groundwater systems in terms of ages.

3. Basic principles for constant flow systems

The *exit age-distribution function*, or the *transit time distribution*, E(t), describes the exit time distribution of incompressible fluid elements of the system (water) which entered the system at a given t = 0. This function is normalized in such a way that:

$$\int_0^\infty E(t)\,dt = 1 \tag{6}$$

According to the definition of the E(t) function, the mean age of water leaving the system is:

$$t_w = \int_0^\infty tE(t)\,dt \tag{7}$$

The *mean transit time of a tracer* (t_t) or the *mean age of tracer* is defined as:

$$t_t = \int_0^\infty tC_I(t)\,dt \Big/ \int_0^\infty C_I(t)\,dt \tag{8}$$

where $C_I(t)$ is the tracer concentration observed at the measuring point as the result of an instantaneous injection at the injection point at t = 0. Equation 8 defines the age of any tracer injected and measured in any mode. In order to avoid possible misunderstandings, in all further considerations, t_t denotes the mean age of a conservative tracer. Unfortunately, it is a common mistake to identify Eq. 7 with Eq. 8 for conservative tracers (or for radioisotope tracers corrected for the decay) whereas the mean age of a conservative tracer leaving the system is equal to the mean age of water only if the tracer is injected and measured in the flux mode and if no stagnant water zones exist in the system. Consequently, because the tracer age may differ from the water age, it is convenient to define a function describing the distribution of a conservative tracer. This function, called the *weighting function*, or the *system response function*, g(t), describes the exit age-distribution of tracer particles which entered the system of a constant flow rate at a given t = 0:

$$g(t) = C_I(t) \Big/ \int_0^\infty C_I(t)\,dt = C_I(t)Q/M \tag{9}$$

because the whole injected mass or activity (M) of the tracer has to appear at the outlet, i.e.:

$$M = Q \int_0^\infty C_I(t)\,dt \tag{10}$$

As mentioned, the g(t) function is equal to the E(t) function, and, consequently, the mean age of tracer is equal to the turnover time of water, if a conservative tracer (or a decaying tracer corrected for the decay) is injected and measured in the flux mode, and if there are no stagnant zones in the system. Systems with stagnant zones are discussed in Sect. 9. In the lumped-parameter approach it is usually assumed that the concentrations are observed in water entering and leaving the system, which means that flux concentrations are applicable. Therefore, in all further considerations the C symbol stays for flux concentrations, and the mean transit time of tracer is equal to the mean transit time of water unless stated otherwise.

Equation 8 is of importance in artificial tracing, and, together with Eq. 9, serves for theoretical findings of the response functions in environmental tracing. For a steady flow through a groundwater system, the output concentration, C(t), can be related to the input concentration (C_{in}) of any tracer by the well known convolution integral:

$$C(t) = \int_0^\infty C_{in}(t-t')\,g(t')\,\exp(-\lambda t')\,dt' \tag{11a}$$

where t' is the transit time, or

$$C(t) = \int_{-\infty}^{0} C_{in}(t')\, g(t-t')\, \exp[-\lambda(t-t')\, dt' \qquad (11b)$$

where t' is time of entry, and t - t' is the transit time.

The type of the model (e.g. the piston flow model, or dispersion model) is defined by the g(t') function chosen by the modeller whereas the model parameters are to be found by calibration (fitting of concentrations calculated from Eq. 11 to experimental data, for known or estimated input concentration records).

4. Models and their parameters

4.1. General

The lumped-parameter approach is usually limited to one- or two-parameter models. However, the type of the model and its parameters define the exit-age distribution function (the weighting function) which gives the spectrum of the transit times. Therefore, if the modeller gives just the type of the model and the mean age, the user of the data can be highly misled. Consider for instance an exponential model and the mean age of 50 years. The user who has no good understanding of the models may start to look for a relatively distant recharge area, and may think that there is no danger of a fast contamination. However, the exponential model (see Sects 4.3 and 9.1) means that the flow lines with extremely short (theoretically equal to zero) transit times exist. Therefore, the best practice is to report both the parameters obtained and the weighting function calculated for these parameters. Another possible misunderstanding is also related to the mean age. For instance, the lack of tritium means that no water recharged in the hydrogen-bomb era is present (i.e., after 1952). However, for highly dispersive systems (e.g. those described by the exponential model or the dispersive model with a large value of the dispersion parameter), the presence of tritium does not mean that an age of 100 years, or more, is not possible.

Sometimes either it is necessary to assume the presence of two water components (e.g., in river bank filtration studies), or it is impossible to obtain a good fit (calibration) without such an assumption. The additional parameter is denoted as β, and defined as the fraction of total water flow with a constant tracer concentration, C_{β}.

4.2. Piston Flow Model (PFM)

In the *piston flow model* (PFM) approximation it is assumed that there are no flow lines with different transit times, and the hydrodynamic dispersion as well as molecular diffusion of the tracer are negligible. Thus the tracer moves from the recharge area as if it were in a parcel. The weighting function is given by the Dirac delta function [$g(t') = \delta(t'-t_t)$], which inserted into Eq. 9 gives:

$$C(t) = C_{in}(t-t_t)\, \exp(-\lambda t_t) \qquad (12)$$

Equation 12 means that the tracer which entered at a given time $t-t_t$ leaves the system at the moment t with concentration decreased by the radio-

active decay during the time span t_t. The mean transit time of tracer (t_t) equal to the mean transit time of water (t_w) is the only parameter of PFM. Cases in which t_t may differ from t_w are discussed in Sect. 9.

4.3. Exponential Model (EM)

In the *exponential model* (EM) approximation it is assumed that the exponential distribution of transit times exists, i.e., the shortest line has the transit time of zero and the longest line has the transit time of infinity. Tracer concentration for an instantaneous injection is: $C_I(t) = C_I(0) \exp(-t/t_t)$. This equation inserted into Eq. 9, and normalized in such a way that the initial concentration is as if the injected mass (M) was diluted in the volume of the system (V_m), gives:

$$g(t') = t_t^{-1} \exp(-t'/t_t) \tag{13}$$

The mean transit time of tracer (t_t) is the only parameter of EM. The exponential model is mathematically equivalent to the well known model of good mixing which is applicable to some lakes and industrial vessels. A lot of misunderstandings result from that property. Some investigators reject the exponential model because there is no possibility of good mixing in aquifers whereas others claim that the applicability of the model indicates conditions for a good mixing in the aquifer. Both approaches are wrong because the model is based on an assumption that no exchange (mixing) of tracer takes place between the flow lines [1, 6, 8]. The mixing takes place only at the sampling site (spring, river or abstraction well). That problem will be discussed further.

A normalized weighting function for EM is given in Fig. 1. Note that the normalization allows to represent an infinite number of cases by a single curve. In order to obtain the weighting function in real time it is necessary to assume a chosen value of t_t and recalculate the curve from Fig. 1.

The mean transit time of tracer (t_t) equal to the mean transit time of water (t_w) is the only parameter of EM. Cases in which t_t may differ from t_w are discussed in Sect. 9.

4.4. Linear Model (LM)

In the *linear model* (LM) approximation it is assumed that the distribution of transit times is constant, i.e., all the flow lines have the same velocity but linearly increasing flow time. Similarly to EM, there is no mixing between the flow lines. The mixed sample is taken in a spring, river, or abstraction well [1, 3, 6]. The weighting function is:

$$\begin{aligned} g(t) &= 1/(2t_t) \quad \text{for } t' \le 2t_t \\ &= 0 \quad\quad\;\; \text{for } t' \ge 2t_t \end{aligned} \tag{14}$$

The mean transit time of tracer (t_t) is the only parameter of LM. A normalized weighting function is given in Fig. 2. In order to obtain the weighting function in real time it is necessary to assume a chosen value of t_t and recalculate the curve from Fig. 2.

The mean transit time of tracer (t_t) equal to the mean transit time of water (t_w) is the only parameter of LM. Cases in which t_t may differ from t_w are discussed in Sect. 9.

4.5. Combined Exponential-Piston Flow Model (EPM)

In general it is unrealistic to expect that single-parameter models can adequately describe real systems, and, therefore, a little more realistic two-parameter models have also been introduced. In the *exponential-piston model* it is assumed that the aquifer consists of two parts in line, one with the exponential distribution of transit times, and another with the distribution approximated by the piston flow. The weighting function of this model is [3, 6]:

$$g(t') = (\eta/t_t)\exp(-\eta t'/t_t + \eta - 1) \quad \text{for } t' \geq t_t(1 - \eta^{-1}) \qquad (15)$$
$$= 0 \quad \text{for } t' \leq t_t(1 - \eta^{-1})$$

where η is the ratio of the total volume to the volume with the exponential distribution of transit times, i.e., $\eta = 1$ means the exponential flow model (EM). The model has two fitting (sought) parameters, t_t and η. The weighting function does not depend on the order in which EM and PFM are combined. An example of a normalized weighting function obtained for $\eta = 1.5$ is given in Fig. 1. However, experience shows that EPM works well for η values slightly larger than 1, e.i., for a dominating exponential flow pattern corrected for the presence of a small piston flow reservoir. In other cases, DM is more adequate.

In order to obtain the weighting function for a given value of η and a chosen t_t value in real time it is necessary to recalculate the curve from Fig. 1. Cases in which t_t may differ from t_w are discussed in Sect. 9.

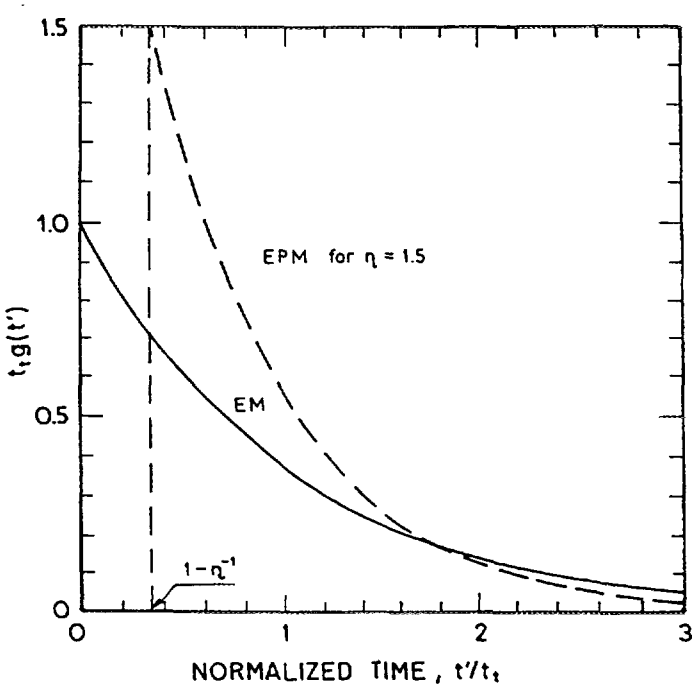

Fig. 1. The g(t') function of EM, and the g(t') function of EPM in the case of $\eta = 1.5$ [3, 6].

4.6. Combined Linear-Piston Flow Model (LPM)

The combination of LM with PFM gives similarly to EPM the *linear-piston model* (LPM). Similarly to EPM the weighting function has two parameters and does not depend on the order in which the models are combined. The weighting function is [3, 6]:

$$g(t') = \eta/(2t_t) \quad \text{for} \quad t_t - t_t/\eta \le t' \le t_t + t_t/\eta \qquad (16)$$
$$= 0 \quad \text{for other } t'$$

where η is the ratio of the total volume to the volume in which linear flow model applies, i.e., $\eta = 1.0$ means the linear flow model (LM). An example of the weighting function is given in Fig. 2. Weighting functions in real time are obtainable in the same way as described above for other models. Cases in which t_t differs from t_w are discussed in Sect. 9.

4.7. Dispersion Model (DM)

In the *dispersion model* (DM) the uni-dimensional solution to the dispersion equation for a semi-infinite medium and flux injection-detection mode, developed in [20] and fully explained in [18], is usually put into Eq. 9 to obtain the weighting function, though sometimes other approximations are also applied. That weighting function reads [3, 6]:

$$g(t') = (4\pi t'^3/Pet_t)^{-1/2} \exp[-(1 - t'/t_t)^2 t_t Pe/t'] \qquad (17)$$

where Pe is the so-called Peclet number. The reciprocal of Pe is equal to the dispersion parameter, $Pe^{-1} = D/vx$, where D is the dispersion coefficient. In the lumped parameter approach the dispersion parameter is treated as a single parameter. The meaning of that parameter is discussed in Sect. 9.1.

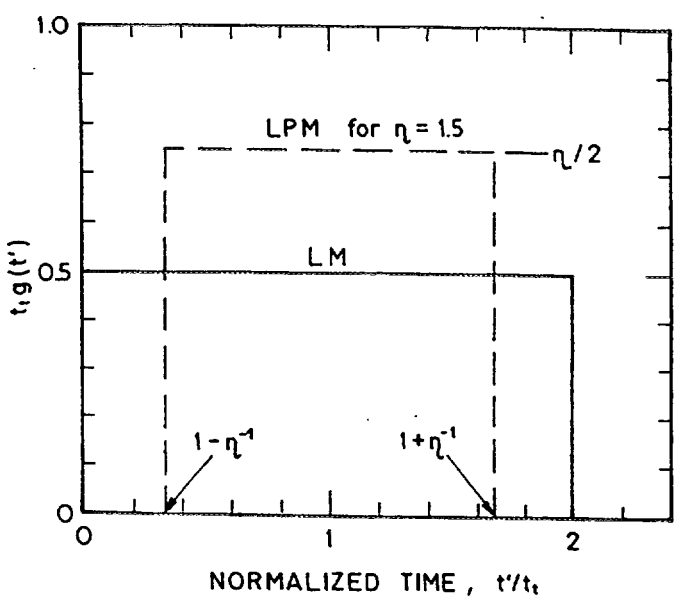

Fig. 2. The g(t') function of LM, and the g(t') function of LPM in the case of $\eta = 1.5$ [3, 6].

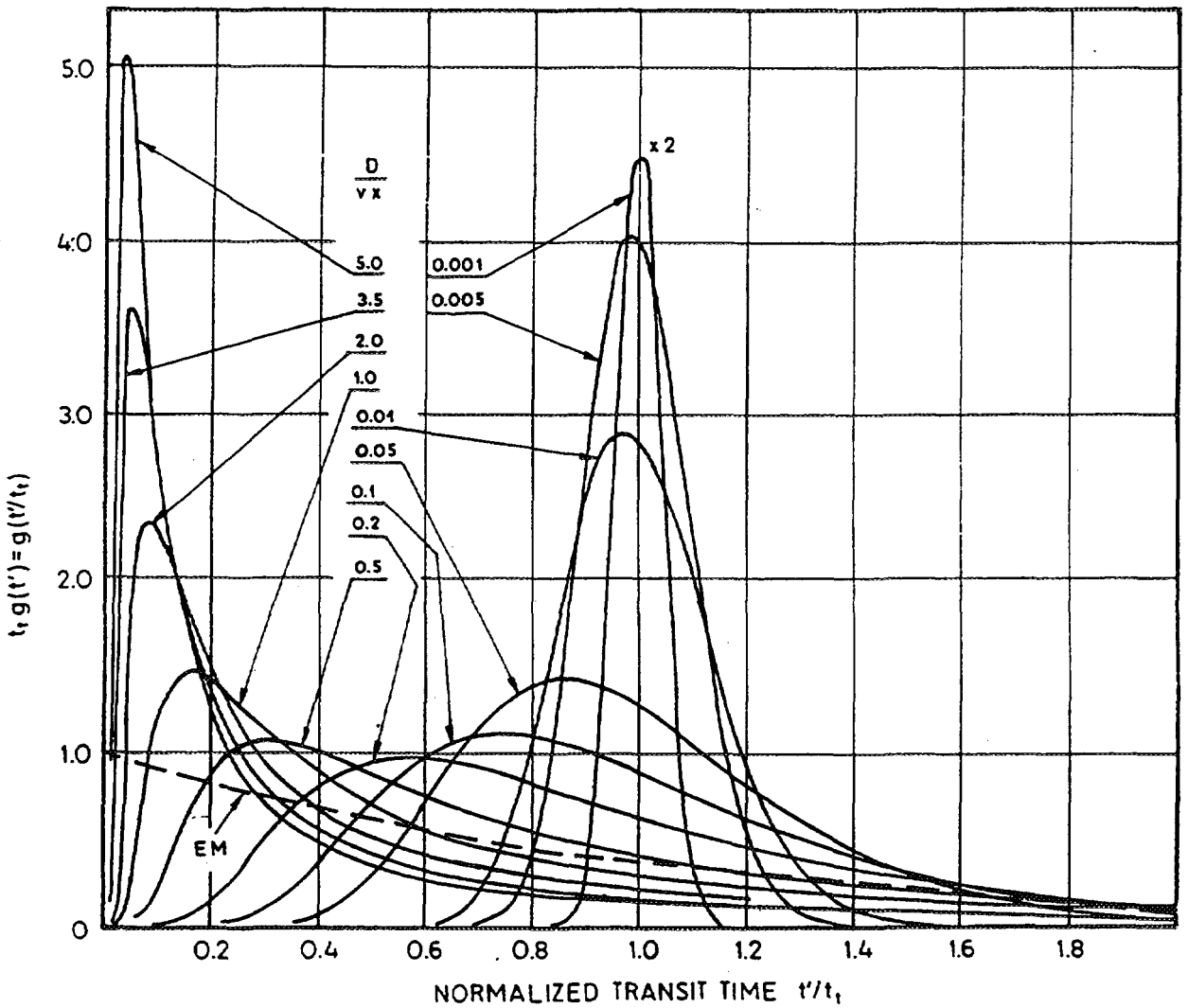

Fig. 3. Examples of the g(t') functions for DM in flux mode [3, 6]. The g(t') function of EM is shown for comparison.

Examples of normalized weighting functions for DM in the flux mode are shown in Fig. 3. Weighting functions in real time are obtainable in the same way as described above for other models. Cases in which t_t differs from t_w are discussed in Sect. 9.

The dispersion model can also be applied for the detection performed in the resident concentration mode (see Eq. 1). Then the weighting function reads [3, 6]:

$$g(t') = \{(\pi t'/Pet_w)^{-1/2} \exp[-(1 - t'/t_w)^2 t_w Pe/t'] - (Pe/2) \exp(Pe) \operatorname{erfc}[(1 + t'/t_w)(4t'/Pet_w)^{-1/2}]\}/t_w \qquad (18)$$

where erfc(z) = 1 - erf(z), erf(z) being the tabulated error function. In the case of Eq. 18 the mean transit time of tracer always differs from the mean transit time of tracer and in ideal cases is given by: $t_t = (1 + Pe^{-1})t_w$, which shows that even if there are no stagnant zones in the system

the mean transit time of a conservative tracer may differ from the mean transit time of water. Cases of stagnant water zones are discussed in Sects 9.2 and 9.3.

A misunderstanding is possible as a result of different applications of the dispersion equation and its solutions. For instance, in the pollutant movement studies the dispersion equation usually serves as a distributed parameter model, especially when numerical solutions are used. Then, the dispersion coefficient (or the dispersivity, D/v, or dispersion parameter, Pe^{-1}, depending on the way in which the solutions are presented) represents the dispersive properties of the rock. If the dispersion model is used in the lumped parameter approach for the interpretation of environmental data in aquifers, the dispersion parameter is an apparent quantity which mainly depends on the distribution of flow transit times, and is practically order of magnitudes larger than the dispersion parameter resulting from the hydrodynamic dispersion, as explained in Sect. 9.1. However, in the studies of vertical movement through the unsaturated zone, or in some cases of river bank infiltration, the dispersion parameter can be related the hydrodynamic dispersion.

5. Cases of constant tracer input

For radioisotope tracers, the cases of a constant input can be solved analytically. They are applicable mainly to ^{14}C and tritium prior to atmospheric fusion-bomb tests in the early 1950s. The following solutions are obtainable from Eq. 9 [1, 3, 6]:

$$C = C_0 \exp(-\lambda/t_a) \qquad \text{for PFM} \qquad (19)$$

$$C = C_0/(1 + \lambda/t_a) \qquad \text{for EM} \qquad (20)$$

$$C = C_0[1 - \exp(-2\lambda t_a)]/(2\lambda t_a) \qquad \text{for LM} \qquad (21)$$

$$C = C_0 \exp\{(Pe/2)\times[1 - (1 + 4\lambda t_a Pe^{-1})^{1/2}]\} \qquad \text{for DM} \qquad (22)$$

where C_0 is a constant concentration measured in water entering the system and t_w is replaced by t_a (radioisotope age) to the reasons discussed in detail in Sect. 9. Here, we shall remind only that for nonsorbable tracers and systems without stagnant zones $t_w = t_a$. Unfortunately, it is a common mistake to identify the radiocarbon age obtained from Eq. 19 with the water age without any information if PFM is applicable and if the radiocarbon is not delayed by interaction between dissolved and solid carbonates.

Relative concentration (C/C_0) given as functions of normalized time (λt_a) are given in Fig. 4 (for tritium $1/\lambda$ = 17.9 a, and for radiocarbon $1/\lambda$ = 8,300 a). From Eqs 19 to 22 and Fig. 4, several conclusions can immediately be drawn. First, for a sample taken from a well, it is in principle not possible to distinguish if the system is mobile or immobile (however, if a short-lived radioisotope is present, it would be unreasonable to assume that the system can be separated from the recharge). Second, the applicability of the piston flow model (PFM) is justified for a constant tracer input to systems with the values of the dispersion parameter, say, not larger than about 0.05. Third, from the measured C/C_0 ratio it is not possible to obtain the radioisotope age without the knowledge on the model of flow pattern even if a single-parameter model is assumed. Fourth, for ages below, say, $0.5(1/\lambda)$,

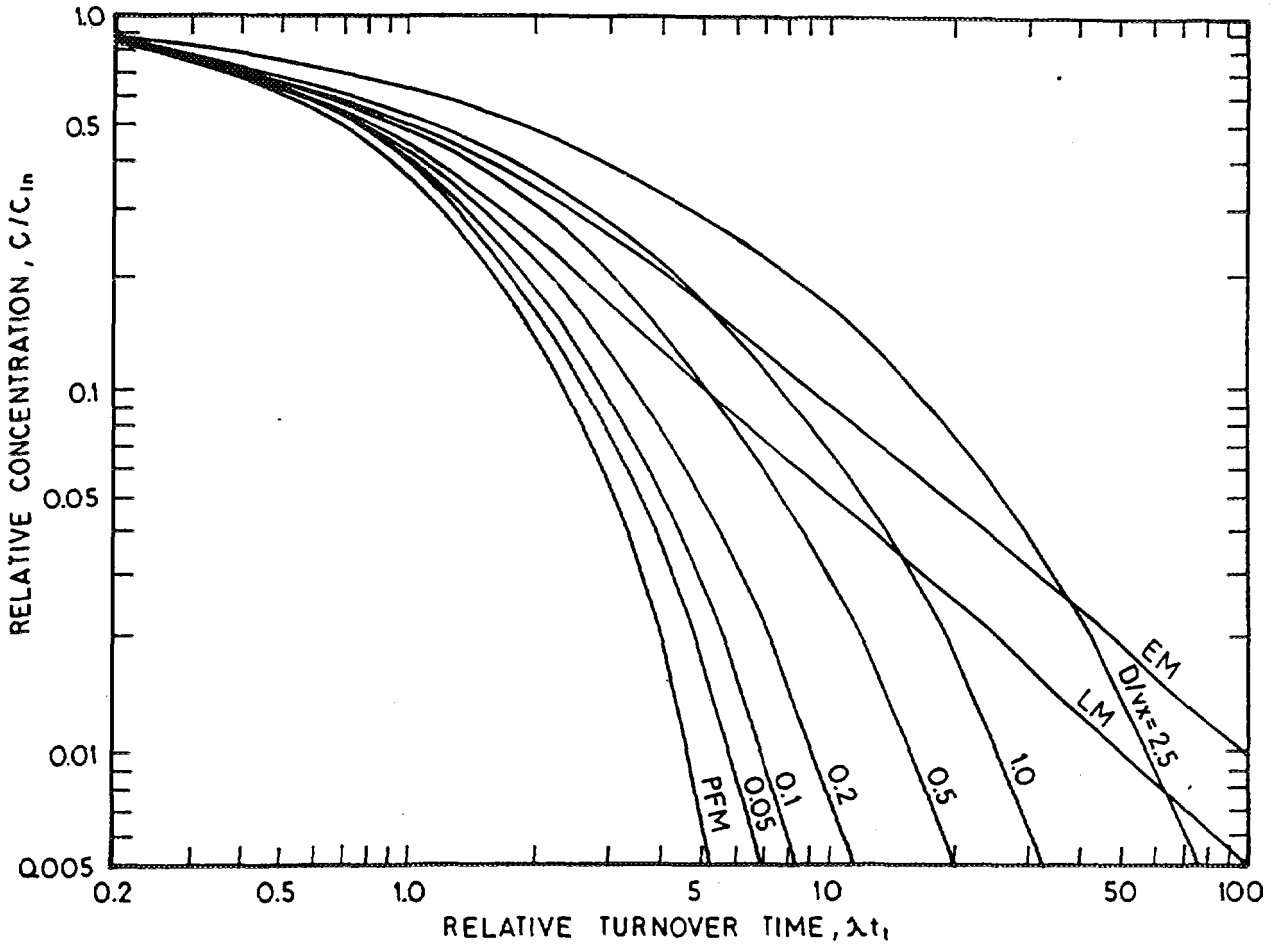

Fig. 4. Relative concentration versus relative radioisotope age (λt_t), in the case of a constant input of a radioactive tracer [3, 6]. EM - exponential model, LM - linear model, PFM - piston flow model, Pe^{-1} - dispersion parameter for the dispersion model in the flux mode.

the flow pattern (type of model) has low influence on the age obtained. Fifth, for two-parameter models it is impossible to obtain the age value (it is like solving a single equation with two unknowns).

When no information is available on the flow pattern, the ages obtained from PFM and EM can serve as brackets for real values, though in some extreme cases DM can yield higher ages (see Fig. 4).

Radioisotopes with a constant input are applicable as tracers for the age determination due to the existence of a sink (radioactive decay), which is adherent to the sought parameter (see the definition of an ideal tracer in Sect. 1.2). Other substances cannot serve as tracers for this purpose though they come under earlier definitions of an ideal tracer. However, those other substances (e.g., Cl^-) may serve as good tracers for other purposes, e.g., for determining the mixing ratio of different waters.

Note that for a constant tracer input, a single determination serves for the calculation of age. Therefore, no calibration can be performed. The only way to validate, or confirm, a model is to compare its results with other independent data, if available.

6. Cases of variable tracer input

6.1. Tritium method

Seasonal variations of the tritium concentration in precipitation cause serious difficulties in calculating the input function, $C_{in}(t)$. The best method would be to estimate for each year the mean concentration weighted by the infiltration rates:

$$C_{in} = \sum_{i=1}^{12} C_i \alpha_i P_i / \sum_{i=1}^{12} \alpha_i P_i \qquad (23)$$

where C_i, α_i and P_i are the ^3H concentrations in precipitation, infiltration coefficients, and monthly precipitation amounts for ith month, respectively. C_i is to be taken from the nearest IAEA network station, and for early time periods by correlations between that station and other stations for which long records are available [2]. The precipitation rates are to be taken from the nearest meteorologic station, or as the mean of two or three stations if the supposed recharge area lies between them. Usually, it is assumed that the infiltration coefficient in the summer months (α_s) is only a given fraction (α) of the winter coefficient (α_w). Then, Eq. 23 simplifies to:

$$C_{in} = [(\alpha \Sigma C_i P_i)_s + (\Sigma C_i P_i)_w]/[(\alpha \Sigma P_i)_s + (\Sigma P_i)_w] \qquad (24)$$

where subscripts "s" and "w" mean the summing over the summer and winter months, respectively. For the northern hemisphere, the summer months are from April to September and winter months from October to March, and the same α value is assumed for each year.

The input function is constructed by applying Eq. 24 to the known C_i and P_i data of each year, and for an assumed α value. In some cases Eq. 23 is applied if there is no surface run-off and α_i coefficients can be found from the actual evapotranspiration and precipitation data. The actual evapotranspiration is either estimated from pan-evaporimeter experiments [21] or by the use of an empirical formula for the potential evapotranspiration [22]. Monthly precipitation has to be measured in the recharge area, or can be taken from a nearby station. Monthly ^3H concentrations in precipitation are known from publications of the IAEA [23] by taking data for the nearest station or by applying correlated data of other stations [2].

It is well known that under moderate climatic conditions the recharge of aquifers takes place mainly in winter and early spring. Consequently, in early publications on the tritium input function, the summer infiltration was either completely neglected [2], or α was taken as equal 0.05 [3, 6]. Similar opinion on the tritium input function was expressed in a recent review of the dating methods for young groundwaters [4]. However, whenever the stable isotopic composition of groundwater reflects that of the average precipitation there is no reason to reject the influence of summer tritium input. This is because even if no net recharge takes place in summer months, the water which reaches the water table in winter months is usually a mixture of both winter and summer water. Otherwise the stable isotopic composition of groundwater would reflect only the winter and early spring precipitation, which is not the case, as observed in many areas of the world, and as discussed below for two case studies in Poland.

Rearranged Eq. 24 can be used in an opposite way in order to find the α value [24]:

$$\alpha = [\sum_i (P_i C_i)_w - C] \sum_i (P_i)_w / [C - \sum_i (P_i C_i)_s] \sum_i (P_i)_s \qquad (25)$$

where C stays for the mean values of $\delta^{18}O$ or δD of the local groundwater originating from the modern precipitation, and C_i represents mean monthly values in precipitation. Theoretically, the summings in Eq. 25 should be performed for the whole time period which contribute to the formation of water in a given underground system. Unfortunately, this time period is unknown prior to the tritium interpretation. Much more serious limitation results from the lack of sufficient records of stable isotope content in precipitation. Therefore, the longer the record of stable isotope content in precipitation, the better the approximation. For a seven year record in Cracow station, and for typical groundwaters in the area, it was found that the α value is about 0.6-0.7, and that the values of model parameters found by calibration slightly depend on the assumed α value in the range of 0.4 to 1.0 (see case studies in Ruszcza and Czatkowice described in Sects 10.1 and 10.2). Therefore, whenever the mean isotopic composition of groundwater is close to that of the precipitation, it is advised to use α = 0.5 to 0.7. Such situations are typically observed under moderate climatic conditions and in tropical humid areas (e.g. in the Amazonia basin). In other areas the tritium input function cannot be found so easily.

Note that unless the input function is found independently, the α parameter is either arbitrarily assumed by the modeller, or tacitly used as hidden fitting parameter (see Sects 10.1 and 10.2 for case studies in which α was used as a fitting parameter in an explicit way).

6.2. Tritium-helium method

As the tritium peak in the atmosphere, which was caused by hydrogen bomb test, passes and ^3H concentration in groundwaters declines slowly approaching the pre-bomb era values, the interest of a number of researchers has been directed to other methods covering similar range of ages. In the ^3H-^3He method either the ratio of tritiugenic ^3He to ^3H is considered, or theoretical contents of both tracers are fitted (calibration process) to the observation data independently [4, 6, 25-31]. The method has several advantages and disadvantages. In order to measure ^3He a costly mass-spectrometer is needed and additional sources and sinks of ^3He in groundwater must be taken into account. The main advantage seemed to result from the $^3He/^3H$ peak to appear much later in groundwater systems than the ^3H peak of 1963. Unfortunately, in some early estimates of the potential abilities of that method, the influence of a low accuracy of the ratio for low tritium contents was not taken into account.

Another advantage consists in the $^3He/^3H$ ratio being independent of the initial tritium content for the piston flow model (PFM). Then the tracer age is:

$$t_t = \lambda_T^{-1} \ln[1 + {}^3He_T/{}^3H] \qquad (26)$$

where λ_T is the radioactive decay constant for tritium ($\lambda_T^{-1} = t_{1/2}/\ln 2 = 12.4/0.693 = 17.9$ a), and ^3He_T stays for tritiugenic ^3He content expressed in T.U. (for ^3He expressed in ml STP of gas per gram of water, the factor is 4.01×10^{14} to obtain the ^3He content in T.U.).

Unfortunately, contrary to the statements of some authors, Eq. 26 does not apply to other flow models. In general, the following equations have to be considered [31]:

$$C_T(t) = \int_0^\infty C_{Tin}(t-t')\, g(t')\, \exp(-\lambda t')\, dt' \qquad (27)$$

for tritium, and

$$C_{He}(t) = \int_0^\infty C_{Tin}(t-t')\, g(t')\, [1 - \exp(-\lambda t')]\, dt' \qquad (28)$$

for the daughter ^3He. From these equations, and from examples of theoretical concentrations curves (solutions to the direct problem) given in [31], it is clear that the results of the ^3H-^3He method depend on the tritium input function.

Several recent case studies show that in vertical transport through the unsaturated zone, or for horizontal flow in the saturated zone, when the particular flow paths can be observed by multi-level samplers, the ^3H-^3He method in the piston flow approximation yields satisfactory or acceptable results [27-30]. However, for typical applications of the lumped-parameter approach, when Eqs 27 and 28 must be used, and where possible sources and sinks of ^3He influence the concentrations measured, the ^3H-^3He method does not seem to yield similar ages as the tritium method [32]. The main sources and sinks result from possible gains and losses of ^3He by diffusional exchange with the atmosphere, if the water is not well separated on its way after the recharge event.

6.3. Krypton-85 method

The ^{85}Kr content in the atmosphere results from nuclear power stations and plutonium production for military purposes. Large scatter of observed concentrations shows that there are spatial and temporal variations of the ^{85}Kr activity. However, yearly averages give relatively smooth input functions for both hemispheres [32-35]. The input function started from zero in early 1950s and monotonically reached about 750 dpm/mmol Kr in early 1980s. The ^{85}Kr concentration is expressed in Kr dissolved in water by equilibration with the atmosphere, and, therefore it does not depend on the temperature at the recharge area, though the concentration of Kr is temperature dependent. Initially, it was hoped that the ^{85}Kr method would replace the tritium method [36] when the tritium peak disappears. However, due to large samples required and a low accuracy, the method is very seldom applied, though, similarly to the ^3H-^3He method, a successful application for determining the water age along flow paths is known [37]. In spite of the present limitations of the ^{85}Kr method, it is, together with man-made volatile organic compounds discussed in Sect. 6.6, one of the most promising methods for future dating of young groundwaters [4], though similar limitations as in the case of the ^3H-^3He method can be expected due to possible diffusional losses or gains [32].

The solutions to the direct problem given in [6] indicate that for short transit times (ages), say, of the order of 5 years, the differences between particular models are slight, similarly as for constant tracer input (see Sect. 5). For longer transit times, the differences become larger, and, contrary to the statements of some authors, long records are needed to differentiate responses of particular models.

6.4. Carbon-14 method as a variable input tracer

Usually the ^{14}C content is not measured in young waters in which tritium is present unless mixing of waters having distinctly different ages is to be investigated. However, in principle, the variable ^{14}C concentrations of the bomb era can also be interpreted by the lumped-parameter approach, though the method is costly and the accuracy limited due to the problems related to the so-called initial carbon content [38, 39]. Therefore, it is possible only to check if the carbon data are consistent with the model obtained from the tritium interpretation [6, 32].

6.5. Oxygen-18 and/or deuterium method

Seasonal variations of $\delta^{18}O$ and δD in precipitation are known to be also observable in small systems with the mean transit time up to about 4 years, though with a strong damping. Several successful applications of the lumped parameter approach to such systems with ^{18}O and D as tracers are known. In order to obtain a representative output concentration curve, a frequent sampling is needed, and a several year record of precipitation and stable isotope data from a nearby meteorologic station. The method proposed in [40, 41] for finding the input function, is also included in the FLOW program within the present manual. The input function is found from the following formula (where C stays for delta values of ^{18}O or D):

$$C_{in}(t) = \bar{C} + [N\alpha_i P_i (C_i - \bar{C})] / \sum_i^N \alpha_i P_i \qquad (29)$$

where $\bar{C}$ is the mean output concentration, and N is the number of months (or weeks, or two-week periods) for which observations are available. Usually, instead of monthly infiltration rates (α_i), the coefficient α given by Eq. 25 is used. For small retention basins the α coefficient can also be estimated from the hydrologic data as $(Q_s/P_s)/(Q_w/P_w)$, where Q_s and Q_w are the summer and winter outflows from the basin, respectively [40, 41]. The Wimbachtal Valley case study showed that the values of the α coefficient determined by these two methods may differ considerably when the snow cover accumulated in winter months melts in summer months.

6.6. Other methods

Among other variable tracers which are the most promising for dating the young groundwaters are freon-12 (CCl_2F_2) and SF_6. In 1970s a number of authors demonstrated the applicability of chlorofluorocarbons (mainly freon-11) to trace the movement of sewage in groundwaters [4]. However, early attempts of dating with freon-11 by the lumped-parameter approach were not very successful [32], most probably due to the adsorption of that tracer and exchange with the atmosphere. However, conclusions reached in several recent publications indicate that freon-11 and freon-12 are in general applicable to trace young waters [4, 42, 43]. In a case study in Maryland a number of sampling wells were installed with screens only 0.9 m long [43]. Therefore, it was possible to use the piston flow approximation (advective transport only) for determining the freon-11 and freon-12 ages which were next used to calibrate a numerical flow and transport model. However, in our opinion, no good fit was obtained for these two tracers, and for the tritium tracer (interpreted both by the advective model and numerical dispersion model), though the conclusion reached was that the calibration was reasona-

bly good. In spite of difficulties encountered with gaseous tracers, some of the man-made gases with monotonically increasing atmospheric concentrations can be considered as promising for dating of young waters, and, therefore, an adequate option is included in the FLOW program mentioned earlier.

Most probably, SF_6 should also be included to the list of promising environmental tracers for groundwater dating [44].

Though technical difficulties with contamination of samples have been overcome [4], still some limitations for dating with all gaseous tracers discussed within this section result from the dependence of their solubility on the temperature at the recharge area, and on possible contamination of groundwater by local pollution sources [4]. The modelling problems are similar as those discussed for ^{85}Kr in Sect. 6.3 with additional difficulties mentioned above.

6.7. Goodness of fit

In the case of variable tracer input, the model is usually fitted (calibrated) to the set of observation data. The goodness of fit is within the present manual given by SIGMA defined as:

$$SIGMA = \left[\sum_{i=1}^{n} (Cm_i - C_i)^2 \right]^{1/2} / n \qquad (30)$$

where Cm_i is the ith measured concentration, C_i is the ith calculated concentration and n is the number of observations.

7. Other models related to the lumped-parameter approach

A number of models have been derived from the piston flow model with a constant input, which take into account possible underground production of the tracer, its interactions with the solid phase, dilution, enrichment due to membrane filtration (ultrafiltration) and diffusion exchange with acquicludes or acquitards. These models mainly serve for the interpretation of such radioisotopes as ^{14}C in a steady state, ^{36}Cl, $^{234}U/^{238}U$, and others. Their review is far beyond the scope of the present manual. References to a number of papers devoted to these models can be found in [8].

8. Variable flow

Groundwater systems are never constant, thus the assumption of a constant flow rate seems to be unjustified. Therefore, there were a number of attempts to solve the problem of variable flow in the lumped-parameter approach. It has been shown that Eq. 11 results from a more general formula in which the flux of tracer, i.e., the product C(t)×Q(t) is convoluted, and the weighting function is defined for the flux [45]. Therefore, it is evident that to interpret the tracer data in variable flow, the records of input and output flow rates are also needed. In some cases, from the record of the outflow rate it is possible to calculate the inflow rate, and to perform the interpretation of tracer data [45, 46]. In a study of a small retention basin (0.76 km^2) with a high changes in flow rate, the variable flow approach was shown to yield slightly better fit, but the mean turnover time was very close to that found from the steady-state approach [46]. Therefore, it was concluded that when the variable part of the investigated system is small in comparison with the total volume of the system, the steady state approxima-

tion is applicable. Most probably the majority of groundwater systems satisfy well this condition. Intuitively, changes in the volume and flow rates should also be short in comparison with the duration of changes in tracer concentration and its half-life time in case of radioisotopes. Under these conditions, the steady-state approach should yield satisfactory results.

9. Relations between model parameters and flow parameters

9.1. Applicability of the models

In principle, the distribution of flow lines within the investigated system in not considered in the lumped-parameter approach. However, in the interpretation of environmental tracer data, where records of data are usually too short to select the most adequate model only by calibration, selection of models can be performed on the basis of available geological or technical information. Such a selection can be performed either prior to calibration or after the calibration of several models. Fig. 5 presents several typical situations to which particular models are applicable.

The piston flow model (PFM) may be used to situations shown in the first part of Fig. 5 under the following conditions: (1) the length of the recharge zone measured in the direction of flow is negligible in comparison with the distance to the sampling site, (2) the aquifer is sufficiently homogeneous to have similar velocities in a given vertical cross-section, (3) the input concentration should either be constant or monotonically slowly changing, and (4) for a radioisotope tracer, its half-life time should preferably be lower than the age of water. These conditions are mostly intuitive, but examples given in Fig. 4 demonstrate how PFM compares with other models for a constant radioisotope tracer input. Examples of direct solutions for ^{85}Kr tracer and different models can be found in [6]. In spite of all its draw- backs, PFM may be convenient for fast and easy estimations.

The piston flow model can also be used in other situations shown in Fig. 5 if a small fraction of a well is screened, which gives a situation similar to that shown in cross-section 1.

The exponential model can be used for situations shown as *a*, *b*, and *d* in cross-section 2 of Fig. 5 providing the transit time through the unsaturated zone is negligible in comparison with the total transit time. This condition results from the shape of the weighting function (Fig. 2) in which the infinitesimally short transit time appears. It is a common mistake to fit EM to the data obtained on samples taken at a great depth, or from an artesian well, or even from a phreatic aquifer but with a thick unsaturated zone. In all such cases the extremely short transit times do not exist, and, consequently, EM is not applicable.

If the transit time through the unsaturated zone is not negligible, or if the abstraction well is screened at a certain depth (see case *c* in cross-section 2, Fig. 5), or finally if the aquifer is partly confined (cross-section 3, Fig. 5), the exponential-piston model and alternatively the dispersion model are applicable.

As mentioned, for the piston flow model no dispersion is allowed and all the flow lines have the same transit time. For the exponential and linear models and for their combinations with the piston flow model (EPM and LPM, respectively), no exchange of tracer between flow lines is assumed. For the dispersion model (DM), no assumption is needed on the dispersivity. However, one should keep in mind that in most cases, the apparent dispersivity results from the distribution of transit times of particular flow lines. In an extreme case (e.g., *d* in cross-section 2, Fig. 5, which can be equivalent to the exponential flow case) the mean distance from the recharge area to the drainage point is $x = 0.5x_o$, where x_o is the length of the recharge zone measured along the direction of flow. Then, the recharge

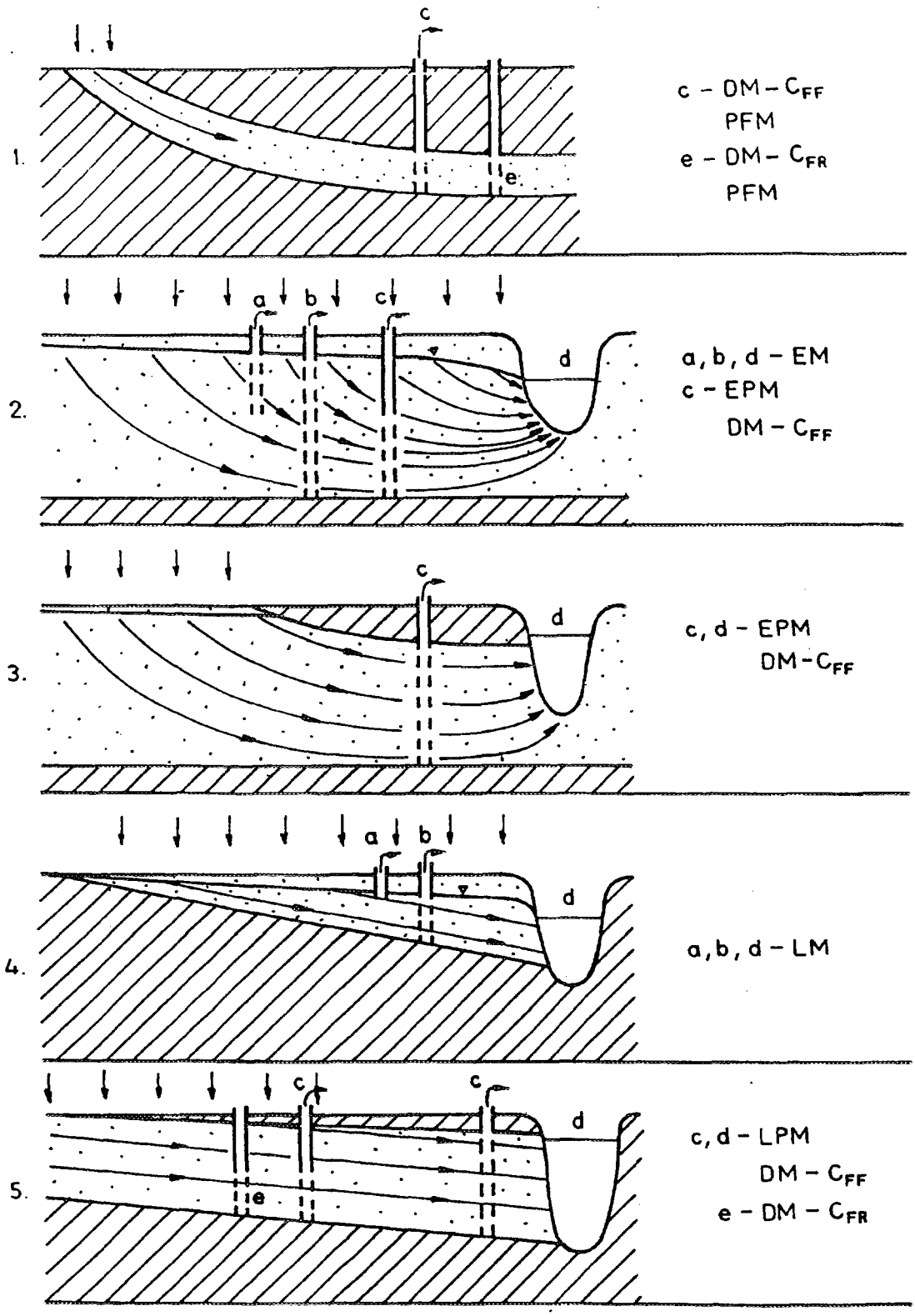

Fig. 5. Schematic situations showing examples of possible applicability of models [3, 6]. Cases *a*, *b*, *c*, and *d* correspond to sampling in outflowing or abstracted water (the sampling is averaged by the flow rates, C_{FF} mode).

Case *e* corresponds to samples taken separately at different depths and next averaged by the depth intervals (C_{FR} mode).

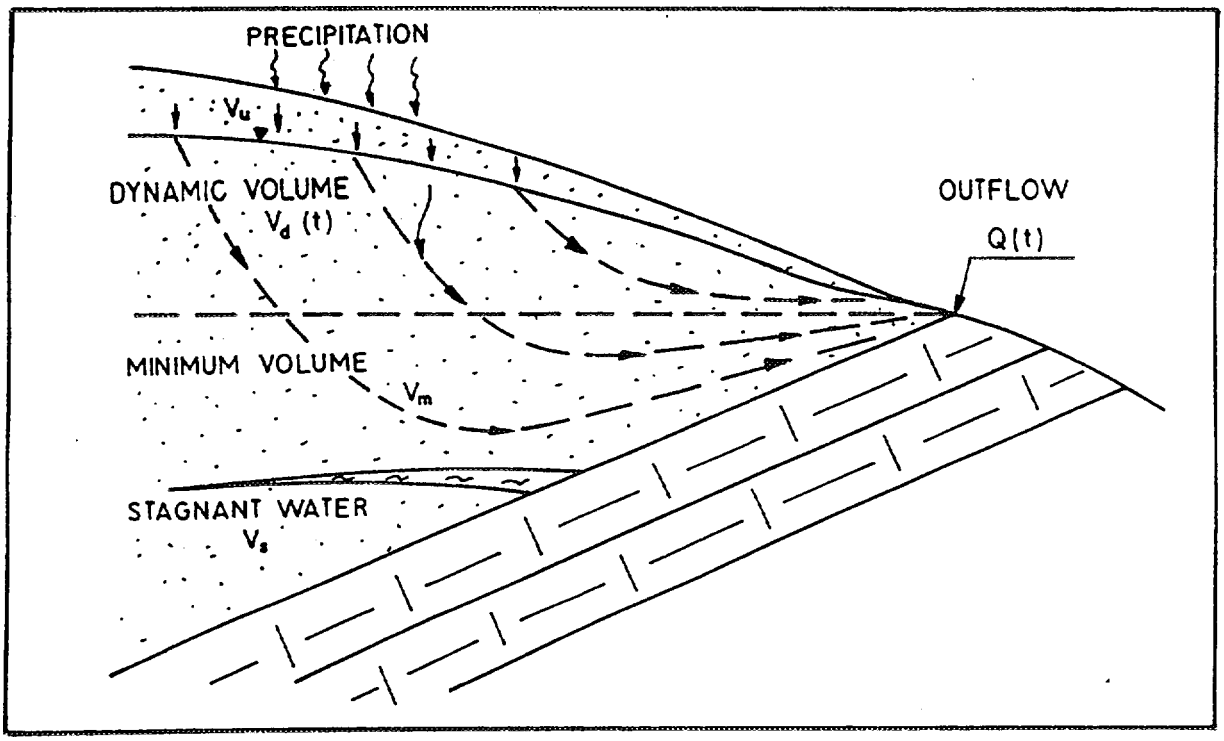

Fig. 6. Schematic presentation of different parts of a groundwater system in relation to the concept of tracer age in the lumped-parameter approach [45]. V_u - volume of water in the unsaturated zone, V_d - dynamic volume which influences the outflow rate, Q, V_{min} - minimum volume which is observed for periods in which Q = 0, V_s - stagnant volume in a sedimentation pocket.

parameter should not exceed 2 because if D/v is the measure of heterogeneity, the dispersion parameter is: $D/vx = x_o/x = 2$. Somewhat similar conclusion can be reached from Fig. 4 for a constant tracer input. For low values of the relative age, the dispersion model with D/vx = 0.5 is close to the exponential model. However, for higher values of the relative age, the dispersion model with D/vx = 2.5 is the closest one to the exponential model (EM).

Note that if the samples are taken in the discharge area (*d*) or in abstracted water (*a*, *b*, or *c*) the dispersion model in the flux mode is applicable (weighting function given by Eq. 17). However, if samples are taken at different depths of the well and the mean value is averaged over the sampled depth interval, Eq. 18 is applicable, because then the detection is in the resident mode (see Appendix A for graphical presentation of possible differences between the weighting functions).

9.2. Granular aquifers

In granular systems there is no difference between the conservative tracer age (t_t) and the radioisotope age (t_a), and, in principle, the tracer age is equal to the water age (t_w). Therefore, when dealing with granular aquifers these different concepts of ages are not necessary. However, even for granular aquifers misunderstandings are possible in relation to the

meaning of parameters obtained from the interpretation of tracer data. In Fig. 6 a schematic presentation of possible flow and tracer paths through an aquifer is shown. The tracer age determined from the interpretation of tracer concentrations in the outflow will yield the total mobile water volume (V_m) which is equal to the sum of water volume in the unsaturated zone (V_u), the dynamic water volume (V_d), and the minimum volume (V_{min}). The stagnant water in a sedimentation pocket (V_s) is neither included in the definition of water age (Eq. 3) nor it distinctly influences the tracer age, if the tracer diffusion is limited due to a small area of contact and a large extension of the pocket. It is evident from Fig. 6 that the dynamic volume which can be determined from the recession curve of the volumetric flow rate should not be identified with the mobile water volume. It is also evident that for some groundwater systems the transit time through the unsaturated zone is not negligible in comparison with the transit time in the saturated zone, and, therefore, the tracer age can be related to the aquifer parameters only if corrected for the transit time through the unsaturated zone (see Sect. 10.1).

A new abstraction well screened at the interval of a sedimentation pocket, like that shown in Fig. 6, will initially yield water with the tracer age much larger than that in the active part of the aquifer. If the pocket has large dimensions, the tracer data will not disclose for a long time that a connection with the active part exists, and a large tracer age may lead to the overestimation of the volume of that part of the investigated system. On the other hand, the tracer data from the active part of the system will lead to the underestimation of the total volume. Therefore, it can be expected that in highly heterogeneous systems the tracer ages obtained from the lumped-parameter approach will differ from the water ages. Numerical simulations performed with two-dimensional flow and transport models and compared with the interpretation performed with the aid of Eq. 11 confirmed that for highly heterogeneous systems the tracer age observed at the outlet is usually smaller than the water age [47].

9.3. Karstified and fractured aquifers

In fractured or karstified rocks the movement of water takes place mainly in fractures or in karstic channels whereas stagnant or quasi stagnant water in the microporous rock matrix is easily available to tracer by molecular diffusion. In such a case the tracer transport is delayed in respect to the mass transport of water (transport of mobile water) due to the additional time spent by the tracer in stagnant zone(s). The retardation factor caused by molecular diffusion exchange between the mobile water in fissures or channels and stagnant water in the matrix is given by the following formula [48, 49, 50]:

$$R_p = v_w/v_t = t_t/t_w = (V_p + V_f)/V_f = (n_p + n_f)/n_f - n_p \cong (n_p + n_f)/n_f \qquad (31)$$

where (R_p) is the retardation factor, n_p is the matrix porosity, and n_f is the fissure porosity (or more generally the mobile water porosity, usually called the effective porosity, and denoted in Eq. 4 as n_e). Note that n_p is defined for a unit volume of the matrix whereas n_f is defined for a representative unit volume of the whole rock. Equation 31 was first derived for a model of the fissure network represented by parallel fissures of equal aperture and spacing, as shown in Fig. 7, and in Fig. 8 in the lumped approach.

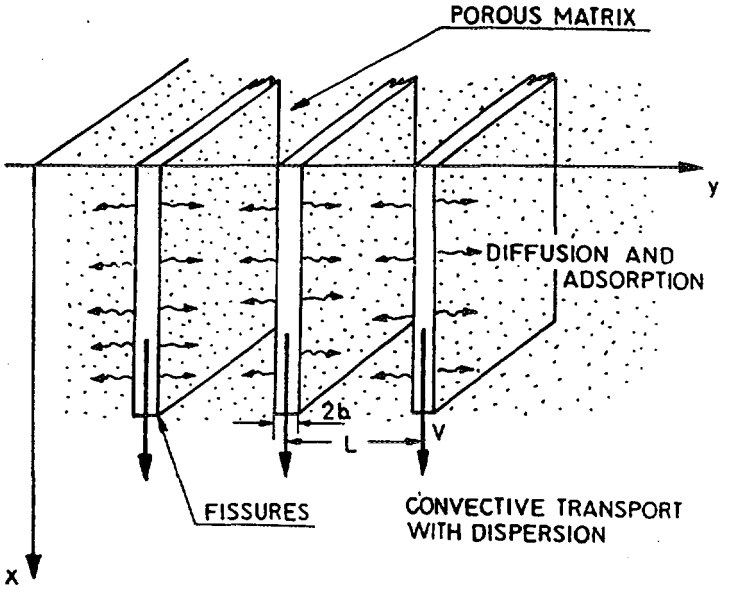

Fig. 7. A model of parallel fissure system with the exchange of tracer between the mobile water in fissures and stagnant water in the micropores.

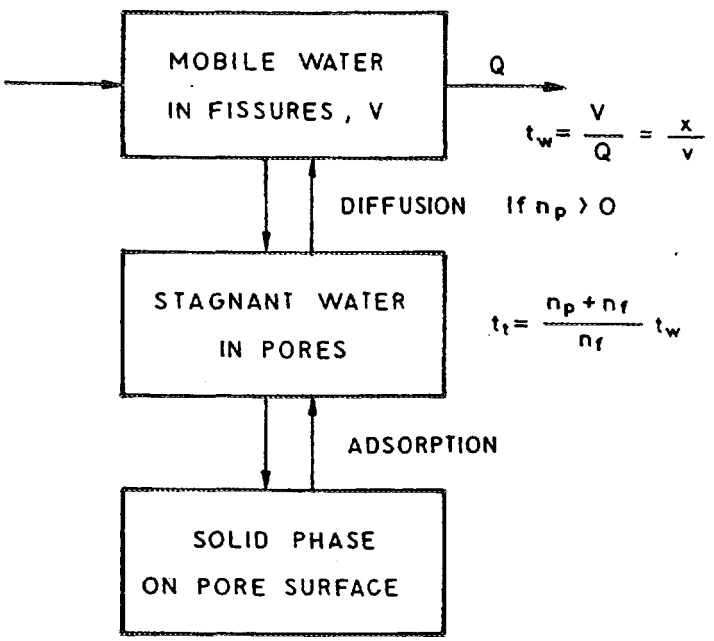

Fig. 8. A lumped-parameter approach to the system shown in Fig. 7. Note that t_w is not influenced by stagnant water volume whereas t_t is governed by matrix porosity, especially when $n_p >> n_f$ which is a common case.

It is evident from Eq. 31 that the retardation factor, i.e., the ratio of tracer age to the mean travel time of mobile water, is independent of the fissure network arrangement and the coefficient of matrix diffusion.

Equation 31 is theoretically applicable at any distance, however, in practice, its applicability is limited to large scales as discussed in [13]. The movement of environmental tracers is usually observed at large scales.

If v_w expressed by Eq. 31 is put into Eq. 4, one gets the following formula for Darcy's velocity [13, 19, 49]:

$$v_f = (n_p + n_f)v_t \cong n_p v_t = n_p(x/t_t) \tag{32}$$

which immediately gives the hydraulic conductivity:

$$k = (n_p + n_f)v_t/(\Delta H/\Delta x) \cong n_p v_t/(\Delta H/\Delta x) = n_p(x/t_t)/(\Delta H/\Delta x) \tag{33}$$

Comparison of Eqs 32 and 33 with Eq. 4 shows that if the tracer velocity is used instead of the mobile water velocity, the total open (accessible for tracer) porosity (i.e. $n_p + n_f$) replaces the fissure porosity. However, the matrix porosity is seldom below 0.02 (2 %) whereas the fissure porosity is seldom above 0.001 (0.1 %), i.e. $n_p >> n_f$. Carbonate rocks are often characterized by fissure porosities of about 0.01, but their matrix porosities are also higher (e.g., for chalks and marls about 0.3 to 0.4). Therefore, the fissure porosity can usually be neglected in a good approximation. Contrary to the fissure porosity, the matrix porosity is easily measurable on rock samples. Then, the approximate forms of Eqs 32 and 33 are applicable, which means that if either the tracer velocity or the tracer age is known, Darcy's velocity and the hydraulic conductivity can be estimated at large scale without any knowledge on the parameters of the fissure network, and vice versa, if the hydraulic conductivity is known (e.g. from pumping tests), the mean velocity of a conservative pollutant can be predicted. Even if the condition $n_p >> n_f$ is not well satisfied, the use of the approximate forms of Eqs 30 and 33 still seem to be better justified than the use of the effective porosity which is either defined as that in which the water flux occurs or undefined (some authors seem to define the effective porosity as that in which the tracer transport takes place, and at the same time to be equal to that in which the water movement takes place).

Some authors identify the specific yield with the effective porosity. However, for granular rocks the specific yield is always lower than the effective porosity defined for water flux, whereas for fissured rocks, the specific yield can be larger than the effective porosity. The identification of the effective porosity with the fissure porosity is an approximation because dead-end fissures may contain stagnant water (then $n_e < n_f$), and in large micropores some movement of water may exist (then $n_e > n_f$). In any case, for typical fissured rocks one can assume that $n_e \cong n_f << n_p$. For fissured rocks with the matrix characterized by large pores, the specific yield is larger than n_f and smaller than n_p.

It is evident from Eqs 31-33 that the solute time of travel is mainly governed by the largest water reservoir available for solute during its transport, although the solute enters and leaves the stagnant reservoir only by molecular diffusion. The mobile water reservoir in fissures is usually negligible for the estimation of the solute time of travel. In other words, the "effective porosity" applied by some workers for diffusable solutes must

be equal to the total porosity, or in approximation to the matrix porosity. However, it must be remembered, that the "effective porosity" defined for the solute transport differs from the effective porosity commonly applied in Darcy's law.

From Eq. 3 and 31 it follows that the total volume of water accessible to the tracer is [13]:

$$V = V_p + V_f = Qt_t \tag{34}$$

and the volume of rock (V_r) is:

$$V_r = V/(n_f + n_p) = Qt_t/(n_f + n_p) \cong Qt_t/n_p \tag{35}$$

It follows from Eqs 31-35 that for $n_p >> n_f$, the stagnant water in the micropores is the main reservoir for the tracer transport in fissured rocks. A serious error can be committed if that fact is not taken into account in the interpretation of water volume from the tracer age. In other words, stagnant water in the micropores, which is not available for exploitation, is the main contributor to the tracer age and the transport of pollutants.

10. Case studies

A number of case studies were reviewed in several papers [3, 6, 51]. Examples given below are selected to help the reader in a better understanding of different problems in practical applications of the lumped-parameter approach to different systems. In all these case studies, long records of tracer data were available. Unfortunately, very often single determinations of tritium, or another, tracer is available. Then, except for a constant tracer input, no age determination is possible. For springs with a constant outflow, two tritium determinations taken in a large time span are often sufficient to estimate the age. If for a given system a number of determinations are available with a short time span (up to about two years), a good practice is to "fit" the models which yield extreme age values (PFM and EM) for each sampling site and to take the mean value.

10.1. Granular aquifers

(a) Ruszcza aquifer (Nowa Huta near Cracow, southern Poland)

A sandy aquifer in Ruszcza is exploited by a number of wells (Figs 9 and 10). Its environmental tracer study was performed in order to compare different tracer techniques and to clarify if there is a flow component of a distant recharge [52]. On the basis of pumping tests it was supposed that all the wells are able to yield 10,000 m^3/d for the recharge area limited by the boundary of the high terrace of Vistula (see Fig. 9). However, a long exploitation of all wells showed that it was possible to get only 6,000 m^3/d, which still was too much for the supposed recharge area. On the other hand, high tritium and ^{14}C contents (76-71 pmc for $\delta^{13}C$ = -15.3 to -17.5 ‰ [6, 33]) excluded the possibility of an underground recharge by older water.

Consider first the tritium interpretation reported in [25]. A number of dispersion models (DM) yielded equally good fits for the values of parameters listed in Table 1. It is evident that the α coefficient cannot be used as a fitting parameter because then a large number of models (i.e., a large number of t_t and Pe pairs). The α coefficient equal to about 0.60 was

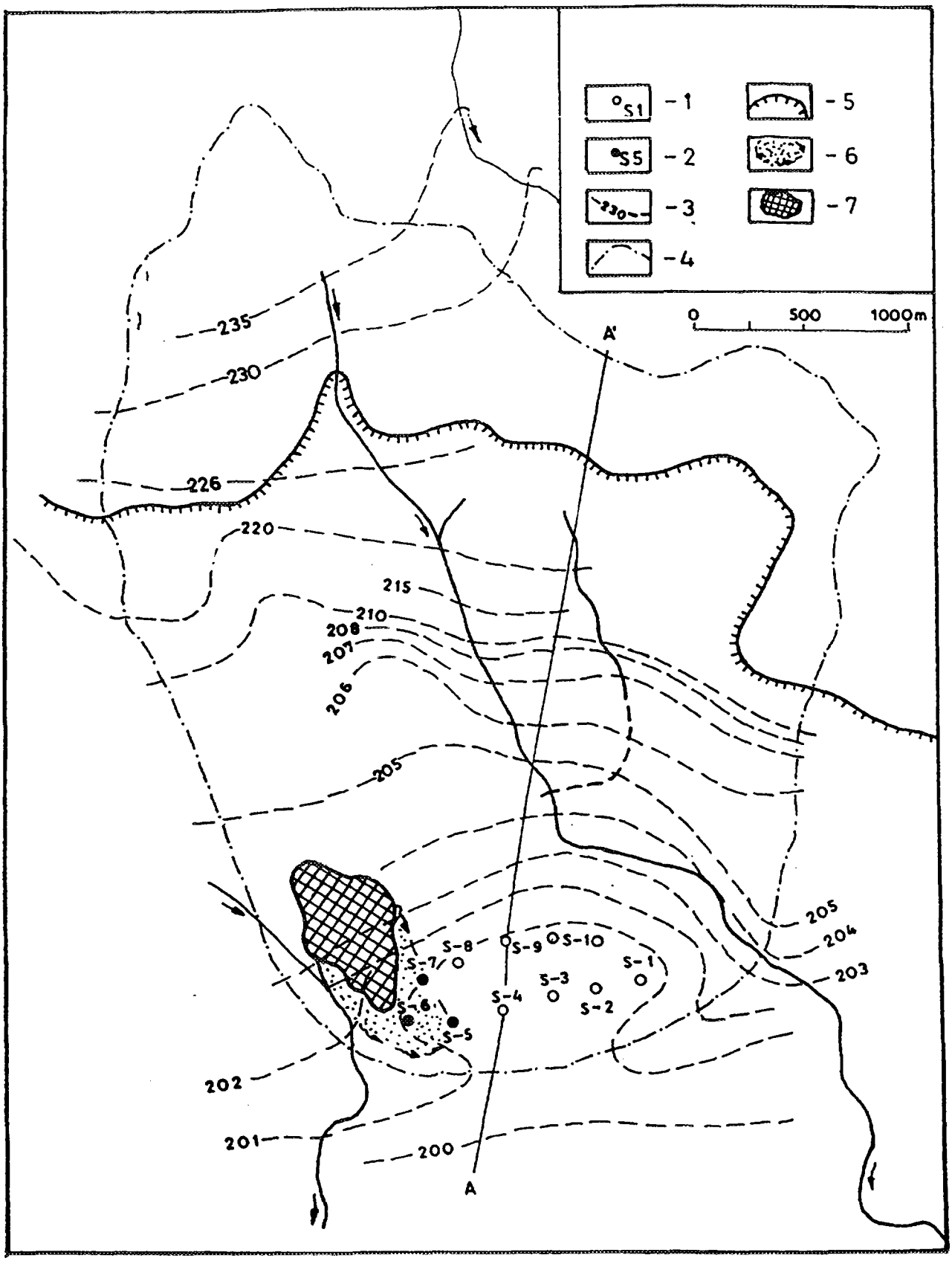

Fig. 9. Map of Ruszcza aquifer [52]. 1 - exploited wells, 2 - contaminated wells pumped as a barrier, 3 - piezometric surface, 4 - boundary of the recharge area defined by the flow lines and by the morphology in the northern part, 5 - boundary of the upper terrace of the Vistula river, 6 - contaminated part of the aquifer, 7 - disposal site.

Table 1. Tritium ages (t_t) and the dispersion parameters (Pe^{-1}) obtained from fitting the dispersion model (DM) to tritium data of Ruszcza wells for several α values [25].

Well	α	t_t [a]	Pe^{-1}
S4	1.00	39.4	0.25
	0.77	38.4	0.25
	0.50	37.2	0.25
	0.40	36.8	0.25
	0.00	25.8	0.15
S1	1.00	30.6	0.15
	0.77	30.0	0.15
	0.50	29.4	0.15
	0.40	27.8	0.13
	0.00	21.3	0.08

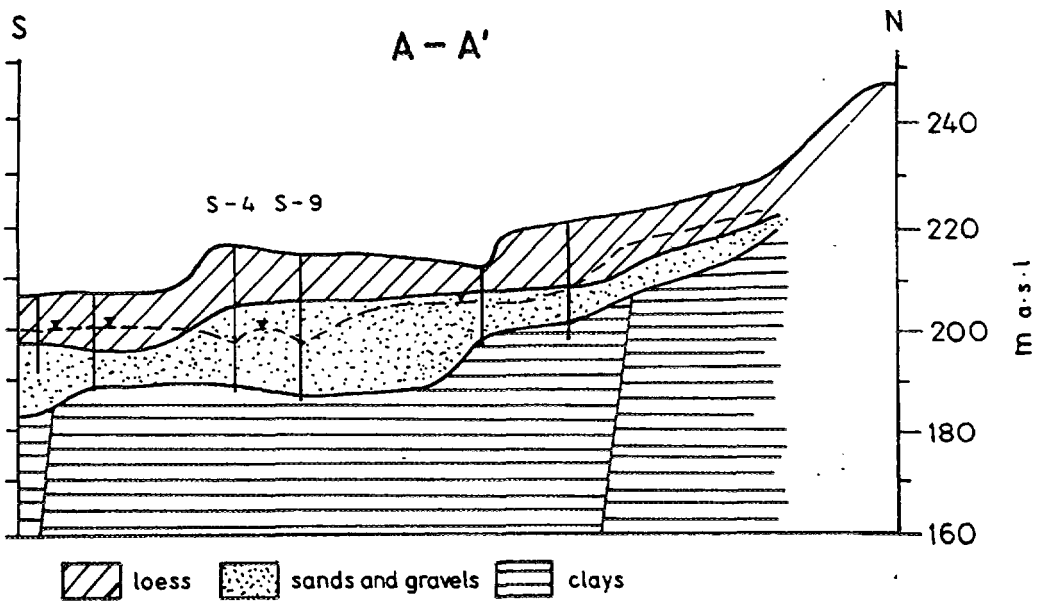

Fig. 10. Geological cross-section of Ruszcza aquifer [52].

found from Eq. 24 [for C_{in} replaced by $\delta^{18}O$ (or δD) of groundwater, and for summer and winter $\delta^{18}O$ (or δD) values calculated from mean monthly deltas and precipitation rates measured in Cracow station]. However, calculations performed for several assumed values of α show that if $\alpha \geq 0.4$, its value does not influence strongly the value of age found from fitting (similar conclusion was reached for the Czatkowice study described further). Though the aquifer is unconfined, a relatively low value of the dispersion parameter qualitatively confirms the inadequacy of EM. On the other hand, due to a large reservoir in the unsaturated zone and its variable thickness, the dispersion model should be adequate.

Taking the mean tritium age of 35 years as equal to the mean water age, the following volume of water (V) in the system is obtained:

$$V = Qt_t = 6000\ m^3/d \times 35\ years \times 365 = 76.7 \times 10^6\ m^3 \quad (25)$$

The mean thickness of water is $H_w = V/S_a = 7.1$ m, where $S_a = 10.8 \times 10^6$ m^2 is the surface of the recharge area defined by the morphology in the northern part and by the flow lines which reach the wells. The mean water thickness in the unsaturated zone (H_{wl}) is in approximation given as the product of the loess layer thickness (12 m) and the mean moisture content by volume (0.32), i.e., about 3.8 m. From that the mean water thickness in the aquifer (H_{wa}) is:

$$H_{wa} = H_w - H_{wl} = 7.1 - 3.8 = 3.3\ m \quad (26)$$

The mean age is also the sum of ages in the unsaturated (t_{tl}) and saturated zones (t_{ta}):

$$t_t = t_{tl} + t_{ta} \quad (27)$$

For the infiltration rate (I) estimated at about 0.20 m/year, the mean transit time through the unsaturated zone is: $t_{tl} = H_{wl}/I = 3.8/0.2 = 19$ years. Therefore, the mean transit time through the saturated zone is from Eq. 27 equal to 35 -19 = 16 years.

It is evident that the mean transit time of sulphates from the disposal site shown in Fig. 9, which was 23 years to the well S6 and 20 years to the well S7, practically resulted from the long transport in the unsaturated zone because the transit time in the saturated zone must be quite short due to a short distance and a large hydraulic gradient.

The mean water velocity (v_w) for a porous aquifer can be estimated as follows:

$$v_w = (l/2)/t_{ta} = 100\ m/year$$

where l/2 is a rough estimate of the mean flow length path (l being the length of the aquifer).

For the mean k value known from pumping tests (6×10^{-4} ms^{-1}), the mean hydraulic gradient of 0.003 and the assumed porosity of 0.35, the water velocity is about 160 m/year, which reasonably agrees with the value estimated from the tracer data. For the total recharge area shown in Fig. 9, i.e., including the loess hills, the available flow rate is: $Q = I \times S_a \cong 6000\ m^3/d$.

It should be mentioned that the model obtained from the tritium data yielded a reasonable agreement also for the ^{14}C data [6, 32] whereas no fit was obtained for the ^3H-He^3 and ^{85}Kr methods [32]. In the case of the ^3H-He^3 method, the observed He^3 concentrations were lower than expected from the prediction obtained with the aid of the tritium model. The escape of He^3 by diffusion from its peak in the unsaturated zone, which is related to the bomb peak of ^3H can be offered as an explanation. On the other hand, ^{85}Kr concentration were about three times higher than predicted values. In that case, a faster diffusion transport of ^{85}Kr from the atmosphere to the aquifer, in comparison with the velocity resulting from the infiltration rate through the unsaturated zone, can be offered as a possible source of the discrepancy. A similar picture was observed for freon-11. Therefore, it was

concluded that the tritium method yielded reasonable results whereas the ^{3}H-He^{3}, ^{85}Kr and freon-11 methods failed. Even if these methods are improved in near future, their accuracy will probably be lower than the present accuracy of the tritium method.

(b) An alpine basin, Wimbachtal Valley, Berchtesgaden Alps, Germany

The Wimbachtal Valley has a catchment area of 33.4 km^2, and its groundwater system consists of three aquifer types with a dominant porous aquifer. The environmental isotope study was performed to provide a better insight into the groundwater storage properties [41]. Due to lack of other possibilities, the system was treated as a single box. The direct runoff is very low and for the period of observations its mean value was estimated to be less than 5 %. However, the presence of direct runoff as well as changes in flow rate and volume contribute to a large scatter of tracer data.

In five river sampling points the tritium output concentrations were measured for 3.5 years and $\delta^{18}O$ values for 3 years. A very favourable situation because the input data were available from a station situated in the valley. The results of fittings for the river sampling points are summarized in Table 2.

Table 2. Mean transit times (t_t, in years) for EM, and for DM with two values of the dispersion parameters (Pe^{-1}), obtained for tritium and $\delta^{18}O$ (in brackets), after [41] with minor corrections.

Sampling point	EM	DM (Pe^{-1} = 0.12)	DM (Pe^{-1} = 0.6)
River, A	4.8	7.0	4.2 (4.1)
B	3.9	6.2	3.8
E	4.1 (4.0)	6.4 (n.o.)	4.0 (4.0)
F	3.9	6.2	3.7 (3.8)
P	4.3 (4.5)	6.5 (n.o.)	4.2 (4.1)

n.o. - a "good fit" was not obtainable.

It is evident from Table 2 that in spite of large number of tritium data no unambiguous calibration of DM was obtained due to a large scatter of tritium contents. Due to a complex hydrogeology of the system, the higher value of the dispersion parameter seems to be more probable, especially as no good fit was obtained for the lower dispersion parameter in the case of oxygen-18 (see Table 2). A good fit obtained for EM also indicates that the dispersion parameter of 0.12 is unacceptable.

For the mean tracer age of 4.15 years, and the mean discharge of 1.75 m^3s^{-1} (in the period 1988-1991), the water volume of 230×10^6 m^3 was obtained. However, the mean water volume estimated from the rock volume and the porosity (with a correction for the unsaturated zone) is 470×10^6 m^3, i.e. about two times more than the volume found from the tracer method. saturated yields the water volume of 600×10^6 m^3. No plausible explanation for this discrepancy was given in the original work. A possible existence of large stagnant zones, i.e., sedimentation pockets or deep layers separated by semipermeable interbeddings from the upper active flow zone, to which the diffusion and advection of tracer are negligible can be offered as an explanation of that discrepancy (see Sect. 9.2).

It should be mentioned that the α coefficient estimated from Eq. 25 was equal to 0.17 (in the original work it was given in approximation as equal to 0.2) whereas a direct estimation from the precipitation and outflow rate data yielded about 1. That discrepancy can be explained by large storage of snow in winter months, which melts in summer months.

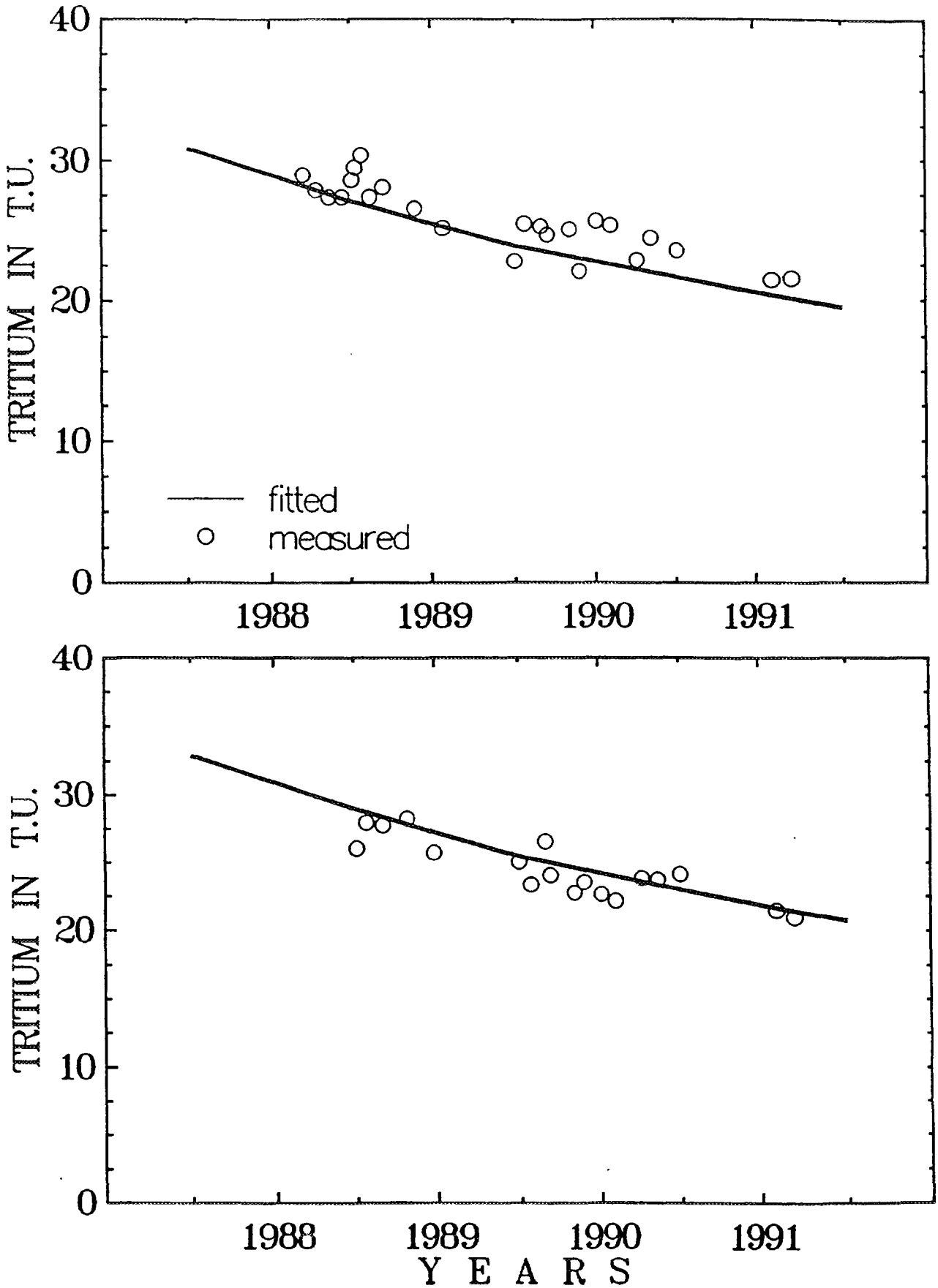

Fig. 11. Upper: Observed and fitted tritium output function for total runoff at Wimbach gauging station (A in Table 2). Lower: Observed and fitted tritium output function for Wimbachquelle (Wimbach spring, F in Table 2).

(c) River bank infiltration, Passau, Germany

In river bank infiltration studies the advantage is taken of the seasonal variations in the stable isotope composition of river water, and of the difference between its mean value and the mean value of groundwater. Measurements of $\delta^{18}O$ were used to determine to fraction of bank infiltrated river water making up the groundwater of a small island (0.3 km^2) in the Danube River near Passau [54]. In Fig. 11 a schematic presentation of flow pattern and its lumped-parameter model is shown. The portion of the river water (p) was calculated from the mean tracer contents applying the following formula:

$$p = \left[\overline{\delta^{18}O}_x - \overline{\delta^{18}O}_{ow}\right] / \left[\delta^{18}O_d - \overline{\delta^{18}O}_{ow}\right] \qquad (28)$$

where subscripts are as follows: x is for the wells on the island, d is for the Danube water, and ow is for the observation well (see Fig. 13).

Due to the seasonal variations of the Danube water, the water exploited in the island has also variable isotopic composition. The following formula was applied adequately to the situation shown in Fig. 13:

$$C(t) = p \int_0^\infty C_{in}(t - t')g(t')dt' + (1 - p)\overline{\delta^{18}O}_{ow} \qquad (29)$$

where $C_{in}(t)$ function was taken as the weighted monthly means of the delta values in Danube water. Due to very short mean transit times (48 to 120 d), it was possible to fit equally well three models, EM, EPM with $\eta = 1.5$ and DM with $Pe^{-1} = 0.12$. Apparent dispersivities (D/v) calculated for particular wells from the dispersion parameter varied between 2.3 m to 25 m as the result of long injection lines along the bank. For the identified input-output relation it was possible to predict response of the wells to hypothetical pollutant concentration in river water (DM was chosen for that purpose). A similar study was presented in [55] whereas in [56] a slightly more complicated case was described, which however was finally simplified to Eq. 29.

10.2. Fractured rocks

(a) Czatkowice springs (Krzeszowice near Cracow, southern Poland)

Czatkowice springs discharge water from a fissured and karstified carbonate formation at a crossing of two fault zones which act as impermeable walls [13]. The Nowe (60 ls^{-1}) and Wrobel (12 ls^{-1}) springs have the same tritium concentration (about 10 T.U.) which is nearly constant in time. The tritium content in the Chuderski spring (18 ls^{-1}) was about 45 T.U. in 1974, and decreased to about 18 T.U. in 1984. Similarly to the case study in Ruszcza, it was shown that when α coefficient is included in the fitting procedure, no unambiguous solution can be obtained. The stable isotopes yielded $\alpha = 0.63 \pm 0.13$ for $\delta^{18}O$ and $\alpha = 0.76 \pm 0.15$ for δD. For more recent fittings shown in Tables 3 and 4, and in Figs 12 and 13, the α coefficient was assumed to be equal to 0.77. Initially, according to [24], it was not possible to obtain good fits for the Nowe and Chuderski springs without assuming the presence of an old water component without tritium. In a recent interpretation, which included additional tritium determinations, it was possible to obtain a good fit for the Nowe spring without an old component (see Table 3) whereas for the Chuderski spring two versions of the old component were considered (see Table 4 and Fig. 13). However, it is evident that in spite of a long tritium record of about 10 years, no unambiguous fitting was possible. The results given for the Nowe and Wrobel springs suggest the EPM to be the

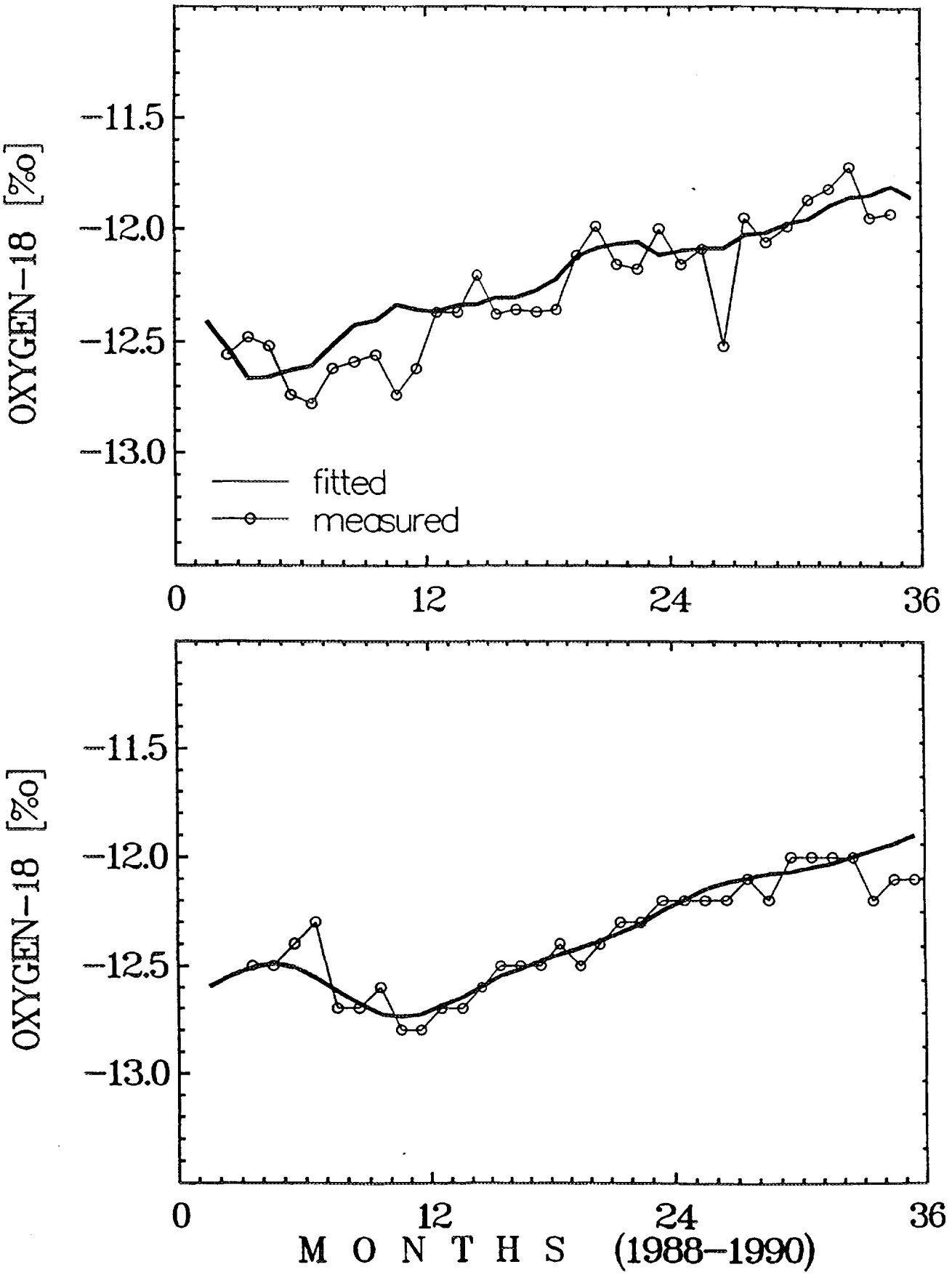

Fig. 12. Upper: Observed and fitted ^{18}O output function for total runoff at Wimbach gauging station (A in Table 2). Lower: Observed and fitted ^{18}O output function for Wimbachquelle (Wimbach spring, F in Table 2).

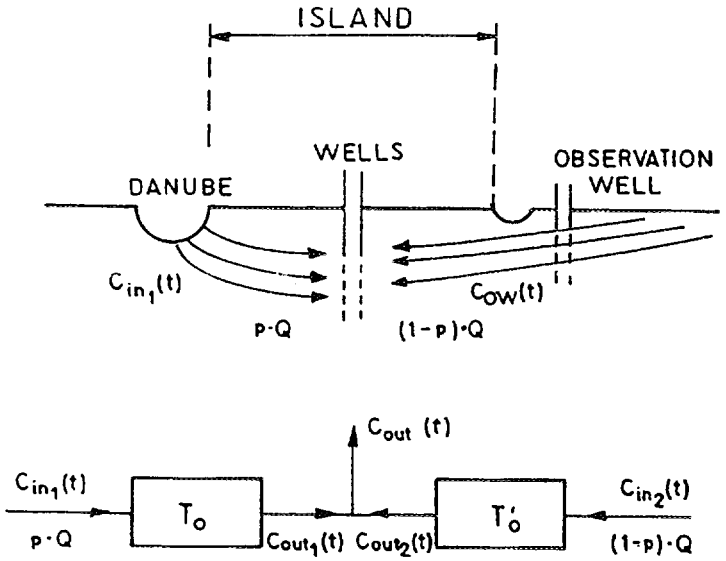

Fig. 13. Conceptual model of river bank filtration in Passau (notation as in the original paper [54]): p - represents the fraction of river water and 1 - p is the fraction of local groundwater. Note that 1 - p is equivalent to β defined in Sect. 4.1 and applied in the FLOW program (Appendix C).

most reliable, because for that model a relatively good fit is obtained for two parameters, whereas in other cases either the number of parameters is larger or the accuracy lower. In other words, it is possible to obtain a reasonable fit without assuming the presence of a tritium free component, but the tritium age is quite high (note that the mean age can be much larger than the time span since the beginning of hydrogen bomb tests, which is the consequence of the wide spectrum of the transit times for given response functions).

Table 3. Models fitted to the Nowe spring tritium data [7].

Number	Model	t_t [a]	Pe^{-1}	η	β	σ [T.U.]
		For 0 T.U. in old component				
1	DM	130	1.0	-	0.70	0.546
2	DM	70	0.5	-	0.78	0.510
3	DM	95	0.5	-	0.58	0.475
		Without old component				
4	DM	190	0.8	-	-	0.622
5	DM	135	0.5	-	-	0.736
6	EM	400	-	(1.00)	-	0.906
7	EPM	300	-	1.04	-	0.522

For the Chuderski spring also a number of models can be fitted, especially as two flow components seem to exist. In the early interpretation, similarly to the Nowe and Wrobel springs, it was assumed that the older component is tritium free [24]. That assumption is represented by models 1, 2, and 3 in Table 4 and Fig. 13. However, if EPM (No 7 in Table 2, i.e., a

model without an old component) is chosen for the Nowe and Wrobel springs, which are situated just at lower elevation than, and close to the Chuderski spring, it is more reasonable to assume that the old component in that spring is exactly the same as water discharged from the other two springs. In such a case, in a good approximation, the tritium content of 10.7 T.U. in the old component can be taken as the mean value for the period of observations. Then, the models No 5-8 in Table 4 and Fig. 13 are obtained. Model No 8 can be selected as that with the lowest number of fitting parameters and the best fit. In conclusion 15 % of water in the Chuderski spring is young and recharged at a local hill, whereas 85 % and 100 % of the Nowe and Wrobel springs come from a larger distance. The whole aquifer is unconfined, but paleo-channels close to the Nowe and Wrobel springs act as a piston flow model of a low volume (about 4 % of the total volume because η = 1.04).

Table 4. Models fitted to the Chuderski spring tritium data [7].

Number	Model	t_t [a]	Pe^{-1}	β	σ [T.U.]
		For 0 T.U. in old component			
1	DM	15	0.25	0.82	0.815
2	DM	20	0.25	0.78	0.766
3	DM	30	1.0	0.73	0.922
		For 10.7 T.U. in old component			
5	DM	12	0.8	0.85	0.837
6	DM	3	0.9	0.75	1.059
7	EM	2.5	-	0.75	1.067
8	EM	11	-	0.85	0.757

Details of the hydrogeological interpretation can be found in [13]. Here, only the most important findings are given. For the mean matrix porosity of 0.030 ± 0.005 (known from laboratory measurements on core samples), the mean distance between the centre of the recharge area and springs of 8000 ± 2000 m, and the mean hydraulic gradient of 0.006 ± 0.001 (both known from the hydrogeological map), Eq. 33 yields $k = (4.2 \pm 1.5)\times10^{-6}$ ms^{-1}, which agrees well with other estimates. Similarly, the local hydraulic conductivity found from the age of the young component in the Chuderski spring agrees reasonable with other estimates.

The fissure porosity of 0.0015 is known from direct observation in a nearby quarry. If the tritium age is wrongly identified with the water age in a simplified form of Darcy's law, it yields $k = n_f x/[t_t(\Delta H/\Delta x) = 0.2\times10^{-6}$ ms^{-1}, which is about 20 times too low.

It should be mentioned that for the Nowe and Chuderski spring, preliminary ^{85}Kr and ^{3}He measurements did not agree with the expected values found for the models fitted to the tritium data [32]. No reinterpretation has been performed so far for the new approach to the tritium data, which is presented here after [7].

(b) Thermal systems in Cieplice and Ladek Spas, Sudetes, Poland

The main granitic thermal system in Cieplice Spa contains water which according to stable isotope composition, ^{14}C content and noble gas data can be dated to the end of the last glacial period [57]. The ^{14}C age was estimated by the piston flow approach for a steady tracer input, whereas the shift in the stable isotope content caused by climatic change can be consid-

ered as a transient state tracer input. Water volume was found from Eq. 34, and for known matrix porosity (about 0.02), the rock volume was given by Eq. 35. That rock volume was shown to reasonably agree with the estimate based on the morphology of the basin and the depth of aquifer, whereas any estimate for a neglected matrix porosity would lead to an unacceptably high rock volume. The simplified form of Eq. 33 yielded a reasonable value of the hydraulic conductivity, which also confirmed the importance of matrix porosity as a transport parameter.

The thermal water in Ladek Spa, which discharges from gneisses of low matrix porosity (about 0.008) was shown to have the PFM-^{14}C age of several thousand years [58]. In spite of low matrix porosity, also in that system Eqs 33-35 were shown to be applicable and yield reasonable results whereas any identification of tracer ages with the mobile water in fissures would yield unacceptable results.

(c) Cheju Island, South Korea

First isotopic investigations performed on Cheju Island were described in [59] where a binomial model was used to interpret the tritium data. The same data were later interpreted with the aid of EM and EPM which yielded much better fits than those obtained in the original paper [3, 6]. For a large coastal spring (site 2), EM yielded age of 19 years whereas EPM gave 21 years with η = 1.1. However, the stable isotope composition showed that the spring has its recharge area at high altitude, at the central part of the island, excluding the possibility of a significant recharge at the large coastal plain. Therefore, EM can be rejected, and η = 1.1 means that the main water body with an exponential flow pattern is probably in the mountains whereas from there water is led to the coast by a small volume system (a lava tunnel?). This example shows how stable isotope data can be used in a qualitative way to identify a more adequate model. Unfortunately, no data are available on the relation between mobile and immobile water volumes. However, the tritium ages are most probably related to a high degree to the stagnant water in a microporous lava.

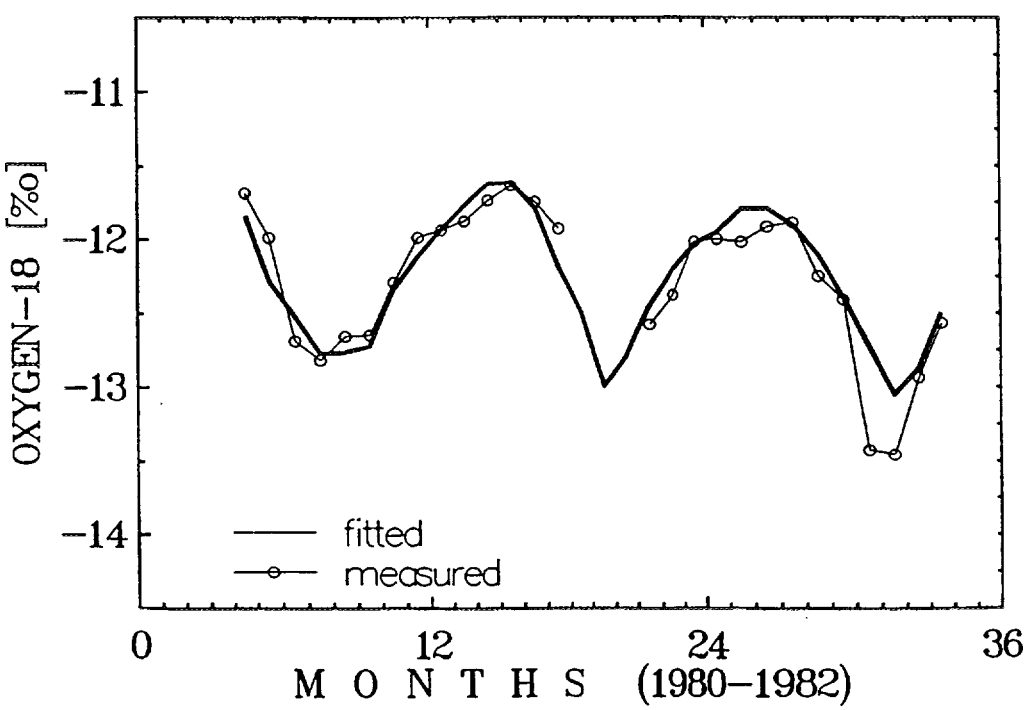

Fig. 14. Observed and fitted ^{18}O output function in PSI well in Passau for DM with t_t = 60 days, D/vx = 0.12, 1 - p = β = 0.80, C_β = -10.4 ‰ [54].

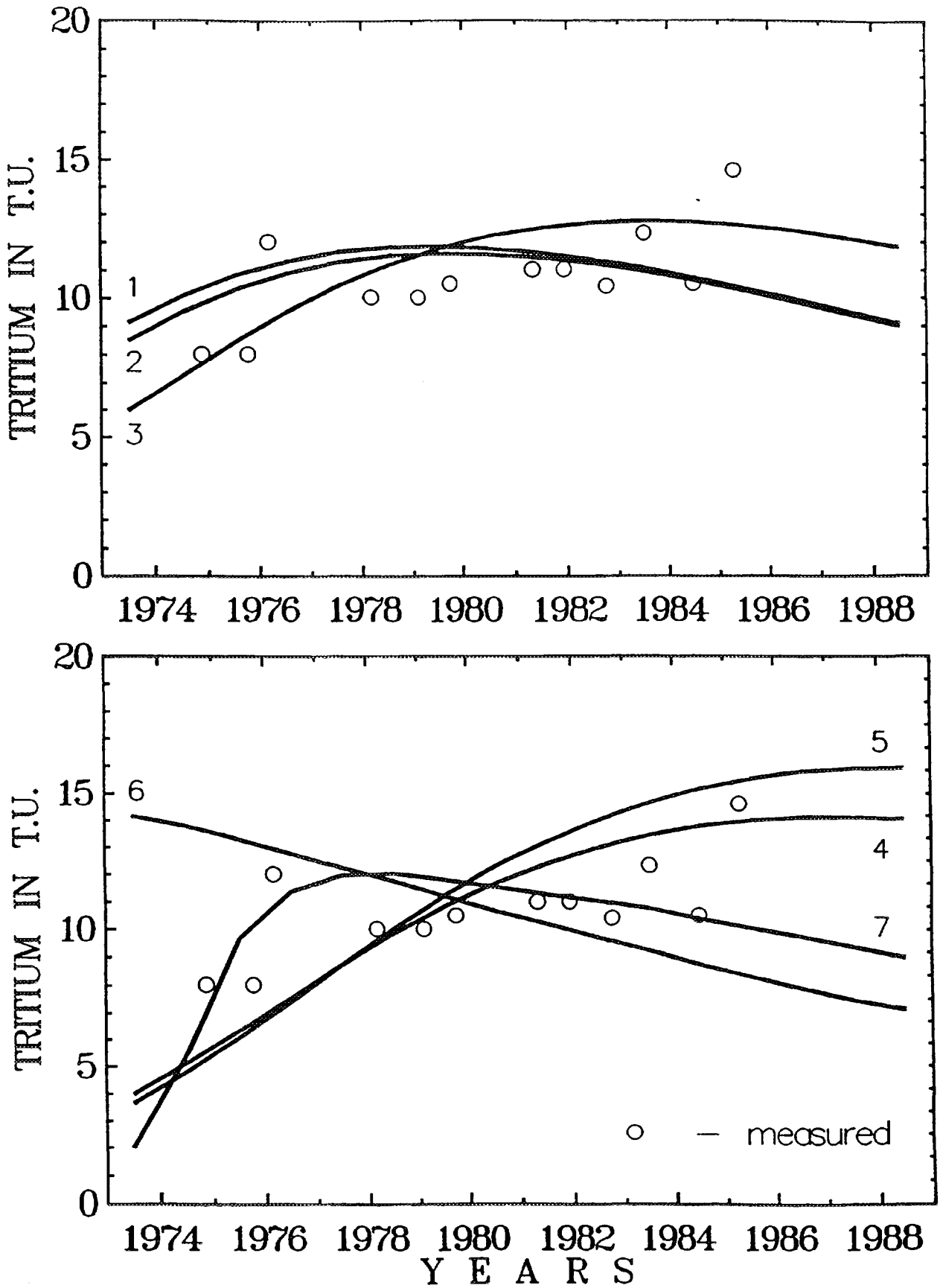

Fig. 15. Different models fitted to the tritium data of the Nowe spring (curve numbers correspond to model numbers in Tab. 3) [7].

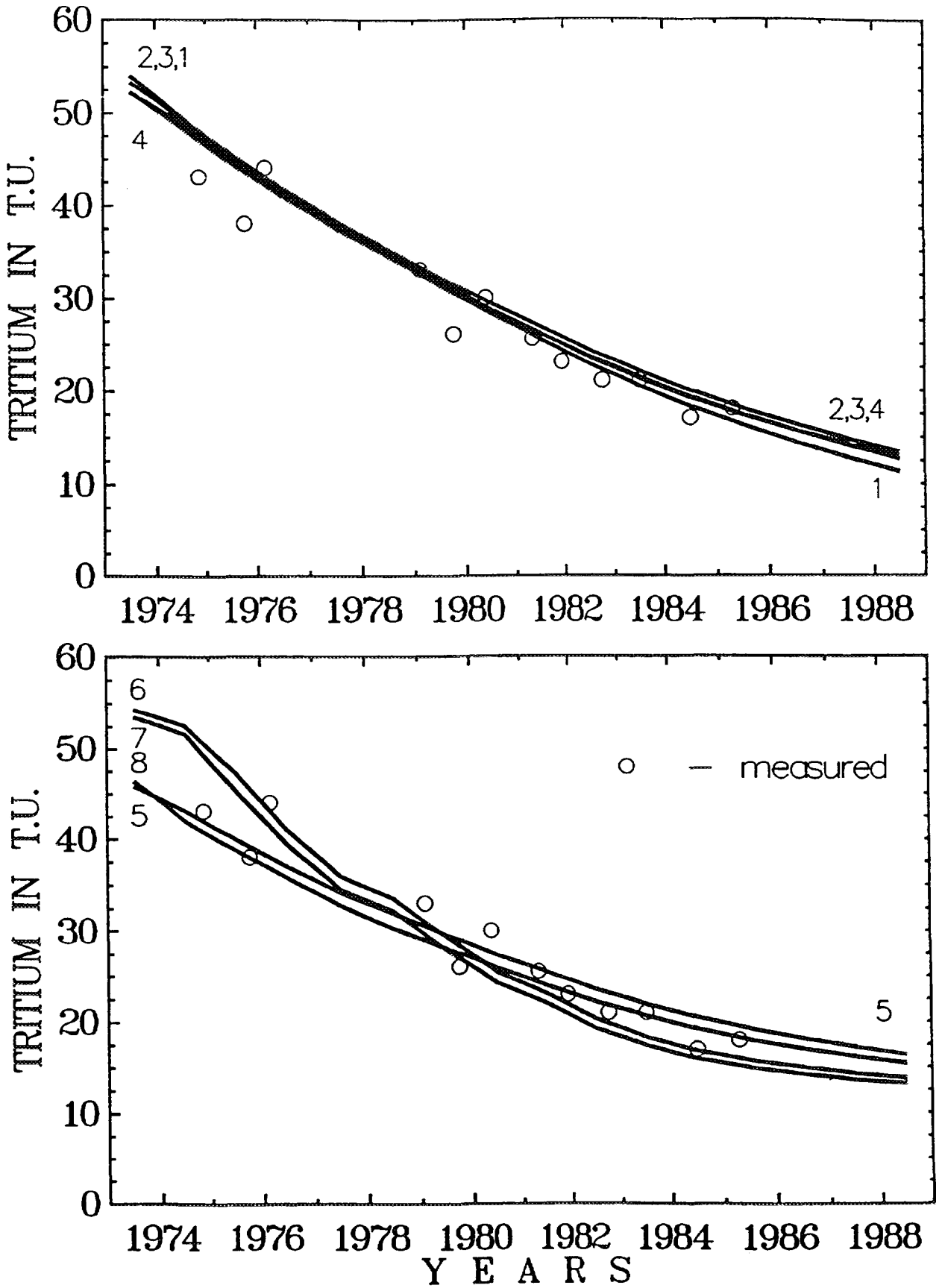

Fig. 16. Different models fitted to the tritium data of the Chuderski spring (curve numbers correspond to model numbers in Tab. 4) [7].

10.3. Complex cases

(a) An alpine basin, Lainbach valley, Germany

A complex interpretation was described for an alpine basin with a catchment area of 18.7 km^2 [60]. Three conceptual models shown in Fig. 14 were considered. First, the direct runoff was eliminated. Another trick to solve a complex problem was to use seasonal variations in deuterium content to find the transit time through the upper reservoir (the tracer is stable, and, therefore, its flow through a large deeper reservoir does not influence the shift of seasonal variations in response). Tritium samples were taken only for base flow and served to calculate the mean transit time both for model 2 and for model 3 (see Fig. 14). For details of the study, the reader is referred to the original paper.

(b) A small basin in Harz Mountains

A detailed study of a small basin (0.76 km^2), Lange Bramke, Harz Mts., Lower Saxonia, was first given in [61] and extented in [60]. The interpretation of tritium data for a single reservoir both for steady flow approximation and variable flow approach was given in [46] as mentioned in Sect. 8.

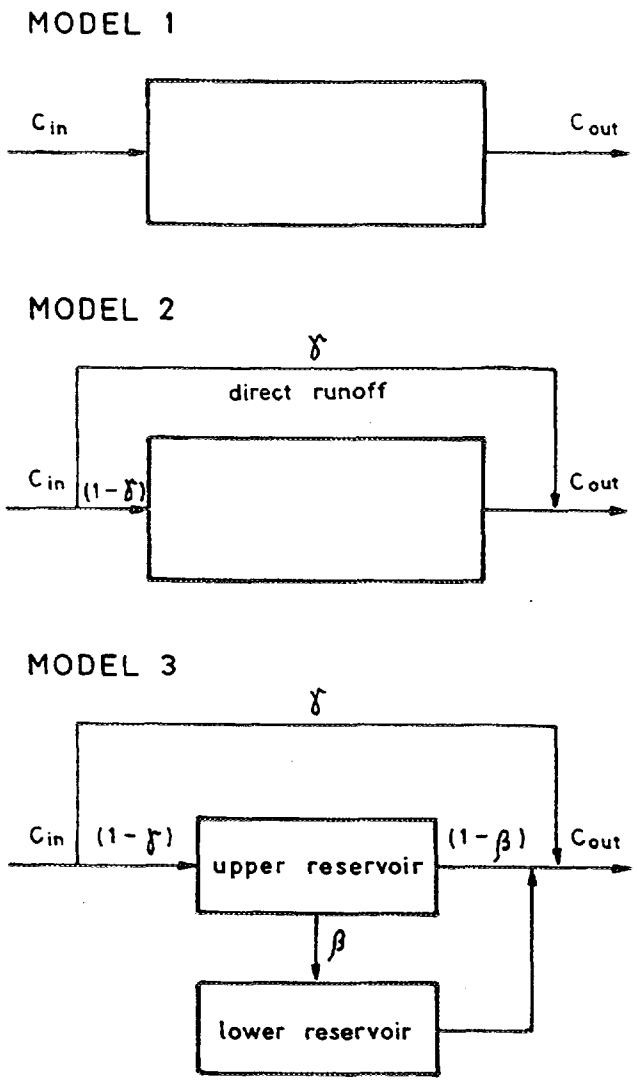

Fig. 17. Three scenarios of the Lainbach valley conceptual model [60].

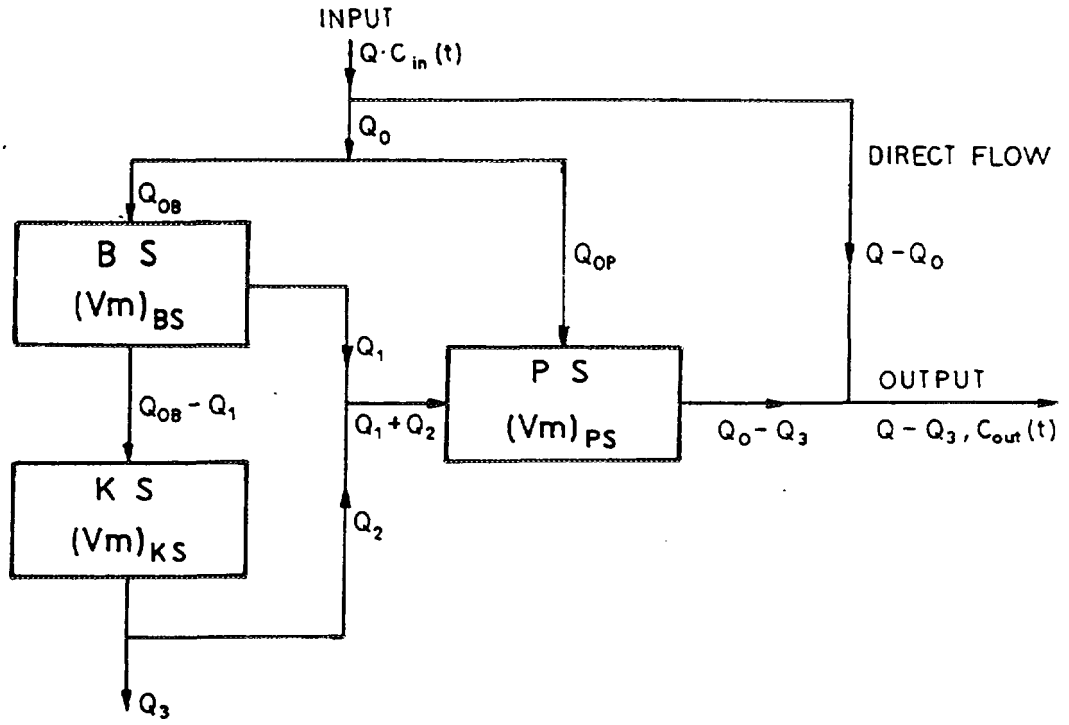

Fig. 18. Lange Bramke conceptual model [61, 62].

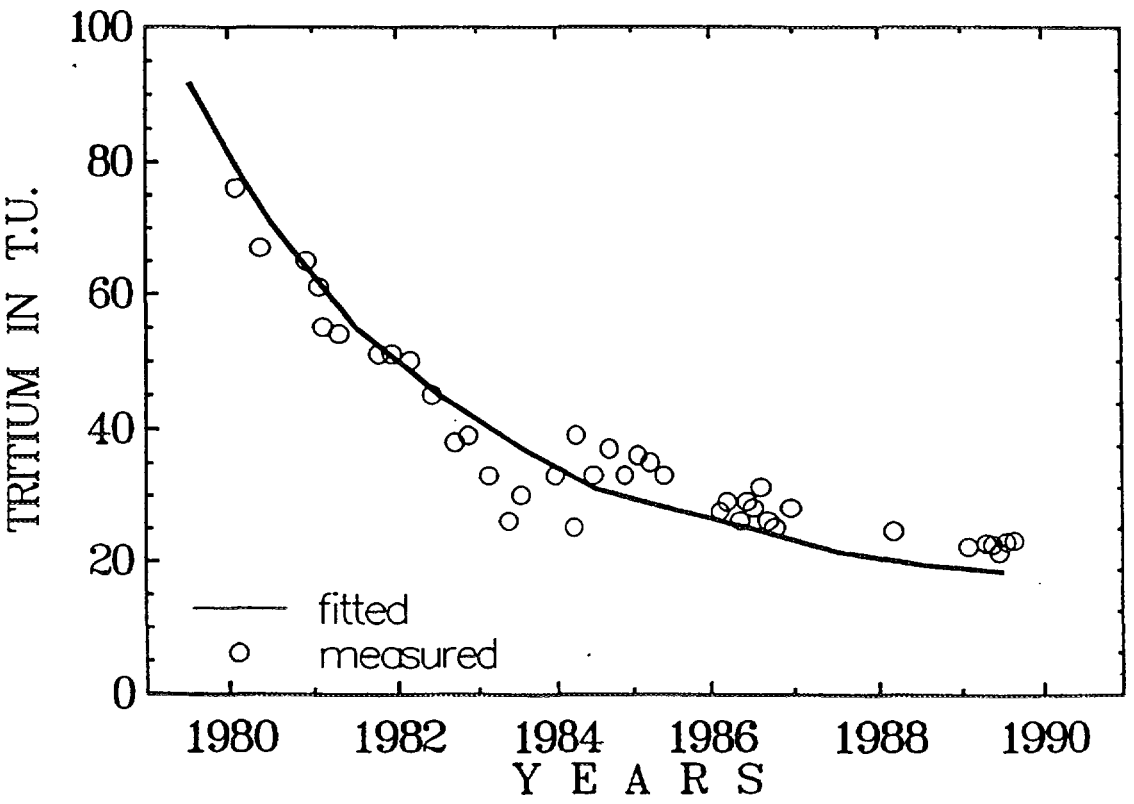

Fig. 19. Observed and fitted tritium output functions for the stream draining the Lange Bramke basin [61, 62].

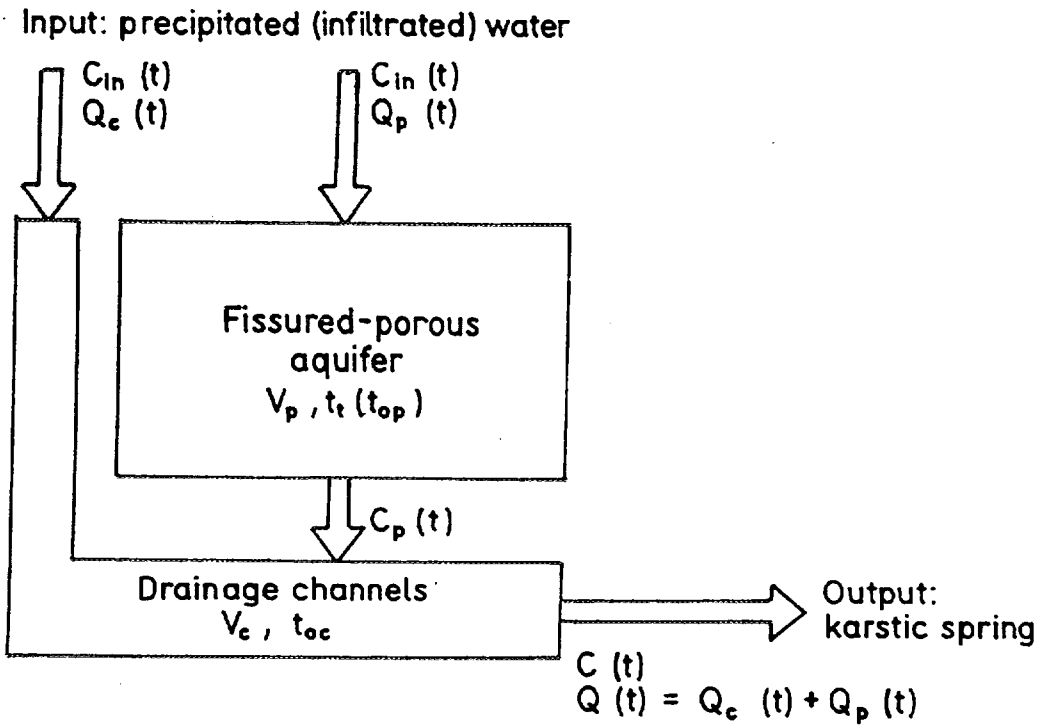

Fig. 20. Schneealpe massif conceptual model (notation as in the original paper [64]).

In Fig. 15 a more complex conceptual model is shown [62]. The BS box represents unsaturated zone associated with different soil materials which cover KS. The KS box represents fissured rock whereas the PS is for the porous reservoir located in the valley bottom. Tritium was measured at the outflow from the basin for low flow (in $Q_o - Q_3$ in Fig. 15). Oxygen-18 was measured in precipitation (Q), direct flow ($Q - Q_o$) and in total surface outflow ($Q - Q_3$). The flux through the BS reservoir was measured by sampling for ^{18}O at different depths whereas the flow in the PS was sampled for the same tracer with the aid of piezometers screened at required depths. However, in spite of considerable expenses, it was not possible to identify fully the whole system due to the lack of information on some flow components and on the fissured part (KS).

10.4. Complex cases in karstic rocks

(a) General comments

Tracer data from karstic rocks, in which large channels collect water only at final stages, can often be interpreted similarly to fissured rocks, i.e. as if the movement were taking place in the total open porosity. This was shown for the Czatkowice springs discussed above. A similar conclusion was reached for a pollutant movement in a karstic-fissured-porous formation in which large karstic forms are developed in vertical direction, and are discontinuous in the direction of flow [63]. However, in karstic rocks, continuous channels extending from sinkholes in the recharge area to springs are often observed, and then the interpretation is difficult. An example of the interpretation of such a system by combination of two tracers is given below.

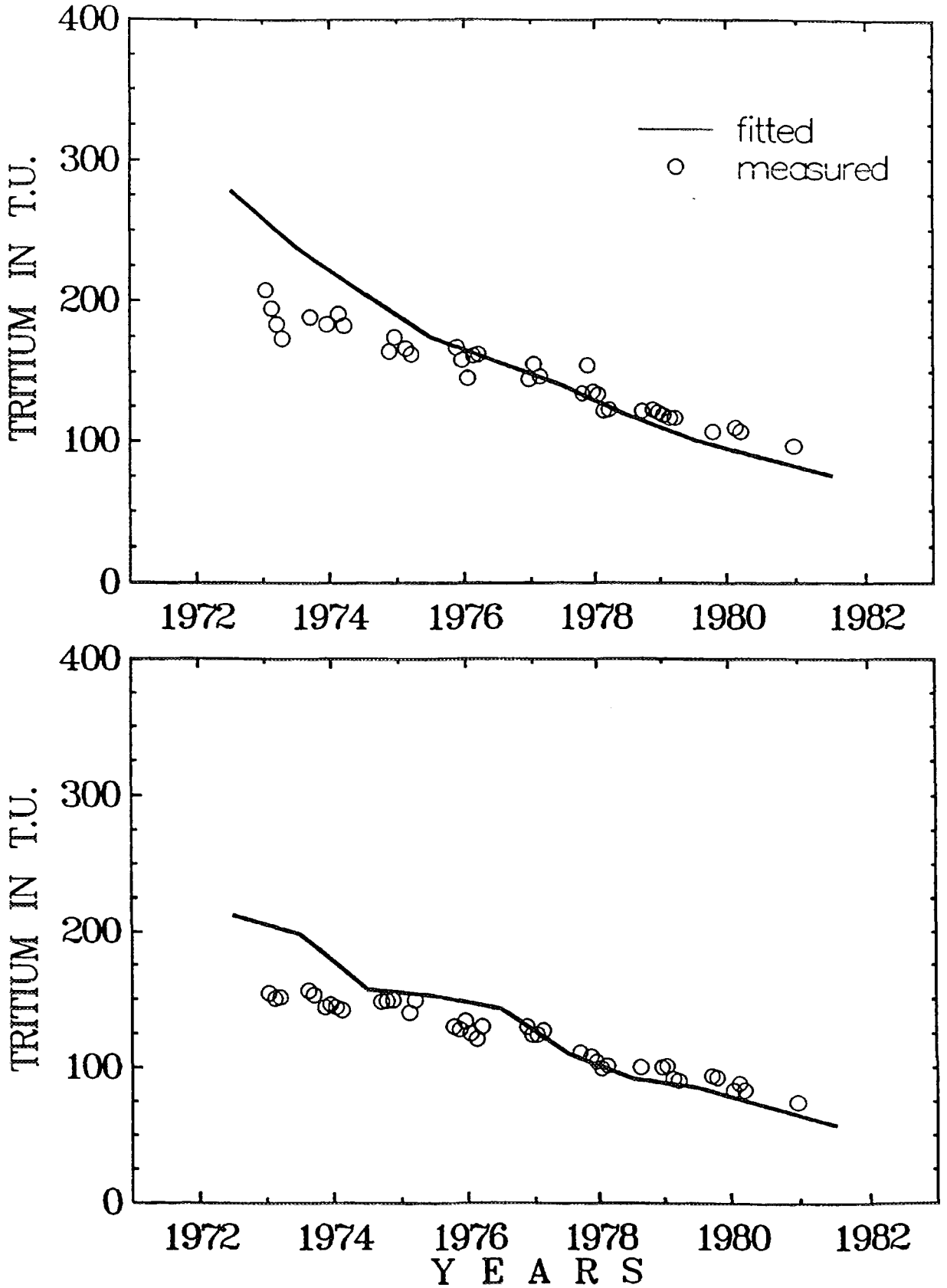

Fig. 21. Schneealpe massif tritium output functions Wasseralquelle (upper) and Siebenquelle (lower) observed for base flow. Dispersion models (DM) with D/vx = 0.5 and t_t of 4.5 and 2.5 years, respectively [64].

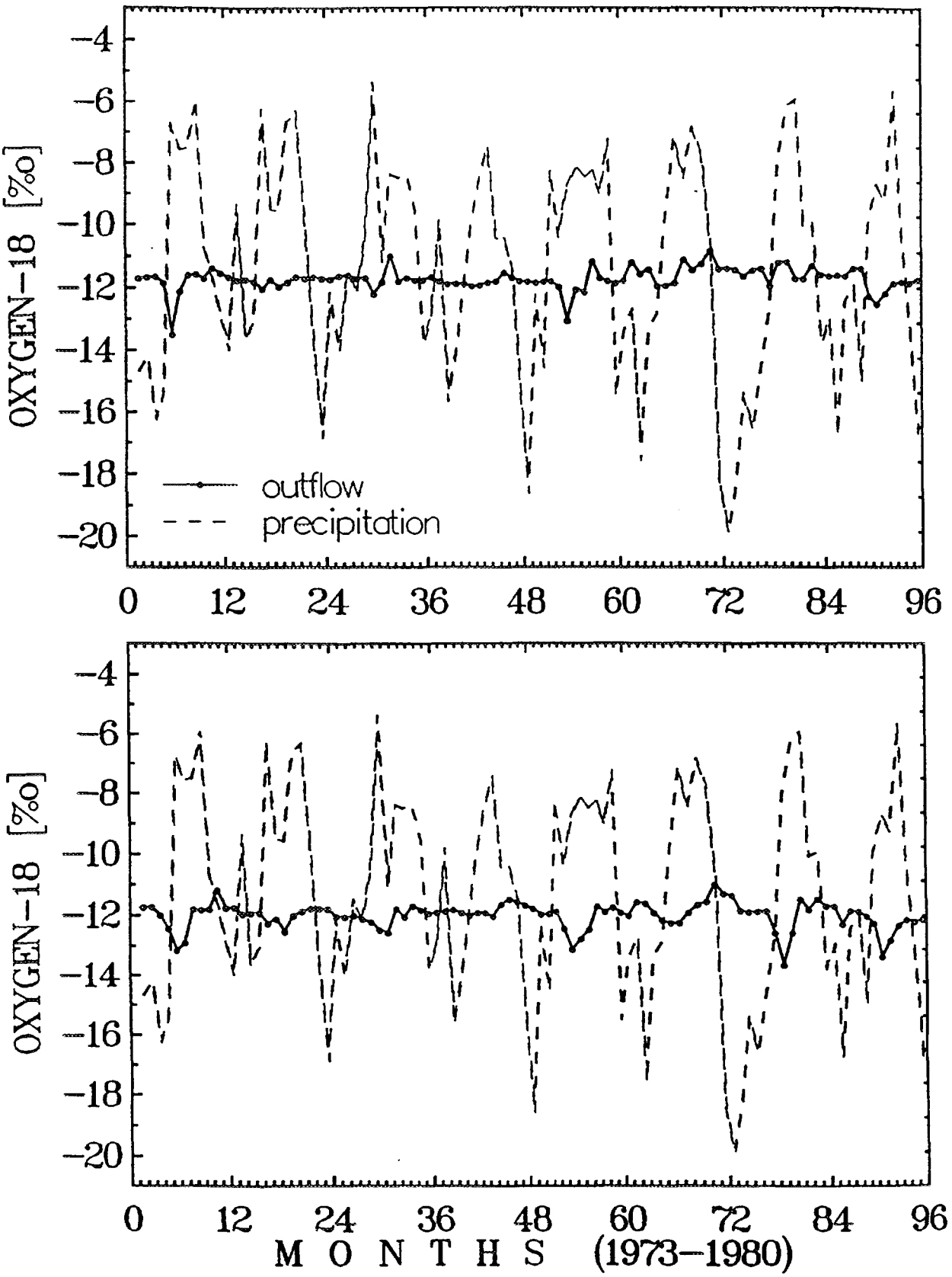

Fig. 22. Schneealpe massif ^{18}O output functions Wasseralquelle (upper) and Siebenquelle (lower) observed for high flows. Piston flow model (PFM) with t_t = 2 months for both springs (only positions of maximal and minimal concentrations were fitted [64]).

(b) An alpine karst massif, Schneealpe, Austria

Changes in tritium and ^{18}O contents were measured in water outflows from a karstic massif of 90 km^2 [64]. The conceptual model for tracer flow is given in Fig. 16. It was assumed that for base flow there is no flow in drainage channels. Then, tritium sampled in springs represented flow through the fissured porous aquifer. On the other hand, during high flow rates, the seasonal variations in ^{18}O were assumed to represent the fast flow through channels. By fitting DM to the tritium data and PFM to the ^{18}O data it was possible to find mean transit times for both sub-systems. Next, knowing the mean discharges for both flow components it was possible to estimate the water volumes of both subsystems.

Another complex karstic system which was identified by combination of artificial and environmental tracer methods was described in [65].

REFERENCES

[1] Eriksson, E., The possible use of tritium for estimating groundwater storage, Tellus **10** (1958) 472-478.

[2] DAVIS, G.H., DINCER, T., FLORKOWSKI, T., PAYNE, B.R., GATTINGER, T., "Seasonal variations in the tritium content of groundwaters of the Vienna basin", Isotopes in Hydrology, IAEA, Vienna (1967) 451-473.

[3] MAŁOSZEWSKI, P., ZUBER, A., Determinig the turnover time of groundwater systems with the aid of environmental tracers, I. Models and their applicability, J. Hydrol. **57** (1982) 207-231.

[4] PLUMMER, L.N., MICHEL, R.L., THURMAN, E.M., GLYNN, P.D., "Environmental tracers for age dating young ground water", Regional Ground-Water Quality (ALLEY, W.M., Ed.), Van Nostrand Reinhold, New York (1993) 255-294.

[5] Nuclear Energy Agency (NEA), The International Hydrocoin Project, Level 2: Model Validation, Paris (1990).

[6] ZUBER, A., "Mathematical models for the interpretation of environmental radioisotopes in groundwater systems", Handbook of Environmental Isotope Geochemistry, Vol. 2, Part B (FRITZ, P., FONTES, J.Ch., Eds.), Elsevier, Amsterdam (1986) 1-59.

[7] MAŁOSZEWSKI, P., ZUBER, A., On the calibration and validation of mathematical models for the interpretation of tracer experiments in groundwater, Adv. Water Resour. **15** (1992) 47-62.

[8] MAŁOSZEWSKI, P., ZUBER, A., Principles and practice of calibration and validation of mathematical models for the interpretation of environmental tracer data in aquifers, Adv. Water Resour. **16** (1993) 173-190.

[9] ZUBER, A., "On calibration and validation of mathematical models for the interpretation of environmental tracer data in aquifers" IAEA-TECDOC, IAEA, Vienna (in press).

[10] KONIKOV, L.F., BREDEHOEFT, J.D., Ground-water models cannot be validated, Adv. Water Resour. **15** 1 (1992) 75-83.

[11] ORESKES, N., SHRADER-FRECHETTE, K., BELITZ, K., Verification, validation, and confirmation of numerical models in the earth sciences, Science **263** (1994) 641-646.

[12] MAŁOSZEWSKI, P., ZUBER, A., Tracer experiments in fractured rocks: Matrix diffusion and the validity of models, Water Resour. Res., **29** 8 (1993) 2723-2735.

[13] ZUBER, A., MOTYKA, J., Matrix porosity as the most important parameter of fissured rocks for solute transport at large scales, J. Hydrol. **158** (1994) 19-46.

[14] SNYDER, W.M., STALL, J.B., Men models, methods and machines in hydrologic analysis, J. Hydraul. Div., ASCE, **91** (1965) 85-99.

[15] LEVENSPIEL, O., TURNER, J.C.R., The interpretation of residence time experiments. Chem. Eng. Sci. **25** (1970) 1605-1609.

[16] GARDNER, R.P., FELDER, R.M., DUNN, T.S., Tracer concentration responses and moments for measurements of laminar flow in circular tubes, Int. J. Appl. Radiat. Isot. **24** (1973) 253-270.
[17] BRIGHAM, W.E., Mixing equations in short laboratory cores, Soc. Pet. Eng. J. **14** (1974) 91-99.
[18] KREFT, A., ZUBER, A, On the physical meaning of the dispersion equation and its solutions for different initial and boundary conditions, Chem. Eng. Sci. **33** (1978) 1471-1480.
[19] ZUBER, A., "Review of existing mathematical models for interpretation of tracer data in hydrology", Mathematical Models for Interpretation of Tracer Data in Groundwater Hydrology, IAEA-TECDOC-381, IAEA, Vienna (1985) 69-116.
[20] LENDA, A., ZUBER, A., "Tracer dispersion in groundwater experiments", Isotope Hydrology 1970, IAEA, Vienna, 619-641.
[21] ANDERSEN, L.J., SEVEL, T., "Six years' environmental tritium profiles in the unsaturated and saturated zones", Isotope Techniques in Groundwater Hydrology 1974, Vol. I, IAEA, Vienna (1974) 3-20.
[22] PRZEWŁOCKI, K., Hydrologic interpretation of the environmental isotope data in the Eastern Styrian Basin, Steir. Beitr. Hydrol. **27** (1975) 85-133.
[23] IAEA, Tech. Rep. Ser., 96, 117, 129, 147, 129, 147, 165, 192, 206, 226, 264, 311, 331 (yearly means up to 1987 are given) IAEA, Vienna (newer data are available on diskettes only).
[24] GRABCZAK, J., MAŁOSZEWSKI, P., RÓŻAŃSKI, K., ZUBER, A., Estimation of the tritium input function with the aid of stable isotopes, Catena **11** (1984) 105-114.
[25] TOLSTIKHIN, I.N., KAMENSKY, I.L., Determination of groundwater ages by the T-^{3}He method, Geochemistry International **6** (1969) 810-811.
[26] TORGERSEN, T., CLARKE, W.B., JENKINS, W.J., "The tritium/helium-3 method in hydrology", Isotope Hydrology 1978, IAEA, Vienna, 917-930.
[27] SCHLOSSER, P., STUTE. M., DORR, H., SONNTAG, C., MUNNICH, K.O., Tritium/^{3}He dating of shallow groundwater, Earth and Planetary Science Letters **89** (1988) 353-362.
[28] SCHLOSSER, P., STUTE. M., SONNTAG, C., MUNNICH, K.O., Tritiugenic ^{3}He in shallow groundwater, Earth and Planetary Science Letters **94** (1989) 245-256.
[29] SOLOMON, D.K., SUDICKY, E.A., Tritium amd helium-3 isotope ratios for direct estimation of spatial variations in groundwater recharge. Water Resour. Res. **27** 9 (1991) 2309-2319.
[30] SOLOMON, D.K., POREDA, R.J., SCHIFF, S.L., CHERRY, J.A., Tritium and helium-3 as groundwater age tracers in the Borden aquifer, Water Resour. Res. **28** 3 741-755.
[31] MAŁOSZEWSKI, P., ZUBER, A., The theoretical possibilities of the ^{3}H-^{3}He method in investigations of groundwater systems, Catena **10** (1983) 189-198.
[32] GRABCZAK, J., ZUBER, A., MAŁOSZEWSKI, P., RÓŻAŃSKI, K, WEISS, W., ŚLIWKA, I., New mathematical models for the interpretation of environmental tracers in groundwaters and the combined use of tritium, C-14, Kr-85, He-3 and freon-11 methods, Beitr. Geol. Schweiz - Hydrologie, **28** (1982) 395-405.
[33] RÓŻAŃSKI, K., Krypton-85 in the atmosphere 1950-1977: a data review. Environ. Int. **2** (1979) 139-143.
[34] RÓŻAŃSKI, K., FLORKOWSKI, T., "Radioactive noble gases in the terrestrial environment" Handbook of Environmental Isotope Geochemistry, Vol. 2, Part B (FRITZ, P., FONTES, J.Ch., Eds.), Elsevier, Amsterdam (1986) 481-506.
[35] WEISS, W., SARTORIUS, H., STOCKBURGER, H., "Global distribution of atmospheric Kr-85: A database for the verification of transport and mixing models", Isotopes of Noble Gases as Tracers in Environmental Studies, IAEA (1992) 29-63.

[36] RÓŻAŃSKI, K., FLORKOWSKI, T., "Krypton-85 dating of groundwater", Isotope Hydrology 1978, Vol. II, IAEA, Vienna (1979) 949-961.
[37] SMETHIE, W.M., Jr., SOLOMON, D.K., SCHIFF, S.L., MATHIEU, G.G., Tracing groundwater flow in the Bordon aquifer using krypton-85, J. Hydrol. **130** (1992) 279-297.
[38] FONTES, J.Ch., GARNIER, J.M., Determination of the initial ^{14}C activity of the total dissolved carbon: a reviev of the existing models and a new approach, Water Resour. Res. **15** (1979) 369-413.
[39] FONTES, J.Ch., "Chemical and isotopic constraints on ^{14}C dating of groundwater", Radiocarbon After Four Decades (TAYLOR, R.A., LONG A., KRA, R.S., Eds.) Springer-Verlag, New York (1992) 242-261.
[40] BERGMAN, H., SACKL, B., MAŁOSZEWSKI, P., STICHLER, W., "Hydrological investigations in a small catchment area using isotope data series", 5th International Symposium on Underground Water Tracing, Institute of Geology and Mineral Exploration (IGME), Athens, 1986.
[41] MAŁOSZEWSKI, P., RAURET, W., TRIMBORN, P., HERRMANN, A., RAU, R., Isotope hydrological study of mean transit times in an alpine basin. J. Hydrol. **140** (1992) 343-360.
[42] BUSENBERG, E., PLUMMER, L.N., Use of chlorofluorocarbons (CCl_3F and CCl_2F_2) as hydrologic tracers and age-dating tools: The alluvium and terrace system of central Oklahoma, Water Resour. Res. **28** 9 (1992) 2257-2283.
[43] REILLY, T.E., PLUMMER L.N., PHILLIPS, P.J., BUSENBERG, E., The use of simulation and multiple environmental tracers to quantify groundwater flow in a shallow aquifer. Water Resour. Res. **30** 2 (1994) 421-433.
[44] MAISS, M., LEVIN, I., global increase of SF_6 observed in the atmosphere, Geophys. Res. Lett. **21** 7 (1994) 569-572.
[45] ZUBER, A., On the interpretation of tracer data in variable flow systems, J. Hydrol. **86** (1986) 45-57.
[46] ZUBER, A., MAŁOSZEWSKI, P., STICHLER, W., HERRMANN, A., "Tracer relations in varaiable flow" 5th International Symposium on Underground Water Tracing, IGME (Institute of Geology and Mineral Exploration), Athens (1986) 355-360.
[47] MAŁOSZEWSKI, P., (in preparation).
[48] NERETNIEKS, I.,Age dating of groundwater in fissured rocks: influence of water volume in micropores. Water Resour. Res. **17** (1981) 421-422.
[49] MAŁOSZEWSKI, P., ZUBER, A., On the theory of tracer experiments in fissured rocks with a porous matrix, J.Hydrol. **79** (1985) 333-358.
[50] MAŁOSZEWSKI, P., ZUBER, A., Influence of matrix diffusion and exchange reactions on radiocarbon ages in fissured carbonate aquifers, Water Resour. Res. **27** (1991) 1937-1945.
[51] MAŁOSZEWSKI, P., Mathematical Modelling of Tracer Experiments in Fissured Aquifers, Freiburger Schriften zur Hydrologie, Band 2, Universität Freiburg, Freiburg (1994).
[52] ZUBER, A., KLECZKOWSKI, A.S., MYSZKA, J., WITCZAK, S., "Pumping rate and mineralization of water from an intake at the high terrace of Vistula, east of Cracow, as explained by isotopic investigations" (in Polish), Aktualne problemy hydrogeologii, AGH, Kraków (1985) 186-195.
[53] MAŁOSZEWSKI, P., RAUERT, W., TRIMBORN, P., HERRMANN, A., RAU, R., Isotope hydrological study of mean transit times in an alpine basin (Wimbachtal, Germany), J. Hydrol. **140** (1992) 343-360.
[54] STICHLER, W., MAŁOSZEWSKI, P., MOSER, H., Modelling of river water infiltration using oxygen-18 data, J. Hydrol. **83** (1986) 355-365.
[55] HÖTZL, H., REICHERT, B., MAŁOSZEWSKI, P., MOSER, H., STICHLER, W., "Contaminant transport in bank filtration - Determining hydraulic parameters by means of artificial and natural labeling", Contaminant Transport in Groundwater (KOBUS, H.E., KINZELBACH, W, Eds), A.A. Balkema, Rotterdam (1989) 65-71.

[56] MAŁOSZEWSKI, P., MOSER, H., STICHLER, W., BERTLEFF, B., HEDIN, K., "Modelling of groundwater pollution by river bank filtration using oxygen-18 data", Groundwater Monitoring and Management, IAHS Publ. no. 173 (1990) 153-161.
[57] CIĘŻKOWSKI, W., GRÖNING, M., LEŚNIAK, P.M., WEISE, S.M., ZUBER, A., Origin and age of thermal waters in Cieplice Spa, Sudeten, Poland, inferred from isotope and noble gas data. J. Hydrol. **140**: 89-117.
[58] ZUBER, A., WEISE, S.M., OSENBRÜCK, K., GRABCZAK, J., CIĘŻKOWSKI, W., Age and recharge area of thermal waters in Ladek Spa (Sudeten, Poland) deduced from environmental isotope and noble gas data. J. Hydrol. (in press).
[59] DAVIS, G.H., LEE, K.CH., BRADLEY, E., PAYNE, B.R., Geohydrologic interpretations of a volcanic island from ebvironmental isotopes. Water Resour. Res. **6** (1970) 99-109.
[60] MAŁOSZEWSKI, P., RAUERT, W. STICHLER, W., HERRMANN, A., Application of flow models in alpine catchment area using tritium and deuterium data, J. Hydrol. **66** (1983) 319-330.
[61] HERRMANN, A., KOLL, J., MAŁOSZEWSKI, P. RAUERT, W., STICHLER, W., Water balance studies in a small catchment area of paleozoic rock using environmental isotope tracer techniques" Conjuctive Water Use, IAHS Publ. no. 156 (1986) 111-124.
[62] HERRMANN, A., KOLL, J., LEIBUNGUT, CH., MAŁOSZEWSKI, P., RAU, R., RAUERT, W., SCHÖNIGER, M., STICHLER, W., Wasserumsatz in einem kleinem Einzubsgebiet im paläozoischen Mittelgebirge (Lange Bramke, Oberharz). Eine hydrologische Systemanalyse mittels Umweltisotopen als Tracer, Landschaftökologie u. Umweltforschung, Heft 17 (1989) 1-186.
[63] MOTYKA, J., WITCZAK, S., ZUBER, A., Migration of lignosulphonates in a karstic-fractured-porous aquifer - history and prognosis for a Zn-Pb mine, Pomorzany, southern Poland, Environ. Geol. (1994) (in press).
[64] RANK, D., VÖLKL, G., MAŁOSZEWSKI, P., STICHLER, W., "Flow dynamics in an alpine karst massif studied by means of environmental isotopes", Isotope Techniques in Water Resources Development 1991, IAEA, Vienna (1992) 327-343.
[65] MAŁOSZEWSKI, P., HARUM, T., BENISCHKE, R., "Mathematical modelling of tracer experiments in the karst of Lurbach system", Transport Phenomena in Different Aquifers, Steirische Beiträge zur Hydrologie, Band 43 (1992) 116-136.
[66] MAŁOSZEWSKI, P., HARUM, T., ZOJER, H., "Modelling of environmental tracer data", Transport Phenomena in Different Aquifers, Steirische Beiträge zur Hydrologie, Band 43 (1992) 136-143.
[67] TAYLOR, G., Dispersion of soluble matter in solvent flowing slowly through a tube, Proc. R. Soc. London, Ser. A, **219** (1953) 186-203.
[68] SUDICKY, E.A., FRIND, E.O., Contaminant transport in fractured porous media: Analytical solutions for a system of parallel fractures, Water Resour. Res. **18** (1982) 1634-1642.

APPENDIX A: Examples of tracer curves (system response functions) for different injection-detection modes

A capillary with a laminar flow can be regarded as one of the simplest systems, though the transport of solute is quite complex. At a short distance the influence of molecular diffusion in negligible and one may assume that tracer particles do not move from one flow line to another, and, consequently the observed tracer distribution results only the parabolic distribution of flow velocity and from the injection-detection mode. For an instantaneous injection the following formulas are obtained [16, 19]:

$$C_{IRR}(t) = (M/2V)/(t/t_w) \qquad (A.1)$$

$$C_{IRF}(t) = C_{IFR}(t) = (M/2V)/(t/t_w)^2 \qquad (A.2)$$

$$C_{IFF}(t) = (M/2V)/(t/t_w)^3 \qquad (A.3)$$

for $t \geq 0.5t_w$

and $C(t) = 0$ for $t < 0$

where M is the injected mass, V is the volume of water in the capillary between the injection and detection cross-section and t_w is the mean transit

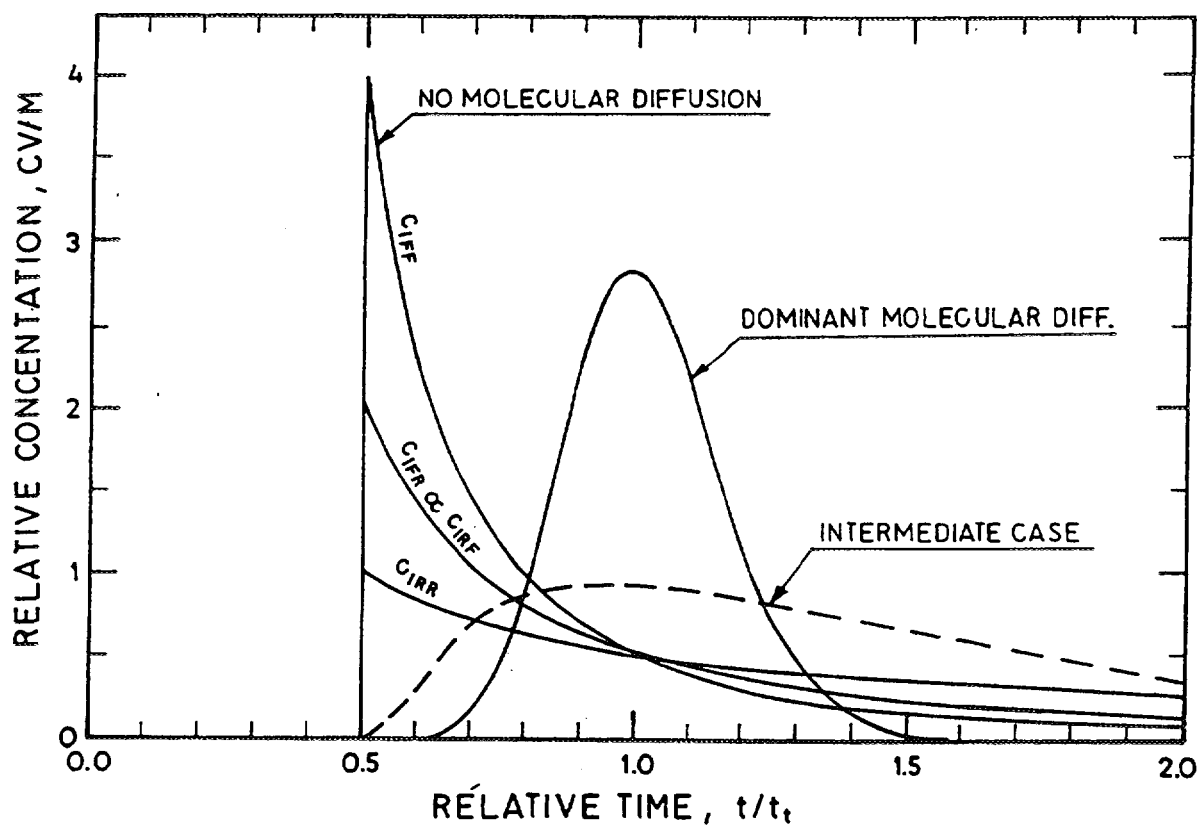

Fig. A.1. Normalized response functions for laminar flow in a capillary for negligible molecular diffusion (they depend on injection-detection mode), and typical examples of response functions in case of dominant molecular diffusion and under intermediate conditions [19].

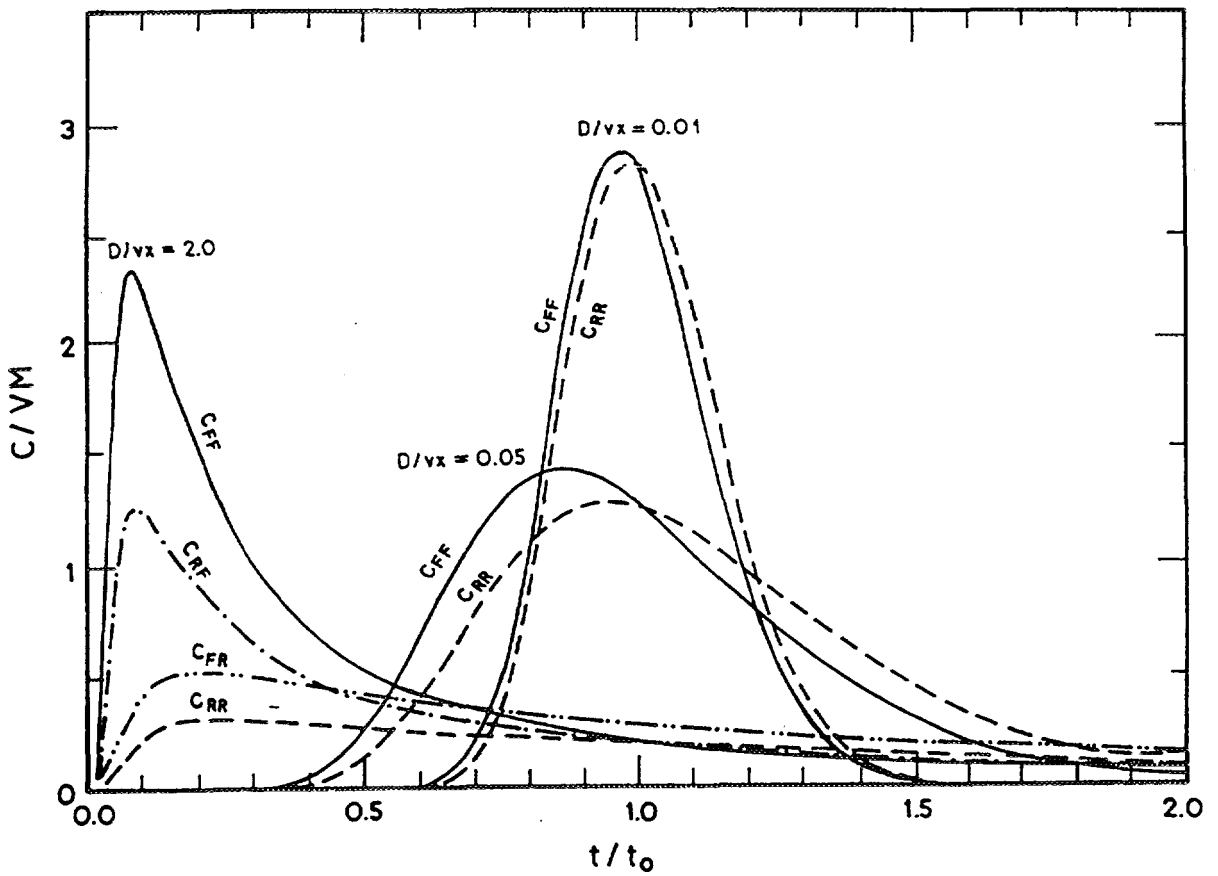

Fig. A.2. Examples of normalized response functions for different injection-detection modes in case of DM (dispersion model) [19].

time (exit age, turnover time) of water defined as $t_w = V/Q$ (Q being the volumetric flow rate).

Relative tracer curves (which after dividing by t_w are equal to the system response functions) are given in Fig. A.1 as cases with no molecular diffusion. It is easy to check that only for Eq. A.3 the mean transit time of tracer (age of tracer) defined by Eq. 8 is equal to the mean transit time of water.

If a capillary is long enough, or/and the mean flow velocity is sufficiently low for the molecular diffusion to become a dominant process in the transverse mixing, the tracer is distributed around the mean transit time of water and the tracer curve is given by a solution to the dispersion equation [67] (an example shown in Fig. A.1 by the curve for dominant molecular diffusion).

For the intermediate cases, no theoretical formula is available. Then, the tracer curves are flat with a long tail (an example shown in Fig. A.1).

In conclusion, the behaviour of a tracer in a capillary, though dependent on the distribution of flow line velocities, does not represent the system in a unique way, because it also depends on the injection-detection mode as well as on the duration of an experiment and the coefficient of molecular diffusion.

Similarly, for systems which can be described by solutions to the dispersion equation, four injection-detection modes exist [19]. In Fig. A.2 examples of tracer curves for three chosen values of the dispersion parameter ($D/vx = Pe^{-1}$) are shown. It is clear that for low values of the dispersion parameter (high Peclet numbers), the influence of the injection-detection mode becomes negligible.

APPENDIX B: An example of differences observed in fissured rocks between the water age (t_w), conservative tracer age (t_t), and radioisotope age (t_a)

Differences between the mean time travel times (ages) of mobile water (t_w), conservative solute (t_t), and decaying tracer (t_a), or the mean velocities of mobile water (v_w), conservative solute (v_t), and decaying tracer (v_a), can be easily demonstrated in a number of ways. An exact analytical solution to the transport equation in the fissures coupled with the diffusion equation in the matrix, for a system of parallel fissures of equal spacing and apertures, is chosen after [13] to serve the purpose. That solution yields the tritium distributions along flow in fissures in the case of a constant input as shown in Fig. B.1 (adapted from Figs. 2 and 4 in [68]).

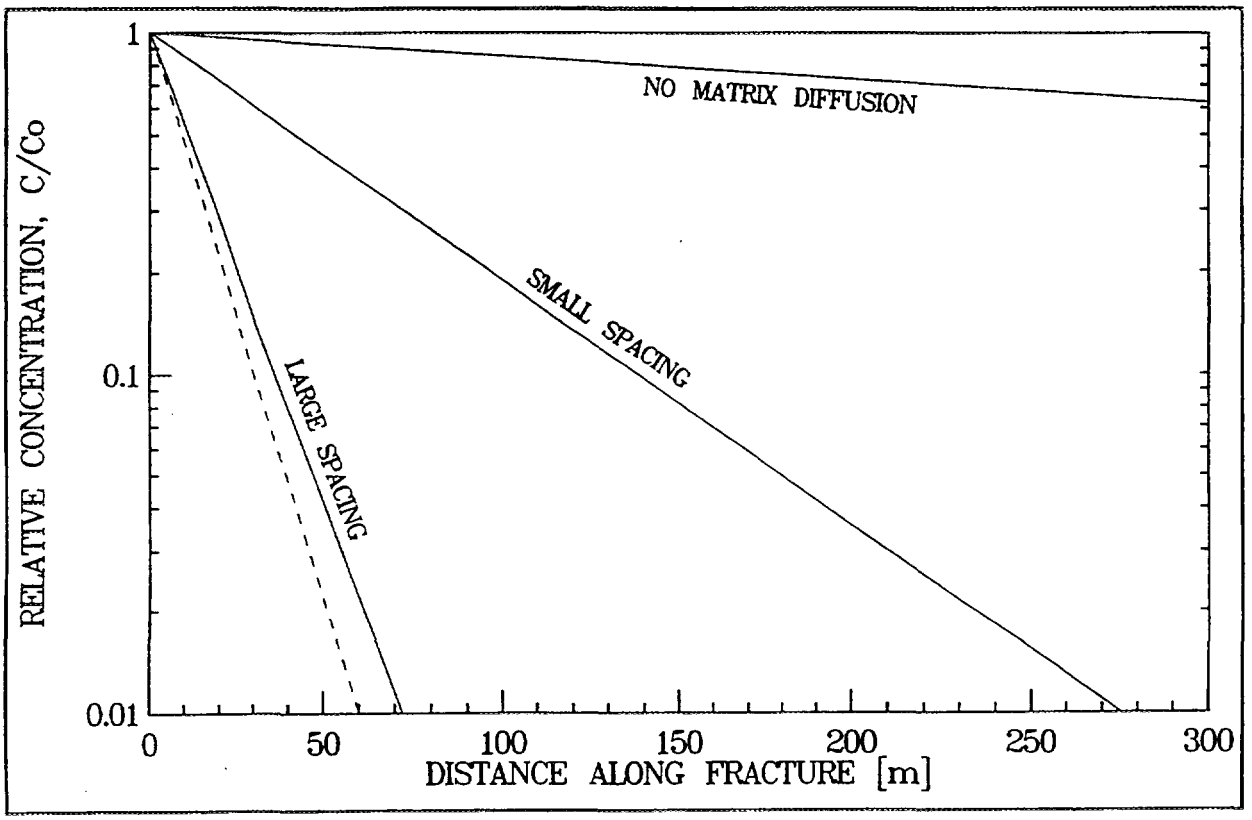

Fig. B.1. An example of the dependence of tracer age on matrix diffusion and the decay of tracer in the matrix (adapted from [13], original calculations after [67]. Case of no matrix diffusion shows the distribution of tritium in fissures when $n_p = 0$ (other parameters given in text). Case of small spacing shows the distribution of tritium for fissure spacing of 0.1 m and matrix porosity of 0.01. This distribution is in a good approximation related to the case of no diffusion by Eq. 31. Case of large spacing (heavy line) shows the distribution of tritium for spacing of 0.5 m (other parameters as above). Dashed line shows the distribution which would be observed if there were no decay in the matrix (related to the case of no diffusion by Eq. 31 which is now less exact but still yields much better results than the assumption of no diffusion).

A matrix porosity of 0.01, and a fissure aperture of 100 μm were assumed. The fissure spacing was 0.5 m (large spacing) and 0.1 m (small spacing). The boundary conditions were chosen in such a way that the flow velocity (v_w) in fissures was in both cases equal to 0.1 m/d.

The fissure porosities are: 0.0001m/0.5m = 0.0002 and 0.0001m/0.1m = 0.001, for large and small spacings, respectively. For these porosities, the retardation factors (R_p) calculated from Eq. 31 are: (0.01 + 0.0002)/0.001 = 51 and (0.01 + 0.001)/0.001 = 11, respectively.

For a steady state, the decaying tracer velocity (v_a) can be calculated for any distance along the fissures. The distances at which the concentration is equal to 0.01 of the initial concentration are chosen here. For large and small fissure spacings these distances are: 72 m and 275 m, respectively (see Fig. B.1). In both cases, the decaying tracer age calculated from Eq. 19 is 82.4 years. The different values of velocities (in m day^{-1}) are summarized as follows:

Velocity:	v_w	$v_t = x/t_t = v_w/R_p$	$v_a = x/t_a$
Large spacing:	0.1	0.00196	0.00239
Small spacing:	0.1	0.0091	0.0091

These results confirm the well-known fact of lower solute velocity in comparison with the flow (mobile water) velocity in fissures. They also show that, for large spacing, the decaying tracer velocity can be larger than the conservative tracer velocity, which is, unfortunately, not well known. In other words, the radioisotope ages defined by Eq. 19 can be lower than the conservative tracer ages in cases of sparsely fissured rocks. However, the differences between the conservative and decaying solute velocities and ages are either negligible or much lower than the differences between the solute and flow velocities. In densely fissured rocks, the differences between decaying and conservative tracer ages are negligible, particularly for large half-life times as in the case of radiocarbon [50].

The differences between exact Darcy's velocities and those estimated from the approximate form of Eq. 32 are also worth considering. For large spacing, the exact value is $n_f v_w = 0.0002 \times 0.1 = 2 \times 10^{-5}$ m day^{-1}, and the approximate one is $n_p v_t = 0.01 \times 0.00196 = 1.96 \times 10^{-5}$ m/d. For small spacing, these velocities are: $0.1 \times 0.001 = 1 \times 10^{-4}$ m/d, and $0.01 * 0.0091 = 0.91 \times 10^{-4}$ m day^{-1}, respectively. It is obvious that even for as low n_p/n_f value as above (i.e. $n_p/n_f = 10$), the approximate forms of Eqs 32 and 33 are sufficiently exact. Typical porosity ratios are higher, as shown in [13].

NUMERICAL MODELS OF GROUNDWATER FLOW AND TRANSPORT

L.F. KONIKOW
US Geological Survey,
Reston, Virginia, USA

Abstract

This chapter reviews the state-of-the-art in deterministic modeling of groundwater flow and transport processes, which can be used for interpretation of isotope data through groundwater flow analyses. Numerical models which are available for this purpose are described and their applications to complex field problems are discussed. The theoretical bases of deterministic modeling are summarized, and advantages and limitations of numerical models are described. The selection of models for specific applications and their calibration procedures are described, and results of a few illustrative case study type applications are provided.

1. INTRODUCTION

In the past, the main driving force for hydrogeologic studies has been the need to assess the water-supply potential of aquifers. However, during the past 20 years, the emphasis has shifted from water-supply problems to water-quality problems. This has driven a need to predict the movement of contaminants through the subsurface environment. One consequence of the change in emphasis has been a shift in perceived priorities for scientific research and data collection. Formerly, the focus was on developing methods to assess and measure the water-yielding properties of high-permeability aquifers. The focus is now largely on transport and dispersion processes, retardation and degradation of chemical contaminants, and the ability of low-permeability materials to contain contaminated ground water.

The past 20 years or so have also seen some major technological breakthroughs in ground-water hydrology. One technological growth area has been in the development and use of deterministic, distributed-parameter, computer simulation models for analyzing flow and solute transport in ground-water systems. These developments have somewhat paralleled the development and widespread availability of faster, larger memory, more capable, yet less expensive computer systems. Another major technological growth area has been in the application of isotopic analyses to ground-water hydrology, wherein isotopic measurements are being used to help interpret and define ground-water flow paths, ages, recharge areas, leakage, and interactions with surface water [1].

Because isotopes move through ground-water systems under the same driving forces and by the same processes as do dissolved chemicals, it is natural that the ground-water flow and solute-transport models applied to ground-water contamination problems be linked to and integrated with isotopic measurements and interpretations. However, many previous applications of isotopic analyses to ground-water systems have assumed overly simplified conceptual models for ground-water flow and transport of dissolved chemicals--either plug flow (with piston-like displacement and no mixing) or a well-mixed reservoir (which unrealistically overestimates the mixing effects of dispersion and diffusion). If the interpretations of isotopic analyses are coupled with more realistic conceptual models of flow and transport, then it is anticipated that the synergistic analysis will lead to a more accurate understanding of the hydrogeologic system being

studied. Dinçer and Davis (1984) provide a review of the application of environmental isotope tracers to modeling in hydrology, and Johnson and DePaolo (1994) provide an example of applying such a coupled approach in their analysis of a proposed high-level radioactive waste repository site [2,3].

The purpose of this chapter is to review the state of the art in deterministic modeling of ground-water flow and transport processes for those who might want to merge the interpretation of isotopic analyses with quantitative ground-water model analysis. This chapter is aimed at practitioners and is intended to help define the types of models that are available and how they may be applied to complex field problems. It will discuss the philosophy and theoretical basis of deterministic modeling, the advantages and limitations of models, the use and misuse of models, how to select a model, and how to calibrate a model. However, as this chapter is only a review, it cannot offer comprehensive and in-depth coverage of this very complex topic; but it does guide the reader to references that provide more details. Other recent comprehensive reviews of the theory and practice of deterministic modeling of ground-water processes are provided by Anderson and Woessner (1992) and Bear and Verruijt (1987) [4,5].

2. MODELS

The word *model* has so many meanings and is so overused that it is sometimes difficult to know to what one is referring [6]. A model is perhaps most simply defined as *a representation of a real system or process*. For clarification, several types of ground-water models will be discussed briefly.

A *conceptual model* is *a hypothesis for how a system or process operates*. The idea can be expressed quantitatively as a mathematical model. *Mathematical models* are abstractions that replace objects, forces, and events by expressions that contain mathematical variables, parameters, and constants [7].

Most ground-water models in use today are *deterministic* mathematical models. Deterministic models are based on conservation of mass, momentum, and energy--that is, on a balance of the various fluxes of these quantities. Experimental laws, such as Darcy's Law, Fourier's Law of thermal diffusion, and Fick's Law of chemical species diffusion, are mathematical statements (or constitutive equations) relating fluxes of mass, momentum, and energy to measurable state variables, such as hydraulic head, temperature, and solute concentration [6]. Deterministic models describe cause and effect relations. The underlying philosophy is that given a high degree of understanding of the processes by which stresses on a system produce subsequent responses in that system, the system's response to any set of stresses can be defined or predetermined through that understanding of the governing (or controlling) processes, even if the magnitude of the new stresses falls outside of the range of historically observed stresses [8]. The accuracy of such deterministic models and predictions thus depends, in part, upon how closely the concepts of the governing processes reflect the processes that in reality are controlling the system's behavior.

Deterministic ground-water models generally require the solution of partial differential equations. Exact solutions can often be obtained analytically, but analytical models require that the parameters and boundaries be highly idealized. Some models treat the properties of the porous media as lumped parameters (essentially, as a black box), but this precludes the representation of heterogeneous hydraulic properties in the model. Heterogeneity, or variability in aquifer properties, is characteristic of all geologic systems and is now recognized as playing a key role in influencing the ground-water flow and solute transport. Thus, it is often preferable to apply distributed-parameter models, which allow

the representation of variable system properties. Numerical methods yield approximate solutions to the governing equation (or equations); they require discretization of space and time. Within the discretized format one approximates the variable internal properties, boundaries, and stresses of the system. Deterministic, distributed-parameter, numerical models relax the idealized conditions of analytical models or lumped-parameter models, and they can therefore be more realistic and flexible for simulating field conditions (if applied properly).

The number and types of equations are determined by the concepts of the dominant governing processes. The coefficients of the equations are the parameters that are measures of the properties, boundaries, and stresses of the system; the dependent variables of the equations are the measures of the state of the system and are mathematically determined by the solution of the equations. Because the state of a ground-water system changes over time, as well as in space, the governing equations are normally written to give the change in the dependent variables with respect to both location and time. In computing changes over time, the solution must start from some point in time when the state of the system is known (or assumed to be known). In terms of mathematically solving the governing equations, these are the initial conditions, which must always be specified for solving a transient (or unsteady-state) equation [8].

A major difficulty is that inadequate and insufficient data limit the reliability of traditional deterministic ground-water models. The data may be inadequate because aquifer heterogeneities occur on a scale smaller than can be defined on the basis of available data, time-dependent variables are monitored too infrequently, and measurement errors exist. Consequently, there is much research under way that is directed towards representing these errors or inadequacies in a stochastic manner and incorporating statistical concepts in an otherwise conceptually based deterministic modeling approach [8]. Regression formulation of ground-water processes (such as described by Cooley, 1982) include random components or uncertainties, so that predictions may be made of confidence intervals instead of point values [9]. Freeze (1982), Neuman (1982), and Dagan (1989) present overviews of stochastic ground-water modeling and they also contrast stochastic and deterministic approaches [10-12].

When a numerical algorithm is implemented in a computer code to solve one or more partial differential equations, the resulting computer code can be considered a *generic* model. When the parameters (such as hydraulic conductivity and storativity), boundary conditions, and grid dimensions of the generic model are specified to represent a particular geographical area, the resulting computer program is a *site-specific* model. Generic models are not so robust as to preclude the generation of significant numerical errors when applied to a field problem. If the user of a model is unaware of or ignores the details of the numerical method, including the derivative approximations, the scale of discretization, and the matrix solution techniques, significant errors can be introduced and remain undetected.

3. FLOW AND TRANSPORT PROCESSES

It generally is assumed that the process of ground-water flow is governed by the relation expressed in Darcy's Law, which was derived in 1856 on the basis of the results of laboratory experiments on the flow of water through a sand column. Darcy's Law states that the ground-water flow rate is proportional to the hydraulic gradient; the constant of proportionality is the hydraulic conductivity, a property which depends on the characteristics of the porous media (such as grain

size, sorting, packing, and orientation) and the fluid (such as density and viscosity). However, Darcy's Law has limits on its range of applicability. It was derived from experiments on laminar flow of water through porous material. Flow probably is turbulent or in a transitional state from laminar to turbulent flow near the screens of many large-capacity wells [13]. Turbulent flows also may occur in rocks that have significant secondary permeability as a result of the development of fractures, joints, or solution openings. What is commonly done in such situations is to ignore local or small-scale turbulence and assume that flow behaves as if it were laminar flow through porous media on the regional scale, and thus that Darcy's Law applies at that scale. Darcy's Law also appears to have a lower limit of applicability and may not be valid in extremely fine-grained material. At the very slow velocities occurring in these typically low-permeability materials, driving forces other than hydraulic gradient (such as temperature gradient, chemical gradient, or even electrical gradient), may cause fluid flow that is comparable to that driven by the hydraulic gradient. Coupling between forces of one type and fluxes of another type are discussed by Bear (1972, p. 85-90), but coupled forces are usually small and will be assumed to be negligible in this chapter.

The purpose of a model that simulates solute transport in ground water is to compute the concentration of a dissolved chemical species in an aquifer at any specified time and place. The theoretical basis for the equation describing solute transport has been well documented in the literature [14-19]. Reilly et al. (1987) provide a conceptual framework for analyzing and modeling physical solute-transport processes in ground water [20]. Changes in chemical concentration occur within a dynamic ground-water system primarily due to four distinct processes: (1) advective transport, in which dissolved chemicals are moving with the flowing ground water; (2) hydrodynamic dispersion, in which molecular and ionic diffusion and small-scale variations in the flow velocity through the porous media cause the paths of dissolved molecules and ions to diverge or spread from the average direction of ground-water flow; (3) fluid sources, where water of one composition is introduced into and mixed with water of a different composition; and (4) reactions, in which some amount of a particular dissolved chemical species may be added to or removed from the ground water as a result of chemical, biological, and physical reactions in the water or between the water and the solid aquifer materials. There are significant problems in quantifying the role of each of these four processes in the field.

Many of the advancements in understanding solute-transport processes have been made as an outcome of society's concern with environmental problems, such as ground-water contamination from industrial activities and waste-disposal practices. The processes affecting contaminant migration in porous media have been reviewed by Gillham and Cherry (1982). They state (p. 32), "Although considerable research on contaminant migration in ground-water flow systems has been conducted during recent decades, this field of endeavor is still in its infancy. Many definitive laboratory and field tests remain to be accomplished to provide a basis for development of mathematical concepts that can be founded on knowledge of the transport processes that exist at the field scale" [21].

The subsurface environment constitutes a complex, three-dimensional, heterogeneous hydrogeologic setting. This variability strongly influences ground-water flow and transport, and such a reality can only be described accurately through careful hydrogeologic practice in the field. However, no matter how much data are collected, the sampling is limited and uncertainty always remains about the properties and boundaries of the ground-water system of interest.

Rocks that have a dominant secondary permeability, such as fractures or solution openings, represent an extreme but common example of heterogeneity. In such subsurface environments, the secondary permeability channels may be

orders of magnitude more transmissive than the porous matrix comprising most of the rock mass. In such rocks, the most difficult problem may be identifying where the fractures are located, how they are interconnected, and what their hydraulic properties are [22]. Where transport occurs through fractured rocks, diffusion of solutes from fractures to the porous blocks can serve as a significant retardation mechanism [23]. Modeling of ground-water flow and transport through fractured rocks is an area of active research, but not an area where practical and reliable approaches are readily available. The state of the art in analyzing and modeling flow and transport in fractured rock is reviewed by Bear et al. (1993) [24].

4. GOVERNING EQUATIONS

The development of mathematical equations that describe the ground-water flow and transport processes may be developed from the fundamental principle of conservation of mass of fluid or of solute. Given a representative volume of porous medium, a general equation for conservation of mass for the volume may be expressed as:

rate of mass inflow - rate of mass outflow + rate of mass production/consumption = rate of mass accumulation (1)

This statement of conservation of mass (or continuity equation) may be combined with a mathematical expression of the relevant process to obtain a differential equation describing flow or transport [15-16, 19].

4.1. Ground-water flow

A quantitative description of ground-water flow is a prerequisite to accurately representing solute transport in aquifers. A general form of the equation describing the transient flow of a compressible fluid in a nonhomogeneous anisotropic aquifer may be derived by combining Darcy's Law with the continuity equation. A general ground-water flow equation may be written in Cartesian tensor notation as:

$$\frac{\partial}{\partial x_i}\left(K_{ij}\frac{\partial h}{\partial x_i}\right) = S_s\frac{\partial h}{\partial t} + W^* \qquad (2)$$

where K_{ij} is the hydraulic conductivity of the porous media (a second-order tensor), L^2T^{-1}; h is the hydraulic head, L; S_S is the specific storage, L^{-1}; t is time, T; W^* is the volumetric flux per unit volume (positive for outflow and negative for inflow), T^{-1}; and x_i are the Cartesian coordinates, L. The summation convention of Cartesian tensor analysis is implied in eq. 2. The sign convention for the source/sink term, W^*, is somewhat arbitrary (and inconsequential, as long as usage is clear and consistent). Equation 2 can generally be applied if isothermal conditions prevail, the porous medium only deforms vertically, the volume of individual grains remains constant during deformation, Darcy's Law applies (and gradients of hydraulic head are the only driving force), and fluid properties (density and viscosity) are homogeneous and constant.

In many ground-water studies, if the aquifer is relatively thin compared to its lateral extent, it can be reasonably assumed that ground-water flow is areally two-dimensional. This allows the three-dimensional flow equation to be reduced to the case of two-dimensional areal flow, for which several additional simplifications are possible. The advantages of reducing the dimensionality of the equations include less stringent data requirements, smaller computer memory requirements, and shorter computer execution times to achieve a numerical solution [25].

An expression similar to eq. 2 may be derived for the two-dimensional areal flow of a homogeneous fluid and written as:

$$\frac{\partial}{\partial x_i}\left(K_{ij}b\frac{\partial h}{\partial x_i}\right)=S_s b\frac{\partial h}{\partial t}+W^* b \tag{3}$$

where b is the saturated thickness of the aquifer, L, and it is assumed that the hydraulic conductivity, specific storage, and hydraulic head represent vertically integrated mean values [26]. The transmissivity of the aquifer may be defined as:

$$T_{ij}=K_{ij}b \tag{4}$$

where T_{ij} is the transmissivity, L^2T^{-1}. Similarly, the storage coefficient of the aquifer may be defined as:

$$S=S_S b \tag{5}$$

where S is the storage coefficient (dimensionless). After substituting the relations indicated by eqs. 4 and 5 into eq. 3, we obtain:

$$\frac{\partial}{\partial x_i}\left(T_{ij}\frac{\partial h}{\partial x_i}\right)=S\frac{\partial h}{\partial t}+W \tag{6}$$

where $W = W(x,y,t) = W^*b$ is the volume flux per unit area, LT^{-1}.

Although fluid sources and sinks may vary in space and time, they have been lumped into one term (W) in the previous development. There are several possible ways to compute W. If we consider only fluid sources and sinks such as (1) direct withdrawal or recharge (for example, pumpage from a well, well injection, or evapotranspiration), and (2) steady-state leakage into or out of the aquifer through a confining layer, streambed, or lake bed, then for the case of two-dimensional horizontal flow, the source/sink terms may be specifically expressed as:

$$W(x,y,t)=Q(x,y,t)-\frac{K_z}{m}(H_s-h) \tag{7}$$

where Q is the rate of withdrawal (positive sign) or recharge (negative sign), LT^{-1}; K_z is the vertical hydraulic conductivity of the confining layer, streambed, or lake bed, LT^{-1}; m is the thickness of the confining layer, streambed, or lake bed, L; and H_s is the hydraulic head in the source bed, stream, or lake, L.

When eq. 6 is applied to an unconfined (water-table) aquifer system, it must be assumed that flow is horizontal and equipotential lines are vertical, that the horizontal hydraulic gradient equals the slope of the water table, and that the storage coefficient is equal to the specific yield (S_y) [4].

The cross-product terms of the hydraulic conductivity tensor drop out when the coordinate axes are aligned with the principal axes of the tensor [27]; that is, $K_{ij} = 0$ when $i \neq j$. Therefore, the only hydraulic conductivity terms with possible nonzero values are K_{xx}, K_{yy}, and K_{zz}. This assumption simplifies the general flow equation (eq. 2), which can now be rewritten to include explicitly all hydraulic conductivity terms as:

$$\frac{\partial}{\partial x}\left(K_{xx}\frac{\partial h}{\partial x}\right)+\frac{\partial}{\partial y}\left(K_{yy}\frac{\partial h}{\partial y}\right)+\frac{\partial}{\partial z}\left(K_{zz}\frac{\partial h}{\partial z}\right)=S_s\frac{\partial h}{\partial t}+W^* \tag{8}$$

Darcy's Law may similarly be written as:

$$\begin{aligned} q_x &= -K_{xx}\,\partial h/\partial x \\ q_y &= -K_{yy}\,\partial h/\partial y \\ q_z &= -K_{zz}\,\partial h/\partial z \end{aligned} \tag{9}$$

where q_i is the specific discharge vector, LT^{-1}.

For the case of two-dimensional areal flow, if the coordinate axes are aligned with the principal directions of the transmissivity tensor, eq. 6 may be written as:

$$\frac{\partial}{\partial x}\left(T_{xx}\frac{\partial h}{\partial x}\right)+\frac{\partial}{\partial y}\left(T_{yy}\frac{\partial h}{\partial y}\right)=S\frac{\partial h}{\partial t}+W \tag{10}$$

In some field situations, fluid properties such as density and viscosity may vary significantly in space or time. This may occur where water temperature or dissolved-solids concentration changes significantly. It is worth noting that in general fluid viscosity is more sensitive to changes in temperature, whereas fluid density is more sensitive to changes in chemical content. When the water properties are heterogeneous and (or) transient, the relations among water levels, hydraulic heads, fluid pressures, and flow velocities are neither simple nor straightforward [22]. In such cases, the flow equation is written and solved in terms of fluid pressures, fluid densities, and the intrinsic permeability of the porous media as:

$$\frac{\partial}{\partial x_i}\left[\frac{\rho g k_{ij}}{\mu}\left(\frac{\partial P}{\partial x_i}+\rho g\frac{\partial z}{\partial x_j}\right)\right]=S_s\frac{\partial P}{\partial t}+W^*\rho' g \tag{11}$$

where k_{ij} is the intrinsic permeability, L^2; ρ is the fluid density, ML^{-3}; μ is the dynamic viscosity, $ML^{-1}T^{-1}$; P is the fluid pressure, $ML^{-1}T^{-1}$; g is the gravitational acceleration constant, LT^{-2}; z is the elevation of the reference point above a standard datum, L; and ρ' is the density of the source/sink fluid, ML^{-3} [28-29]. The intrinsic permeability is related to the hydraulic conductivity as:

$$K_{ij}=\frac{\rho g}{\mu}k_{ij} \tag{12}$$

4.2. Seepage velocity

The migration and mixing of chemicals dissolved in ground water will obviously be affected by the velocity of the flowing ground water. The specific discharge calculated from eq. 9 is sometimes called the Darcy velocity, presumably because it has the same dimensions as velocity. However, this nomenclature can be misleading because q_i does not actually represent the speed of the water movement. Rather, q_i represents a volumetric flux per unit cross-sectional area. Thus, to calculate the actual seepage velocity of ground water, one must account for the actual cross-sectional area through which flow is occurring. This is usually calculated as follows:

$$V_i=\frac{q_i}{\varepsilon} \tag{13}$$

where V_i is the seepage velocity (or average interstitial velocity), LT^{-1}; and ε is the effective porosity of the porous medium. It can also be written in terms of Darcy's Law as:

$$V_i=-\frac{K_{ij}}{\varepsilon}\frac{\partial h}{\partial x_j} \tag{14}$$

4.3. Solute-transport equation

An equation describing the transport and dispersion of a dissolved chemical in flowing ground water may be derived from the principle of conservation of mass (eq. 1), just as a general flow equation was so derived [14-17, 25, 30]. The principle of conservation of mass requires that the net mass of solute entering or leaving a specified volume of aquifer during a given time interval must equal the accumulation or loss of mass stored in that volume during the interval. This relationship may then be expressed mathematically by considering all fluxes into and out of a representative elementary volume (REV), as described by Bear (1972, p. 19).

A generalized form of the solute-transport equation is presented by Grove (1976), in which terms are incorporated to represent chemical reactions and solute concentration both in the pore fluid and on the solid surface, as:

$$\frac{\partial(\varepsilon C)}{\partial t} = \frac{\partial}{\partial x_i}\left(\varepsilon D_{ij}\frac{\partial C}{\partial x_j}\right) - \frac{\partial}{\partial x_i}\left(\varepsilon C V_i\right) - C'W^* + CHEM \qquad (15)$$

where *CHEM* equals :

$-\rho_b \frac{\partial \overline{C}}{\partial t}$ for linear equilibrium controlled sorption or ion-exchange reactions,

$\sum_{k=1}^{s} R_k$ for s chemical rate-controlled reactions, and (or)

$-\lambda\left(\varepsilon C + \rho_b \overline{C}\right)$ for decay,

and where D_{ij} is the coefficient of hydrodynamic dispersion (a second-order tensor), L^2T^{-1}, C' is the concentration of the solute in the source or sink fluid, $\overline{C}$ is the concentration of the species adsorbed on the solid (mass of solute/mass of sediment), ρ_b is the bulk density of the solid, ML^{-3}, R_k is the rate of production of the solute in reaction k, $ML^{-3}T^{-1}$, and λ is the decay constant (equal to *ln* 2/half life), T^{-1} [31].

The first term on the right side of eq. 15 represents the change in concentration due to hydrodynamic dispersion. This expression is analogous to Fick's Law describing diffusive flux. This Fickian model assumes that the driving force is the concentration gradient and that the dispersive flux occurs in a direction from higher concentrations towards lower concentrations. However, this assumption is not always consistent with field observations and is the subject of much ongoing research and field study. The second term represents advective transport and describes the movement of solutes at the average seepage velocity of the flowing ground water. The third term represents the effects of mixing with a source fluid that has a different concentration than the ground water at the location of the recharge or injection. The fourth term lumps all of the chemical, geochemical, and biological reactions that cause transfer of mass between the liquid and solid phases or conversion of dissolved chemical species from one form to another. The chemical attenuation of inorganic chemicals can occur by sorption/desorption, precipitation/dissolution, or oxidation/reduction; organic chemical can adsorb or degrade by microbiological processes. There has been considerable progress in modeling these reaction processes; however, a comprehensive review of the reaction processes and their representation in transport models is beyond the scope of this chapter.

If reactions are limited to equilibrium-controlled sorption or exchange and first-order irreversible rate (decay) reactions, then the general governing equation (eq. 15) can be written as:

$$\frac{\partial C}{\partial t}+\frac{\rho_b}{\varepsilon}\frac{\partial \overline{C}}{\partial t}=\frac{\partial}{\partial x_i}\left(D_{ij}\frac{\partial C}{\partial x_j}\right)-\frac{\partial}{\partial x_i}(CV_i)+\frac{C'W^*}{\varepsilon}-\lambda C-\frac{\rho_b}{\varepsilon}\lambda\overline{C} \tag{16}$$

The temporal change in sorbed concentration in eq. 16 can be represented in terms of the solute concentration using the chain rule of calculus, as follows:

$$\frac{d\overline{C}}{dt}=\frac{d\overline{C}}{dC}\frac{\partial C}{\partial t} \tag{17}$$

For equilibrium sorption and exchange reactions $d\overline{C}/dC$, as well as $\overline{C}$, is a function of C alone. Therefore, the equilibrium relation for $\overline{C}$ and $d\overline{C}/dC$ can be substituted into the governing equation to develop a partial differential equation in terms of C only. The resulting single transport equation is solved for solute concentration. Sorbed concentration can then be calculated using the equilibrium relation. The linear-sorption reaction considers that the concentration of solute sorbed to the porous medium is directly proportional to the concentration of the solute in the pore fluid, according to the relation

$$\overline{C}=K_dC \tag{18}$$

where K_d is the distribution coefficient, L^3M^{-1}. This reaction is assumed to be instantaneous and reversible. The curve relating sorbed concentration to dissolved concentration is known as an isotherm. If that relation is linear, the slope (derivative) of the isotherm, $d\overline{C}/dC$, is known as the equilibrium distribution coefficient, K_d. Thus, in the case of a linear isotherm,

$$\frac{d\overline{C}}{dt}=\frac{d\overline{C}}{dC}\frac{\partial C}{\partial t}=K_d\frac{\partial C}{\partial t} \tag{19}$$

After substituting this relation into eq. 16, we can then rewrite eq. 16 as:

$$\frac{\partial C}{\partial t}+\frac{\rho_bK_d}{\varepsilon}\frac{\partial C}{\partial t}=\frac{\partial}{\partial x_i}\left(D_{ij}\frac{\partial C}{\partial x_j}\right)-\frac{\partial}{\partial x_i}(CV_i)+\frac{C'W^*}{\varepsilon}-\lambda C-\frac{\rho_bK_d}{\varepsilon}\lambda C \tag{20}$$

Factoring out the term $(1+\rho_b K_d/\varepsilon)$ and defining a retardation factor, R_f (dimensionless), as:

$$R_f=1+\frac{\rho_bK_d}{\varepsilon} \tag{21}$$

and substituting this relation into eq. 20, results in:

$$R_f\frac{\partial C}{\partial t}=\frac{\partial}{\partial x_i}\left(D_{ij}\frac{\partial C}{\partial x_j}\right)-\frac{\partial}{\partial x_i}(CV_i)+\frac{C'W^*}{\varepsilon}-R_f\lambda C \tag{22}$$

Because R_f is constant under these assumptions, the solution to this governing equation is identical to the solution for the governing equation with no sorption effects, except that the velocity, dispersive flux, and source strength are reduced by a factor R_f. The transport process thus appears to be "retarded" because of the instantaneous equilibrium sorption onto the porous medium.

In the conventional formulation of the solute-transport equation (eq. 15), the coefficient of hydrodynamic dispersion is defined as the sum of mechanical dispersion and molecular diffusion [15]. The mechanical dispersion is a function both of the intrinsic properties of the porous media (such as heterogeneities in hydraulic conductivity and porosity) and of the fluid flow. Molecular diffusion in a porous media will differ from that in free water because of the effects of porosity and tortuosity. These relations are commonly expressed as:

$$D_{ij} = \alpha_{ijmn} \frac{V_m V_n}{|V|} + D_m, \qquad i,j,m,n = 1,2,3 \tag{23}$$

where α_{ijmn} is the dispersivity of the porous medium (a fourth-order tensor), L; V_m and V_n are the components of the flow velocity of the fluid in the m and n directions, respectively, LT^{-1}; D_m is the effective coefficient of molecular diffusion, L^2T^{-1}; and $|V|$ is the magnitude of the velocity vector, LT^{-1}, defined as $|V| = \sqrt{V_x^2 + V_y^2 + V_z^2}$ [15-16, 32]. Scheidegger (1961) and Bear (1979) show that the dispersivity of an isotropic porous medium can be defined by two constants. These are the longitudinal dispersivity of the medium, α_L, and the transverse dispersivity of the medium, α_T. These are related to the longitudinal and transverse dispersion coefficients by $D_L = \alpha_L|V|$ and $D_T = \alpha_T|V|$. Most applications of transport models to ground-water problems that have been documented to date have been based on this conventional formulation.

Bear (1979, p. 320) notes that the separation between mechanical dispersion and diffusion is rather artificial as the processes are inseparable. However, because diffusion occurs even at zero velocity, its contribution to overall dispersion is greatest for low-velocity systems. In many ground-water transport problems, the velocity is relatively high, such that the separable contribution of diffusion is negligible and the magnitude of the mechanical dispersion (essentially αV) may be much greater than D_m. After expanding eq. 23, substituting Scheidegger's (1961) identities, and eliminating terms with coefficients that equal zero, the components of the dispersion coefficient for two-dimensional flow in an isotropic aquifer may be stated explicitly as:

$$D_{xx} = \alpha_L \frac{(V_x)^2}{|V|} + \alpha_T \frac{(V_y)^2}{|V|} + D_m \tag{24}$$

$$D_{yy} = \alpha_T \frac{(V_x)^2}{|V|} + \alpha_L \frac{(V_y)^2}{|V|} + D_m \tag{25}$$

$$D_{xy} = D_{yx} = (\alpha_L - \alpha_T) \frac{V_x V_y}{|V|} \tag{26}$$

The consideration of solute transport in a porous medium that is anisotropic would require the estimation of more than two parameters. For example, for the case of transversely isotropic media (such as a stratified system in which the hydraulic conductivity is different in the vertical direction than in the horizontal direction), the dispersion tensor can be characterized by six scalar invariants [18, 33]. In practice, it is rare that field values for even the two constants α_L and α_T can be defined uniquely. Thus, it appears impractical to be able to measure or define as many as six dispersivity constants in the field. Therefore, although anisotropy in hydraulic conductivity (a second-order tensor) is recognized and accounted for in ground-water flow simulation, it is commonly assumed out of convenience that the same system is isotropic with respect to dispersion. This essentially means that α_L and α_T do not vary as a function of direction, so that even assuming isotropy with respect to dispersion, the overall spreading of a solute is anisotropic in the sense that a plume or tracer will typically exhibit greater spreading in the direction of flow compared to the amount of spreading transverse to the direction of flow (and α_L will have a different magnitude than α_T).

The error that can be introduced by neglecting material anisotropy is illustrated in field data where α_T has been shown to be sensitive to direction. In a study of a contaminant plume at Barstow, California, two-dimensional solute-transport models were applied in both areal and cross-sectional planes [34-35]. To achieve a best fit to the field data, the value of α_T in the cross-sectional model had to be reduced by a factor of 100 from the value of about 20 m used in the areal model ($\alpha_L \approx 65$ m in both planes) [34-35]. Robson (1978) explains the change in dispersivity values by stating, "In the areal-oriented model D_L and D_T are essentially measures of mixing along aquifer bedding planes, as D_L in the profile model, whereas D_T in the profile model is primarily a measure of mixing across bedding planes."

If single values of α_L or α_T are used in predicting solute transport when the flow direction is not always parallel to one of the principal directions of anisotropy, then dispersive fluxes will be either overestimated or underestimated for various parts of the flow system (depending on whether the values of α_L and α_T are characteristic of dispersive transport in the horizontal or vertical direction). This will lead to errors in predicted concentrations. Voss (1984) included in his solute-transport model an *ad-hoc* relation to account for dispersion in anisotropic media by making α_L and α_T a function of flow direction. He assumes that α_L and α_T have two principal directions aligned with the principal directions of the permeability (or hydraulic conductivity) tensor [36]. The values of longitudinal and transverse dispersivity are thereby calculated as:

$$\alpha_L = \frac{\alpha_{L(\max)}\alpha_{L(\min)}}{\left(\alpha_{L(\min)}\cos^2\theta_{kv} + \alpha_{L(\max)}\sin^2\theta_{kv}\right)} \tag{27a}$$

$$\alpha_T = \frac{\alpha_{T(\max)}\alpha_{T(\min)}}{\left(\alpha_{T(\min)}\cos^2\theta_{kv} + \alpha_{T(\max)}\sin^2\theta_{kv}\right)} \tag{27b}$$

where $\alpha_{L(\max)}$ and $\alpha_{L(\min)}$ are the longitudinal dispersivities for flow in the directions of maximum and minimum permeabilities, respectively, L; $\alpha_{T(\max)}$ and $\alpha_{T(\min)}$ are the transverse dispersivities for flow in the directions of maximum and minimum permeabilities, respectively, L; and θ_{kv} is the angle from the maximum permeability direction to the local flow direction [36].

Although conventional theory holds that α_L is generally an intrinsic property of the aquifer, it is found in practice to be dependent on and proportional to the scale of the measurement. Most reported values of α_L fall in a range from 0.01 to 1.0 of the scale of the measurement, although the ratio tends to decrease at larger scales [23, 37-38]. Smith and Schwartz (1980) conclude that macroscopic dispersion results from large-scale spatial variations in hydraulic conductivity and that the use of relatively large values of dispersivity with uniform hydraulic conductivity fields is an inappropriate basis for describing transport in geologic systems [39]. Dagan (1989) provides a comprehensive review of stochastic theory of ground-water flow and transport, an approach that directly relates scale-dependent dispersion to the statistical measures of heterogeneity of the porous media [12]. From another perspective, some part of the scale dependence of dispersivity may be explained as an artifact of the models used, in that a scaling up of dispersivity will occur whenever an (n-1)-dimensional model is calibrated or used to describe an n-dimensional system [40]. Numerical experiments also show that variations in hydraulic conductivity contribute significantly to observed dispersion [41]. If a model is applied to a system having variable hydraulic conductivity but uses mean values and does not explicitly represent the variability, the model calibration will likely yield compensating errors in which values for the dispersivity coefficients are larger than would be measured locally in the field area. Similarly, representing a transient flow field

by a mean steady-state flow field, as is commonly done, inherently ignores some of the variability in velocity and must also be compensated for by increased values of dispersivity (primarily transverse dispersivity) [42].

Because advective transport and hydrodynamic dispersion both depend on the velocity of ground-water flow, the mathematical simulation model must solve at least two simultaneous partial differential equations. One is the equation of flow, from which ground-water flow velocities are obtained, and the second is the solute-transport equation, which describes the chemical concentration in ground water. If the properties of the water are affected significantly by changes in solute concentration, as in a saltwater intrusion problem, then the flow and transport equations should be solved simultaneously (or at least iteratively). If not, then the flow and transport equations can be decoupled and solved sequentially, which is simpler numerically.

5. NUMERICAL METHODS TO SOLVE EQUATIONS

The partial differential equations describing ground-water flow and transport can be solved mathematically using either analytical solutions or numerical solutions. The advantages of an analytical solution, when it is possible to apply one, are that it usually provides an exact solution to the governing equation and is often relatively simple and efficient to obtain. Many analytical solutions have been developed for the flow equation; however, most applications are limited to well hydraulics problems involving radial symmetry [e.g. 43-45]. The familiar Theis type curve represents the solution of one such analytical model. Analytical solutions are also available to solve the solute-transport equation [15, 46-48]. In general, obtaining the exact analytical solution to the partial differential equation requires that the properties and boundaries of the flow system be highly and perhaps unrealistically idealized. For simulating most field problems, the mathematical benefits of obtaining an exact analytical solution are probably outweighed by the errors introduced by the simplifying assumptions of the complex field environment that are required to apply the analytical approach.

Alternatively, for problems where the simplified analytical models no longer describe the physics of the situation, the partial differential equations can be approximated numerically. In so doing, the continuous variables are replaced with discrete variables that are defined at grid blocks (or nodes). Thus, the continuous differential equation, which defines hydraulic head or solute concentration everywhere in the system, is replaced by a finite number of algebraic equations that defines the hydraulic head or concentration at specific points. This system of algebraic equations generally is solved using matrix techniques. This approach constitutes a numerical model, and generally, a computer program is written to solve the equations on a computer.

The equations describing ground-water flow and solute transport are second-order differential equations, which can be classified on the basis of their mathematical properties. Peaceman (1977) states that there are basically three types of second-order differential equations, which are parabolic, elliptic, and hyperbolic [49]. Such equations can be classified and distinguished based on the nature and magnitude of the coefficients of the equation. This is important because the numerical methods for the solution of each type have should be considered and developed separately for optimal accuracy and efficiency in the solution algorithm. Peaceman (1977) shows that if you consider a general form of a second-order differential equation in which you have two independent variables

(e.g. x and t) and a generalized dependent variable, u, then the equations may be written in the following general form:

$$A\frac{\partial^2 u}{\partial x^2}+B\frac{\partial^2 u}{\partial t^2}=f\left(\frac{\partial u}{\partial x},\frac{\partial u}{\partial t},u\right) \tag{28}$$

The equation is elliptic if $A \cdot B>0$; parabolic if $A \cdot B=0$; and hyperbolic if $A \cdot B<0$ [49].

Examples of parabolic equations include the equations describing diffusion, heat conduction, and transient ground-water flow. Examples of elliptic equations include Laplace's equation, Poisson's equation, and the steady-state ground-water flow equation. Examples of hyperbolic equations include the wave equation and the first-order advection (or convection) transport equation. The first two types are most amenable to accurate and efficient solution using standard numerical methods.

Two major classes of numerical methods have come to be well accepted for solving the ground-water flow equation. These are the finite-difference methods and the finite-element methods. Each of these two major classes of numerical methods includes a variety of subclasses and implementation alternatives. Comprehensive treatments of the application of these numerical methods to ground-water problems are presented by [50-51]. Both of these numerical approaches require that the area of interest be subdivided by a grid into a number of smaller subareas (cells or elements) that are associated with node points (either at the centers of peripheries of the subareas).

Finite-difference methods approximate the first derivatives in the partial differential equations as difference quotients (the differences between values of variables at adjacent nodes, both in space and time, with respect to the interval between those adjacent nodes). There are several advanced text books that focus primarily on finite-difference methods [49-50, 52]. Finite-element methods use assumed functions of the dependent variables and parameters to evaluate equivalent integral formulations of the partial differential equations. Huyakorn and Pinder (1983) present a comprehensive analysis and review of the application of finite-element methods to ground-water problems [53]. In both numerical approaches, the discretization of the space and time dimensions allows the continuous boundary-value problem for the solution of the partial differential equation to be reduced to the simultaneous solution of a set of algebraic equations. These equations can then be solved using either iterative or direct matrix methods.

Each approach has advantages and disadvantages, but there are very few ground-water problems for which either is clearly superior. In general, the finite-difference methods are simpler conceptually and mathematically, and are easier to program for a computer. They are typically keyed to a relatively simple, rectangular grid, which also eases data entry tasks. Finite-element methods generally require the use of more sophisticated mathematics but, for some problems, may be more accurate numerically than standard finite-difference methods. A major advantage of the finite-element methods is the flexibility of the finite-element grid, which allows a close spatial approximation of irregular boundaries of the aquifer and (or) of parameter zones within the aquifer when they are considered. However, the construction and specification of an input data set is much more difficult for an irregular finite-element grid than for a regular rectangular finite-difference grid. Thus, the use of a model preprocessor, which includes a mesh generator and a scheme to efficiently number the nodes and elements of the mesh and to specify the spatial coordinates of each node, is valuable to effectively utilize the advantageous features of a finite-element model. Figure 1 illustrates a hypothetical aquifer system, which has impermeable boundaries and a well field of interest (fig. 1a), which has been discretized using

finite-difference (fig. 1b) and finite-element (fig. 1c) grids. Figures 1b and 1c illustrate conceptually how their respective grids can be adjusted to use a finer mesh spacing in selected areas of interest. The rectangular finite-difference grid approximates the aquifer boundaries in a step-wise manner, resulting in some nodes or cells outside of the aquifer, whereas sides of the triangular elements of the finite-element grid can closely follow the outer boundary using a minimal number of overall nodes.

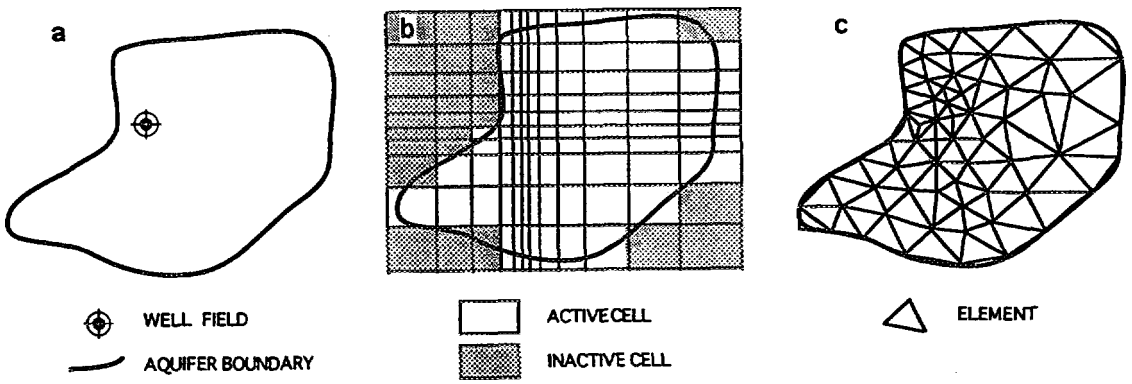

Figure 1. Hypothetical application of finite-difference and finite-element grids to an irregularly bounded aquifer.

Boundary elements or boundary integral methods can also be applied to solve the flow equation. Their main advantage is that the precision of the calculations is not a function of the size of the elements used, contrary to finite-difference or finite-element methods [54]. Thus, a few very large elements can be used, so that the method is very efficient in terms of computer time. In a two-step process, the numerical solution is only calculated along the boundaries of the elements in the first step; if the solution is also explicitly required inside an element, its value is calculated in a second step by numerical integration inside the element. The main restriction is that the properties of the porous medium in a given element are assumed to be constant. If heterogeneities are such that a large number of elements are required to describe them adequately, then the boundary integral method loses its superiority, and finite-difference or finite-element methods can be used just as well. This method is, therefore, much less flexible and general than the previous ones. More details on the boundary integral method are given by Brebbia (1978) and Liggett (1987) [55-56].

The solute-transport equation is in general more difficult to solve numerically than the ground-water flow equation, largely because the mathematical properties of the transport equation vary depending upon which terms in the equation are dominant in a particular situation. When solute transport is dominated by advective transport, as is common in many field problems, then eq. 15 approximates a hyperbolic type of equation (similar to equations describing the propagation of a wave or of a shock front). But if a system is dominated by dispersive fluxes, such as might occur where fluid velocities are relatively low and aquifer dispersivities are relatively high, then eq. 15 becomes more parabolic in nature (similar to the transient ground-water flow equation).

The numerical methods that work best for parabolic partial differential equations are not best for solving hyperbolic equations, and vice versa. Thus, no one numerical method or simulation model will be ideal for the entire spectrum of

ground-water transport problems likely to be encountered in the field. Further compounding this difficulty is the fact that in the field, the seepage velocity of ground water is highly variable, even if aquifer properties are relatively homogeneous (because of the effects of complex boundary conditions). Thus, in low permeability zones or near stagnation points, the velocity may be close to zero and the transport processes will be dominated by dispersion processes; in high permeability zones or near stress points (such as pumping wells), the velocity may be several meters per day and the transport processes will be advection dominated. In other words, for the same system, the governing equation may be more hyperbolic in one area (or at one time) and more parabolic in nature in another area (or at another time). Therefore, no matter which numerical method is chosen as the basis for a simulation model, it will not be ideal or optimal over the entire domain of the problem, and significant numerical errors may be introduced somewhere in the solution. The transport modeling effort must recognize this inherent difficulty and strive to minimize and control the numerical errors.

Although finite-difference and finite-element models are commonly applied to transport problems, other types of numerical methods have also been applied to transport problems, including method of characteristics, particle tracking, random walk, Eulerian-Lagrangian methods, and adaptive grid methods. All of these have the ability to track sharp fronts accurately with a minimum of numerical dispersion. Documented models based on variants of these approaches include Konikow and Bredehoeft (1978), Sanford and Konikow (1985), Prickett et al. (1981), Engineering Technologies Associates (1989), and Zheng (1990) [29, 57-60].

Finite-difference and finite-element methods also can be applied to solve the transport equation, particularly when dispersive transport is large compared to advective transport. However, problems of numerical dispersion and oscillations may induce significant errors for some problems. The numerical errors can generally be reduced by using a finer discretization (either time steps or spatial grid). Examples of documented three-dimensional, transient, finite-difference models that simultaneously solve the fluid pressure, energy-transport, and solute-transport equations for nonhomogeneous miscible fluids include Kipp (1987) and Reeves et al. (1986) [61-62]. A two-dimensional finite-element transport model is documented by Voss (1984) [36]. Because none of the standard numerical methods are ideal for a wide range of transport problems, there is currently still much research on developing better mixed or adaptive methods that aim to minimize numerical errors and combine the best features of alternative standard numerical approaches [63-66].

The method of characteristics was developed to solve hyperbolic differential equations. A major advantage is that the method minimizes or eliminates numerical dispersion [17, 30, 57, 67-68]. The approach taken by the method of characteristics is not to solve eq. 15 or 22 directly, but rather to solve an equivalent system of ordinary differential equations. Equation 22 can be further modified for improved compatibility with this method by expanding the advection term, substituting relations from Darcy's Law and the flow equation, and rearranging terms to obtain [25]:

$$\frac{\partial C}{\partial t} = \frac{1}{R_f}\frac{\partial}{\partial x_i}\left(D_{ij}\frac{\partial C}{\partial x_j}\right) - \frac{V_i}{R_f}\frac{\partial C}{\partial x_i} + \frac{W^*(C - C')}{\varepsilon R_f} - \lambda C \qquad (29)$$

If we consider the material derivative of concentration with respect to time, dC/dt, as describing the change in concentration of a parcel of water moving at the seepage velocity of water, it may be defined for a two-dimensional system as:

$$\frac{dC}{dt} = \frac{\partial C}{\partial t} + \frac{\partial C}{\partial x}\frac{dx}{dt} + \frac{\partial C}{\partial y}\frac{dy}{dt} . \quad (30)$$

The second and third terms on the right side include the material derivatives of position, which are defined by the velocity in the x and y directions. We then have:

$$\frac{dx}{dt} = \frac{V_x}{R_f} \quad (31)$$

$$\frac{dy}{dt} = \frac{V_y}{R_f} \quad (32)$$

and

$$\frac{dC}{dt} = \frac{1}{R_f}\frac{\partial}{\partial x_i}\left(D_{ij}\frac{\partial C}{\partial x_j}\right) + \frac{W^*(C - C')}{\varepsilon R_f} - \lambda C . \quad (33)$$

The solutions of the system of equations comprising eqs. 31-33 may be given as $x = x(t)$, $y = y(t)$, and $C = C(t)$, and are called the characteristic curves of eq. 29. Given solutions to eqs. 31-33, a solution to the partial differential equation may be obtained by following the characteristic curves. This may be accomplished by introducing a set of moving points (or reference particles) that can be traced within the stationary coordinates of a finite-difference grid. Each particle corresponds to one characteristic curve, and values of x, y, and C are obtained as functions of t for each characteristic [67]. Each point has a concentration and position associated with it and is moved through the flow field in proportion to the flow velocity at its location (see fig. 2). Equation 33 can be solved using finite-difference approaches [57]. Random walk models make use of the analogy between dispersion and probability theory and solve eq. 33 by moving particles to account for advection (i.e. the mean velocity) and then adjusting their positions statistically to account for dispersion (i.e. by assuming that dispersion is mostly related to deviations in velocity about the mean, and representing that by a random function) [58-59].

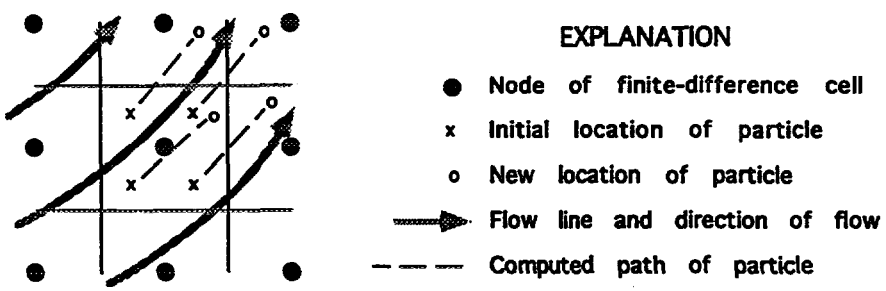

Figure 2. Part of a hypothetical finite-difference grid showing relation of flow field to movement of points (or particles) in method-of-characteristics model for simulating solute transport (modified from Konikow and Bredehoeft, 1978 [57]).

The conventional solute-transport equation is a Fickian model. However, most mechanical dispersion actually arises from variations in velocity about the mean, so essentially are an advective process. In discussing the development and derivation of the solute-transport equation, Bear (1979, p. 232) states, "As a working hypothesis, we shall assume that the dispersive flux can be expressed as a Fickian type law." This, in effect, is a practical engineering approximation for

the dispersion process that proves adequate for some field problems but inadequate for many others [8]. Field-scale dispersion (commonly called macrodispersion) results from large-scale spatial variations in hydraulic properties and the use of relatively large values of dispersivity with uniform hydraulic properties is an inappropriate basis for describing transport in geological systems [39]. Transport in stratified porous media may be non-Fickian in nature [69-70]. Thus, no matter how accurately we can solve the governing solute-transport equation, that equation itself is not necessarily a definitive and sufficient description of the processes controlling solute transport at the scale of most field problems. Overall, the more accurately a model can represent or simulate the true velocity distribution, the less of a problem will be the uncertainty concerning representation of dispersion processes.

There are additional complications when the solutes of interest are reactive. The reaction terms included in eq. 15 are mathematically simple ones. They do not necessarily represent the true complexities of many reactions. Also, particularly difficult numerical problems arise when reaction terms are highly nonlinear, or if the concentration of the solute of interest is strongly dependent on the concentration of other chemical constituents. In reality, isotherms may not be linear and may not be equilibrium controlled. Rubin (1983) discusses and classifies the chemical nature of reactions and their relation to the mathematical problem formulation [71]. Bahr and Rubin (1987) compare kinetic and local equilibrium formulations for solute transport affected by surface reactions [72]. For field problems in which reactions are significantly affecting solute concentrations, simulation accuracy is less limited by mathematical constraints than by data constraints. That is, the types and rates of reactions for the specific solutes and minerals in the particular ground-water system of interest are rarely known and require an extensive amount of data to assess accurately. Yeh and Tripathi (1989) review hydrogeochemical transport models and discuss various mathematical approaches to modeling transport of multiple reacting species [73].

5.1. Basics of finite-difference methods

The partial differential equations describing the flow and transport processes in ground water include terms representing derivatives of continuous variables. Finite-difference methods are based on the approximation of these derivatives (or slopes of curves) by discrete linear changes over small discrete intervals of space or time. If the intervals are sufficiently small, then all of the linear increments will represent a good approximation of the true curvilinear surface.

If we consider the observation wells in a confined aquifer, as illustrated in fig. 3a, Bennett (1976) [74] shows that a reasonable approximation for the derivative of head, $\partial h/\partial x$, at a point (d) midway between wells 1 and 0 is:

$$\left(\frac{\partial h}{\partial x}\right)_d \approx \frac{h_0 - h_1}{\Delta x} \tag{34}$$

Note that the observation wells are spaced an equal distance apart. Similarly, a reasonable approximation for the second derivative, $\partial^2 h/\partial x^2$, at point 0 (the location of the center well) can be given as:

$$\left(\frac{\partial^2 h}{\partial x^2}\right) \approx \frac{\left(\frac{\partial h}{\partial x}\right)_e - \left(\frac{\partial h}{\partial x}\right)_d}{\Delta x} = \frac{\frac{h_2 - h_0}{\Delta x} - \frac{h_0 - h_1}{\Delta x}}{\Delta x} = \frac{h_1 + h_2 - 2h_0}{(\Delta x)^2} \tag{35}$$

If we also consider wells 3 and 4 shown in fig. 3b, located on a line parallel to the y-axis, we can similarly approximate $\partial^2 h/\partial y^2$ at point 0 (the same point 0 as in fig. 3a) as [74]:

$$\left(\frac{\partial^2 h}{\partial y^2}\right) \approx \frac{h_3 + h_4 - 2h_0}{(\Delta y)^2} \tag{36}$$

If the spacing of the wells in fig. 3b is uniform (that is, $\Delta x = \Delta y = a$), then we can develop the following approximation:

$$\frac{\partial^2 h}{\partial x^2} + \frac{\partial^2 h}{\partial y^2} \approx \frac{h_1 + h_2 + h_3 + h_4 - 4h_0}{a^2} \tag{37}$$

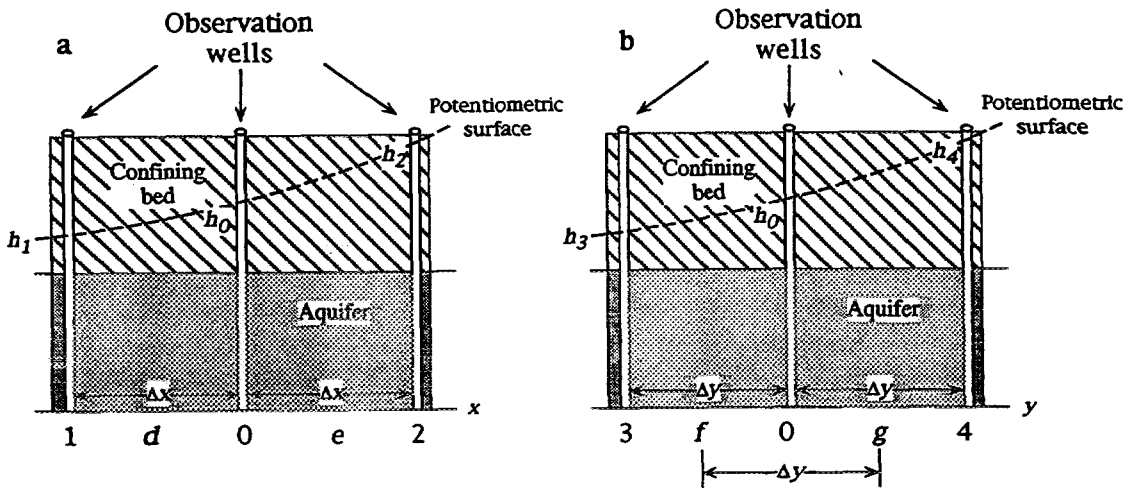

Figure 3. Schematic cross section through confined aquifer to illustrate numerical approximation to derivatives of head, $\partial h/\partial x$ (a) and $\partial h/\partial y$ (b) (modified from Bennett, 1976 [74]).

These approximations can also be obtained through the use of Taylor series expansions. A certain error is involved in approximating the derivatives by finite-differences, but this error will generally decrease as a (or Δx and Δy) is given smaller and smaller values. This error is called a "truncation error" because the replacement of a derivative by a difference quotient is equivalent to using a truncated Taylor series, so that the exact solution of a difference equation differs from the solution of the corresponding differential equation [49]. Also, it may not be possible to achieve an "exact" solution of the difference equation because of limits of precision in storing numbers in a digital computer. In solving a large set of difference equations, many arithmetic operations are performed, and round-off errors may sometimes accumulate.

Next consider the construction of a rectangular finite-difference grid. Two possible modes of construction of a grid to subdivide the solution region in the x-y plane are illustrated in fig. 4. In the first (fig. 4a) the calculation points (or nodes) are located at the centers of the blocks (or cells) formed by the grid lines. This type of grid is commonly called a *block-centered* grid. In the second type (fig. 4b) the nodes are considered to be located at the intersections of the grid lines. This type has been variously called a *point-centered*, *node-centered*, *mesh-centered*, or *lattice-centered* grid. Although there is no overall inherent advantage of one type over the other, there will be some operation differences between the two approaches in the treatment of boundaries and in areas of influence around

nodes. Most, but not all, finite-difference ground-water models are based on the use of block-centered grids.

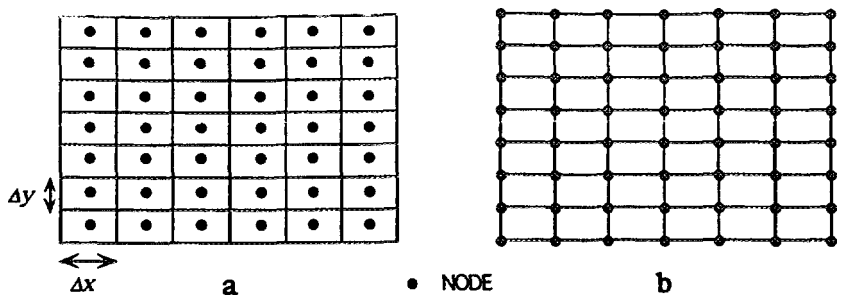

Figure 4. Two possible formulations of finite-difference grids; (a) block-centered grid and (b) node-centered grid.

Figure 5 shows a closer view of a representative part of a two-dimensional, variably-spaced, block-centered grid. The integer i is used as the index in the x-direction, and the integer j is the index in the y-direction. Thus, for example, x_i is the i^{th} value of x. Double indexing is normally used to identify functions and variables within the two-dimensional region. For example, $h_{i,j}$ is the head at node i,j. Note that some commonly available finite-difference ground-water models use a different convention for indexing in the y-direction, in that they assume that the j-index increases from the top towards the bottom of the grid, so that node $(1,1)$ is in the upper-left corner of the grid. Of course, which convention is used is arbitrary and makes no substantive difference.

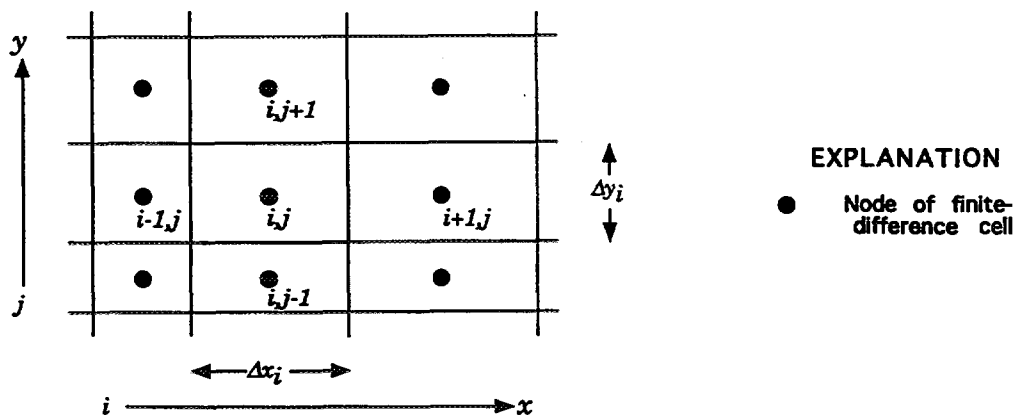

Figure 5. Part of a two-dimensional, block-centered, variably-spaced, finite-difference grid showing typical indexing scheme used to label nodes and cells.

We must also consider the discretization of time, which may be viewed as another dimension, and hence represented by another index. If we consider a representative segment of a hydrograph (see fig. 6), in which head is plotted against time for a transient flow system, n is the index or subscript used to denote the time at which a given head value is observed. The slope of the hydrograph at any point is the derivative of head with respect to time, and it can be approximated as $\partial h/\partial t \approx \Delta h/\Delta t$. In terms of the heads calculated at specific time increments (or time nodes), the slope of the hydrograph at time n can be approximated by:

$$\left(\frac{\partial h}{\partial t}\right)_{n\Delta t} \approx \frac{h_{n+1} - h_n}{\Delta t} \tag{38}$$

or

$$\left(\frac{\partial h}{\partial t}\right)_{n\Delta t} \approx \frac{h_n - h_{n-1}}{\Delta t} \tag{39}$$

We are calculating the derivative at $t = n\Delta t$ in eq. 38 by taking a "forward difference" from time n to time $n+1$, and by taking a "backward difference" in eq. 39. In terms of solving the ground-water flow equation for a node (i,j) of a finite-difference grid, we have to consider heads at five nodes and at two time levels, as illustrated in fig. 7. In fig. 7a, we have expressed the spatial derivatives of head at time level n, where all values are known, and the time derivative as a forward difference to the unknown head at time step $n+1$. Then for every node of the grid we will have a separate difference equation, each of which contains only one unknown variable. Thus, these equations can be solved explicitly. Explicit finite-difference equations are thus simple and straightforward to solve, but they may have stability criteria associated with them. That is, if time increments are too large, small numerical errors or perturbations may propagate into larger errors at later stages of the computations.

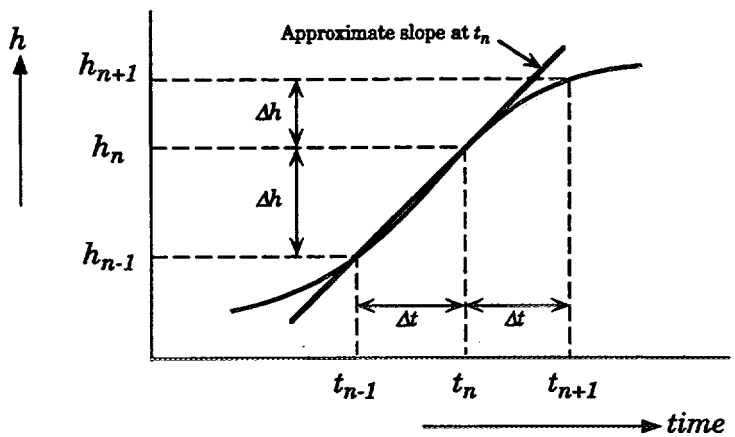

Figure 6. Part of a hydrograph showing that the derivative (or slope, $\partial h / \partial t$) at time node t_n may be approximated by $\Delta h / \Delta t$.

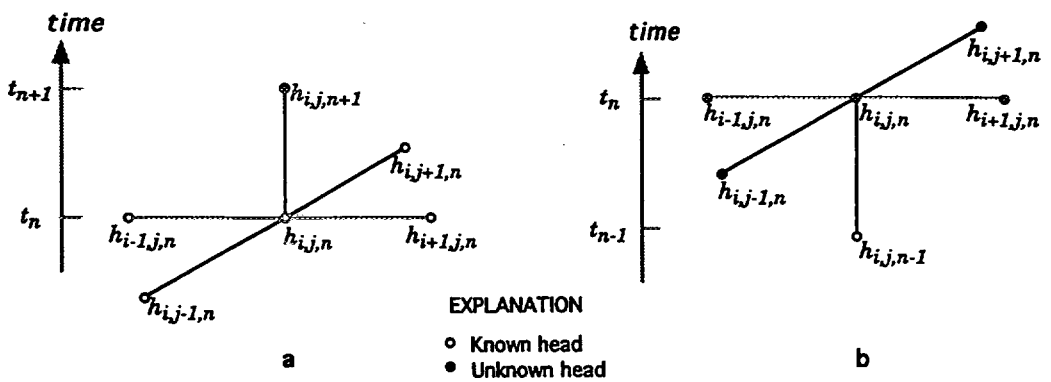

Figure 7. Grid stencil showing discretization of time at node (i,j) in two-dimensional finite-difference grid: (a) explicit (forward-difference) formulation and (b) implicit (backward-difference) formulation.

In fig. 7b we have expressed the time derivative as a backward difference from the heads at time level n, which are thereby the unknown heads, whereas the heads at the previous time level, n-1, are known (either from specified initial conditions for the first time step or from subsequent solutions at later time steps). The spatial derivatives of head are written at time level n, where all values are unknown, so for every node of the grid we will have one difference equation that contains five unknowns, which cannot be solved directly. However, for the entire grid, which contains N nodes, we would have a system of N equations containing a total of N unknowns. Such a system of simultaneous equations, together with specified boundary conditions, can be solved implicitly. Although implicit solutions are more complicated, they also have the advantage of generally being unconditionally stable. This implies that a solution will be obtained, not necessarily that the estimate of the derivative that is calculated will be accurate if the time steps are large relative to the rate of change of head. Most available ground-water flow models solve an implicit finite-difference approximation to the flow equation.

We may next consider a two-dimensional ground-water flow equation for a heterogeneous, anisotropic aquifer (eq. 10), in which the coordinate system is aligned with the major axes of the transmissivity tensor, and in which the source term is represented by eq. 7. This may be approximated by the following finite-difference equation for representative node (i,j) as:

$$T_{xx[i-\frac{1}{2},j]}\left(\frac{h_{i-1,j,n}-h_{i,j,n}}{(\Delta x)^2}\right)+T_{xx[i+\frac{1}{2},j]}\left(\frac{h_{i+1,j,n}-h_{i,j,n}}{(\Delta x)^2}\right)$$
$$+T_{yy[i,j-\frac{1}{2}]}\left(\frac{h_{i,j-1,n}-h_{i,j,n}}{(\Delta y)^2}\right)+T_{yy[i,j+\frac{1}{2}]}\left(\frac{h_{i,j+1,n}-h_{i,j,n}}{(\Delta y)^2}\right) \qquad (40)$$
$$=S\left(\frac{h_{i,j,n}-h_{i,j,n-1}}{\Delta t}\right)+\frac{q_{i,j}}{\Delta x\Delta y}-\frac{K_z}{m}\left(H_{s[i,j]}-h_{i,j,n}\right)$$

where $q_{i,j}$ is the volumetric rate of withdrawal or recharge at the i,j node, L^3T^{-1}. This formulation inherently assumes that any stresses, such as represented by $q_{i,j}$, are applied over the entire surface area of cell i,j rather than at a point (or at node i,j). This implies that if a pumping well is represented at node i,j, then the head will be calculated as if it were being withdrawn from a well that had a borehole surface area equal to $\Delta x\Delta y$ rather than its actual value. In eq. 40 the transmissivity terms represent the harmonic means of the transmissivity of the two adjacent cells. The harmonic mean can be shown to be appropriate and consistent with the assumption that transmissivity is constant and uniform within each cell but may be different between cells. Other types of means for interblock transmissivity may be more appropriate for other assumptions about the transmissivity distribution, such as smoothly varying transmissivity [75].

5.2. Matrix solution techniques

As indicated, each numerical approximation leads to an algebraic equation for each node point. These are combined to form a matrix equation, which may be solved numerically by one of two basic methods: direct or iterative. In direct methods, a sequence of operations is performed only once, providing a solution that is exact, except for machine round-off error. Iterative methods attempt solution by a process of successive approximation. They involve making an initial

guess at the matrix solution, then improving this guess by some iterative process until an error criterion is satisfied. Therefore, in these techniques, convergence and the rate of convergence are of concern.

Numerical solution can be illustrated using a simple example having two equations with two unknowns. Say you have the following two simultaneous equations, and wish to solve for x and y:

$$x + y = 3 \tag{41}$$

$$x + 2y = 4 \tag{42}$$

These can first be rearranged to express each unknown separately, as:

$$x = 3 - y \tag{43}$$

$$y = \left(\frac{4 - x}{2}\right) \tag{44}$$

Then each of these two equations can be solved iteratively by substituting the previous value of the variable on the right side (the "known" variable) into each equation, and solving for the "unknown" variable on the left side; the solution sequence is initiated using some initial (and perhaps arbitrary) "guess" for each variable as a starting point. The following table illustrates such a calculation sequence for the above two equations, solving both equations at each level of iteration by substituting the value of the "known" variable from the previous level of iteration.

	Iteration Number	x (eq. 43)	y (eq. 44)
initial guess ⇒	0	0	0
	1	$x = 3\text{-}0 = 3$	$y = (4\text{-}0)/2 = 2$
	2	$x = 3\text{-}2 = 1$	$y = (4\text{-}3)/2 = ½$
	3	2½	1½
	4	1½	¾
	5	2¼	1¼
	⋮	⋮	⋮
	∞	2	1

It can be seen in the above example that the solution is converging on the true values of $x = 2$ and $y = 1$. However, the rate of convergence can be speeded up by modifying the iterative routine to substitute the most recently updated value of the variables on the right side of the equations, as illustrated in the following table.

	Iteration Number	x (eq. 43)	y (eq. 44)
initial guess ⇒	0	0	0
	1	$x = 3\text{-}0 = 3$	$y = (4\text{-}3)/2 = ½$
	2	$x = 3\text{-}½ = 2½$	$y = (4\text{-}2½)/2 = ¾$
	3	2¼	⅞
	4	2⅛	15/16
	5	2 1/16	31/32
	⋮	⋮	⋮
	∞	2	1

In the second example, the convergence to the solution is much faster and smoother (which helps assure numerical stability). This approach is sometimes called a Gauss-Seidel method of iteration (or method of successive displacements), whereas the former is sometimes called the Jacobi method (or method of simultaneous displacements) [49]. There are many other variants possible when the number and complexity of the system of equations grows large.

Another alternative to solving the system of simultaneous equations is to solve them directly, which can be illustrated for the simple set above. First substitute eq. 43 into eq. 44 (or vice versa) to obtain:

$$y = \left(\frac{4-(3-y)}{2}\right) = \left(\frac{1+y}{2}\right) \tag{45}$$

Rearranging terms and solving for y yields the result $y = 1$. Then back substitute into eq. 43 to obtain: $x = (3-y) = (3-1)$, or $x = 2$.

Direct methods can be further subdivided into: (1) solution by determinants, (2) solution by successive elimination of the unknowns, and (3) solution by matrix inversion. Direct methods have two main disadvantages. The first problem deals with storage requirements and computation time for large problems. The matrix is sparse (contains many zero values) and in order to minimize computational effort, several techniques have been proposed. Various schemes of numbering the nodes have been studied; an efficient one for finite-difference nodes is alternating direction (D4) ordering [76]. Other methods have been attempted with the finite-element method. However, for finite-difference and finite-element methods, storage requirements may still prove to be unavoidably large for three-dimensional problems. The second problem with direct methods deals with round-off errors. Because many arithmetic operations are performed, round-off errors can accumulate for certain types of matrices.

Iterative schemes avoid the need for storing large matrices, which make them attractive for solving problems with many unknowns. Numerous schemes have been developed; a few of the more commonly used ones include successive over-relaxation methods, iterative alternating-direction implicit procedure, and the strongly implicit procedure [49-50, 52, 77].

Because iterative methods start with an initial estimate for the solution, the efficiency of the method depends somewhat on this initial guess. To speed up the iterative process, relaxation and acceleration factors are used. Unfortunately, the definition of best values for these factors commonly is problem dependent. In addition, iterative approaches require that an error tolerance be specified to stop the iterative process. An optimal value for the tolerance, which is used to evaluate when the iterative calculations have converged on a solution, may also be problem dependent. If the tolerance is set too large, then the iterations may stop before adequate numerical accuracy is achieved. If the tolerance is set too small, then the iterative process may consume excessive computational resources in striving for numerical precision that may be orders of magnitude smaller than the precision of the field data, or the iterative process may even fail to converge.

More recently, a semi-iterative method, or class of methods, known as conjugate-gradient methods, has gained popularity. One advantage of the conjugate-gradient method is that it does not require the use or specification of iteration parameters, thereby eliminating this partly subjective procedure. A comparison of the efficiency of 17 different iterative methods for the solution of the nonlinear three-dimensional ground-water flow equation indicated that, in general, the conjugate gradient methods did the best [78].

5.3. Boundary and initial conditions

In order to obtain a unique solution of a partial differential equation corresponding to a given physical process, additional information about the physical state of the process is required. This information is described by boundary and initial conditions. For steady-state problems, only boundary conditions are required, whereas for transient problems, boundary and initial conditions must be specified. A steady-state solution for ground-water flow may be achieved by setting the storativity equal to 0.0 (as in eq. 6 or eq. 40), which effectively determines that there will be no change in head with respect to time.

Mathematically, the boundary conditions include the geometry of the boundary and the values of the dependent variable or its derivative normal to the boundary. In physical terms, for ground-water model applications, the boundary conditions are generally of three types: (1) specified value (head or concentration), (2) specified flux (corresponding to a specified gradient of head or concentration), or (3) value-dependent flux (or mixed boundary condition, in which the flux across a boundary is related to both the normal derivative and the value) [79]. An example where the third type of boundary condition might be applicable is to represent leakage or exchange between a stream and an adjacent aquifer, in which the leakage may change over time as the head in the aquifer changes, even though the head in the stream might remain fixed. A no-flow boundary is a special case of the second type of boundary condition. The types of boundaries appropriate to a particular field problem may require careful consideration.

The initial conditions are simply the values of the dependent variable specified everywhere inside the boundary. If initial conditions are specified so that transient flow is occurring in the system at the start of the simulation, it should be recognized that heads will change during the simulation, not only in response to the new pumping stress, but also due to the initial conditions [77]. This may or may not be intended by the model user.

6. MODEL DESIGN, DEVELOPMENT, AND APPLICATION

The first step in model design and application is to define the nature of the problem and evaluate the purpose of the model. Although this may seem obvious, it is an important first step that is sometimes overlooked in a hasty effort to take action. This step is closely linked with the formulation of a conceptual model, which again is required prior to development of a simulation model. A possible outcome of such a preliminary assessment might even be that a deterministic simulation model is not needed. In formulating a conceptual model, the analyst must evaluate which processes are significant in the system being investigated for the particular problem at hand. Some processes may be important to consider at one scale of study, but negligible or irrelevant at another scale of investigation. The analyst must similarly decide on the appropriate dimensionality for the numerical model. Good judgment is required to evaluate and balance the tradeoffs between accuracy and cost, with respect to both the model and to data requirements. The key to efficiency and accuracy in modeling a system probably is more affected by the formulation of a proper and appropriate conceptual model than by the choice of a particular numerical method or code.

Once a decision to develop a model has been made, a code (or generic model) must be selected (or modified or constructed) that is appropriate for the given problem. Next, the generic code must be adapted to the specific site or region being simulated. Development of a numerical deterministic, distributed-parameter, simulation model involves selecting or designing spatial grids and

time increments that will yield an accurate solution for the given system and problem. The analyst must then specify the properties of the system (and their distributions), stresses on the system (such as recharge and pumping rates), boundary conditions, and initial conditions (for transient problems). All of the parameter specifications and boundary conditions are really part of the overall conceptual model of the system, and the initial numerical model reflects the analyst's conceptual model of the system.

It must always be remembered that a model is an approximation of a very complex reality, and a model is used to simplify that reality in a manner that captures or represents the essential features and processes relative to the problem at hand. In the development of a deterministic ground-water model for a specific area and purpose, we must select an appropriate level of complexity (or, rather, simplicity). We are inclined to believe that finer resolution in a model will yield greater accuracy, and there is a legitimate basis for this. However, there also exists the practical constraint that even when appropriate data are available, a finely discretized three-dimensional numerical model may be too large to run on available computers, especially if transport processes are included. The selection of the appropriate model and appropriate level of complexity remains subjective and dependent on the judgment and experience of the analysts, the objectives of the study, and level of prior information on the system of interest. The trade-off between model accuracy and model cost will always be a difficult one to resolve, but will always have to be made. In any case, water managers and other users of model results must be made aware that these trade-offs and judgments have been made and may affect the reliability of the model.

In general, it is more difficult to calibrate a solute-transport model of an aquifer than it is to calibrate a ground-water flow model. Fewer parameters need to be defined to compute the head distribution with a flow model than are required to compute concentration changes using a solute-transport model. Because the ground-water seepage velocity is determined from the head distribution, and because both advective transport and hydrodynamic dispersion are functions of the seepage velocity, a model of ground-water flow is often calibrated before a solute-transport model is developed. In fact, in a field environment perhaps the single most important key to understanding a solute-transport problem is the development of an accurate definition (or model) of the flow system. This is particularly relevant to transport in fractured rocks, where simulation is commonly based on porous-media concepts. Although the potential (or head) field can often be simulated, the required velocity field may be greatly in error.

Major questions in the application of a ground-water model concern the model's ability to represent the processes that are controlling responses in the system of interest and the reliability of the predictions. Regarding concepts and parameters, Watson's (1969) cautioning statement is relevant [80]: "*Just because we do or must describe the world in a given way does not mean that the world is really that way.*"

6.1. Model verification

One of the first things that must be demonstrated is that the generic model accurately solves the governing equations for various boundary value problems, an evaluation that is often called model "verification." This is checked by demonstrating that the code gives good results for problems having known solutions. This test is usually done by comparing the numerical model results to that of an analytical solution. Numerical accuracy is rarely a problem for the

solution to the flow equation, but may sometimes be a significant obstacle in transport modeling.

It must be remembered that numerical solutions are sensitive to spatial and temporal discretization. Therefore, even a perfect agreement for test cases only proves that the numerical code *can* accurately solve the governing equations, not that it *will* under any and all circumstances.

Analytical solutions generally require simple geometry, uniform properties, and idealized boundary and initial conditions. The power of the numerical methods is that they relax the simplification imposed by analytical methods and allow the introduction of nonhomogeneous, anisotropic parameter sets, irregular geometry, mixed boundary conditions, and even nonlinearities into the boundary value problems. Usually, analytical solutions approximating these complexities are unavailable for comparison. The problem is: *Once these complexities are introduced, how does one know the computer code is calculating an accurate solution to the governing equations?* The answer is: *One cannot be sure!* You can do simple tests, such as checking mass conservation and evaluating the global mass-balance error, but in the final analysis you cannot be sure [6].

One approach that improves confidence for complex heterogeneous problems is to compare the model results to experimental data, to results of other well accepted models, or to some other accepted standard. Such evaluations might best be termed *benchmarking*. The HYDROCOIN Project used standardized problem definitions as a basis for intercode comparisons [81]. While this type of benchmarking helps assure consistency, it does not guarantee or measure accuracy. A collection and detailed discussion of a number of classical ground-water problems that have been used historically as a basis of model evaluation are presented and documented by Ségol (1994) [82].

6.2. Grid design

The dimensionality of the model (i.e. one-, two-, or three-dimensions) should be selected during the formulation of the conceptual model. If a one- or two-dimensional model is selected, then it is important that the grid be aligned with the flow system so that there is no unaccounted flux into or out of the line or plane of the grid. For example, if a two-dimensional areal model is applied, then there should be no significant vertical components of flow and any vertical leakage or flux must be accounted for by boundary conditions; if a two-dimensional profile model is applied, then the line of the cross section should be aligned with an areal streamline, and there should not be any lateral flow into or out of the plane of the cross section.

To minimize a variety of sources of numerical errors, the model grid should be designed using the finest mesh spacing and time steps that are possible, given limitations on computer memory and computational time. To the extent possible, the grid should be aligned with the fabric of the rock and with the average direction of ground-water flow. The boundaries of the grid also should be aligned, to the extent possible, with natural hydrologic and geologic boundaries of the system of interest. Where it is impractical to extend the grid to a natural boundary, then an appropriate boundary condition should be imposed at the edge of the grid to represent the net effects of the continuation of the system beyond the grid. This can typically be accomplished using head-dependent leakage (third type) boundary conditions. These boundaries should also be placed as far as possible away from the area of interest and areas of stresses on the system, so as to minimize any impact of conceptual errors associated with these artificial boundary conditions.

In designing the grid, the length to width ratio (or aspect ratio) of cells or elements should be kept as close to one as possible. Long linear cells or elements can lead to numerical instabilities or errors, and should be avoided, particularly if the aspect ratio is greater than about five [4]. However, this is a loose guideline as aspect ratios exceeding 100:1 are often used with no problem. In applying this guideline to triangular finite-element methods, Torak (1992) recommends that angles less than 22.5 degrees in a triangle should be avoided [83]. However, in anisotropic materials, the effective aspect ratio is equivalent to a transformed isotropic domain [4]. Freeze and Cherry (1979, p. 174-178) show that this transformation is based on the ratio of the square roots of the principal hydraulic conductivity values. For example, if $K_z = 1$ and $K_x = 100$, then the ratio of $\sqrt{K_z}/\sqrt{K_x} = 0.1$; if Δz is 1 m and Δx is 10 m, then the effective aspect ratio is one.

In specifying boundary conditions for a particular problem and grid design, care must be taken to not overconstrain the solution. That is, if dependent values are fixed at too many boundary nodes, at either internal or external nodes of a grid, the model may have too little freedom to calculate a meaningful solution. At the extreme, by manipulating boundary conditions, one can force any desired solution at any given node. While this may assure a perfect match to observed data used for calibration, it is of course not an indicator of model accuracy or reliability, and in fact is meaningless.

To optimize computational resources in a model, it is generally advisable to use an irregular (or variably-spaced) mesh in which the grid is finest in areas of point stresses, where gradients are steepest, where data are most dense, where the problem is most critical, and (or) where greatest numerical accuracy is desired. It is generally advisable to increase the mesh spacing by a factor no greater than about two between adjacent cells or elements. Similarly, time steps can often be increased geometrically during a simulation. At the initial times or after a change in the stress regime, very small time steps should be imposed, as that is when changes over time are the greatest. With increased elapsed time, the rate of change in head typically decreases, so time steps can often be safely increased by a factor of two or more.

Equation 26 describes the cross-product terms of the dispersion tensor. Because transmissivity is a property of the porous media, the cross-product terms of the transmissivity tensor can typically be dropped out of the governing flow equation that is solved in a model by aligning the model grid with the major axes of the transmissivity tensor (as represented in eq. 10). However, this cannot typically be done for the dispersion tensor in the transport equation because it is related to, and depends on, the flow direction, which changes orientation over space and time. There is, in general, no way to design a fixed grid that will always be aligned with a changing flow field.

6.3. Model calibration

Deterministic ground-water simulation models impose large requirements for data to define all of the parameters at all of the nodes of a grid. To determine uniquely the parameter distribution for a field problem would require so much expensive field testing that it is seldom feasible either economically or technically. Therefore, the model typically represents an attempt, in effect, to solve a large set of simultaneous equations having more unknowns than equations. It is inherently impossible to obtain a unique solution to such a problem.

Uncertainty in parameters logically leads to a lack of confidence in the interpretations and predictions that are based on a model analysis, unless it can be demonstrated that the model is a reasonably accurate representation of the real system. To demonstrate that a deterministic ground-water simulation model is realistic, it is usual to compare field observations of aquifer responses (such as changes in water levels for flow problems or changes in concentration for transport problems) to corresponding values calculated by the model. The objective of this calibration procedure is to minimize differences between the observed data and calculated values. Usually, the model is considered calibrated when it reproduces historical data within some acceptable level of accuracy. What level is acceptable is, of course, determined subjectively. Although a poor match provides evidence of errors in the model, a good match in itself does not prove the validity or adequacy of the model [6].

Because of the large number of variables in the set of simultaneous equations represented in a model, calibration will not yield a unique set of parameters. Where the match is poor, it suggests (1) an error in the conceptual model, (2) an error in the numerical solution, or (3) a poor set of parameter values. It may not be possible to distinguish among the several sources of error [6]. Even when the match to historical data is good, the model may still fail to predict future responses accurately, especially under a new or extended set of stresses than experienced during the calibration period.

Matalas and Maddock (1976) argue that model calibration is synonymous with parameter estimation [84]. The calibration of a deterministic ground-water model is often accomplished through a trial and error adjustment of the model's input data (aquifer properties, sources and sinks, and boundary and initial conditions) to modify the model's output. Because a large number of interrelated factors affect the output, this may become a highly subjective and inefficient procedure. Advances in parameter identification procedures help to eliminate some of the subjectivity inherent in model calibration [9, 85-88]. The newer approaches tend to treat model calibration as a statistical procedure. Thus, multiple regression approaches allow the simultaneous construction, application, and calibration of a model using uncertain data, so that the uncertainties are reflected as estimated uncertainties in the model output and hence in predictions or assessments to be made with the model [89].

However, even with regression modeling, the hydrologic experience and judgment of the modeler continues to be a major factor in calibrating a model both accurately and efficiently, even if automated procedures are used. In any case, the modeler should be very familiar with the specific field area being studied to know that both the data base and the numerical model adequately represent prevailing field conditions. The modeler must also recognize that the uncertainty in the specification of sources, sinks, and boundary and initial conditions should be evaluated during the calibration procedure in the same manner as the uncertainty in aquifer properties. Failure to recognize the uncertainty inherent both in the input data and in the calibration data may lead to "fine-tuning" of the model through artificially precise parameter adjustments strictly to improve the match between observed and calculated variables. This may only serve to falsely increase the confidence in the model without producing an equivalent (or any) increase in its predictive accuracy. This was illustrated by Freyberg (1988) in an exercise in which several groups were given the task of modeling a particular hypothetical problem [90]. He showed that the group that achieved the best calibration, as measured by the minimum root mean square error, was not the group that developed the model that yielded the best prediction (measured by the same criteria). He concluded that simple measures of goodness

of a calibrated fit are inadequate to evaluate the true worth of a calibrated parameter set [90].

Figure 8 illustrates in a general manner the use and role of deterministic models in the analysis of ground-water problems. The value of the modeling approach is its capability to integrate site-specific data with equations describing the relevant processes as a quantitative basis for predicting changes or responses in a ground-water system. There must be allowances for feedback from the stage of interpreting model output both to the data collection and analysis phase and to the conceptualization and mathematical definition of the relevant governing processes. One objective of model calibration should be to improve the conceptual model of the system. Because the model numerically integrates the effects of the many factors that affect ground-water flow or solute transport, the calculated results should be internally consistent with all input data, and it can be determined if any element of the conceptual model should be revised. In fact, prior concepts or interpretations of aquifer parameters or variables, such as represented by potentiometric maps or the specification of boundary conditions, may be revised during the calibration procedure as a result of feedback from the model's output. In a sense, any adjustment of input data constitutes a modification of the conceptual model.

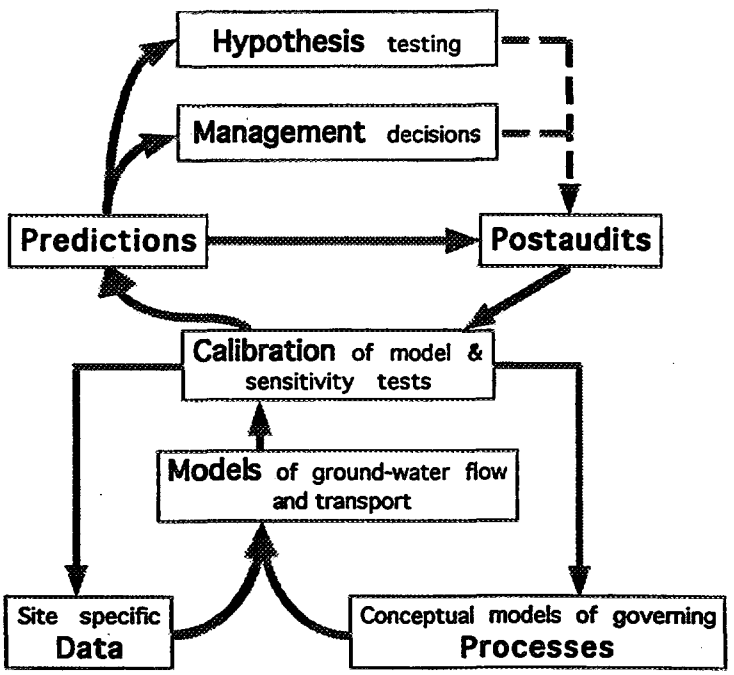

Figure 8. The use and role of models in the analysis of ground-water problems.

Automated parameter-estimation techniques improve the efficiency of model calibration and have two general components--one part that calculates the best fit (sometimes called automatic history matching) and a second part that evaluates the statistical properties of the fit. The objective of automatic history matching is to obtain the estimates of system parameters that yield the closest match (minimizes deviations) between observed data and model calculations. Least squares deviation is usually chosen as a criteria. The minimization procedure uses sensitivity coefficients that are based on the change in calculated value divided by the change in the parameter. For ground-water flow, for

example, this may take the specific form of $\partial h/\partial T$; that is, the change in head with changing transmissivity. The sensitivity coefficients themselves may be useful in the consideration of additional data collection.

Parameter uncertainty is commonly addressed using a sensitivity analysis. A major objective of sensitivity analysis of simulation models is to determine the change in model results as a result of changes in the model input or system parameters. Conventional sensitivity analysis uses direct parameter sampling in which parameters are perturbed one by one and the complete set of system equations are resolved [91]. Sensitivity coefficients for each of these perturbed parameters may be derived by a finite-difference approximation. Considerable research in parameter uncertainty in ground-water models has been conducted since Freeze's (1975) paper [92] that considered the parameters in model equations to be stochastic, rather than fixed. Comprehensive reviews of the available literature are provided by [11, 93-94].

6.4. Errors

Discrepancies between observed and calculated responses of a system are the manifestation of *errors* in the mathematical model. In applying ground-water models to field problems, there are three sources of error [6]. One source is conceptual errors--that is, theoretical misconceptions about the basic processes that are incorporated in the model. Conceptual errors include both neglecting relevant processes as well as representing inappropriate processes. Examples of such errors include the application of a model based upon Darcy's Law to media or environments where Darcy's Law is inappropriate, or the use of a two-dimensional model where significant flow or transport occurs in the third dimension. A second source of error involves numerical errors arising in the equation-solving algorithm. These include truncation errors, round-off errors, and numerical dispersion. A third source of error arises from uncertainties and inadequacies in the input data that reflect our inability to describe comprehensively and uniquely the aquifer properties, stresses, and boundaries. In most model applications conceptualization problems and uncertainty concerning the data are the most common sources of error.

Numerical methods in general yield approximate solutions to the governing equations. There are a number of possible sources of numerical error in the solution. If the modeler is aware of the source and nature of these errors, they can control them and interpret the results in light of them. In solving advection dominated transport problems, in which a relatively sharp front (or steep concentration gradient) is moving through a system, it is numerically difficult to preserve the sharpness of the front. Obviously, if the width of the front is narrower than the node spacing, then it is inherently impossible to calculate the correct values of concentration in the vicinity of the sharp front. However, even in situations where a front is less sharp, the numerical solution technique can calculate a greater dispersive flux than would occur by physical dispersion alone or would be indicated by an exact solution of the governing equation. That part of the calculated dispersion introduced solely by the numerical solution algorithm is called *numerical dispersion*, as illustrated in fig. 9. Because the hydrologic interpretation of isotopic data is sensitive to mixing phenomena in an aquifer, numerical mixing (or dispersion) can have the same effect on the interpretation of model-calculated isotopic values. Therefore, care must be taken to assess and minimize such numerical errors that would artificially add "numerical" mixing to the calculated mixing attributable to physical and chemical processes.

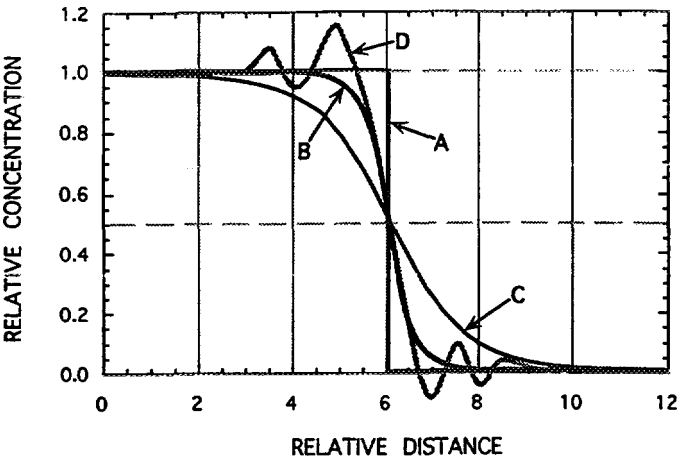

Figure 9. Representative breakthrough curves for a simple flow and transport problem to illustrate types of numerical errors that may occur in numerical solution to transport equation: (A) plug flow having no dispersion, (B) "exact" solution for transport with dispersion, (C) numerical solution for case *B* that exhibits effects of numerical dispersion, and (D) numerical solution for case *B* that exhibits oscillatory behavior.

Figure 9 illustrates calculated breakthrough curves for a hypothetical problem of uniform flow and transport to the right, at some time and distance after a tracer having a relative concentration of 1.0 was injected at some point upstream. Curve *A* represents the breakthrough curve and position of a sharp front for a case having no dispersion (plug flow). Curve *B* represents an exact analytical solution for a nonzero dispersivity. Curve *C* illustrates the breakthrough curve calculated using a numerical method that introduces numerical dispersion.

Numerical dispersion can be controlled by reducing the grid spacing (Δx and Δy). However, reduction to a tolerable level may require an excessive number of grid points for a particular region to be simulated and render the computational costs unacceptably high [49]. It may also be controlled in finite-element methods by using higher order basis functions or by adjusting the formulation of the difference equations (using different combinations of forward, backward, or centered in time and/or space, or using different weighting functions). Unfortunately, many approaches that eliminate or minimize numerical dispersion introduce oscillatory behavior, causing overshoot behind a moving front and possibly undershoot ahead of the front (see curve *D* in fig. 9), and *vice versa*. Undershoot can result in the calculation of negative concentrations, which are obviously unrealistic. However, overshoot can introduce errors of equal magnitude that may go unnoticed because the value is positive in sign (although greater than the source concentration, so still unrealistic). Oscillations generally do not introduce any mass balance errors, and often dampen out over time. However, in some cases, oscillatory behavior can become unbounded, yielding an unstable solution or failure to converge numerically.

In solving the advective-dispersive transport equation, some numerical errors (mainly oscillations) can be related to two dimensionless parameter groups (or numbers). One is the Peclet number, P_e, which may be defined as $P_e = \Delta l/\alpha$, where Δl is a characteristic nodal spacing (although it should be noted that there are several alternative, though essentially equivalent, ways to define P_e) [4].

Anderson and Woessner (1992) recommend that the grid be designed so that $\Delta l < 4\alpha$ (or $P_e < 4$), although Ségol (1994) recommends a criteria of $P_e \leq 2$. Similarly, time discretization can be related to the Courant number, C_O, which may be defined as $C_O = V\Delta t / \Delta l$ [4]. Anderson and Woessner (1992) also recommend that time steps be specified so that $\Delta t < \Delta l / V$ (or $C_O < 1.0$), which is equivalent to requiring that no solute be displaced by advection more than one grid cell or element during one time increment. The deviations of curves *C* and *D* from the exact solution can be significant in some locations, although such errors tend to be minimal at the center of a front (relative concentration of 0.5).

In solving the transport equation, classical numerical methods exhibit the proportionately largest numerical errors where the relative (or dimensionless) concentrations (C/C_{max}) are lowest [95]. Dougherty and Bagtzoglou (1993) show that the error-to-signal (or noise-to-signal) ratio can become quite large (>0.1) where the relative concentrations are less than 0.01 [95]. In isotope analyses of ground-water systems, the samples from areas of interest frequently reflect concentrations less than 0.01 of the source concentration, so caution is warranted.

In transport models there may also be a grid-orientation effect, in which the solute distribution, calculated for the same properties and boundary conditions, will vary somewhat depending on the angle of the flow relative to the grid. This phenomena is largely related to the cross-product terms in the governing equation, and generally is not a serious source of error, but the model user should be aware of it.

6.5. Mass Balance

One measure of model accuracy is how well the model conserves mass. This can be measures by comparing the net fluxes calculated or specified in the model (e.g. inflow and sources minus outflow and sinks) with changes in storage (accumulation or depletion). Mass-balance calculations should always be performed and checked during the calibration procedure to help assess the numerical accuracy of the solution.

As part of these calculations, the hydraulic and chemical fluxes contributed by each distinct hydrologic component of the flow and transport model should be itemized separately to form hydrologic and chemical budgets for the system being modeled. The budgets are valuable assessment tools because they provide a measure of the relative importance of each component to the total budget.

Errors in the mass balance for flow models should generally be less than 0.1 percent. However, because the solute-transport equation is more difficult to solve numerically, the mass-balance error for a solute may be greater than for the fluid, but this will depend also on the nature of the numerical method implemented. Finite-difference and finite-element methods are inherently mass conservative, while some implementations of the method of characteristics and particle tracking approaches may not be (or their mass balance calculations themselves are only approximations). It must also be remembered that while a large mass-balance error provides evidence of a poor numerical solution, a perfect mass balance in itself does not and cannot prove that a true or accurate solution has been achieved or that the overall model is valid. That is, a perfect mass balance can be achieved if the model includes compensating errors. For example, the solutions *C* and *D* in fig. 9 that exhibit significant numerical dispersion or oscillatory behavior arise from solutions that show a near-perfect mass balance, but they are still wrong.

6.6. Parameter adjustment

Many input data are required for a numerical model, and the accuracy of these data will affect the reliability of the calculated results. In all field problems there are some inadequate data, so values of parameters will have to be estimated. A common approach is to first assume the best estimate of values for parameters, and then adjust their values until a best fit is achieved between the observed and computed dependent variables. Although this can be accomplished most efficiently using a parameter-estimation model, such as MODFLOWP [96], a trial and error method is still commonly used.

In order to maintain the value of the process-oriented structure of a deterministic model, the degree of allowable adjustment should generally be directly proportional to the uncertainty of its value or specification, and limited to its range of expected values or confidence interval. For example, in a study of the Madison Limestone regional aquifer system, historical pumping rates were relatively well known, so their values were not adjusted [97]. But because the transmissivity was poorly defined, various values were assumed over a possible range of several orders of magnitude.

Parameter adjustment produces changes in model output. The responses to parameter adjustment should be evaluated quantitatively to provide the modeler with a measure of progress during model calibration and a guide for determining the direction and magnitude of subsequent changes in the goodness of fit between the observed data and the model output. One procedure for evaluation is to plot changes of the mean difference between observed and computed data and changes in the standard error of estimate for successive simulation tests during model calibration.

As an example, this procedure was used in calibrating a flow and transport model for contaminant migration in an alluvial aquifer system in Colorado [98]. In this case, the water-table configuration served as the basis for evaluating goodness of fit with respect to adjustments of transmissivity, net recharge in irrigated areas, and some boundary conditions. Initial estimates of net recharge were used in a preliminary calibration of the model. Next, initial estimates of transmissivity values and boundary conditions were adjusted between successive simulations with an objective of minimizing the differences between observed and computed water-table elevations in the irrigated area. As shown in fig. 10a, the standard error of estimate (a statistical measure of scatter similar to the standard deviation) generally decreased as successive simulation tests were made. After about seven tests, additional parameter adjustments produced only small improvements in the fit. At this point, the standard error of estimate was about 0.35 m, which was approximately the same as the reliability of the water-table elevations, which was limited because of variability in the times of measurements, measurement errors, unknown vertical components of flow, varying distances of observation wells to stress points, uncertain and varying depths of well screens and openings. Therefore, it was judged that further refinements would essentially represent calibration to the noise in the data, and would not lead to a better model. A final estimate of the net recharge rate in irrigated areas was made using the values for other parameters developed for the previous test having a minimum standard error of estimate. The mean of the differences between observed and computed heads at all nodes in the irrigated area was then minimized (equal to zero) when a net recharge rate of about 0.47 m/yr was assumed, so this was the value selected for the model (see fig. 10b). A drawback to this trial and error approach is that the uniqueness of the solution cannot be easily demonstrated.

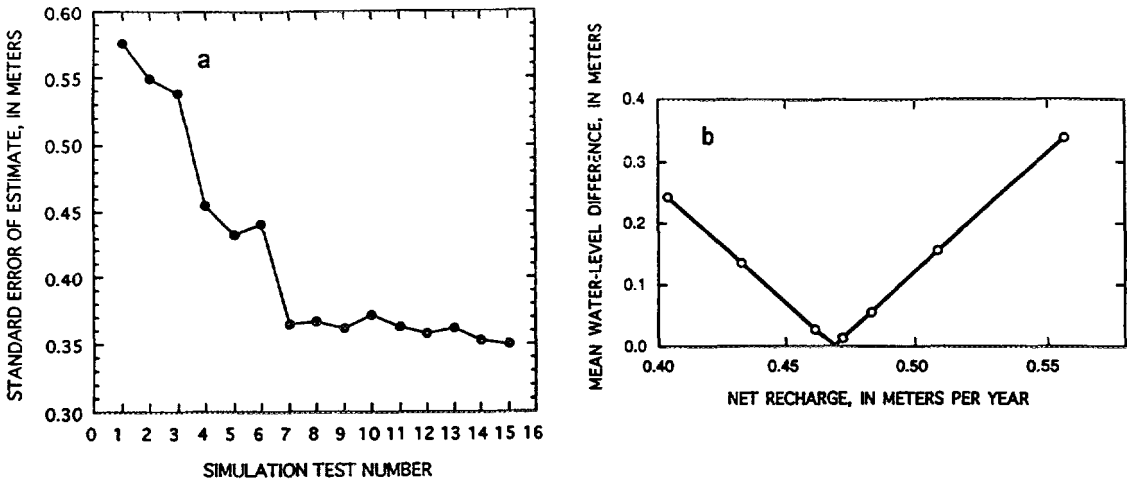

Figure 10. Selected calibration criteria for ground-water model of shallow aquifer at the Rocky Mountain Arsenal, Colorado; (a) change in standard error of estimate for successive simulation tests during calibration, and (b) relation between net recharge rate in irrigated areas and mean error in head (modified from Konikow, 1977 [98]).

6.7. Sensitivity tests

Assuming various values for given parameters also helps to achieve another objective of the calibration procedure, namely to determine the sensitivity of the model to factors that affect ground-water flow and transport and to errors and uncertainty in the data. Evaluating the relative importance of each factor helps determine which data must be defined most accurately and which data are already adequate or require only minimal further definition. If additional data can be collected in the field, such a sensitivity analysis helps you decide which types of data are most critical and how to get the best information return on the costs of additional data collection. If additional data cannot be collected, then the sensitivity tests can help to assess the reliability of the model by demonstrating the effect of a given range of uncertainty or error in the input data on the output of the model. The relative sensitivities of the parameters that affect flow and transport will vary from problem to problem. Furthermore, the sensitivities may change over time as the stress regime imposed on a system evolves. Thus, one generalization is that a sensitivity analysis should be performed during the early stages of a model study.

The sensitivity of the solution to the grid design (or spacing), time-step criteria, nature and placement of boundary conditions, and other numerical parameters should also be evaluated, even if an inverse or regression modeling approach has been used. This is frequently overlooked, but failure to do so may cause critical design flaws to remain undetected. For example, parameter-estimation models cannot calculate the sensitivity to grid spacing or certain boundary conditions that are fixed in the model by the user. A general approach that works is after a preliminary calibration has be achieved with a model, it should be rerun for the same stresses and properties using a finer grid, smaller time steps, and perhaps alternative boundary conditions. If such a test yields significantly different results, then the model should be recalibrated using design criteria that yield a more accurate numerical solution. If such a test yields no

model; one of their conclusions was that parameter estimation methods should use only discrete data points in order to produce answers that are free of contouring interpretations [101].

When the statistical analyses of the fits between observed and computed values of relevant variables indicate the attainment of an acceptable level of accuracy for the problem at hand, then the model may be accepted as calibrated. However, if any major additions or revisions are made to the observed data base at a later time, the model should be recalibrated.

6.9. Predictions and postaudits

As model calibration and parameter estimation are keyed to a set of historical data, the confidence in and reliability of the calibration process is proportional to quality and comprehensiveness of the historical record. The time over which predictions are made with a calibrated model should also be related to, and limited by, the length of the historical record. A reasonable guideline is to predict only for a time comparable to the period that was matched.

The accuracy of a model's predictions is the best measure of its reliability. However, that can only be evaluated after the fact. There have been several published studies in which the predictive accuracy of a deterministic ground-water model was evaluated several years after the prediction had been made [102-107]. The results suggest that extrapolations into the future were rarely very accurate. Predictive errors often related to having used a period of history match that was too short to capture an important element of the model or of the system, or to an incomplete conceptual model. For example, processes and boundary conditions that are negligible or insignificant under the past and present stress regime may become nontrivial or even dominant under a different set of imposed stresses. Thus, a conceptual model founded on observed behavior of a ground-water system may prove to be inadequate in the future, when existing stresses are increased or new stresses are added. A major source of predictive error is sometimes attributable primarily to the uncertainty of future stresses. But if the range or probability of future stresses can be estimated, then the range or probability of future responses can be predicted. An encouraging trend is that many analysts are now attempting to place confidence bounds on predictions arising out of the uncertainty in parameter estimates. However, these confidence limits still would not bound errors arising from the selection of a wrong conceptual model or from problems in the numerical solution algorithms [108].

It should be recognized that when model parameters have been adjusted during calibration to obtain a best fit to historical data, there is a bias towards extrapolating existing trends when predicting future conditions, in part because predictions of future stresses are often based on existing trends [104]. The model calibration procedure, which is clearly required for field applications, essentially forces a deterministic model to become, at least in part, a statistical model, and thus to acquire the same types of limitations that are characteristic of all statistically-based models and predictions.

If a model is to be used for prediction in a problem or system that is of continuing interest or significance to society, then field monitoring should continue and the model should be periodically postaudited, or recalibrated, to incorporate new information, such as changes in imposed stresses or revisions in the assumed conceptual model. A postaudit offers a means to evaluate the nature and magnitude of predictive errors, which may itself lead to a large increase in the understanding of the system and in the value of a subsequently revised model. Revised predictions can then be made with greater reliability.

significant differences, then the coarser design is probably adequate for that particular problem.

6.8. Calibration criteria

Model calibration may be viewed as an evolutionary process in which successive adjustments and modifications to the model are based on the results of previous simulations. The modeler must decide when sufficient adjustments have been made to the representation of parameters and processes and at some time accept the model as being adequately calibrated (or perhaps reject the model as being inadequate and seek alternative approaches). This decision is often based on a mix of subjective and objective criteria. The achievement of a best fit between values of observed and computed variables is a regression procedure and can be evaluated as such. That is, the residual errors should have a mean that approaches zero and the deviations should be minimized. Cooley (1977) discusses several statistical measures that can be used to assess the reliability and goodness of fit of ground-water flow models [99]. The accuracy tests should be applied to as many dependent variables as possible. The types of observed data that are most valuable for model calibration include head and concentration changes over space and time, and the quantity and quality of ground-water discharges from the aquifer.

While it is necessary to evaluate quantitatively the accuracy of the model, it is equally important to assure that the dependent variables that serve as a basis for the accuracy tests are reliable indicators of the computational power and accuracy of the model. For example, if a particular variables were relatively insensitive to the governing parameters, then the existence of a high correlation between its observed and computed values would not necessarily be a reflection of a high level of accuracy in the overall model. For example, in modeling an alluvial stream-aquifer system in Colorado, the computed streamflow at the downstream end of the study reach coincided almost exactly with the observed streamflow [100]. However, the greatest component of computed outflow at the downstream end of the study reach, which averaged about 4.1 m^3/s, was the observed inflow at the upstream end of the study reach, which averaged about 3.8 m^3/s. Because stream gains and losses within the study reach were small (about 8 percent) relative to the actual streamflow, the accuracy of the fit between observed and computed streamflow values for the downstream gauging station is a poor indicator of the reliability of the model. A better indicator is the *change* in streamflow in the study reach. However, during periods of high flow, the change in streamflow represented only about 3 percent of the actual flow, which is about the same order of magnitude as the measurement errors. Therefore, the lack of a precise fit during these high-flow periods does not indicate that the model is poor or uncalibrated.

Similarly, caution must be exercised when the "observed data" contain an element of subjective interpretation. For example, matching an observed potentiometric surface is sometimes used as a basis for calibrating a ground-water flow model, and an observed concentration distribution may serve as a basis for calibrating a solute-transport model. Both represent interpretative contouring of observed point data that have some limited frequency and accuracy. Thus, a contoured surface serves as a weak basis for model calibration because it includes a variability or error introduced by the contourer, in addition to measurement errors present in the observed data at the specific points. Cooley and Sinclair (1976) evaluated the uniqueness of a steady-state ground-water flow

6.10. Model validation

It is natural for people who apply ground-water models, as well as those who make decisions based on model results, to want assurance that the model is valid. This has led to programs for verification or validation of hydrogeological models, such as the INTRACOIN, HYDROCOIN, and INTRAVAL projects. For example, the INTRAVAL project was established to evaluate the validity of mathematical models for predicting the potential transport of radioactive substances in the geosphere [109].

Ground-water models are embodiments of various scientific theories and hypotheses. Karl Popper argues that "as scientists we can never validate a hypothesis, only invalidate it" [110]. Stephen Hawking argues that physical theories are always provisional and can never be proven [111]. He states, "No matter how many times the results of experiments agree with some theory, you can never be sure that the next time the result will not contradict the theory." The same philosophy has been applied specifically to ground-water models [6, 112].

Several available definitions of model validation are presented in terms of providing assurances or building confidence that the model adequately represents reality. However, the criteria for labeling a model as validated are inherently subjective. In practice, validation is attempted through the same process that is typically identified as calibration, "... by comparison of calculation with observations and experimental measurements" [113]. However, the nonuniqueness of model solutions means that a good comparison can be achieved with an inadequate or erroneous model. Also, because the definition of "good" is subjective, under the common operational definitions of validation, one competent and reasonable scientist may declare a model as validated while another may use the same data to demonstrate that the model is invalid. In science and engineering, such an operational definition would not appear to be meaningful [6]. To the general public, proclaiming that a ground-water model is validated carries with it an aura of correctness that many modelers would not claim [108]. Because labeling a model as having been "validated" has very little objective or scientific meaning, such "certification" does little beyond instill a false sense of confidence in such models. Konikow and Bredehoeft (1992) recommend that the term *validation* not be applied to ground-water models [6].

7. OVERVIEW OF REPRESENTATIVE MODEL--*MODFLOW*

One of the most popular and comprehensive deterministic ground-water models available today is the MODFLOW code of McDonald and Harbaugh (1988) [114]. This is actually a family of compatible codes that centers on an implicit finite-difference solution to the three-dimensional flow equation that was coded in FORTRAN in a modular style to allow and encourage the development of additional packages or modules that can be added on or linked to the original code. The flexibility and comprehensiveness of this package is indicated by the list in table 1, which presents a summary of features and modules presently available for MODFLOW. The basic model uses a block-centered finite-difference grid that allows variable spacing of the grid in three dimensions. Flow can be steady or transient. Layers can be simulated as confined, unconfined, or a combination of both. Aquifer properties can vary spatially and hydraulic conductivity (or transmissivity) can be anisotropic. Flow associated with external stresses, such as wells, areally distributed recharge, evapotranspiration, drains, and streams, can also be simulated through the use of specified head, specified

flux, or head-dependent flux boundary conditions. The implicit finite-difference equations can be solved using either the Strongly Implicit Procedure (SIP) or Slice-Successive Overrelaxation (SSOR) methods. Newer modules offer several additional solution algorithms. Although the input and output systems of the program were designed to permit maximum flexibility, usability and ease of interpretation of model results can be enhanced by using one of several commercially available preprocessing and postprocessing packages; some of these operate independently of MODFLOW whereas others are directly integrated into reprogrammed and (or) recompiled versions of the MODFLOW code.

The pathline program MODPATH (Pollock, 1989) uses the results of the MODFLOW model and determines that paths and travel times of water movement under steady-state conditions [115]. The additional information required for the pathline analysis, beyond that required for MODFLOW, include porosity and the top and bottom elevations of simulated layers. MODPATH uses a semianalytical particle-tracking scheme. The method assumes that each directional velocity component varies linearly within a grid cell in its own coordinate direction. MODPATH-PLOT presents the results graphically [116].

The parameter-estimation package, MODFLOWP, can be used to estimate parameters (such as transmissivity, storage coefficient, leakance coefficients, recharge rates, evapotranspiration, and hydraulic head at constant-head boundaries) using nonlinear regression [96]. Parameters are estimated by minimizing a weighted least-squares objective function by either the modified Gauss-Newton method or a conjugate-direction method. Data used to estimate parameters can include independent estimates of parameter values, observed heads or drawdowns, and observed gains or losses in streamflow. The MODFLOWP output includes statistics for analyzing the reliability of the estimated parameters and of the model.

As shown in table 1, a variety of other packages and modules are available. Most of these are summarized by Appel and Reilly (1994) [136].

8. CASE HISTORIES

8.1. Regional-scale flow in a deep confined aquifer

The Powder River Basin of northeastern Wyoming and southeastern Montana contains large coal reserves that have not yet been developed fully. The future development of such energy resources in the Powder River Basin will be accompanied by increased demands for water, which is not abundantly available in this semiarid area. One plan had been formulated to construct a coal-slurry pipeline to transport coal out of the area; it would have required about 0.6 to 0.8 m^3/s of water. In the mid-1970s, a plan was proposed to supply this water from up to 40 wells drilled about 1000 m into the Mississippian Madison Limestone in Niobrara County, Wyoming. The Madison aquifer is an areally extensive Paleozoic carbonate rock system that underlies an area exceeding 260,000 km^2 in the Northern Great Plains.

Concern that such relatively large ground-water withdrawals might cause significant water-level declines in the Madison aquifer, perhaps extending into adjacent states, as well as possibly causing decreases in streamflow and spring discharge in or near the outcrop areas, resulted in the need to predict the effects of the proposed large ground-water withdrawals on potentiometric levels, recharge, and discharge. Because the Madison lies at such great depths (from 300 to 5,000 m) in most of the area, it is relatively undeveloped, and sufficient

Table 1. Summary of selected features and modules for the MODFLOW model.

FEATURE or MODULE	REFERENCE
3-D or quasi-3D ground-water flow using implicit, block-centered, finite-difference methods; includes transient flow, variety of boundary conditions, heterogeneity, and anisotropy; solvers include SIP and SSOR	McDonald and Harbaugh (1988) [114]
Preconditioned conjugate gradient matrix solvers	Kuiper (1987) [117]
Statistical processor (MMSP)	Scott (1990) [118]
Integrate with geographical information system (GIS) files (MODFLOWARC); linked to ARC/INFO software	Orzol and McGrath (1992) [119]
Calculation of water budgets (ZONEBUDGET)	Harbaugh (1990) [125]
Aquifer compaction	Leake and Prudic (1991) [121]
River routing and accounting (RIV2)	Miller (1988) [122]
Narrow canyons and faults and layer pinchouts	Hansen (1993) [123]
Stream-aquifer relations; stream stage calculated using Manning formula for rectangular channel	Prudic (1989) [124]
Contouring package for heads or drawdowns	Harbaugh (1990) [120]
Calculation of pathlines for advective transport (MODPATH & MODPATH-PLOT)	Pollock (1989, 1990) [115-116]
Preconditioned conjugate-gradient matrix solver (PCG2)	Hill (1990) [126]
Parameter estimation (MODFLOWP) using nonlinear regression; confidence intervals	Hill (1992, 1994) [96, 127]
Generalized finite-difference formulation	Harbaugh (1992) [128]
Cylindrical flow to a well	Reilly and Harbaugh (1993) [129]
Alternative interblock transmissivity conceptualizations	Goode and Appel (1992) [75]
Horizontal flow barriers (HFB)	Hsieh and Freckleton (1993) [130]
Rewetting of dry cells	McDonald et al. (1992) [131]
Transient leakage from confining units (TLK1)	Leake, Leahy, and Navoy (1994) [132]
Coupled surface-water and ground-water for stream-aquifer interaction with unsteady open-channel flow (MODBRANCH)	Swain and Wexler (1993) [133]
Direct flow connections in coupled ground-water and surface-water model (Streamlink)	Swain (1993) [134]
Advective-dispersive solute transport (RAND3D)	Engineering Technologies Assoc., Inc. (1989) [59]
Advective-dispersive solute transport (MT3D)	Zheng (1990) [60]
Advective-dispersive solute transport (MOC3D)	Goode and Konikow (1991) [135]

data are not available to define the head distribution and the hydraulic properties of the aquifer accurately and precisely. In light of this uncertainty, and as a prelude to a planned subsequent 5-yr hydrogeologic investigation of the Madison, a preliminary digital model of the aquifer was developed using the two-dimensional, finite-difference model of Trescott et al. (1976) [77, 97]. The objectives of the preliminary model study were to: (1) improve the conceptual model of ground-water flow in the aquifer system; (2) determine deficiencies in existing data, and help set priorities for future data collection by identifying the most sensitive parameters, assuming the model is appropriate; and (3) make a preliminary estimate of the regional hydrologic effects of the proposed well field [97].

The results indicated that the aquifer can probably sustain increased ground-water withdrawals as much as several tenths of m^3/s, but that these withdrawals probably would significantly lower the potentiometric surface in the Madison aquifer in a large part of the basin. Because of the great uncertainty in most of the parameters, the model study and predictions were framed in terms of a sensitivity analysis. For example, fig. 11 shows drawdown predictions made for an area near the proposed well field for an assumed reasonable range of values for the storage and leakance coefficients (K_z/m), where K_z and m are the vertical hydraulic conductivity and the thickness, respectively, of the confining layer. The curves show that the range in plausible drawdowns, even after 1 yr, is extremely large. The solutions also illustrate that sensitivities vary with time. At late times (about 100 years), there is no significant difference in drawdown for different values of S, and at early times the drawdown is about the same for all values of leakance at a given value of S.

This preliminary model analysis helped in formulating an improved conceptual model of the Madison aquifer. For example, the important influences on ground-water flow in the Madison of temperature differences and aquifer discontinuities were recognized and documented. Although it could be argued

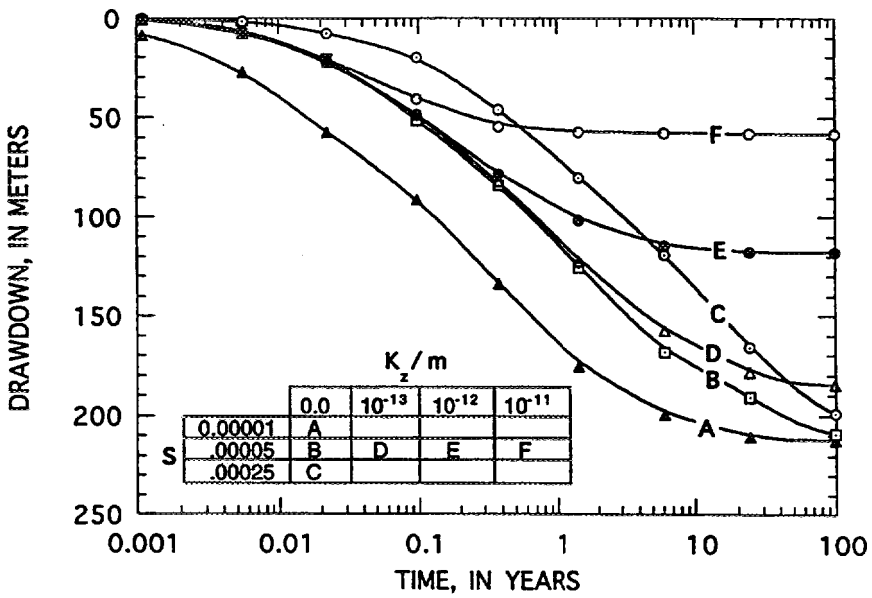

Figure 11. Time-drawdown curves for model node located near proposed well field to pump ground water from the Madison Limestone (modified from Konikow, 1976 [97].)

that the importance of these influences could have been (or should have been) recognized on the basis of hydrogeologic principles without the use of a simulation model, the fact is that none of the earlier published studies of this aquifer system indicated that these factors were of major significance. The difference from earlier studies arose from the quantitative hypothesis-testing role of the model; the nature of the inconsistencies between observed head distributions and those calculated using the initial estimates of model parameters helped direct the investigators towards testing hypotheses that would resolve or minimize the inconsistencies. The demonstrated high sensitivity of drawdown to the leakance coefficient emphasized the need to reevaluate the system in a true three-dimensional framework so as to better consider vertical components of flow. This was done in later studies (e.g. Downey and Weiss, 1980; Woodward-Clyde Consultants, 1981) [137-138]. The latter used a five-layer model and a Monte Carlo simulation approach to incorporate and assess the effects of uncertainties in the parameters. The predicted effects were then presented as probability distribution curves showing the likelihood of different drawdowns occurring at the specified points.

Cooley et al. (1986) applied a nonlinear-regression ground-water flow model to this same aquifer system [89]. Their two-dimensional model was based on a Galerkin finite-element discretization. The finite-element grid and boundary conditions are shown in fig. 12. The grid includes 535 quadrilateral (composites of four triangles) and triangular elements and 555 nodes. The grid was designed to be finer where more data were available and (or) where hydraulic gradients are relatively steep. Regression analysis was used to estimate parameters, including intrinsic permeabilities of the main aquifer and separate lineament zones, discharges from eight major springs, and specified heads on the model boundaries. The regression approach also yielded statistical measures of the reliability of those parameter estimates [89]. The regression model was applied using sequential F testing, so that the fewest number and simplest zonation of intrinsic permeabilities, combined with the simplest overall model, were evaluated initially; additional complexities were then added in stages to evaluate the subsequent degree of improvement in model results. Analysis by Cooley et al. (1986) tends to confirm the existence of lineament zones, which appear to strongly influence the flow and head distribution in the Madison aquifer [89].

Thus, a variety of models were used to understand the sensitivity of the conceptualized Madison aquifer to changes in simulated aquifer parameters. From these sensitivity analyses, improved predictions of aquifer responses can be made, and the confidence in the predictions can be assessed.

Further refinements and understanding evolved on the basis of isotopic analyses, used by Back et al. (1983) to analyze the ground-water flow system and geochemical reactions in this same regional aquifer system [139]. Among other things, they estimated flow paths, flow velocities, and hydraulic properties for the system. After their assumed locations and lengths of flow paths to the sampling sites were reinterpreted in light of flow modeling results, the resulting velocity and permeability values were remarkably close to independently derived, hydrologically based, parameter estimates [140]. Of particular relevance to isotopic interpretation and age dating in stressed regional systems is the fact that each water sample may reflect a long travel history of perhaps thousands of years through the aquifer, which has occurred almost entirely under the influence of natural steady-state hydraulic gradients and flow paths. However, as ground-water withdrawals from the aquifer during the past 50 to 100 years may have significantly influenced the observed heads and hydraulic gradients, there will be an error if the estimated ages are used to calculate hydraulic parameters on the

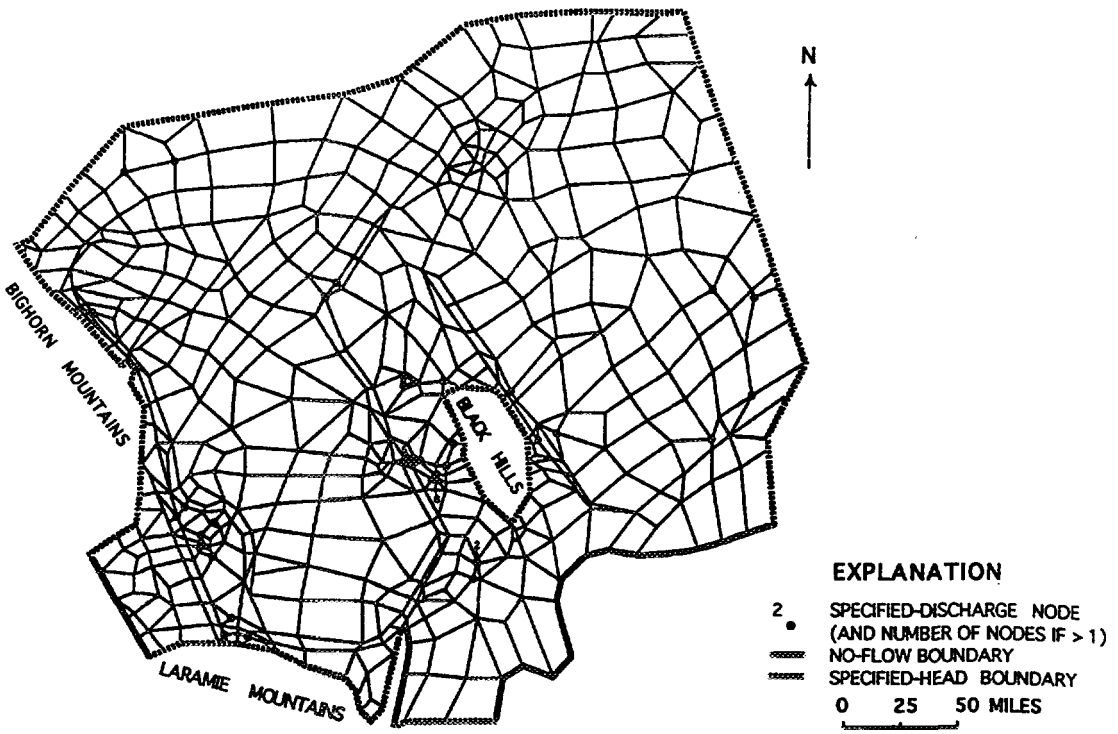

Figure 12. Finite-element grid showing boundary conditions and locations of specified-discharge points (modified from Cooley et al., 1986 [89]).

basis of today's head distribution [140]. This inconsistency can be resolved by linking the isotopic interpretation to a ground-water model analysis for simulating the hydraulic evolution of the system. In the analysis of the Madison aquifer system, the modeling analyses and the isotopic analyses clearly complemented each other, and together yielded better estimates of hydraulic parameters and higher confidence in the interpretations than either approach could have achieved independently.

8.2. Local-scale flow and transport in a shallow unconfined aquifer

Reilly et al. (1994) combined the application of environmental tracers and deterministic numerical modeling to analyze and estimate recharge rates, flow rates, flow paths, and mixing properties of a shallow ground-water system near Locust Grove, in eastern Maryland, USA [141]. The study area encompassed about 2.6×10^7 m^2 of mostly agricultural land on the Delmarva Peninsula. The surficial aquifer includes unconsolidated permeable sands and gravel that range in thickness from less than 6 m to more than 20 m. This surficial aquifer is underlain by relatively impermeable silt and clay deposits, which form a confining unit.

In this study, chlorofluorocarbons (CFCs) and tritium were analyzed from a number of water samples collected from observation wells to estimate the age of ground water at each sampling location and depth [141]. Because errors and uncertainty are associated with estimates of age based on environmental tracers, just as errors and uncertainty are associated with deterministic models of ground-

water flow and transport, the authors applied a feedback or iterative process based on comparisons of independent estimates of travel time [141]. Their approach is summarized and outlined in fig. 13. Each task shown was designed to improve either the estimates of parameters or the conceptualization of the system.

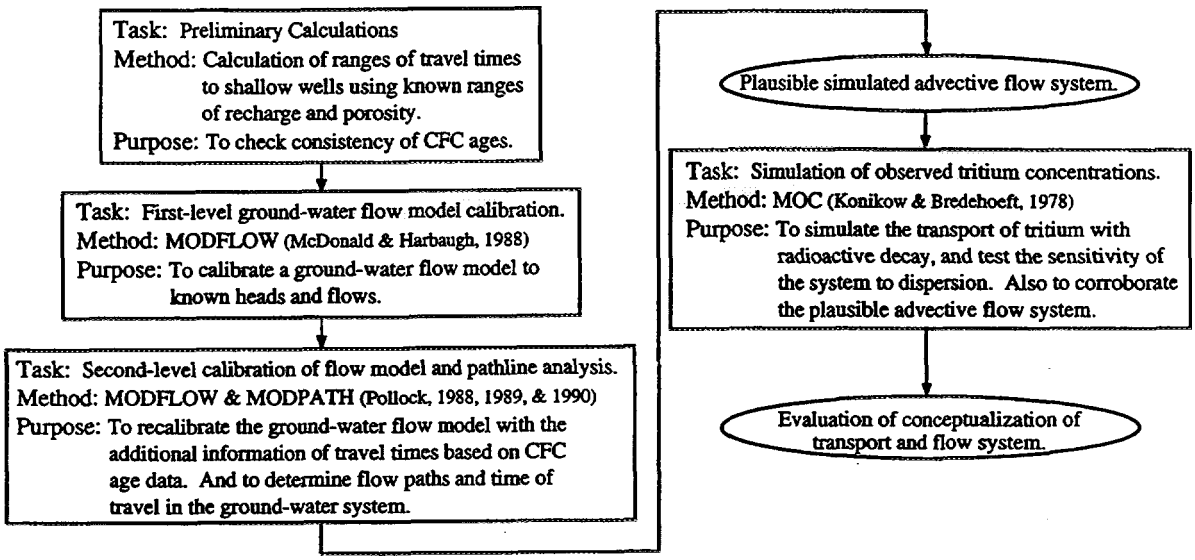

Figure 13. Flow diagram of the steps taken to quantify the flow paths in the Locust Grove, Maryland, ground-water flow system (modified from Reilly et al., 1994 [141]).

As described by Reilly et al. (1994), the preliminary calculations (first task) were used to set bounds on the plausibility of the more complex simulations and chemical analyses. The first-level calibration of a ground-water flow model (second task) provided the initial system conceptualization. The third task was a second-level calibration and analysis involving simulation of advective transport, which provided quantitative estimates of flow paths and time of travel to compare with those obtained from the CFC analyses. The fourth task involved the application of a solute-transport model to simulate tritium concentrations in the ground-water flow system as influenced by the processes of advection, dispersion, radioactive decay, and time-varying input (source concentration) functions.

The sampling wells were located approximately along an areal flow line, so a two-dimensional cross-sectional model was developed for the simulation. The MODFLOW model [114] was used to simulate ground-water flow and advective transport. The finite-difference grid consisted of 24 layers and 48 columns of nodes, with each cell having dimensions of 1.143 by 50.801 m, as shown in fig. 14, which also shows the wells that lie in the cross section. The simulation was designed to represent average steady-state flow conditions. The boundary conditions include (1) water table having a specified and constant rate of recharge, (2) an upgradient boundary as a no-flow condition to represent a ground-water divide, (3) a no-flow boundary on the bottom to represent the underlying confining layer, (4) a specified-head drain boundary condition to represent a stream in the upper right corner of the grid, and (5) a lateral boundary under the stream assumed to be a flow line, thus represented as a no-flow boundary condition [141].

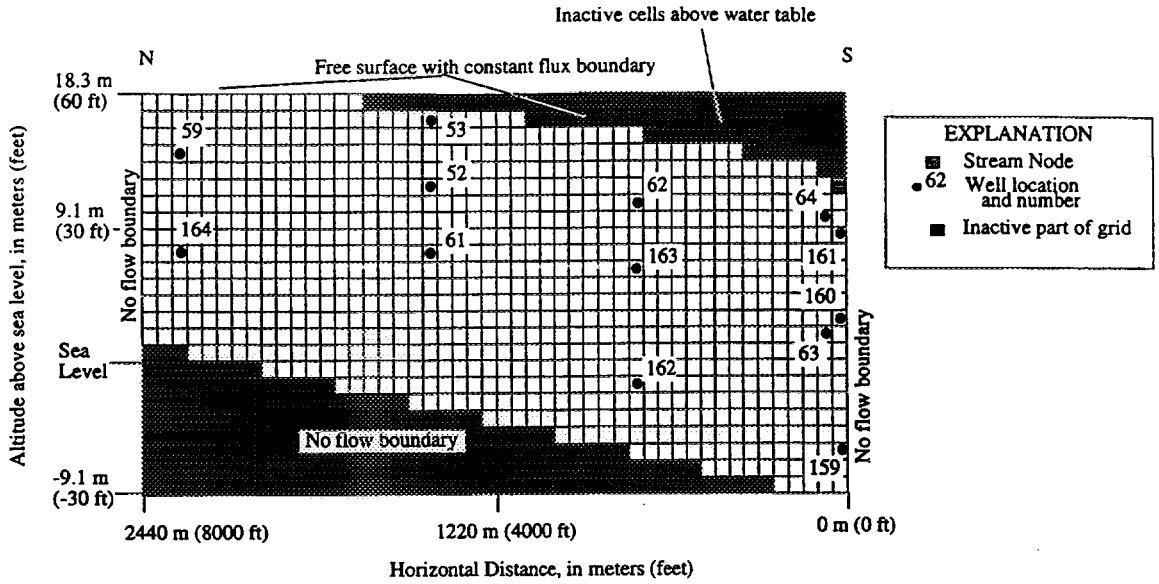

Figure 14. Model grid used to simulate Locust Grove cross section, showing well locations (modified from Reilly et al., 1994 [141]).

After the flow model was calibrated, pathline and travel time analysis was undertaken and comparisons to CFC age estimates were made. Figure 15 shows the pathlines calculated using MODPATH after the second-level calibration with MODFLOW. A flow tube diagram for the same cross section is shown in fig. 16, in which each flow tube is bounded by flow lines and contains an equal amount of flow. Distances traveled in 10-year increments of travel time from points of recharge at the water table are also indicated on each flow line. The comparison with CFC estimates were generally good. However, Reilly et al. (1994) note that close to the stream, many flow lines converge, and the convergence of pathlines representing the entire range of travel times present in the aquifer causes waters of different ages to be relatively near each other [141]. Thus, at the scale and grid spacing of the model, in the area near the stream the convergent flow lines cannot be readily differentiated in the model and the locations of individual well screens cannot be accurately represented directly under the stream. After the second-level calibration, the root mean squared error between the simulated ages and the CFC ages for the 10 wells furthest from the stream (i.e. excluding points 159, 160, and 161) was 3.4 years [141].

Tritium concentrations of recharge waters have varied considerably over the last 40 years [141]. Thus, the time of travel would not always be readily apparent from the concentration in a measured water sample. Also, mixing of these relatively sharp changes of input concentrations can make the interpretation of time of travel from tritium concentrations even more uncertain [141]. Thus, the authors simulated solute transport of tritium within the system using a model that accounts for mixing (dispersion), radioactive decay, and transient input functions, which would also allow a further evaluation of consistency with the results of the previous flow and advective transport model. They applied the MOC solute-transport model of Konikow and Bredehoeft (1978) [57] for this purpose.

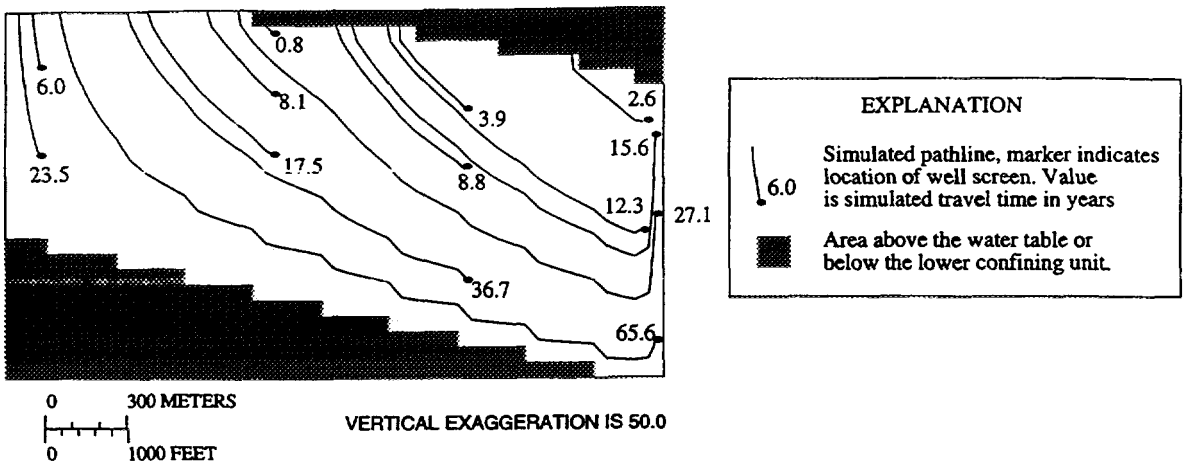

Figure 15. Pathlines (calculated using MODPATH after second-level calibration) in Locust Grove cross section to observation wells showing time of travel (in years) from the water table (modified from Reilly et al., 1994 [141]).

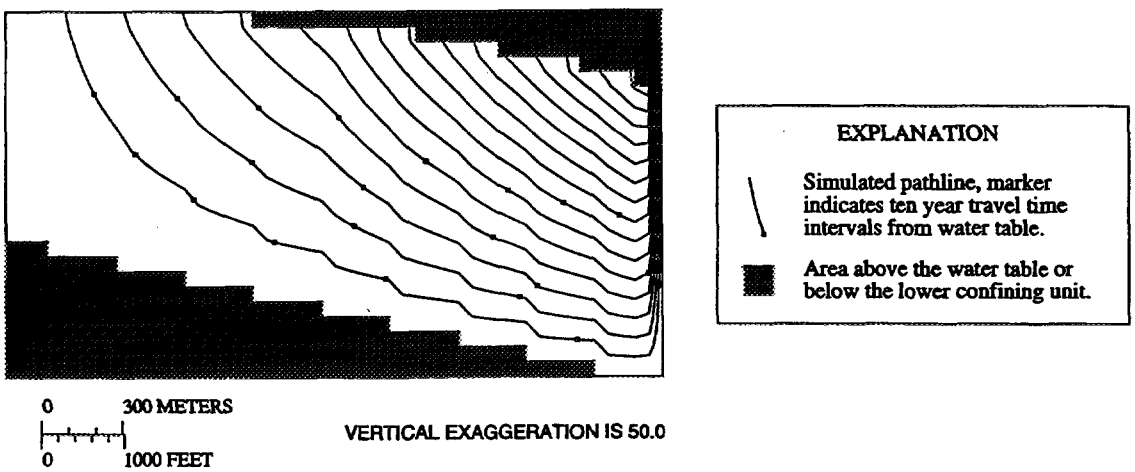

Figure 16. Flow tube diagram of the Locust Grove ground-water flow system in cross section. Markers on pathlines indicate 10-year periods of travel from the water table (modified from Reilly et al., 1994 [141]).

The results of the simulation assuming (1) no dispersion and (2) assuming α_L of 0.15 m and α_T of 0.015 m are shown in fig. 17. The limiting case simulation of no dispersion yielded acceptable results and was used as the best estimate of the tritium distribution in November 1990 [141]. This case reproduces the sharp concentration gradients required to reproduce the low tritium values observed. The MOC model was advantageous for this problem because it minimizes numerical dispersion that might interfere with the analysis and it can solve the governing equations for α_L of 0.0, which many other transport models based on finite-difference or finite-element methods cannot do. The results of the solute-transport simulation are consistent with the advective flow system determined by the second-level calibration and thus support the reasonableness of the conceptual model [141]. The coupling of the tritium analyses and the transport model indicates where discrepancies between the measured and simulated

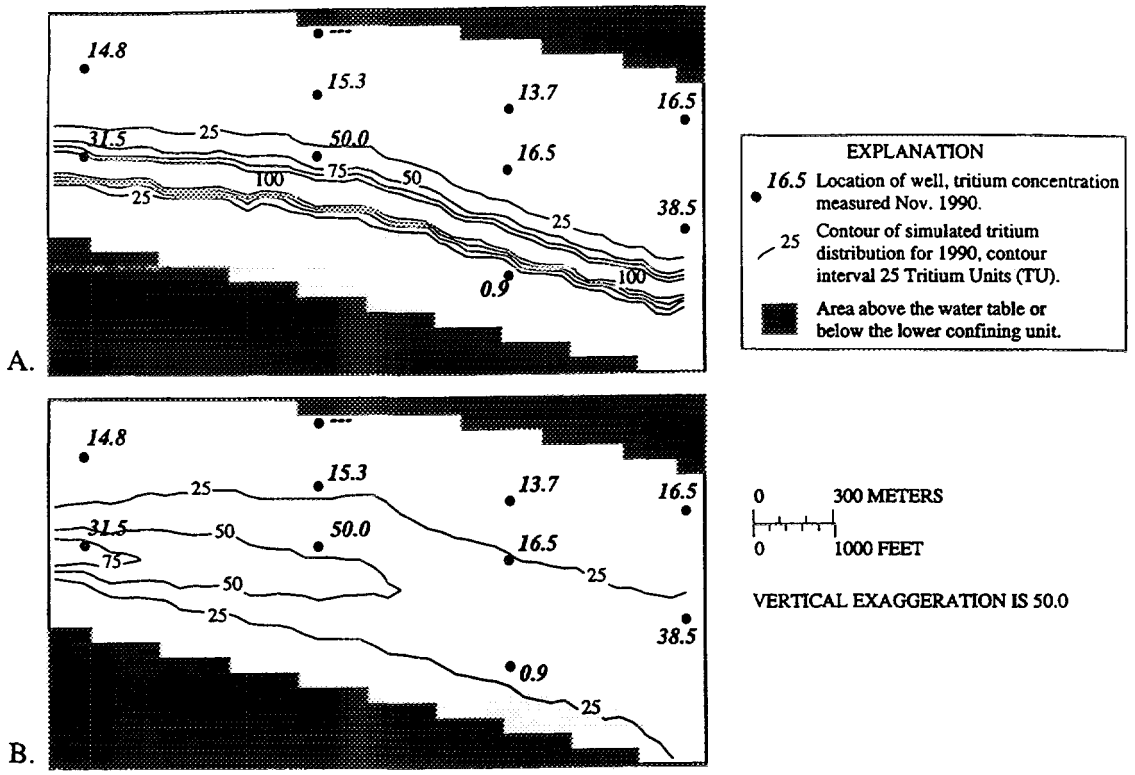

Figure 17. Simulated tritium distribution at the end of 1990: (A) with dispersivity α_L = 0.0 m and α_T = 0.0 m, and (B) with dispersivity α_L = 0.15 m and α_T = 0.015 m. Contour interval 25 tritium units (TU). Measured concentrations from samples obtained from wells in November 1990 are given for their location in bold italics (modified from Reilly et al., 1994 [141]).

concentrations occur, and where additional data collection or refinement of the conceptual model may be warranted [141].

This case study illustrates that environmental tracers and numerical simulation in combination are effective tools that complement each other and provide a means to quantitatively estimate the flow rate and path of water moving through a ground-water system. Reilly et al. (1994) found that the environmental tracers and numerical simulation methods also provide a "feedback" that allows a more objective estimate of the uncertainties in the estimated rates and paths of movement [141]. The ages of water samples, as determined from the environmental tracers, define the time of travel at specific points in the ground-water system, but the quantities of water and paths taken are unknown. The numerical simulations in the absence of the environmental tracer information provide nonunique and therefore uncertain estimates of the quantities of water and flow paths. Together the two methods enabled a coherent explanation of the flow paths and rates of movement while indicating weaknesses in the understanding of the system that would require additional data collection and refinement of conceptual models of the ground-water system [141].

9. AVAILABILITY AND SOURCES OF GROUND-WATER MODELS

There are a large number of deterministic ground-water models available today, based on a variety of numerical methods and a variety of conceptual models. The selection of a numerical method or generic model for a particular

field problem depends on several factors, including accuracy, efficiency/cost, and usability. The first two factors are related primarily to the nature of the field problem, availability of data, and scope or intensity of the investigation. The usability of a method may depend partly on the mathematical background of the modeler, as it is preferable for the model user to understand the nature of the numerical methods implemented in a code. Greater efficiency is usually attained if the modeler can readily modify and adapt the program to the specific problem of interest, and this may sometimes require program modifications to the source code. In selecting a model that is appropriate for a particular application, it is most important to choose one that incorporates the proper conceptual model; one must avoid force fitting an inappropriate model to a field situation solely because of convenience, availability, or familiarity to the user. Usability is also enhanced by the availability of preprocessing and postprocessing programs or features, and by the availability of comprehensive yet understandable documentation.

There have been a number of surveys of available models published in recent years [136, 142-143]. Van der Heijde et al. (1985) reports on an international survey of 399 models, of which 206 had been documented at that time [142]. This was a significant increase from 245 models available for a similar review 5 years earlier. Appel and Reilly (1994) summarize the nature and availability of 89 ground-water flow and quality models produced by and available from the U.S. Geological Survey [136]. Anderson et al. (1992), in their review of ground-water models, list 19 separate software distributors and provide brief descriptions of several codes [144]. A directory and review of programs applicable to radioactive waste disposal problems, including ground-water flow and transport models, was prepared by the Commission of the European Communities in 1983 [145]. The International Ground Water Modeling Center maintains a clearinghouse and distribution center for ground-water simulation models. It also maintains extensive databases on ground-water software and research data, and provides limited technical support services for model users.

A large number of public and private organizations distribute public domain and (or) proprietary software for ground-water modeling. A few are listed in table 2, and they should be contacted directly for the latest availability and costs. There are also many other public and private sources of modeling software (e.g. see Anderson et al., 1992 [144]).

Table 2. Selected list of organizations that distribute ground-water models.

Organization	*Address*	*Phone/Fax/e-mail*
International Ground Water Modeling Center – USA	IGWMC Colorado School of Mines Institute for Ground-Water Research & Education Golden, CO 80401-1887, USA	Phone: 303-273-3103 Fax: 303-273-3278 e-mail: igwmc@flint.mines.colorado.edu
International Ground Water Modeling Center – Europe	IGWMC TNO Institute of Applied Geoscience P.O. Box 6012 2600 JA Delft, The Netherlands	Phone: 31.15.697215 Fax: 31.15.564800
U.S. Geological Survey	U.S. Geological Survey NWIS Program Office 437 National Center Reston, VA 22092 USA	Phone: 703-648-5695 Fax: 703-648-5295 e-mail: oahollow@nwisqvarsa.er.usgs.gov

REFERENCES

[1] COPLEN, T.B., Uses of Environmental Isotopes, *in* Regional Ground Water Quality, Chap. 10 (Alley, W.A., Ed.), Van Nostrand Reinhold, New York (1993) 227-254.

[2] DINÇER, T., DAVIS, G.H., Application of environmental isotope tracers to modeling in hydrology, Jour. Hydrology 68 (1984) 95-113.

[3] JOHNSON, T.M., DEPAOLO, D.J., Interpretation of isotopic data in groundwater-rock systems, Model development and application to Sr isotope data from Yucca Mountain, Water Resources Res. **30** 5 (1994) 1571-1587.

[4] ANDERSON, M.P., WOESSNER, W.W., Applied Groundwater Modeling, Academic Press, San Diego (1992) 381 pp.

[5] BEAR, J., VERRUIJT, A., Modeling Groundwater Flow and Pollution, Reidel Publishing Co., Dordrecht, Holland (1987) 414 pp.

[6] KONIKOW, L.F., BREDEHOEFT, J.D., Ground-water models cannot be validated, Advances in Water Resources **15** 1 (1992) 75-83.

[7] KRUMBEIN, W.C., GRAYBILL, F.A., An Introduction to Statistical Models in Geology: McGraw-Hill, New York (1965) 475 pp.

[8] KONIKOW, L.F., PATTEN, E.P., JR., Groundwater Forecasting: *in* Hydrological Forecasting, (ANDERSON, M.G., BURT, T.P., Eds.), John Wiley and Sons Ltd., New York (1985) 221-270.

[9] COOLEY, R.L., Incorporation of prior information on parameters into nonlinear regression groundwater flow models, 1, Theory, Water Resources Res. **18** 4 (1982) 965-976.

[10] FREEZE, R.A., Hydrogeological Concepts in Stochastic and Deterministic Rainfall-Runoff Predictions, *in* Recent Trends in Hydrogeology (NARASIMHAN, T.N., Ed.) Geol. Soc. Am. Spec. Paper 189 (1982) 63-79.

[11] NEUMAN, S.P., Statistical Characterization of Aquifer Heterogeneities: An Overview, *in* Recent Trends in Hydrogeology (NARASIMHAN, T.N., Ed.) Geol. Soc. Am. Spec. Paper 189 (1982) 81-102.

[12] DAGAN, G., Flow and Transport in Porous Formations, Springer-Verlag, Berlin (1989) 465 pp.

[13] FERRIS, J.G., KNOWLES, D.B., BROWN, R.H., STALLMAN, R.W., Theory of Aquifer Tests, U.S. Geol. Survey Water-Supply Paper 1536-E (1962) 69-174.

[14] BEAR, J., Dynamics of Fluids in Porous Media, Am. Elsevier Publishing Co., New York (1972) 764 pp.

[15] BEAR, J., Hydraulics of Groundwater, McGraw-Hill, New York (1979) 569 pp.

[16] DOMENICO, P.A., SCHWARTZ, F.W., Physical and Chemical Hydrogeology, John Wiley & Sons, New York (1990) 824 pp.

[17] BREDEHOEFT, J.D., PINDER, G.F., Mass transport in flowing groundwater, Water Resources Res. **9** 1 (1973) 194-210.

[18] GREENKORN, R.A., Flow Phenomena in Porous Media, Marcel Dekker, New York (1983) 550 pp.

[19] FREEZE, R.A., CHERRY, J.A., Groundwater, Prentice-Hall, Englewood Cliffs (1979) 604 pp.

[20] REILLY, T.E., FRANKE, O.L., BUXTON, H.T., BENNETT, G.D., A conceptual framework for ground-water solute-transport studies with emphasis on physical mechanisms of solute movement, U.S. Geol. Survey Water-Res. Inv. Rept. 87-4191 (1987) 44 pp.

[21] GILLHAM, R.W., CHERRY, J.A., Contaminant migration in saturated unconsolidated geologic deposits, *in* Recent Trends in Hydrogeology (NARASIMHAN, T.N., Ed.) Geol. Soc. Am. Spec. Paper 189 (1982) 31-61.

[22] NATIONAL RESEARCH COUNCIL, Ground Water Models: Scientific and Regulatory Applications, National Academy Press, Washington, D.C. (1990) 303 pp.

[23] ANDERSON, M.A., Movement of contaminants in groundwater: Groundwater transport--Advection and dispersion, *in* Groundwater Contamination, National Academy Press, Washington, D.C. (1984) 37-45.

[24] BEAR, J., TSANG, C.-F., DE MARSILY, G. [Eds.], Flow and Contaminant Transport in Fractured Rock, Academic Press, Inc., San Diego (1993) 560 pp.

[25] KONIKOW, L.F., GROVE, D.B., Derivation of Equations Describing Solute Transport in Ground Water, U.S. Geol. Survey Water-Res. Inv. 77-19 (1977) 30 pp.

[26] COOLEY, R.L., Finite Element Solutions for the Equations of Ground-Water Flow, Hydrology and Water Resources Pub. no. 18, Desert Research Inst., Univ. Nevada (1974) 134 pp.

[27] BREDEHOEFT, J.D., Finite difference approximations to the equations of ground-water flow, Water Resources Res. 5 2 (1969) 531-534.
[28] REILLY, T.E., GOODMAN, A.S., Quantitative analysis of saltwater-freshwater relationships in groundwater systems--A historical perspective, Jour. Hydrology 80 (1985) 125-160.
[29] SANFORD, W.E., KONIKOW, L.F., A Two-Constituent Solute-Transport Model for Ground Water Having Variable Density, U.S. Geol. Survey Water-Res. Inv. Rept. 85-4279 (1985) 88 pp.
[30] REDDELL, D.L., SUNADA, D.K., Numerical Simulation of Dispersion in Groundwater Aquifers, Colorado State University, Ft. Collins, Hydrology Paper 41 (1970) 79 pp.
[31] GROVE, D.B., Ion Exchange Reactions Important in Groundwater Quality Models, *in* Advances in Groundwater Hydrology, Am. Water Res. Assoc. (1976) 409-436.
[32] SCHEIDEGGER, A.E, General theory of dispersion in porous media, Jour. Geophys. Research 66 10 (1961) 3273-3278.
[33] MORANVILLE, M.B., KESSLER, D.P., GREENKORN, R.A., Directional dispersion coefficients in anisotropic porous media, Ind. Eng. Chem., Fundam. 16 3 (1977) 327-332.
[34] ROBSON, S.G., Feasibility of Digital Water-Quality Modeling Illustrated by Application at Barstow, California, U.S. Geol. Survey Water-Res. Inv. 46-73 (1974) 66 pp.
[35] ROBSON, S.G., Application of Digital Profile Modeling Techniques to Ground-Water Solute-Transport at Barstow, California, U.S. Geol. Survey Water-Supply Paper 2050 (1978) 28 pp.
[36] VOSS, C.I., SUTRA--Saturated Unsaturated Transport--A Finite-Element Simulation Model for Saturated-Unsaturated Fluid-Density-Dependent Ground-Water Flow With Energy Transport or Chemically-Reactive Single-Species Solute Transport, U.S. Geol. Survey Water-Res. Invest. Rep. 84-4369 (1984) 409 pp.
[37] GELHAR, L.W., Stochastic subsurface hydrology from theory to applications, Water Resources Res. 22 9 (1986) 135S-145S.
[38] GELHAR, L.W., WELTY, C., REHFELDT, K.R., A critical review of data on field-scale dispersion in aquifers, Water Resources Res. 28 7 (1992) 1955-1974.
[39] SMITH, L., SCHWARTZ, F.W, Mass transport, 1, A stochastic analysis of macroscopic dispersion, Water Resources Res. 16 2 (1980) 303-313.
[40] DOMENICO, P.A., ROBBINS, G.A., A dispersion scale effect in model calibrations and field tracer experiments, J. Hydrology 70 (1984) 123-132.
[41] DAVIS, A.D., Deterministic modeling of dispersion in heterogeneous permeable media, Ground Water 24 5 (1986) 609-615.
[42] GOODE, D.J., KONIKOW, L.F., Apparent dispersion in transient groundwater flow, Water Resources Res., 26 10 (1990) 2339-2351.
[43] WALTON, W.C., Selected Analytical Methods for Well and Aquifer Evaluation, Illinois State Water Survey Bull. 49 (1962) 81 pp.
[44] LOHMAN, S.W., Ground-Water Hydraulics, U.S. Geol. Survey Prof. Paper 708 (1972) 70 pp.
[45] REED, J.E., Type Curves for Selected Problems of Flow to Wells in Confined Aquifers, Techniques of Water-Res. Invests. of the U.S. Geol. Survey, Book 3, Ch. B3 (1980) 106 pp.
[46] JAVANDEL, I., DOUGHTY, D., TSANG, C.-F., Groundwater Transport: Handbook of Mathematical Models, Am. Geophysical Union, Water Res. Monograph 10 (1984) 228 pp.
[47] VAN GENUCHTEN, M.T., ALVES, W.J., Analytical Solutions of the One-Dimensional Convective-Dispersive Solute-Transport Equation, U.S. Dept. of Agric. Tech. Bulletin 1661 (1982) 151 pp.
[48] WEXLER, E.J., Analytical Solutions for One-, Two-, and Three-Dimensional Solute Transport in Ground-Water Systems with Uniform Flow, Techniques of Water-Res. Invests. of the U.S. Geol. Survey, Book 3, Ch. B7 (1992) 190 pp.
[49] PEACEMAN, D.W., Fundamentals of Numerical Reservoir Simulation, Elsevier, Amsterdam (1977) 176 pp.
[50] REMSON, I., HORNBERGER, G.M., MOLZ, F.J., Numerical Methods in Subsurface Hydrology, Wiley, New York, NY (1971) 389 pp.
[51] WANG, J.F., ANDERSON, M.P., Introduction to Groundwater Modeling, Freeman, San Francisco, CA, (1982) 237 pp.
[52] VON ROSENBERG, D.U., Methods for the Numerical Solution of Partial Differential Equations, Elsevier, New York (1969) 128 pp.
[53] HUYAKORN, P.S., PINDER, G.F., Computational Methods in Subsurface Flow, Academic Press, New York, N.Y. (1983) 473 pp.

[54] DE MARSILY, G., Quantitative Hydrogeology, Academic Press, New York, N.Y. (1986) 440 pp.
[55] BREBBIA, C.A., The Boundary Element Method for Engineers, Pentech Press, London (1978) 189 pp.
[56] LIGGETT, J.A., Advances in the boundary integral equation method in subsurface flow, Water Resources Bull. 23 4 (1987) 637-651.
[57] KONIKOW, L.F., BREDEHOEFT, J.D., Computer Model of Two-Dimensional Solute Transport and Dispersion in Ground Water, Techniques of Water-Res. Invests. of the U.S. Geol. Survey, Book 7, Ch. C2 (1978) 90 pp.
[58] PRICKETT, T.A., NAYMIK, T.G., LONNQUIST, C.G., A "Random-Walk" Solute Transport Model for Selected Groundwater Quality Evaluations, Ill. State Water Survey Bulletin 65 (1981) 103 pp.
[59] ENGINEERING TECHNOLOGIES ASSOCIATES, INC., Three Dimensional Solute Transport Using the Random-Walk Algorithm and MODFLOW, User's Manual for RAND3D, Engineering Technologies Associates, Inc., Ellicott City, MD (1989) 102 pp.
[60] ZHENG, C., MT3D: A Modular Three-Dimensional Transport Model, S.S. Papadopulos and Associates, Inc., Bethesda, MD (1990).
[61] KIPP, K.L., JR., HST3D: A Computer Code for Simulation of Heat and Solute Transport in Three-Dimensional Ground-Water Flow Systems, U.S. Geol. Survey Water-Res. Inv. Rept. 86-4095 (1987) 517 pp.
[62] REEVES, M., WARD, D.S., JOHNS, N.D., CRANWELL, R.M., Theory and Implementation for SWIFT II, the Sandia Waste-Isolation Flow and Transport Model for Fractured Media, Release 4.84, Sandia Natl. Labs., Albuquerque, NM, Rept. NUREG/CR-3328, SAND83-1159 (1986) 189 pp.
[63] CARRERA, J., MELLONI, G., The Simulation of Solute Transport: An Approach Free of Numerical Dispersion, Sandia Natl. Labs., Albuquerque, NM, Rept. SAND86-7095 (1987) 59 pp.
[64] NEUMAN, S.P., Adaptive Eulerian-Lagrangian finite-element method for advection-dispersion, Int. Jour. Numer. Methods Eng. 20 (1984) 321-337.
[65] CELIA, M.A., RUSSELL, T.F., HERRERA, I., EWING, R.E., An Eulerian-Lagrangian localized adjoint method for the advection diffusion equation, Adv. Water Res. 13 4 (1990) 187-206.
[66] GOTTARDI, G., VENUTELLI, M., One-dimensional moving finite-element model of solute transport, Ground Water 32 4 (1994) 645-649.
[67] GARDER, A.O., PEACEMAN, D.W., POZZI, A.L., Numerical calculation of multidimensional miscible displacement by the method of characteristics, Soc. Petroleum Eng. Jour. 4 1 (1964) 26-36.
[68] PINDER, G.F., COOPER, H.H., JR., A numerical technique for calculating the transient position of the saltwater front, Water Resources Res. 6 3 (1970) 875-882.
[69] GELHAR, L.W., GUTJAHR, A.L., NAFF, R.L., Stochastic analysis of macrodispersion in a stratified aquifer, Water Resources Res., 15 6 (1979) 1387-1397.
[70] MATHERON, G., DE MARSILY, G., Is transport in porous media always diffusive? A counterexample, Water Resources Res. 16 5 (1980) 901-917.
[71] RUBIN, J., Transport of reacting solutes in porous media: Relation between mathematical nature of problem formulation and chemical nature of reaction, Water Resources Res. 19 5 (1983) 1231-1252.
[72] BAHR, J.M., RUBIN, J., Direct comparison of kinetic and local equilibrium formulations for solute transport affected by surface reactions, Water Resources Res. 23 3 (1987) 438-452.
[73] YEH, G.T., TRIPATHI, V.S., A critical evaluation of recent developments in hydrogeochemical transport models of reactive multichemical components, Water Resources Res., 25 1 (1989) 93-108.
[74] BENNETT, G.D., Introduction to Ground-Water Hydraulics: A Programmed Text for Self-Instruction, Techniques of Water-Res. Invests. of the U.S. Geol. Survey, Book 3, Ch. B2 (1976) 172 pp.
[75] GOODE, D.G., APPEL, C.A., Finite-Difference Interblock Transmissivity for Unconfined Aquifers and for Aquifers Having Smoothly Varying Transmissivity, U.S. Geol. Survey Water-Res. Inv. Rept. 92-4124 (1992) 79 pp.

[76] PRICE, H.S., COATS, K.H., Direct methods in reservoir simulation, Soc. Petroleum Eng. Jour. 14 3 (1974) 295-308.
[77] TRESCOTT, P.C., PINDER, G.F., LARSON, S.P., Finite-Difference Model for Aquifer Simulation in Two Dimensions with Results of Numerical Experiments, Techniques of Water-Res. Invests. of the U.S. Geol. Survey, Book 7, Ch. C1 (1976) 116 pp.
[78] KUIPER, L.K., A comparison of iterative methods as applied to the solution of the nonlinear three-dimensional groundwater flow equation, SIAM Jour. Sci. Stat. Comput. 8 4 (1987) 521-528.
[79] MERCER, J.W., FAUST, C.R., Ground-Water Modeling, Natl. Water Well Assoc., Worthington, Ohio (1981) 60 pp.
[80] WATSON, R.A., Explanation and prediction in geology, Jour. of Geology 77 (1969) 488-494.
[81] SWEDISH NUCLEAR POWER INSPECTORATE, The International HYDROCOIN Project--Background and Results, OECD, Paris (1987) 25 pp.
[82] SÉGOL, G., Classic Groundwater Simulations: Proving and Improving Numerical Models, PTR Prentice Hall, Englewood Cliffs (1994) 531 pp.
[83] TORAK, L.J., A Modular Finite-Element Model (MODFE) for Areal and Axisymmetric Ground-Water-Flow Problems, Part 1: Model Description and User's Manual, U.S. Geol. Survey Open-File Rept. 90-194 (1992) 153 pp.
[84] MATALAS, N.C., MADDOCK, T., III, Hydrologic semantics, Water Resources Res. 12 1 (1976) 123.
[85] KNOPMAN, D.S., VOSS, C.I., Behavior of sensitivities in the one-dimensional advection-dispersion equation: Implications for parameter estimation and sampling design, Water Resources Res. 23 2 (1987) 253-272.
[86] NEUMAN, S.P., A statistical approach to the inverse problem of aquifer hydrology, 3, Improved solution method and added perspective, Water Resources Res. 16 2 (1980) 331-346.
[87] WAGNER, B.J., GORELICK, S.M., A statistical methodology for estimating transport parameters: Theory and applications to one-dimensional advective-dispersive systems, Water Resources Res. 22 8 (1986) 1303-1315.
[88] YEH, W.W.-G., Review of parameter identification procedures in groundwater hydrology: The inverse problem, Water Resources Res. 22 1 (1986) 95-108.
[89] COOLEY, R.L., KONIKOW, L.F., NAFF, R.L., Nonlinear-regression groundwater flow modeling of a deep regional aquifer system, Water Resources Res. 10 3 (1986) 546-562.
[90] FREYBERG, D.L., An exercise in ground-water model calibration and prediction, Ground Water 26 3 (1988) 350-360.
[91] KONIKOW, L.F., MERCER, J.M., Groundwater flow and transport modeling, Jour. Hydrology 100 2 (1988) 379-409.
[92] FREEZE, R.A., A stochastic-conceptual analysis of one-dimensional groundwater flow in nonuniform homogeneous media, Water Resources Res. 11 5 (1975) 725-741.
[93] DETTINGER, M.D., WILSON, J.L., First-order analysis of uncertainty in numerical models of groundwater flow, Part I. Mathematical development, Water Resources Res. 17 1 (1981) 149-161.
[94] COOLEY, R.L., VECCHIA, A.V., Calculation of nonlinear confidence and prediction intervals for ground-water flow models, Water Resources Bull. 23 4 (1987) 582-599.
[95] DOUGHERTY, D.E., BAGTZOGLOU, A.C., A caution on the regulatory use of numerical solute transport models, Ground Water 31 6 (1993) 1007-1010.
[96] HILL, M.C., A Computer Program (Modflowp) for Estimating Parameters of a Transient, Three-Dimensional, Ground-Water Flow Model Using Nonlinear Regression, U.S. Geol. Survey Open-File Rept. 91-484 (1992) 358 pp.
[97] KONIKOW, L.F., Preliminary Digital Model of Ground-Water Flow in the Madison Group, Powder River Basin and Adjacent Areas, Wyoming, Montana, South Dakota, North Dakota, and Nebraska, U.S. Geol. Survey Water-Res. Inv. 63-75 (1976) 44 pp.
[98] KONIKOW, L.F., Modeling Chloride Movement in the Alluvial Aquifer at the Rocky Mountain Arsenal, Colorado, U.S. Geol. Survey Water-Supply Paper 2044 (1977) 43 pp.
[99] COOLEY, R.L., A method of estimating parameters and assessing reliability for models of steady state ground-water flow, 1., Theory and numerical properties, Water Resources Res. 13 2 (1977) 318-324.
[100] KONIKOW, L.F., BREDEHOEFT, J.D., Modeling flow and chemical quality changes in an irrigated stream-aquifer system, Water Resources Res. 10 3 (1974) 546-562.

[101] COOLEY, R.L., SINCLAIR, P.J., Uniqueness of a model of steady-state ground-water flow, Jour. Hydrology **31** (1976) 245-269.
[102] LEWIS, B.D., GOLDSTEIN, F.J., Evaluation of a Predictive Ground-Water Solute-Transport Model at the Idaho National Engineering Laboratory, Idaho, U.S. Geol. Survey Water-Resources Inv. Rept. 82-25 (1982) 71 pp.
[103] KONIKOW, L.F., PERSON, M.A., Assessment of long-term salinity changes in an irrigated stream-aquifer system, Water Resources Res. **21** 11 (1985) 1611-1624.
[104] KONIKOW, L.F., Predictive accuracy of a ground-water model – Lessons from a postaudit, Ground Water **24** 2 (1986) 173-184.
[105] ALLEY, W.M., EMERY, P.A., Groundwater model of the Blue River basin, Nebraska--Twenty years later, Jour. Hydrology **85** (1986) 225-249.
[106] PERSON, M.A., KONIKOW, L.F., The recalibration and predictive reliability of a solute-transport model of an irrigated stream-aquifer system, Jour. Hydrology **87** (1986) 145-165.
[107] KONIKOW, L.F., SWAIN, L.A., Assessment of predictive accuracy of a model of artificial recharge effects in the Upper Coachella Valley, California: *in* Selected Papers on Hydrogeology, Vol. 1 (SIMPSON, E.S., SHARP, J.M., JR., Eds.), International Assoc. of Hydrogeologists, Proc. 1989 IGC Meeting, Washington, D.C. (1990) 433-449.
[108] BREDEHOEFT, J.D., KONIKOW, L.F., Ground-water models: Validate or invalidate, Ground Water **31** 2 (1993) 178-179.
[109] SWEDISH NUCLEAR POWER INSPECTORATE, The International INTRAVAL Project--Background and Results, OECD, Paris (1990) 45 pp.
[110] POPPER, SIR KARL, The Logic of Scientific Discovery, Harper and Row, New York (1959) 480 pp.
[111] HAWKING, S.W., A Brief History of Time: From the Big Bang to Black Holes, Bantam Books, New York (1988) 198 pp.
[112] ORESKES, N., SHRADER-FRECHETTE, K., BELITZ, K., Verification, validation, and confirmation of numerical models in the earth sciences, Science **263** (1994) 641-646.
[113] INTERNATIONAL ATOMIC ENERGY AGENCY, Radioactive Waste Management Glossary, IAEA-TECDOC-264, International Atomic Energy Agency, Vienna (1982).
[114] MCDONALD, M.G., HARBAUGH, A.W., A Modular Three-Dimensional Finite-Difference Ground-Water Flow Model, Techniques of Water-Res. Invests. of the U.S. Geol. Survey, Book 6, Ch. A1 (1988) 586 pp.
[115] POLLOCK, D.W., Documentation of Computer Programs to Compute and Display Pathlines Using Results from the U.S. Geological Survey Modular Three-Dimensional Finite-Difference Ground-Water Flow Model, U.S. Geol. Survey Open-File Rept. 89-381 (1989) 188 pp.
[116] POLLOCK, D.W., A Graphical Kernel System (GKS) Version of Computer Program Modpath-Plot for Displaying Path Lines Generated from the U.S. Geological Survey Three-Dimensional Ground-Water Flow Model, U.S. Geol. Survey Open-File Rept. 89-622 (1990) 49 pp.
[117] KUIPER, L.K., Computer Program for Solving Ground-Water Flow Equations by the Preconditioned Conjugate Gradient Method, U.S. Geol. Survey Water-Res. Inv. Rept. 87-4091 (1987) 34 pp.
[118] SCOTT, J.C., A Statistical Processor for Analyzing Simulations Made Using the Modular Finite-Difference Ground-Water Flow Model, U.S. Geol. Survey Water-Res. Inv. Rept. 89-4159 (1990) 218 pp.
[119] ORZOL, L.L., MCGRATH, T.S., Modifications of the U.S. Geological Survey Modular, Finite-Difference, Ground-Water Flow Model to Read and Write Geographical Information System Files, U.S. Geol. Survey Open-File Rept. 92-50 (1992) 202 pp.
[120] HARBAUGH, A.W., A Simple Contouring Program for Gridded Data, U.S. Geol. Survey Open-File Rept. 90-144 (1990) 37 pp.
[121] LEAKE, S.A., PRUDIC, D.E., Documentation of a Computer Program to Simulate Aquifer-System Compaction Using the Modular Finite-Difference Ground-Water Flow Model, Techniques of Water-Res. Invests. of the U.S. Geol. Survey, Book 6, Ch. A2 (1988) 68 pp.
[122] MILLER, R.S., User's Guide for RIV2--A Package for Routing and Accounting of River Discharge for a Modular, Three-Dimensional, Finite-Difference, Ground-Water Flow Model, U.S. Geol. Survey Open-File Rept. 88-345 (1988) 33 pp.
[123] HANSEN, A.J., JR., Modifications to the Modular Three-Dimensional Finite-Difference Ground-Water Flow Model Used for the Columbia Plateau Regional Aquifer-System Analysis, Washington, Oregon, and Idaho, U.S. Geol. Survey Open-File Rept. 91-352 (1993) 162 pp.

[124] PRUDIC, D.E., Documentation of a Computer Program to Simulate Stream-Aquifer Relations Using a Modular, Finite-Difference, Ground-Water Flow Model, U.S. Geol. Survey Open-File Rept. 88-729 (1989) 113 pp.
[125] HARBAUGH, A.W., A Computer Program for Calculating Subregional Water Budgets Using Results from the U.S. Geological Survey Modular Three-Dimensional Finite-Difference Ground-Water Flow Model, U.S. Geol. Survey Open-File Rept. 90-392 (1990) 46 pp.
[126] HILL, M.C., Preconditioned Conjugate-Gradient 2 (PCG2)--A Computer Program for Solving Ground-Water Flow Equations, U.S. Geol. Survey Water-Res. Inv. Rept. 90-4048 (1990) 43 pp.
[127] HILL, M.C., Five Computer Programs for Testing Weighted Residuals and Calculating Linear Confidence and Prediction Intervals on Results from the Ground-Water Parameter-Estimation Computer Program MODFLOWP, U.S. Geol. Survey Open-File Rept. 93-481 (1994) 81 pp.
[128] HARBAUGH, A.W., A Generalized Finite-Difference Formulation Program for the U.S. Geological Survey Modular Three-Dimensional Finite-Difference Ground-Water Flow Model, U.S. Geol. Survey Open-File Rept. 91-494 (1992) 60 pp.
[129] REILLY, T.E., HARBAUGH, A.W., Source Code for the Computer Program and Sample Data Set for the Simulation of Cylindrical Flow to a Well Using the U.S. Geological Survey Modular Finite-Difference Ground-Water Flow Model, U.S. Geol. Survey Open-File Rept. 92-659 (1993) 7 pp.
[130] HSIEH, P.A., FRECKLETON, J.R., Documentation of a Computer Program to Simulate Horizontal-Flow Barriers Using the U.S. Geological Survey Modular Three-Dimensional Finite-Difference Ground-Water Flow Model, U.S. Geol. Survey Open-File Rept. 92-477 (1993) 32 pp.
[131] MCDONALD, M.G., HARBAUGH, A.W., ORR, B.R., ACKERMAN, D.J., A Method of Converting No-Flow Cells to Variable-Head Cells for the U.S. Geological Survey Modular Finite-Difference Ground-Water Flow Model, U.S. Geol. Survey Open-File Rept. 91-536 (1992) 99 pp.
[132] LEAKE, S.A., LEAHY, P.P., NAVOY, A.S., Documentation of a Computer Program to Simulate Transient Leakage from Confining Units Using the Modular Finite-Difference Ground-Water Flow Model, U.S. Geol. Survey Open-File Rept. 94-59 (1994) 70 pp.
[133] SWAIN, E.D., WEXLER, E.J., A Coupled Surface-Water and Ground-Water Flow Model for Simulation of Stream-Aquifer Interaction, U.S. Geol. Survey Open-File Rept. 92-138 (1993) 162 pp.
[134] SWAIN, E.D., Documentation of a Computer Program (Streamlink) to Represent Direct-Flow Connections in a Coupled Ground-Water and Surface-Water Model, U.S. Geol. Survey Water-Res. Inv. Rept. 93-4011 (1993) 62 pp.
[135] GOODE, D.J., KONIKOW, L.F., Testing a method-of-characteristics model of three-dimensional solute transport in ground water: *in* Symposium on Ground Water, Proc. Internat. Symposium, Nashville, Tenn., (LENNON, G.P., Ed.) American Soc. Civil Engineers, New York (1991) 21-27.
[136] APPEL, C.A., REILLY, T.E., Summary of Computer Programs Produced by the U.S. Geological Survey for Simulation of Ground-Water Flow and Quality--1994, U.S. Geol. Survey Circular 1104 (1994) 98 pp.
[137] DOWNEY, J.S., WEISS, E.J., Preliminary Data Set for Three-Dimensional Digital Model of the Red River and Madison Aquifers, U.S. Geol. Survey Open-File Rept. 80-756 (1980).
[138] WOODWARD-CLYDE CONSULTANTS, Well-Field Hydrology Technical Report for the ETSI Coal Slurry Pipeline Project, Bureau of Land Management, Washington, D.C. (1981) 448 pp.
[139] BACK, W., HANSHAW, B.B., PLUMMER, L.N., RAHN, P.H., RIGHTMIRE, C.T., RUBIN, M., Process and rate of dedolomitization: Mass transfer and ^{14}C dating in a regional carbonate aquifer, Geol. Soc. of America Bull. 94 12 (1983) 1415-1429.
[140] KONIKOW, L.F., Extended interpretation of "Process and rate of dedolomitization: Mass transfer and ^{14}C dating in a regional carbonate aquifer", Geol. Soc. of America Bull. 96 6 (1985) 1096-1098.
[141] REILLY, T.E., PLUMMER, L.N., PHILLIPS, P.J., BUSENBERG, E., The use of simulation and multiple environmental tracers to quantify groundwater flow in a shallow aquifer, Water Resources Res. 30 2 (1994) 421-433.

[142] VAN DER HEIJDE, P.K.M., BACHMAT, Y., BREDEHOEFT, J.D., ANDREWS, B., HOLTZ, D., SEBASTIAN, S., Groundwater Management: The Use Of Numerical Models, American Geophys. Union, Washington, D.C., Water Res. Monograph 5 [2nd Ed.] (1985) 180 pp.
[143] VESTED, H.J., OLESEN, K.W., REFSGAARD, A., ENGESGAARD, P., MALGREN-HANSEN, A., Advection-Dispersion Review, Rivers and Groundwater, Comm. of the European Communities, Instit. for Systems Eng. and Informatics Rept. ISEI/IE2423/93 (1992) 142 pp.
[144] ANDERSON, M.P., WARD, D.S., LAPPALA, E.G., PRICKETT, T.A., Computer Models for Subsurface Water, *in* Handbook of Hydrology (MAIDMENT, D.R., Ed.), McGraw-Hill, Inc., New York (1992) 22.1-22.34.
[145] BROYD, T.W., DEAN, R.B., HOBBS, G.D., KNOWLES, N.C., PUTNEY, J.M., WRIGLEY, J., A Directory of Computer Programs for Assessment of Radioactive Waste Disposal in Geological Formations, Comm. of the European Communities, Rept. EUR8669en (1983) 530 pp.

QUANTITATIVE EVALUATION OF FLOW SYSTEMS, GROUNDWATER RECHARGE AND TRANSMISSIVITIES USING ENVIRONMENTAL TRACERS

E.M. ADAR
Water Resources Center,
Department of Geology and Minerology
Ben-Gurion University of Negev,
Sede Boker Campus,
Israel

Abstract

This chapter provides an overview of the basic concepts and formulations on the compartmental (mixing-cell) approach for interpretation of isotope and natural tracer data to arrive at quantitative estimates related to groundwater systems. The theoretical basis of the models and the specific solution algorithms used are described. The application of this approach to field cases are described as illustrative examples. Results of sensitivity analyses of the model to different parameters are provided.

INTRODUCTION

To properly manage groundwater resources, there is a need for accurate information about inflows (recharge), outflows (discharge) and the physical characteristics of aquifers. Yet, in many semi-arid and arid basins it has been common to exploit aquifers based on partial information about the hydrologic characteristics. A major source of uncertainty stems from the hydrologist's inability to reliably estimate the spatial and temporal distribution of recharge rates. Similarly, incomplete information of hydraulic conditions along the boundaries, such as fluxes and heads, imposes tremendous difficulties in aquifer numerical modeling. The difficulty is especially acute in semi-arid and arid regions where recharge is often occurs in pulses from floods of relatively short duration, and lasts from several hours to several days (Zimmerman, et al., 1966, 1967). In basins with limited number of wells and hence, limited knowledge of the hydrogeological structure, it is often difficult to precisely define the flow system or the boundary conditions. Furthermore, the lack of observation wells and pumping test data eliminate the possibility of proper calibration processes. For basins with a complex geological structure and with scarce hydrologic information, a method is introduced for a quantitative assessment of groundwater flow system, components of recharge, and transmissivities by incorporating environmental tracers such as dissolved minerals and isotopes.

Models that assess recharge by equating it to infiltration at the soil surface, (including stream beds), in response to rainfall, irrigation and stream flow abound in the literature. Examples can be found in the works of Eakin (1966), Feth, et al. (1966), Briggs and Werho (1966), Burkham (1970), Rantz and Eakin (1971), Belan (1972), Kafri and Ben-Asher (1978), Howard and Lloyd (1979), and others. Of particular interest for recharge from ephemeral stream losses in the

arid southern United States are the studies of Matlock (1965), Marsh (1968) and Keith (1981). Since not all the water infiltrated reaches the water table, the volume and rate of the water table recharge are generally less than those of infiltration. Only that water which actually reaches the water table, and in this way becomes part of the saturated zone, should be considered as recharge. For the computation of net input one needs to transform the infiltration into volumes or rates of deep percolation beneath the root zone, including the root zone of phreatophytes near streams and washes. Methods for effecting such a transformation have been described by numerous authors including Thornwaite and Mather (1957), Mero (1963), Walker (1970), Olmsted et al. (1973), Bos and Nugteren (1974), Heerman and Kincaid (1974), Wind and Van Doorne (1975), King and Lambert (1976), , Tanji (1977), Wilmot (1977) and Karmeli et al. (1978). While some of these methods may work well in humid regions, their applicability to semi-arid and arid conditions is in question.

Among the most readily available hydrologic data that one could use to estimate groundwater recharge in semi-arid and arid regions are stream flow records and hydrographs of nearby wells. Very often, the fluctuation of water levels in wells situated close to streams reflects fluctuation in the rate of recharge as well as the rate of deep percolation beneath the stream. The idea of using groundwater level fluctuations as an indicator of recharge dates back to the early work of Jacob (1943, 1944). Various methods based on this idea have been discussed by Wilson and DeCook (1968), Matlock (1970), Moench and Kisiel (1970), Venetis (1971), Matlock and Davis (1972), Gelhar (1974), Besbes, et al. (1978), Duffy, et al. (1978) and Flug, et al. (1980). When stream flow infiltration is the main source of recharge, some of these methods may yield acceptable results. However, none of the techniques mentioned thus far are able to deal with situations where the relative importance of diverse potential recharge sources is unknown.

In this work a methodology is developed for the identification and quantification of multiple recharge sources, subsurface fluxes, and aquifer physical parameters on the basis of hydrochemical and isotope data. This means using such data to elucidate the spatial distribution of recharge sources, flow components, and to estimate the relative as well as absolute strength of each such source. Under certain conditions this can be accomplished by solving an "inverse problem" of aquifer hydrology in which recharge is estimated jointly with the hydraulic parameters of a numerical aquifer flow model (Carrera and Neuman, 1986a, b & c). This, however, works only if the hydraulic properties of the aquifer are reasonably well characterized, and there is abundant information about its hydraulic response. While such information is often inadequate, data about groundwater chemistry and environmental isotopes can often be collected rapidly and at a relatively small expense. It is therefore important to examine the extent to which such data can be used for the identification and quantification of groundwater flow system.

In the past, hydrologists have used chemical and isotope data for recharge studies primarily in a qualitative sense. Environmental isotopes played a dominant role in such studies, as exemplified by the works of Verhagen, et al. (1970, 1978), Gat and Dansgaard (1972), Blake, et al. (1973), Bredenkamp, et al.

(1974), Mazor et al, (1974), Yurtsever and Payne (1978a & b), Shampine, et al. (1979), Levin, et al. (1980), Issar and Gat (1981), Issar and Gilad (1982), Mazor (1982) and Issar (1983). In some studies, tritium was used to obtain quantitative estimates of recharge (Dincer, et al., 1974; Bredenkamp, et al., 1974; Vogel, et al., 1974). More recent attempts to extract quantitative information about recharge from hydrochemical data often rely on statistical analyses. As an example, Lawrence and Upchurch (1982) use factor analysis to identify the recharge source for certain groups of dissolved chemical species in an aquifer. In all such works, the authors either evaluate the magnitude of a given recharge source, or evaluate the potential of recharge without providing quantitative estimates of recharge rates.

A serious attempt to incorporate hydrologic and hydrochemical information into a mathematical groundwater model for the purpose of source identification and quantification was presented by Gorelick, et al. (1983) and Wagner and Gorelick (1986a & b). They deal with the question of identifying the location and magnitude of pollution sources that might have contributed to the contamination of an aquifer. For this, they utilize a two-dimensional numerical model of solute transport in the aquifer, coupled with various optimization techniques. The method might, in principle, be used for recharge estimation provided one had abundant information about the hydraulic and transport properties of the aquifer.

2. PRINCIPALS OF THE MIXING CELL APPROACH

In this chapter a mathematical model is presented for the estimation of recharge and hydraulic parameters of an aquifer under conditions where the hydraulic and transport characteristics of the aquifer are unknown or poorly known. In the model, the aquifer is divided into cells within which the isotopes and dissolved constituents are assumed to undergo complete mixing. This idea derives from the mixing cell approach of Simpson and co-workers (Simpson, (1975), Simpson and Duckstein, 1976; Campana and Simpson, 1984). This approach had been already used for describing the spatial hydrodynamic behavior of a one dimensional non steady flow. Yurtsever and Payne (1978b & 1985) applied the convolution integral to describe the tritium response function in a simplified lumped parameter multi-cell model. Storage coefficients for each cell, mean travel time and aquifer dispersivity were estimated. Campana and Mahin (1985) used the mixing cell approach to assess mean water age, effective porosity and storage coefficient in a limestone aquifer.

In this approach, mass-balance equations are written for each mixing cell, expressing the conservation of water, isotopes and dissolved chemicals. These equations are solved simultaneously by quadratic programming for the estimation of flow components and aquifer hydraulic parameters in a lumped system. A similar approach was used by Woolhiser et al. (1982) to estimate the inflow rate into a river reach. The latter being analogous to a single cell in our model.

In the approach used here the degree to which individual dissolved constituent may be considered conservative is tested a priori by means of a chemical equilibrium model such as WATEQF (Plummer et al., 1976) or NETPATH ((Plummer et al., 1991) Constituents which do not pass this test are either disregarded or assigned a suitably small weight in the quadratic program.

The model presented below relies basically on three types of conceptual models applied in hydrology (and in hydrodynamics): (a) Evaluation of the motion of water and solutes with a multi-compartmental mixing cell model as suggested by Rasmussen (1982) and Campana and Simpson (1984): (b) solution of a set of water and dissolved constituents mass balance equations via a quadratic programming optimization scheme exemplified by works carried out by Woolhiser, et al. (1982); Adar (1984) and Adar, et al. (1988) and (c) a mathematical model combining an inverse process to estimate compartmental conductances and storage coefficients distribution in a multi-compartmental model for a non-steady flow as described by Adar and Sorek (1989, 1990)

The model is based on accounting for natural available tracers such as dissolved chemicals, stable isotope ratios and electrical conductivity measurements that are relatively easily obtained and measured in an aquifer and in potential recharge sources. It conceptualizes an aquifer that is discretized into finite cells such that the spatial distribution of any aquifer characteristic such as dissolved constituents and hydraulic heads are approximated by unique values for each tracer and head assuming a complete dilution within each cell (the mixing cell principle). The following assumptions are considered to be true in the aquifer:

1. Tracers are conservative: all reactions, dissolution and/or precipitation are negligible. The spatial change in the concentration of the solute is solely due to dilution. In principle, non-conservative tracers can be utilized as long as the rate of change due to subsurface water mineral interaction or rate of decay functions are known.

2. Seasonal pulsation of fluxes for each cell can be represented by mean values spanning over a time interval in which the hydraulic head may be regarded as a constant value or as an average value of cyclic process in time. Pulsation of hydraulic heads throughout observation points in the aquifer may change in amplitude. yet their period phases remain alike.

3. Transport of dissolved constituents are dominated by advection process (i.e. compartmental Peclet number is infinite).

Further practical assumptions are embedded in the model: (a) Concentrations of solutes, which are constant within each cell for specific time step, are measurable and known together with the concentrations of the same tracers in the inflow and outflow components; (b) all of the flows entering or leaving the aquifer system are known qualitatively, yet most of the source-sink and discharge flow components are known quantitatively, including the associated concentration of the dissolved constituents.

Being aware of the fact that in groundwater flow, solutes and isotope concentrations change in space and time, we discretized the aquifer into finite cells assuming that within each cell (for a specific time step) solutes and isotopes are fully mixed, yet their concentrations may differ from one cell to another. Thus, it is justified to assign each cell a mean indicative set of solutes and/or isotopes. With respect to the second assumption one can identify each potential recharge source and represent a potential water source that can contribute to the system via the set of tracers.

3. ASSESSMENT OF GROUNDWATER FLUXES AND RECHARGE COMPONENTS

In this model the aquifer is subdivided into a finite number of discrete cells **N** and time is represented by discrete intervals Δt. Each dissolved constituents is taken to be uniformly distributed within any space-time domain due to complete mixing. Each constituent **k** is taken to be conservative. Seasonal fluctuations in flow rates are smoothed out by considering their temporal integrals over semi-annual cycles. With regard to the above ideas, we will now write a set of balance equations for the flux and solutes within a given time period Δt and for each cell **n** separately.

For a fluid with constant density, the water balance for the **n**-th compartment is expressed by the following equation:

$$Q_n - W_n + \sum_{i=1}^{I_n} q_{in} - \sum_{j=1}^{J_n} q_{nj} = S_n^* \frac{dh_n}{dt} \qquad (1)$$

where **In** and **Jn** denote the number of sources and/or compartments from which flow enters the **n**-th compartment, and leaves it, respectively; q_{in} and q_{nj} denote the fluxes from the **i**-th source or compartment into the **n**-th one, and from the **n**-th one into the **j**-th one, respectively; Q_n and W_n denote the fluid sources (such as point injection) and sinks (such as pumping), respectively; S_n^* represents the storage capacity within cell **n**: and h_n denotes the hydraulic head associated with that compartment. Figure 1 illustrates the aforementioned flow parameters in a schematic compartmental system.

As the head (h_n) for each compartment varies, we may identify points in time, say t_1 and t_2 ($t_2 > t_1$), at which the hydraulic heads are the same (e.g. at the beginning and at the end of a specific season). This means that over that time interval $t=t_2—t_1$ (regardless of the sequence of changes in heads during this time interval), the total magnitude of the derivatives (dh_n/dt) in each compartment has not changed. Hence, since $S_n^* \pi S_n^*(t)$, we obtain:

$$\frac{1}{\tau}\int_{t_1}^{t_2} S_n^* \frac{dh_n}{dt} dt = 0 \quad ; \quad h_{n;t_1} \equiv h_{n;t_2} \qquad (2)$$

Thus, by integrating equation (1) over a time period $t=t_2—t_1$ and dividing by t we obtain accordingly:

$$\overline{Q}_n - \overline{W}_n + \sum_{i=1}^{I_n} \overline{q}_{in} - \sum_{j=1}^{J_n} \overline{q}_{nj} = 0 \qquad (3)$$

where all the parameters have the same meaning as in (1), but represent average values over time interval Δt e.g.:

$$\overline{q}_{in} = \frac{1}{\tau} \int_{t_1}^{t_2} q_{in} dt \qquad (4)$$

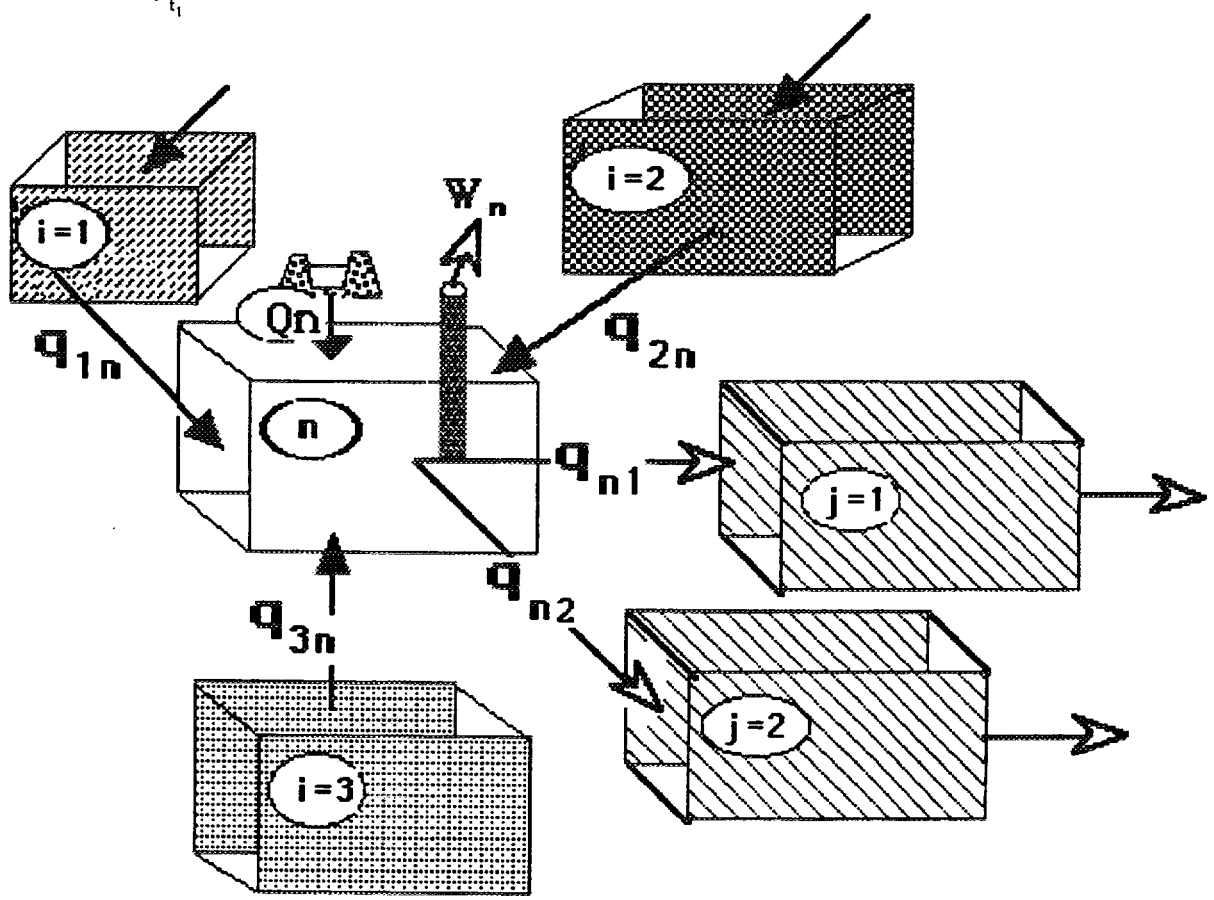

Figure 1. Symbols of designating fluxes, sinks, sources and schematic flow configuration between cells through permeable boundaries.

Note that equation (3) expresses a quasi-steady state situation resulting from the time averaging process.

For quasi-steady state variations of concentrations, when mixing cell concept is applied, and in view of assumption 1 and equation (1c), we write a mass balance expression for a dissolved constituent **k**, in cell **n**.

$$\tilde{C}_{nk}\overline{Q}_n - \overline{C}_{nk}\left[\overline{W}_n + \sum_{j=1}^{J_n} \overline{q}_{nj}\right] + \sum_{i=1}^{I_n} \overline{q}_{in}\overline{C}_{ink} = 0 \quad k=1,2,....,K \qquad (5)$$

where $\bar{C}_{ink}$ is the average concentration of solute **k** entering cell **n** together with the flux coming from cell **I**; $\bar{C}_{nk}$ denotes average concentration of the k^{th} constituent within cell **n** ; and $\tilde{C}_{nk}$ is the average concentration of **k** associated with source Q_n. However, when constructing balance equations from field measurements, equations (3) and (5) should account for various errors. Water balance (equation (3)) may not hold because of an error in identifying and measurements of fluxes or rates of pumpage. Mass balance of solutes (equation (5)) may be affected by analytical errors in measuring concentrations. especially in quantifying cell concentrations. To reflect the above mentioned inconsistencies, we introduce an error term into equation (3) and (5) respectively.

$$\bar{Q}_n - \bar{W}_n + \sum_{i=1}^{I_n} \bar{q}_{in} - \sum_{j=1}^{J_n} \bar{q}_{nj} = e_n \tag{6}$$

$$\tilde{C}_{nk}\bar{Q}_n - \bar{C}_{nk}\left[\bar{W}_n + \sum_{j=1}^{J_n} \bar{q}_{nj}\right] + \sum_{i=1}^{I_n} \bar{q}_{in}\bar{C}_{ink} = e_{nk} \tag{7}$$

where e_n, and e_{nk} are the deviations from flux and solute balance in cell **n**, respectively. Upon combining equations (6) and (7) to a matrix form for each compartment, **n**, we obtain:

$$\underline{\underline{C}}_n \underline{q}_n + \underline{D} = \underline{E}_n \tag{5}$$

where $\underline{\underline{C}}_n$ is a matrix with known concentrations in cell **n** of the form

$$\underline{\underline{C}}_n = \begin{bmatrix} 1 & ,1 & ,\ldots,1 & ,-1 & ,-1 & ,\ldots,-1 \\ C_{1n1}, & C_{2n1}, & \ldots, C_{I_n n1}, & -C_{n1}, & -C_{n1}, & \ldots, -C_{n1} \\ C_{1n2}, & C_{2n2}, & \ldots, C_{I_n n2}, & -C_{n2}, & -C_{n2}, & \ldots, -C_{n2} \\ . & . & . & . & . & . \\ . & . & . & . & . & . \\ C_{1nK}, & C_{2nK}, & \ldots, C_{I_n nK}, & -C_{nK}, & -C_{nK}, & \ldots, -C_{nK} \end{bmatrix} (K+1)*(In+Jn) \tag{8}$$

where the first row accounts for water balance, and the other **K** rows express solute mass balance where **K** is the total number of tracers used in the analysis. Negative sign denotes coefficients which are associated with outgoing fluxes. $\bar{C}ink$ denotes the concentration of the **k**-th species flowing into cell **n** from cell **i**. $\underline{q}_n$ is a vector of the unknown fluxes through the boundaries of cell **n**, described by:

$$\underline{q}_n = \left[\bar{q}_{1n}, \bar{q}_{2n}, \ldots, \bar{q}_{I_n n}, \bar{q}_{n1}, \bar{q}_{n2}, \ldots, \bar{q}_{nJ_n}\right] (In+Jn)*1. \tag{9}$$

$\underline{D}_n$ is a vector containing elements that are measured and known quantitatively in cell **n** (such as known fluxes of pumpage), described by:

$$\underline{D}_n = \left[\left(\bar{Q}_n - \bar{W}_n\right), \left(\tilde{C}_{n1}\bar{Q}_n - C_{n1}\bar{W}_n\right), \left(\tilde{C}_{n2}\bar{Q}_n - C_{n2}\bar{W}_n\right), \ldots, \left(\tilde{C}_{nK}\bar{Q}_n - C_{nK}\bar{W}_n\right)\right] (K+1)*1 \tag{10}$$

E is the error vector in cell n, described by:

$$\underline{E} = [e_n, e_{n1}, e_{n2}, \ldots, e_{nK}](1+K)*1 \qquad (11)$$

The total flux components in the aquifer can now be estimated by a minimization of the square error sums **J**. Similar to a procedure suggested by Adar (1984), by virtue of equation (5) and by assembling the square error terms over all cells we obtain:

$$J = \sum_{n=1}^{N} \left[\underline{E}_n^T \underline{\underline{W}} \underline{E}_n \right] = \sum_{n=1}^{N} \left[\left(\underline{\underline{C}}_n q_n + \underline{D}_n \right)^T \underline{\underline{W}} \left(\underline{\underline{C}}_n q_n + \underline{D}_n \right) \right] \qquad (12)$$

where $(\ )^T$ denotes transpose and $\underline{\underline{W}}$ represents a diagonal matrix comprised of weighting values about estimated errors (independent of each other) expected for each of the terms building the mass balance for the fluid and the dissolved constituents. The weighting matrix, $\underline{\underline{W}}$ also reflects the degree of confidence to which the tracers are assumed conservative and the degree of accuracy of the chemical and isotope analyses. The solution of equation (12) for $\mathbf{q_n}$ is decomposed into linear and non-linear parts and **J** can be minimized to evaluate $\mathbf{q_n}$ by an algorithm developed, for example, by Wolf (1967)

3.1 MODEL TESTING WITH SYNTHETIC DATA

Test has been made of the mathematical model for which sets of synthetic data have been generated for a hypothetical aquifer divided into mixing cells. The test was conducted to evaluate the ability of the computer code to solve the mathematical model for the unknown fluxes. A schematic representation of the flow regime prevailing during the first test is given in Figure 2.

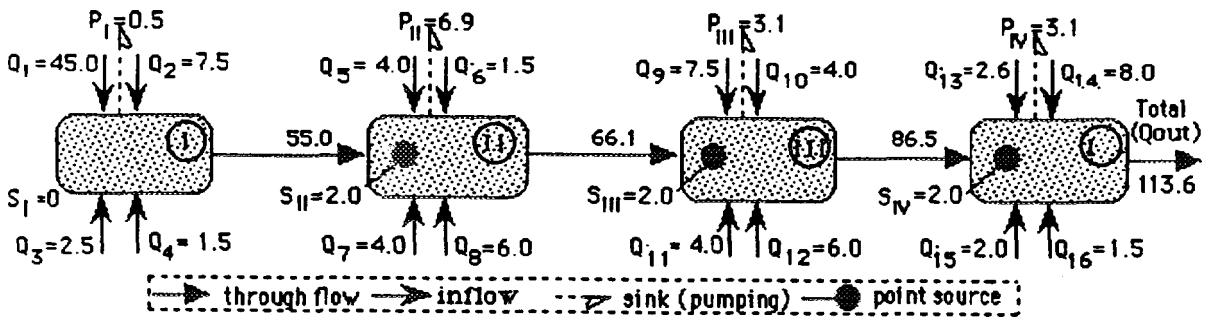

Figure 2: Schematic compartmental aquifer used for testing the mathematical algorithm. Q = rate of inflow (m^3/t); P = rate of discharge (m^3/t).

Recharge into the aquifer derives from nineteen sources. Discharge (**Qout**) occurs at the outlet from cell IV, and via pumpage from each of the four cells. To generate the synthetic data, the corresponding recharge and discharge rates were

assigned arbitrary values (consistent with water balance requirements) in discharge units as indicated in the figure.

In this schematic flow system, the number of unknown flow rates exceeds the number of isotopic and chemical species by 19 to 14. There are four inflows into cell 1 and five into each of cells 2, 3 and 4. One inflow into each of the last tree cells is considered as a point source term (S). The assigned inflows and sources are posted in Figure 2, and the assigned concentrations appear in Table 1. Inflows Q_4, S_{II}, S_{III} and Q_{16} have identical isotopes and chemical signatures. Q_4 and Q_{16} could represent, for example recharge from floods, and so have inflows Q_8, Q_{12}, and Q_{15} which could represent, for example stream bed infiltration due to perennial effluent. S_{II} and S_{III} might designate a common point source such as leakage from surface water tank. The sink terms (such as pumpage) are 0.5, 6.9, 3.1 and 3.1 (volumetric flux units) for cells I, II, III and IV, respectively.

Table 1. Synthetic concentrations used in Test 1.

inflow	EC[a]	Mg	Ca	Na	K	HCO_3	Cl	NO_3	SO_4	F	Li	Si	D[b]	^{18}O[c]
1	353.8	0.74	1.97	0.97	0.062	3.08	0.205	0.082	0.42	0.023	0.0026	18.01	-73.8	-9.73
2	187.1	0.36	0.81	0.39	0.035	0.89	0.093	0.001	0.80	0.001	0.0003	18.18	-66.3	-8.56
3	146.0	0.53	1.13	0.51	0.049	1.40	0.081	0.035	0.66	0.006	0.0012	17.53	-60.6	-8.55
4	332.3	0.62	2.31	0.69	0.174	2.97	0.151	0.030	0.38	0.025	0.0013	16.83	-58.7	-7.41
5	304.5	0.10	0.24	2.01	0.048	2.52	0.263	0.022	0.05	0.036	0.0022	14.00	-67.2	-8.70
6	370.3	0.77	1.67	1.70	0.069	3.04	0.690	0.224	0.14	0.008	0.0032	8.80	-63.1	-6.52
7	454.0	1.28	2.52	0.98	0.028	3.71	0.419	0.059	0.64	0.012	0.0016	16.35	-76.3	-10.18
8	242.0	0.39	1.51	0.33	0.063	1.20	0.086	0.044	0.63	0.030	0.0020	17.70	-67.1	-8.98
source	332.3	0.62	2.31	0.69	0.174	2.97	0.151	0.030	0.38	0.025	0.0013	16.83	-58.7	-7.41
9	356.0	1.72	3.18	0.73	0.034	3.64	0.140	0.046	1.93	0.015	0.0016	14.80	-67.0	-8.43
10	147.8	0.84	0.41	0.33	0.030	0.07	0.070	0.008	0.98	0.120	0.002	7.80	-68.9	-9.36
11	362.0	0.66	2.06	0.87	0.050	2.93	0.140	0.080	0.51	0.022	0.0023	17.10	-69.3	-9.66
12	242.0	0.39	1.51	0.33	0.063	1.20	0.086	0.044	0.63	0.030	0.0020	17.70	-67.1	-8.98
source	332.3	0.62	2.31	0.69	0.174	2.97	0.151	0.030	0.38	0.025	0.0013	16.83	-58.7	-7.41
13	355.5	0.70	2.10	0.89	0.050	2.90	0.175	0.142	0.56	0.024	0.0023	18.55	-72.3	-9.68
14	444.2	1.15	3.21	0.76	0.029	3.39	0.275	0.027	1.36	0.052	0.0016	14.58	-68.6	-9.56
15	242.0	0.39	1.51	0.33	0.063	1.20	0.086	0.044	0.63	0.030	0.0020	17.70	-67.1	-8.98
16	332.3	0.62	2.31	0.69	0.174	2.97	0.151	0.030	0.38	0.025	0.0013	16.83	-67.7	-9.70
source	302.8	0.05	0.30	2.89	0.020	2.52	0.320	0.021	0.19	0.080	0.0037	14.25	-74.8	-9.44
Cell 1	321.9	0.677	1.788	0.865	0.0608	2.712	0.1832	0.0678	0.480	0.0194	0.0022	17.98	-71.82	-9.461
Cell 2	322.9	0.655	1.733	0.902	0.06	2.646	0.2019	0.065	0.468	0.0207	0.0021	17.44	-70.89	-9.303
Cell 3	314.4	0.734	1.807	0.818	0.060	2.538	0.1793	0.0594	0.623	0.0254	0.0020	16.78	-69.885	-9.156
Cell 4	324.2	0.744	1.895	0.844	0.0583	2.593	0.1871	0.0575	0.657	0.0286	0.0020	16.62	-69.856	-9.235

Concentrations in meq l^{-1} unless otherwise indicated.
a-μMHOcm^{-1}
b- Deuterium (0/00)
c- Oxygen-18 (0/00)

These values, while arbitrarily chosen (so as to maintain isotopic and chemical balance for each species, are nevertheless in accord with actual data from the Aravaipa Valley in southern Arizona to be later presented in the field application section. With the assigned flow rates and concentrations, the error terms in equations. (6) and (7) should be zero, and the minimization of J. in equation (12) should yield a zero value for the optimum J.

For the purpose of our exercise, we treated the discharge, Q_{out}, and pumpage rates, P_1- P_4, as known terms, and the recharge rates, Q_1-Q_{19}, as unknowns. To facilitate convergence of the quadratic program we followed the approach of Woolhiser, et al. (1982) setting the components of the diagonal weight matrix W_n, corresponding to each cell n equal to:

$$Wn_{11} = Q_{0ut}^{-2} \quad ; \quad Wn_{1=k,1+k} = C_{ok}^{-2} \quad ; \qquad k=1,2,3,...,K \tag{13}$$

where C_{ok} is the concentration of the k^{th} species at the outlet from the aquifer. The effect of this weighting scheme is to normalize the balance equations so they are all expressed on a scale relative to the downstream outflow equations.

Table 2 compares the calculated and assigned inflow rates, and Table 3 juxtaposes the calculated and assigned mass flow rates for the isotopic and chemical species. Again, the results are seen to be very good, the total water balance and the total isotopic and chemical balance errors are negligible, and attributed to the computer round off procedure.

Table 2. Comparison between assigned and calculated inflows obtained with exact data.

Inflow	Q_1	Q_2	Q_3	Q_4	Q_5	Q_6	Q_7	Q_8	Q_9	Q_{10}	Q_{11}	Q_{12}	Q_{13}	Q_{14}	Q_{15}	Q_{16}	TOTAL
Assigned inflows (m^3/t)	45.00	7.50	2.50	1.50	4.00	1.50	4.00	6.00	7.50	4.00	4.00	6.00	2.60	8.00	2.00	1.50	113.60
Calculated inflows (m^3/t)	44.30	7.40	2.36	1.44	4.17	1.56	4.37	6.30	7.58	3.97	3.76	6.04	2.68	8.07	2.08	1.54	113.59

Flow between cells	I to II	II to III	III to IV
Assigned flow)m^3/t)	55.0	66.1	86.5
Calculated flow (m^3/t)	55.368	66.372	86.396

m^3/t - cubic meters per unit time

The computed flow rates in Table 2 are seen to be very close to the true (assigned) values. Q_4, and Q_{16}, or Q_8, Q_{12}, and Q_{15} derived from the same source (carry same isotopic and chemical signature) but contributing to two separate cells, are correctly identified. The errors in Tables 2 and 3 stem essentially from rounding off and incomplete convergence of the Wolf algorithm. Indeed, experience has shown, that for the same test case, these small deviations vary with the type of computer system. Other tests with different cell and flow configurations are reported in Adar (1984) and Adar et al. (1988).

The tests show that, as long as the input data are precise including a proper aquifer discretization into mixing cells, the algorithm is able to estimate correctly fluxes of recharge and subsurface flow components. It is important to note that within a particular cell, each potential flow component must have a unique chemical and isotopic values. The same source, however, may contribute to

several cells. The number of computed fluxes (unknowns) may be less or more than the number of isotopic and chemical species entering into the model. The number of mass balance expressions, however, should exceed by far the number of unknowns.

Table 3. Comparison between assigned and calculated mass flow rates obtained with exact data.

Ionic and isotopic species	True mass flow	Estimated mass flow	Percentage error
EC*	36,815.94	36,788.62	0.074
Mg	1,019.42	1,019.21	0.021
Ca	4,289.66	4,285.13	0.106
Na	2,211.36	2,211.69	-0.015
K	260.52	260.18	0.130
HCO_3	17,984.83	17,987.77	0.016
Cl	756.67	756.13	0.074
NO_3	406.21	408.85	0.651
SO_4	3,570.12	3,562.35	0.218
F	60.55	60.41	0.228
Li	1.61	1.58	0.749
Si	1,894.77	1,894.87	-0.005
^2H	-7,942.92	-7,943.85	-0.012
^{18}O	-1,049.62	-1,049.50	-0.009
Total	325,133.7	325,326.6	0.060

* Electrical conductivity.

3.2 FIELD APPLICATIONS

The above-mentioned model has been implemented to assess the rate of recharge and groundwater fluxes in two arid basins: the Aravaipa basin in Arizona, USA, and in the Arava Valley shared by Israel and Jordan. In these basins, a simple longitudinal aquifer is recharged through mountain front alluvial fans. Other sources of recharge to be considered are temporal erratic floods and upward leakage from deep semi-confined aquifers.

3.2.1 ARAVAIPA BASIN, ARIZONA, U.S.A.

The Aravaipa Valley is located in the eastern Sonora desert in Arizona, USA (Fig 3). The valley is surrounded by the Galiuro volcanics (a sequence of andesitic and rhyolitic tuffs and lava) on the west, and the Santa Teresa granitic pluton, and the Pinaleno granodioritic pluton from the eastern boundary of the valley.

The Aravaipa Valley is a narrow graben filled with fluvial sediment interbedded with thin lake deposits. The main water course is the ephemeral Aravaipa Creek that becomes perennial at the Aravaipa Springs at the head of the Aravaipa Canyon. Annual precipitation from large winter storms and high intensity convective summer storms range from 355 mm in the lower valley, to 430 mm in the upper valley, and to 510 mm in the surrounding mountains (For further geologic and geophysical information, the reader is referred to Adar, 1984).

Three hydrological units were identified in the Aravaipa watershed: a mountain aquifer and two alluvial aquifers, separated by lacustrine clay layers. The lower alluvial unit is formed mainly by the older alluvium. It is confined from above by low permeability layers which are continuous across the width of the valley except for the western pediments. This suggests that this unit may be recharged directly from the eastern mountains and by infiltrating rainfall and runoff from the alluvial pediments. The main source of water in the valley is the upper water table unit. This aquifer is limited to the course of the Aravaipa Creek and to the alluvial fans of the confluences with major tributaries. This aquifer is 20 kilometers long and is generally narrow ("1,000 m), except near major alluvial fans where its width may exceed 1,500-2,000 m.

In general, available hydrological information for the valley is very poor and consists of an approximated depth of wells, a few driller's logs and two transmissivity values for the upper and confined aquifers respectively. Discharge from the lower confined aquifer by livestock and irrigation wells is estimated at 62,000 m3/year. Discharge from the water table aquifer by domestic use and irrigation wells is estimated at 2.96×10^6 m3/year; and discharge from the valley through the Aravaipa spring is estimated at 1.22×10^7 m3/year. Twenty five years of records regarding the hydrological activities of the valley suggest that it is in a steady state (Arad and Adar, 1981).

Chemistry and environmental isotopes are used to identify potential sources of recharge and possible mixing and dilution of waters from different sources. For this we make use of the fact that water that infiltrates to a depth at which evaporation ceases usually maintains constant ^{18}O and D ratios, unless mixing or dilution with waters having different isotopic compositions takes place.

One hundred and sixty two water samples from 109 well sites, springs and stream gages (including floods) were analyzed for major cations (including Li), anions (including F), Si, TDI, electrical conductivity and temperature. Water from 74 sites were analyzed for Oxygen-18 and 47 of the latter sites were checked for deuterium (D) values. The upper and lower aquifers exhibit different ranges for temperature, water level and ratios of environmental isotopes. Higher temperatures and heavier stable isotopes are found throughout the entire area of the lower aquifer.

Higher piezometric heads in the lower confined unit is a clear indication that water may leak upward from the confined aquifer along the entire valley, through electrical conductivity and temperature logs throughout the confining layer were not sensitive enough to indicate the presence of such leaking. The

hydraulic connection between the two aquifers has been implied on the basis of Tritium and Carbon-14 variations during a pumping test, and by the relationship between Tritium (H-3) and C-14 ratios. (Adar & Neuman, 1986, 1988).

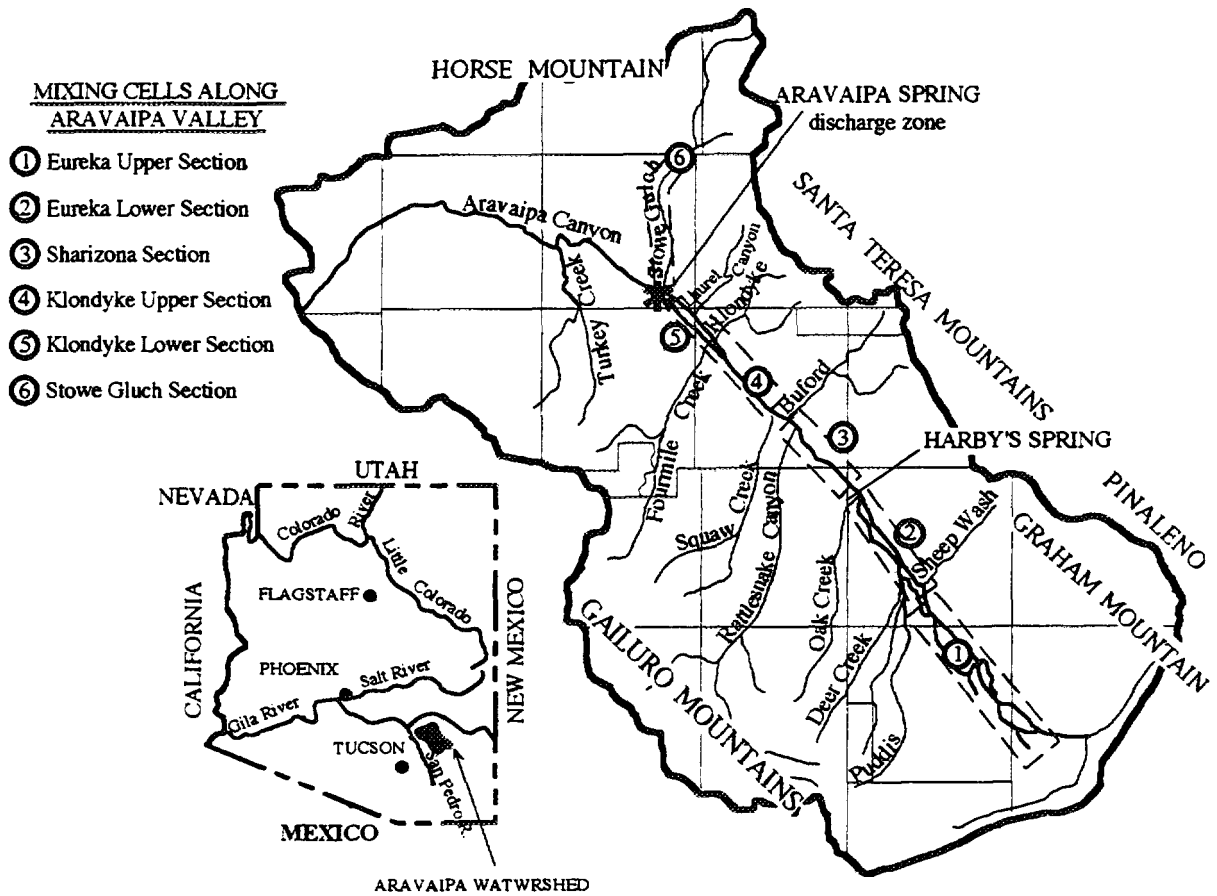

Figure 3: Aravaipa Valley, Arizona, USA.

Most of the mountain springs in the basin have a low discharge rate and present a different dissolved chemical content. It suggests that the mountain springs drain small local aquifers within high fractured zones. Based on the local geology it is possible that these small aquifers, which are in direct contact with the alluvial units, recharge the valley aquifers. Although the mountains on both sides of the valley are at almost the same elevation, the isotopic ratio of the collected rainfall was found to be extremely different (Adar and Long, 1987). Furthermore significant different in geology and type of mineralogy have been observed along the mountains surrounding the valley. The aforementioned

differences between the mountain aquifers can be used in the above-mentioned model to elaborate on the relative quantities that recharge the alluvial aquifers.

Aquifer Division into Mixing Cells

The modeling area is subdivided into five mixing cells as marked in Figure 3. The chemical concentration assigned to each cell are taken to be the average of values determined in wells, tapping the unconfined aquifer within the confines of the suggested cell. In general, multi-variables cluster analysis may provide the tool for aquifer partitioning as long as the group division makes sense regarding the geographic and hydrogeologic distribution. As an added check on the manner in which the water samples were grouped into representative cell values, we used activity diagrams as exemplified via the WATEQF computer program (Truesdel and Jones, 1973, Plummer et al., 1976).

The division of the upper aquifer into cells and the considered flow components are illustrated in Figure 4. The major components of potential sources of recharge into the water table aquifer are: (1) intermittent stream recharge along Aravaipa Creek during and after winter and summer floods; (2) inflows through the alluvial fans at the confluences with major mountain washes; (3) lateral inflows through the upper layers of the Old Alluvium, and (4) upward leakage from the deep aquifer (**ul** in Fig. 4). Rates of known fluxes at the Aravaipa Springs (**Qout**) and known rates of pumping (**P**) from each cell, are also given in Figure 4. In this model, recharge due to direct infiltration of rainfall is disregarded due to: (1) the limited outcrops of the alluvial aquifer; (2) an arid climate with extremely high temperature, and (3) the depth of the water table. This recharge component is deemed to be insignificant. To include it formally in our model would require sampling of infiltrating rain water below the root zone within which major chemical changes are expected. This was beyond the scope of our research.

A complete description of chemical and isotopic characteristics associated with each cell and with outflows and potential inflow components is given in Adar and Neuman, 1988. The data were used to establish the known matrix of concentrations - matrix **C** (equation 4). The unknown flow component **q** were obtained by minimizing J (equation 12) via quadratic programming utilizing Wolf algorithm (1967).

The weight matrix **W** (equation 13) is taken to be diagonal and the non-zero terms are assigned in the following manner: $W_{11} = Q_{out}^{-2}$ and $W_{ll} = w_k^{-2}(C_{ok}\beta_k)^{-2}$ where l=k+1; k=1,2,3,...,k. Here $\mathbf{Q_{out}}$ and $\mathbf{C_{ok}}$ are known rate of outflow from the downstream cell and the concentration of the k^{th} species at the Aravaipa Spring respectively. β_k is the coefficient of variation in determining the laboratory standards and w_k is a coefficient varying between 0 and 1 describing the conservancy level of the k^{th} species. Actual values used for β and ω_K for various species are given in Chapter 6 (Table 8). The balance equation are normalize so that they are all expressed on a scale relative to the outflow at

Aravaipa Spring. Furthermore, the effect of dividing by βk^2 is to reduce the weight of the k^{th} constituent in proportion to measured laboratory errors.

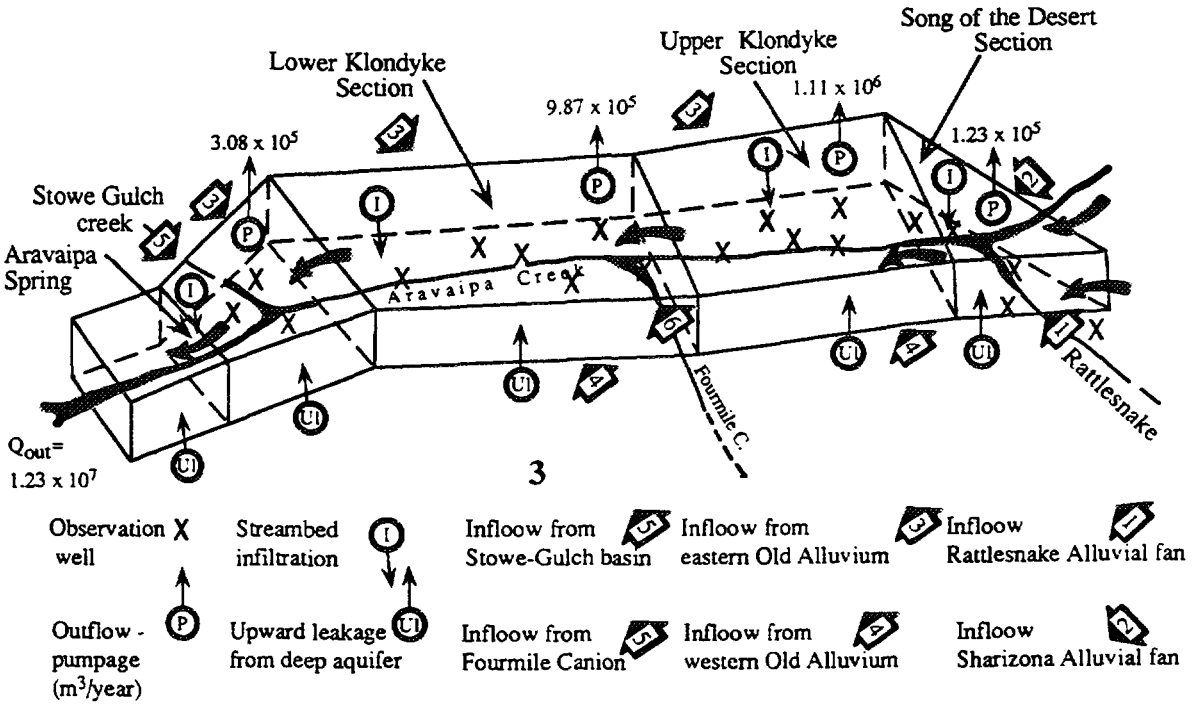

Figure 4: Outline of the modeled portion of the water table aquifer in the Aravaipa Valley

The total number of unknown flow rates in the model, including flow rates in-between the cells, is 23. For each cell there is a water balance and 14 chemical and isotopic balance expressions, resulting in a total of 75 equation. The most probable result with the lowest water and salt balance deviations is given in Table 4.

The results as presented in Table 4 reveal the following findings about recharge in the lower portion of the Aravaipa Valley:

1. Most of the lateral (mountain front) recharge derives from the eastern pediments. The western pediments probably recharge mainly the lower aquifer.
2. Stream bed infiltration contributes about 4% of the total recharge per year. This can be explained in the light of the short length and duration of floods in Aravaipa Creek.
3. Among all the alluvial fans, Stowe-Gulch seems to provide most of the inflow, almost 46% of the total recharge.
4. In the absence of significant pumpage from the lower confined aquifer, the only major avenue of discharge from the deep aquifer is by upward leakage. This flow component provides an important source of fresh water for the upper aquifer.

Table 4: Computed inflow rates into the water table aquifer

Cell No.	Source		Rate of inflow as percent of the total recharge
1	Inflow from	upper valley	3.606
		alluvial fans	0.213
		winter floods	0.000
		summer floods	0.000
		eastern pediments	0.893
		upward leakage	0.020
2	Inflow from	western pediments	7.738
		eastern pediments	4.362
		winter floods	0.030
		summer floods	2.131
		upward leakage	3.908
3	Inflow from	alluvial fans	0.684
		eastern pediments	7.526
		western pediments	1.022
		winter floods	0.000
		summer floods	0.748
4	Inflow from	Stowe-Gulch Basin	46.332
		upward leakage	14.640
		winter floods	0.000
		summer floods	0.000
5		upward leakage	2.333
Water balance			-3.808
Salt balance			+0.310

Although detailed sensitivity analysis of the model to errors in data and to the weight parameters is not presented in this chapter, results must be interpreted with caution. For further descriptions of results the reader is referred to Adar and Nueman, 1988. Nevertheless, the model appears to be a useful to extract and support subsurface flow and recharge information.

3.2.2 ARAVA VALLEY, NEGEV DESERT, ISRAEL & JORDAN

The southern Arava valley is a narrow down faulted rift valley, about 16 km. wide and extending about 80 km. north to the Gulf of Eilat. It is an extremely arid

basin with average annual precipitation of about 50 mm. Due to its geological and geophysical nature, the rift forms a low base level into which surface, as well as subsurface, flows drain from the surrounding mountains. In the valley, water were found in (a) sandstone of Paleozoic age, (b) sandstone of Lower Cretaceous, (c) limestone of Cretaceous age, and (d) alluvial fill of Quaternary age. Figure 5 illustrates the geography, various geological outcrops and location of well fields along the valley. Due to extremely complex hydrogeologic structures caused by

tilted faults followed by upward and/or downward movement of blocks, it was almost impossible to obtain detailed and reliable information on the physical properties of each structural component of the aquifer system. Therefore a quantitative assessment of the flow system including the sources of recharge by numerical modeling is not possible at this stage.

Groundwater of varying chemical and isotopic qualities are exploited by wells drilled in the valley and along its margins. Wells drilled into different blocks and layers and springs showed that due to differences in lithology and mineralogy, each source of recharge provides the alluvial aquifer with water of a specific chemical composition. Also, the isotopic ratios of oxygen-18 to oxygen-16, and deuterium to hydrogen are determined by the geographic location, including prevailing temperatures and the altitude of the area in which recharge occurs. The spatial isotopic and ionic distribution within the alluvial aquifer along the Southern Arava Valley seems to be affected mainly by the relative proportion of recharge contribution from each source. Hence, dilution and mixing are assumed to be the major mechanisms which control the hydrochemical and isotopic composition of the alluvial groundwater reservoir.

The temporal distribution of dissolved ions have revealed almost constant concentrations over the last twelve years. Furthermore, the piezometric head distribution and the pumping regime also seem to be constant for that period. Hence, changes in heads and concentrations of most species within cell **n** during time interval Δt turned out to be very small and thus negligible for modeling purposes. This implies an almost steady state hydrological flow regime, at least for the past decade. For further hydrogeological description and for the detailed flow pattern, as suggested by the environmental tracer's distribution the reader is referred to Rosenthal et al., (1990).

Six ions, TDI, deuterium (D) and oxygen-18 (^{18}O) parameters were used in a multi-variable cluster analyses to isolated and characterize 12 major potential sources of recharge and to divide the alluvial aquifer into 6 homogeneous compartments (Adar et al. 1992). Several close configurations of cells and potential inflows were modeled. For only four close configurations, the Wolf Algorithm solver provided a solution. For the remainder, unbounded or no solutions were obtained. A comprehensive description of the quantitative assessment of subsurface fluxes within the southern Arava basin is given in Adar et al. (1992).

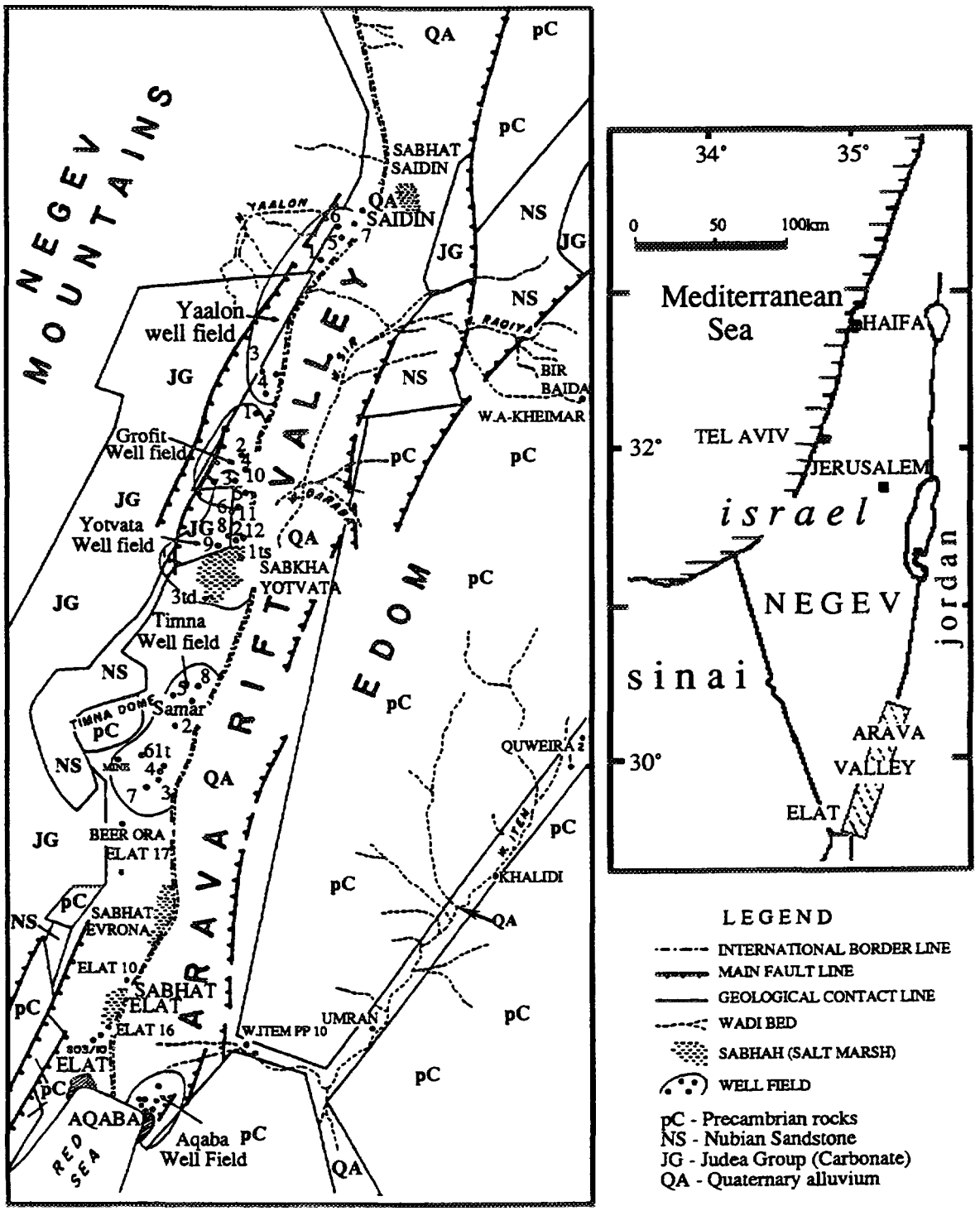

Figure 5: A map of southern Arava basin showing the location of main well fields and a schematic appearance of major geological units.

Figure 6 presents the results for 12 potential inflows obtained with 7 dissolved ions and 2 isotopes. Subsurface recharge components and internal fluxes are given in 10^6 m^3/year. The errors associated with the optimization of mass balance equations of dissolved ions varies from 0.45% to 6.85%. It is important to notice, however, that the calculated fluxes are heavily dependent upon the rates assigned to the known outflows. The absolute values of these deviations have no real meaning aside from the fact that for more reliable flow configurations, one may expect to obtain lower deviations. As a result of the model, for the first time, a quantitative estimation of the contribution from the Nubian sandstone aquifer is obtained. Also, the significant contribution from the mountain - front recharge to the alluvial aquifer is clearly demonstrated.

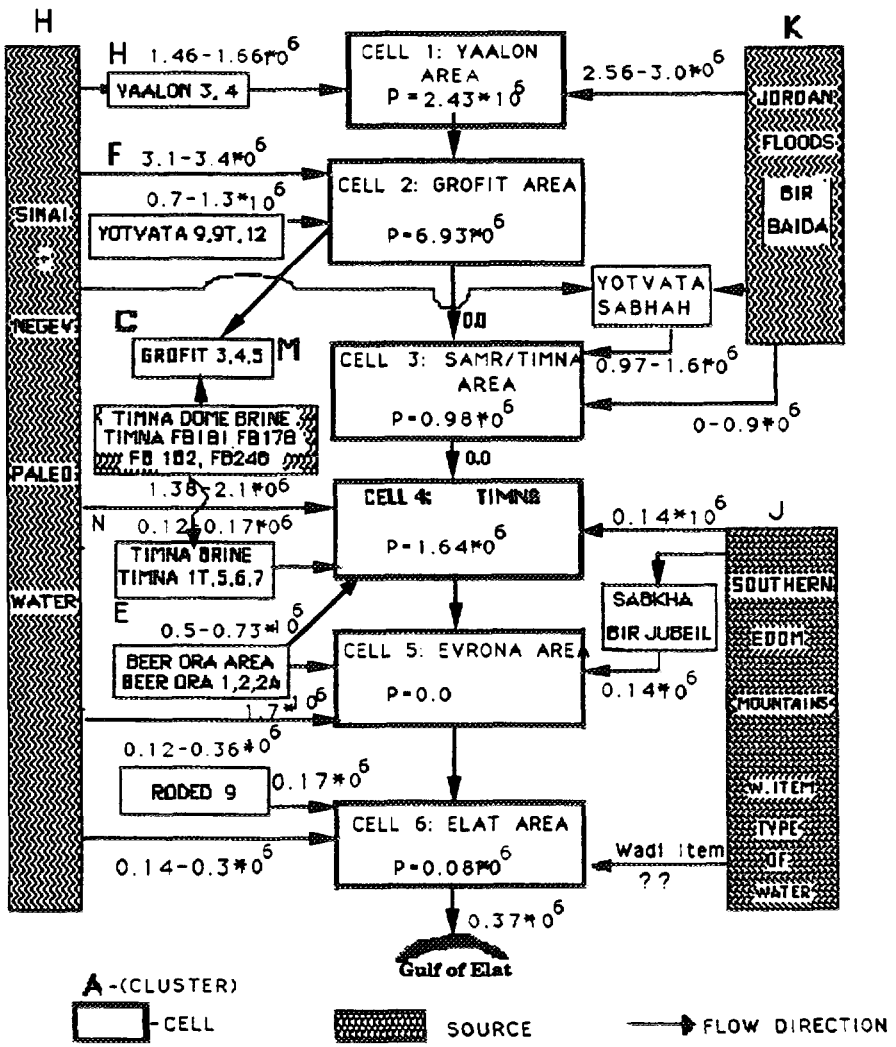

Figure 6: Calculated fluxes and recharge components in the Southern Arava valley.

4. ESTIMATION OF TRANSMISSIVITIES ACROSS FLOWING BOUNDARIES

The solved time averaged fluxes are now used to estimate conductances through cell's boundaries. Conductance is defined as the ability of an active boundary to transmit a unit flux per unit head gradient across the boundary. It can be related to transmissivity as further be discussed below. The flux through a common permeable boundary, is proportional to the hydraulic head difference across this boundary. Integrating Darcy's linear momentum expression for any time interval over a control volume surrounding such a boundary for inflow from cell **i** into cell **n**, yields:

$$\bar{q}_{in} = T^*_{in}\left(\bar{h}_i - \bar{h}_n\right) \tag{14}$$

where T_{ij}^* (= T_{ji}^*) denotes conductance at the common boundary between cells **i** and **j**, and $\bar{h}$ denotes the time average of measured hydraulic head. Similarly, the outflow from cell **n** to cell **j**, reads

$$\bar{q}_{nj} = T^*_{nj}\left(\bar{h}_n - \bar{h}_j\right) \tag{15}$$

Writing equations (14) and (15) for all permeable boundaries of the multi-compartmental system, we obtain a global set of the form:

$$\underline{q} = \underline{\underline{h}}\,\underline{T}^* \tag{16}$$

where $\underline{\underline{h}}$ is a diagonal matrix of hydraulic head differences given by:

$$h_{\xi\eta} = \delta_{\xi\eta}\left(\bar{h}_i - \bar{h}_j\right) \quad ; \quad \xi,\eta = 1,2,3,\ldots,N_b \tag{17}$$

and $\underline{q}$ denotes the vector of solved averaged fluxes across permeable boundaries, given by:

$$q = \left[\, \bar{q}_1, \bar{q}_2, \bar{q}_3, \ldots, \bar{q}_{N_b} \,\right]_{N_b * 1} \tag{18}$$

Here, N_b denotes the number of permeable boundaries in the aquifer cell system. δ_{xh} is the Kronecker delta, where **x=h** for permeable (active) boundary. $(h_i - h_j)$ represents the averaged head difference governing outflow from cell **i** into cell **j**. The vector of conductances. $\underline{T}^*$, is given by:

$$\underline{T}^* = \left[T_1^*, T_2^*, T_3^*, \ldots, T_{N_b}^*\right]_{N_b * 1} \tag{19}$$

Hence, conductances in the aquifer cell system $\underline{T}^*$, are solved using the set of equations as described in equation (16).

In a compartmental simulation of an aquifer, conductances coefficient T* replaces transmissivity term T used in a continuum approach. In view of equation (14), e.g. for inflow boundaries, we may write the relation between T* and T in the following form:

$$\bar{q}_{in} = T^{*}_{in}\left(\bar{h}_i - \bar{h}_n\right) = T_{in} b_{in} \frac{\bar{h}_i - \bar{h}_n}{l_{in}} \qquad (20)$$

where T_{in} denotes the transmissivity between observation wells **i** and **n**, which represent the characteristic properties of the respective cells (the mixing cell approach). b_{in} denotes the length of the (**in**) boundary between those cells and l_{in} represents the distance between observation wells **i** and **n**, normal to the boundary (**in**) as depicted in Figure 7.

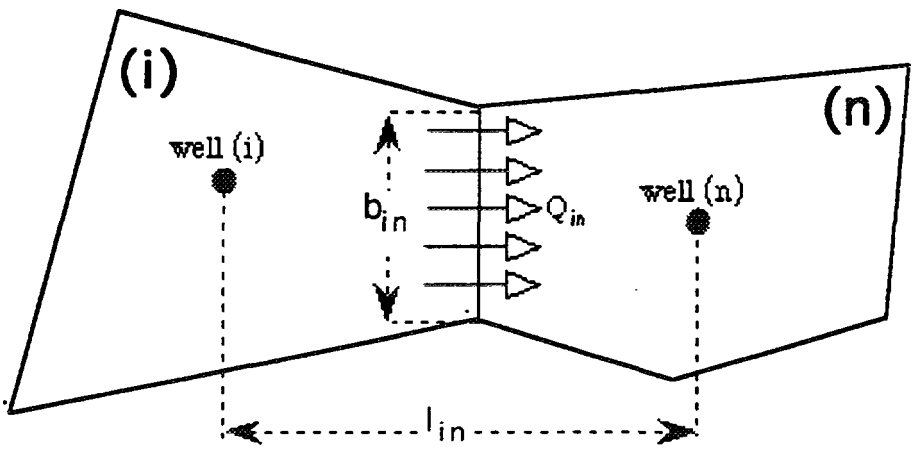

Figure 7. Scheme of flow between two compartments (i) and (n) and illustration of the l_{in} and b_{in} dimensions.

4.1 TESTING THE MODEL WITH SYNTHETIC DATA

The conceptual model and the computer code were tested with a set of synthetic data which was generated for a hypothetical aquifer divided into mixing cells. The test was conducted to evaluate the ability of the computer code to solve the mathematical model for unknown fluxes and transmissivities simultaneously. The test was conducted with four cells. The set up of the cell's configuration and the assigned fluxes, sinks, sources (volume per unit time), and transmissivities (area per unit time) for the internal boundaries are given in Figure 8. Not as in the previous test, a multi-flow cell configuration was assigned for testing the algorithm and the computer code. Cell I has a sink (pumping) term and receives four inflows through external boundaries without a source term. Fluxes leaving cell I contribute water to cells II and III [36 and 20 (l^3/t), respectively]. Cell II also receives water from four external sources and has both sink and source terms (No. 9 in Fig. 8). Subsurface fluxes leave cell II and flow

into cells III [5(l^3/t)] and IV [45(l^3/t)]. Cell III has three external sources with a sink term and water leaves this cell only into cell IV [40(l^3/t)]. Cell IV has two sources with a sink term. The total subsurface outflow is 100 (l^3/t). Two sources contribute the same type of water to more than one cell. Sources #13 and #16 are the same and recharge cells X and XII, respectively. Sources #10, # 14 and #15 are also the same and contribute the same type of water to cells IX, XI and XII, respectively. All together seventeen unknown external sources. The total number of unknowns is 37 (17 external inflows, 15 internal fluxes and 15 transmissivities). Some of the cells: VI, VII, VIII, X, XI and XII were also assigned sink (pumping rates) terms. The numbers in the ellipsoids designate rates of inflows (recharge) from external sources.

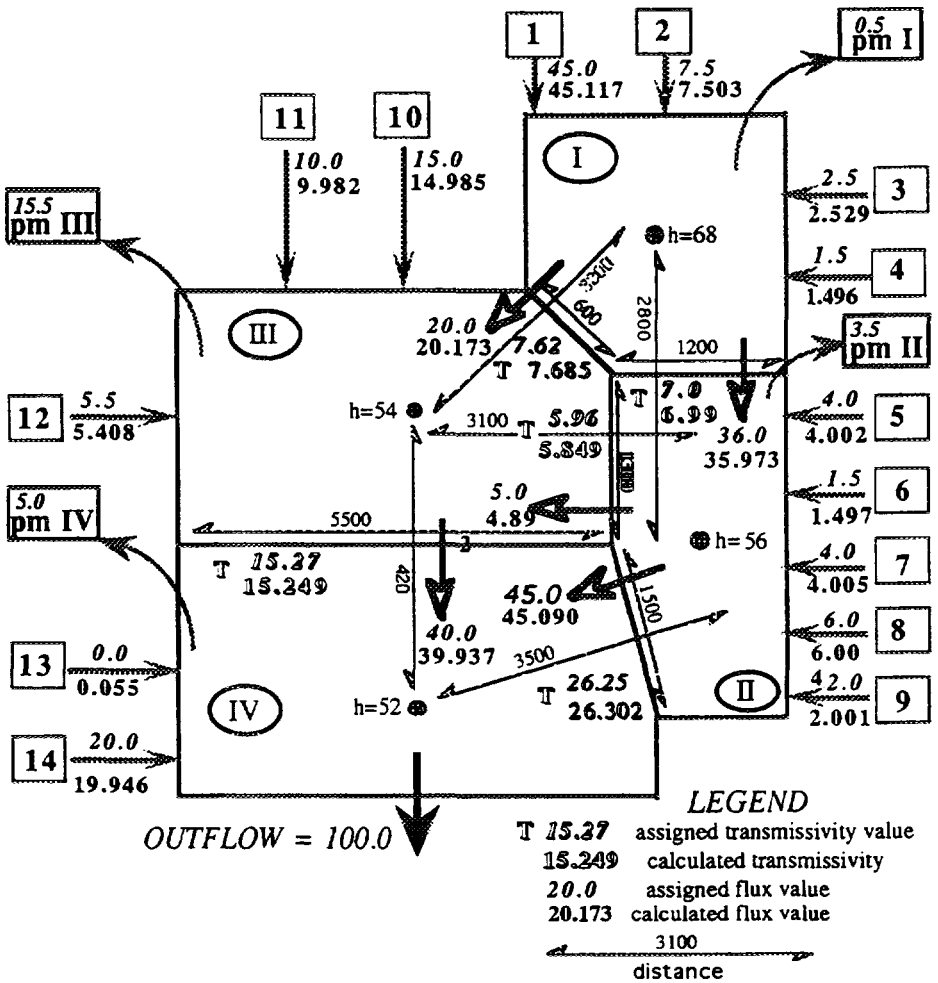

Fig. 8 Schematic compartmental aquifer used for testing the mathematical algorithm. P_m = rate of discharge (in volume per unit time).

To test the ability of the model to evaluate transmissivities across active boundaries, equations (14) and (15) were embedded in equations (6) and (7). The transmissivities then can be calculated using Darcy's type of equation as given in Equation (20). So far, to solve for the time - averaged fluxes, the only data that was required aside from the qualitative knowledge of the flow system were the

spatial distribution of environmental tracers. However, for the calculation of transmissivities, one should add the distribution of hydraulic heads as well as the dimensions of the cells; mainly the size of active boundaries. The combination between head distribution and cell geometry suggests which of the boundaries is active and require evaluation of the transmissivities. All the above-mentioned dimensions are also posted in Figure 8.

In Figure 8 the upper numbers designate the assigned fluxes or transmissivities and the lower numbers are the results obtained from the model. The assigned fluxes were used to calculate the tracers' concentrations for every cell, an information which was later used as known or "measured" data for testing the algorithm. As expected for synthetic data and zero error terms in the water and mass balance equations, the calculated transmissivities and fluxes are almost identical. The negligible differences may attributed to the numerical round off errors. The test show that, as long as the input data are precise including a proper aquifer discretization into mixing cells, the algorithm is able to estimate correctly transmissivities, fluxes of recharge and subsurface flow components.

4.2 FIELD APPLICATION: DISTRIBUTION OF TRANSMISSIVITIES IN THE SOUTHERN ARAVA VALLEY.

The same mixing cell configuration as obtained by the multi variable cluster analysis (Figure 6), and the data set of the dissolved minerals and isotopes were used to assess the spatial distribution of transmissivities over the southern Arava valley. Hydraulic heads were assigned to imaginary wells located at the center of each cell by interpolation from piezometric maps. Additional information on cell's geometry, in particular, the width of the boundaries and the length between the wells, was estimated from topographic maps. A new set of water and chemical (including isotopes) mass balance expressions (equations 6 & 7) were introduced into the mathematical algorithm, such that the flux terms q_{in} & q_{nj} were replaced by conductance terms as defined in equations 14 and 15 respectively. Then, transmissivities were estimated using equation (20).

Figure 9 presents the range of results obtained by a simultaneous optimization for transmissivities and components of recharge (inflows). The range of calculated transmissivities and fluxes is a result of modifications made in flow configurations and in cell geometry.

The concentrations and the hydraulic heads which represent each compartment are assigned to the geometric center of the cell. In other words, an imaginary well is posted at the geometric center of a cluster of observation holes presenting a similar type of water. Therefore, the actual location of boundaries between cells is not known precisely. In fact, the most one can say is that the boundary should be somewhere between the closest extreme well of the nearby cluster forming each cell.

Table 5. Calculated versus measured transmissivities in three sections along the southern Arava Valley (m^2/day).

Section		Measured	Calculated
Yaalon-Grofit area.			**997-1016**
	Ketora 4 (DD)*	1849	
	" (R)**	1209	
	Yotvata 2 (R)	2665	
	" 2 (IT8)***	1400	
	Yotvata11 (DD)	980	
	" 11 (DD	1000	
	" 11 (R)	1060	
	Yotvata12 (R)	2010	
Samar-Timna area			**104-350**
	Samar 2 (?)	400	
	Timna 4 (R)	370	
	Timna FC(IT?)	807	
	Timna 4 (IT3)	4600	
	" (IT1)	2800	
Eilat area			**284-345**
	Eilat 10 (R)	496	
	Eilat m.s. (R)	105	
	Eilat 16 (R)	273	

Since the location of the representative imaginary wells is assigned arbitrarily to the geometric center of the well's cluster (not to the center of the entire cell's area), the exact location of the cells boundaries has no effect on the distance l_{in} between the centers of cells. However, the position of the boundaries, which are always normal to the flow trajectory, affects the width b_{in} of permeable boundaries. The width of the boundaries in the southern Arava Valley were assigned according to the contact between the alluvium and the surrounding hills, as determined from maps and air photos.

Transmissivity values that were obtained by various types of pumping tests in key wells along the valley are listed in Table 5. For most cases, each method provided a different transmissivity. Furthermore, recovery tests with different orientations also revealed different results, which probably reflects the non homogeneity of the aquifer across very short distances. The transmissivity values assessed by the above-mentioned model (also listed in Table 5) are in fairly good agreement with the values found from the pumping tests. It is important to notice, however, that this model allows the evaluation of transmissivities for segments of aquifer with active steady fluxes. For cells with heavy rates of pumping, as in the central section of the `Southern Arava basin, transmissivities can not be evaluated since the inter-cell fluxes are zero. Therefore, it is necessary

to assess simultaneously both transmissivities and fluxes. Similar to the results obtained with the inverse numerical solution, the calculated transmissivities are average values between the nodes. In a compartmental scheme, the values are an assortment of conductances across permeable boundary between cells. In other words, it describes the ability of the boundary to transmit a certain volume of water per unit length of the boundary per unit time.

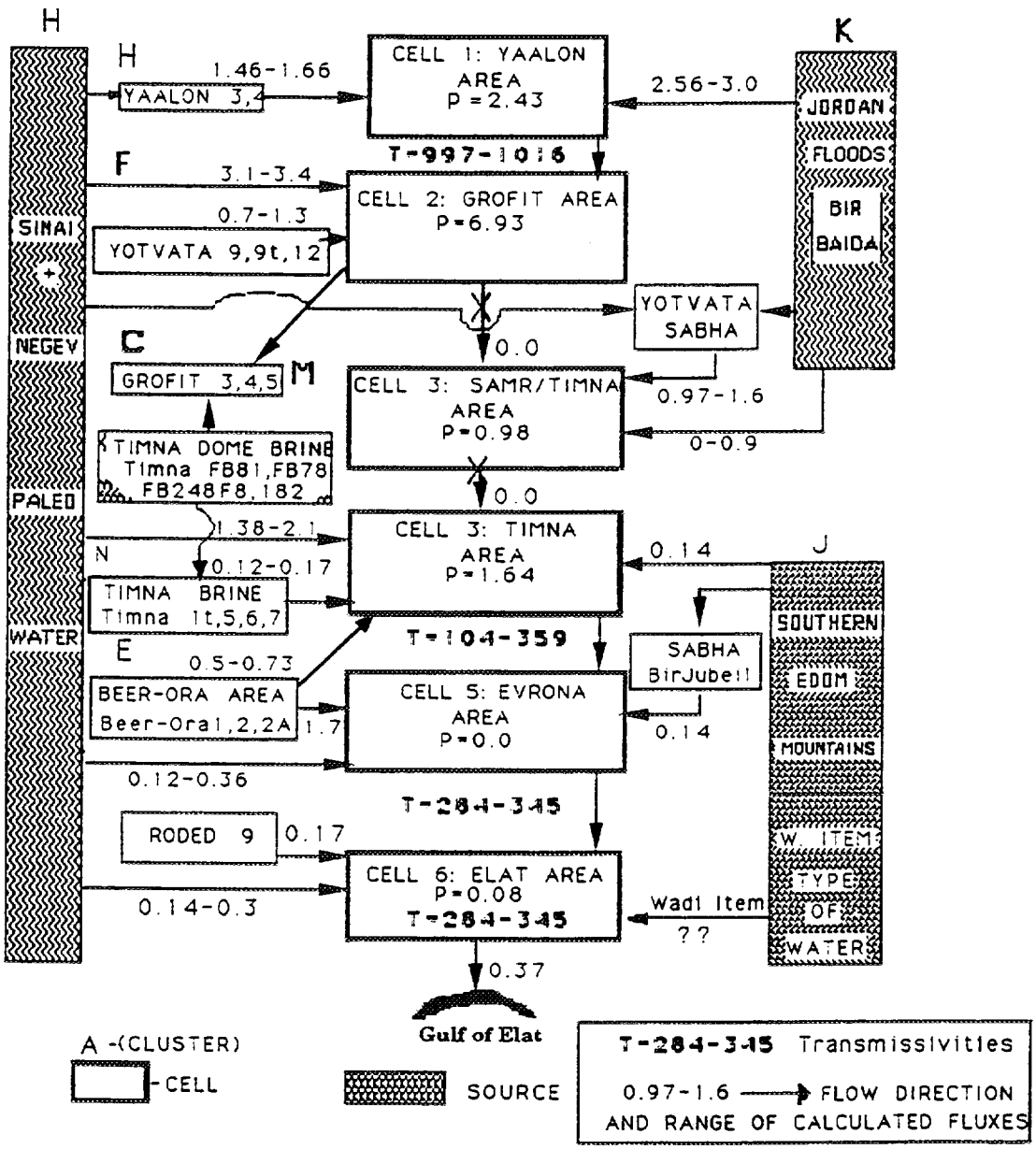

Fig. 9 A schematic flow pattern for the southern Arava Valley with computed transmissivities (in m^2/day) and fluxes (in 10^6 m^3/year).

5. ESTIMATION OF AQUIFER STORAGE COEFFICIENTS

Thus far, fluxes and conductances have been evaluated based on time average compartmental heads and concentrations obtained for time interval Δt. Estimated transmissivities for every active boundary can then be calculated by equation (20).

For the assessment of compartmental storage coefficients, one may use the information about temporary head variations in the flow domain during (or within) the time period Δt (Adar and Sorek, 1989). Suppose one assigns **M** specific observations for compartmental head $h_n^{(m)}$ during time period Δt; (m = 1, 2, ...,M) where $h_n^{(m)}$ denotes the head in cell **n** at time **m** as illustrated in Figure 10.

In view of equations (14) and (15), one may write the temporal values of boundary inflow ($q_{in}^{(m)}$) and outflow ($q_{nj}^{(m)}$) fluxes for each time observation **m** in the following manner:

$$q_{in}^{(m)} = T_{in}^{*}\left(h_i^{(m)} - h_n^{(m)}\right) \tag{21}$$

and

$$q_{nj}^{(m)} = T_{nj}^{*}\left(h_n^{(m)} - h_j^{(m)}\right) \tag{22}$$

In the above equations T_{nj}^{*} is already a known parameter since conductances were already solved. Substituting equations (21) & (22) into equation (1) and assembling for all **N** aquifer compartments, one obtains a global set of linear ordinary equations at time observation **m** of the form

$$\underline{\underline{S}}^{*}\frac{d\underline{h}^{(m)}}{dt} + \underline{\underline{T}}^{*}\underline{h}^{(m)} = \underline{R}^{(m)} \tag{23}$$

where $\underline{\underline{S}}^{*}$ denotes a diagonal matrix of compartmental storage capacity coefficients; $\underline{\underline{T}}^{*}$ denotes the matrix of conductances in which the two terms T_{in}^{*}, and T_{nj}^{*} are associated with permeable boundaries (inflow and outflow respectively). No-flow boundary is expressed by zero term; $\underline{h}^{(m)}$ is a vector of compartmental head terms measured at time observation **m**; and $\underline{R}^{(m)}=(\underline{Q}^{(m)}-\underline{W}^{(m)})$ is a vector of the known compartmental sources (inflows) and sink flux terms.

The goal is to solve for the S_n^{*} storage capacities, for each compartment **n** in the aquifer, given that $h_n^{(m)}$, $R_n^{(m)}$ and T_{in}^{*} (or T_{nj}^{*}) values are known. To do that we rewrite equation (23) to the form:

$$\underline{\underline{X}}^{(m)}\underline{S}^{*} = \underline{Y}^{(m)} \tag{24}$$

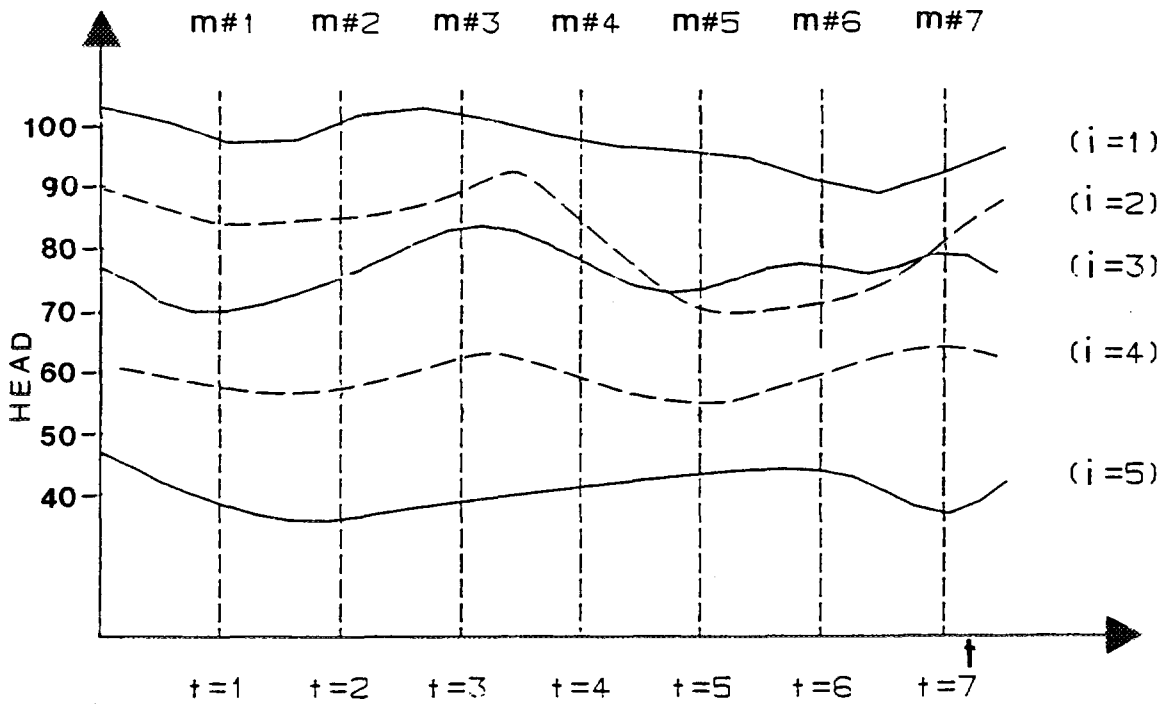

Figure 10 Change of hydraulic head **h** in cells: i=1, i=2, i=3, i=4, and i=5 as function of discrete time observations **m**: t_1 to t_7

where $\underline{\underline{X}}^{(m)}$ is a diagonal matrix of known head rates for all aquifer compartments at time observation **m**

$$X_{ij}^{(m)} = \delta_{ij} \frac{dh_{ij}^{(m)}}{dt} \quad ; \quad i,j = 1,2,3,\ldots,N \tag{25}$$

$\underline{Y}^{(m)}$ is a vector of known terms at observation time **(m)**.

$$\underline{Y}(m) = \left[\underline{R}^{(m)} - \underline{\underline{T}}^{*}\underline{h}^{(m)}\right]_{N*1} \tag{26}$$

and $\underline{S}^{*}$ is the vector of unknown storage capacities for all **n** compartments at observation **(m)**.

$$\underline{S}^{*} = \left[S_1^{*}, S_2^{*}, S_3^{*}, \ldots\ldots, S_N^{*}\right]_{N*1}. \tag{27}$$

Next, upon implementing the Gauss-Markov method (Bard, 1974) for equation (24) through all **M** time observations, we obtain an optimal solution for $\underline{S}^{*}$, of the form

$$\underline{S}^{*} = \left[\underline{\underline{X}}^{T}\underline{\underline{X}}\right]^{-1}\underline{\underline{X}}^{T}\underline{Y} \tag{28}$$

where

$$\underline{\underline{X}} = \begin{bmatrix} \underline{\underline{X}}^{(1)} \\ \underline{\underline{X}}^{(2)} \\ \underline{\underline{X}}^{(3)} \\ . \\ . \\ \underline{\underline{X}}^{(M)} \end{bmatrix}_{(N*M)*N} \tag{29}$$

$$\underline{Y} = \left[\left(\underline{R}^{(1)} - \underline{\underline{T}}^{*}\underline{h}^{(1)}\right), \left(\underline{R}^{(2)} - \underline{\underline{T}}^{*}\underline{h}^{(2)}\right), \ldots, \left(\underline{R}^{(M)} - \underline{\underline{T}}^{*}\underline{h}^{(M)}\right)\right]_{(N*M)*1}. \tag{30}$$

Since $\underline{\underline{X}}^{(m)}$ is a diagonal matrix, we can write an explicit expression for S_n^* commencing from equation (28).

$$S_n^{*} = \frac{\sum_{m=1}^{M} \frac{dh_n^{(m)}}{dt}\left[R_n^{(m)} - \sum_{\eta=1}^{N} T_{n\eta}^{*} h_{\eta}^{(m)}\right]}{\sum_{m=1}^{M}\left[\frac{dh_n^{(m)}}{dt}\right]^2} \tag{31}$$

where **h=1, 2,..., N** denotes numbers of active boundaries.

The $h_n^{(m)}$ and $dh_n^{(m)}/dt$ values are at discrete time observations (**m=1,2,...,M**) for each cell **n**.

Compartmental storage capacity S_n^* is related to the storativity S_{sn} or to specific yield S_{yn} for confined and water table aquifers, respectively, by the following expressions

$$S_n^{*} = \phi_n V_n S_{sn} \tag{32}$$

and

$$S_n^{*} = A_n S_{y_n} \tag{33}$$

where A_n is the area of cell **n**, V_n is its saturated volume, and ϕ_n, is the porosity.

5.1 ASSESSMENT OF TRANSMISSIVITIES AND STORAGE COEFFICIENTS FOR OSCILLATING PIEZOMETRIC HEADS

The next test (Test 2) of the mathematical algorithm and the computer code was performed for calculating transmissivities and storage coefficients in an aquifer with periodic distribution of hydraulic heads. It was performed on the same layout of the flow system (16 unknown external fluxes and 16 transmissivities, 3 sources and 4 sink terms) as illustrated in Figure 2. In this test, instead of using a given average head for each of the relevant cells, a temporal distribution of heads is given for each cell and across every active boundary. The time-head distribution was created arbitrarily, i.e. utilizing a sinusoidal function around an average value $\mathbf{h_{av}}$:

$$h(t) = h_{av} + \alpha \sin\left(\frac{2\pi t}{M}\right) \tag{34}$$

where α is the allowed amplitude and **M** is the total number of observations. Twelve head values were assigned for each cell, but not necessarily at the same time observation. Figure 11 shows an arbitrary periodic distribution of hydraulic heads across sixteen active boundaries in four cells. Later in the program, a spline method for curve fitting was used to obtain a polynomial expression describing the time-head distribution in each cell. These expressions were then integrated and the average heads were obtained from the quotients of the integrals over the head distributions and the length of the time intervals. These polynomial expressions were then used to obtain **M=12** synchronized tabulated piezometric heads. Next, upon implementing the **Gauss-Markov** algorithm (equations (28) to (31)) through all **M** observations of heads, an optimal solution for the storage coefficients $\mathbf{S^*}$ was obtained.

The implementation of the Gauss-Markov method through all M observations in equation (31) for the four (n=4) system cells resulted in the following storage coefficients for each cell (Table 6):

Table 6. Estimated storage coefficients for each cell in Figure 2.

$S_I^* = 1.1799$	$S_{II}^* = 34.5764$	$S_{III}^* = 5.6183$	$S_{IV}^* = 1.4791$

The relations between $\mathbf{S^*}$ to $\mathbf{S_S}$ or $\mathbf{S_y}$ are given in equations (32) and (33), respectively. Specific storage and/or specific yield can be estimated providing that the porosity and either the volume or the area of the saturated layer are available for confined or phreatic aquifers respectively. The large value of $\mathbf{S_2^*}$ emerges from the fact that a relatively large rate of pumping (sink term, Table 6) was assigned to Cell **II**, where also the inflows are very low relative to the other system cells.

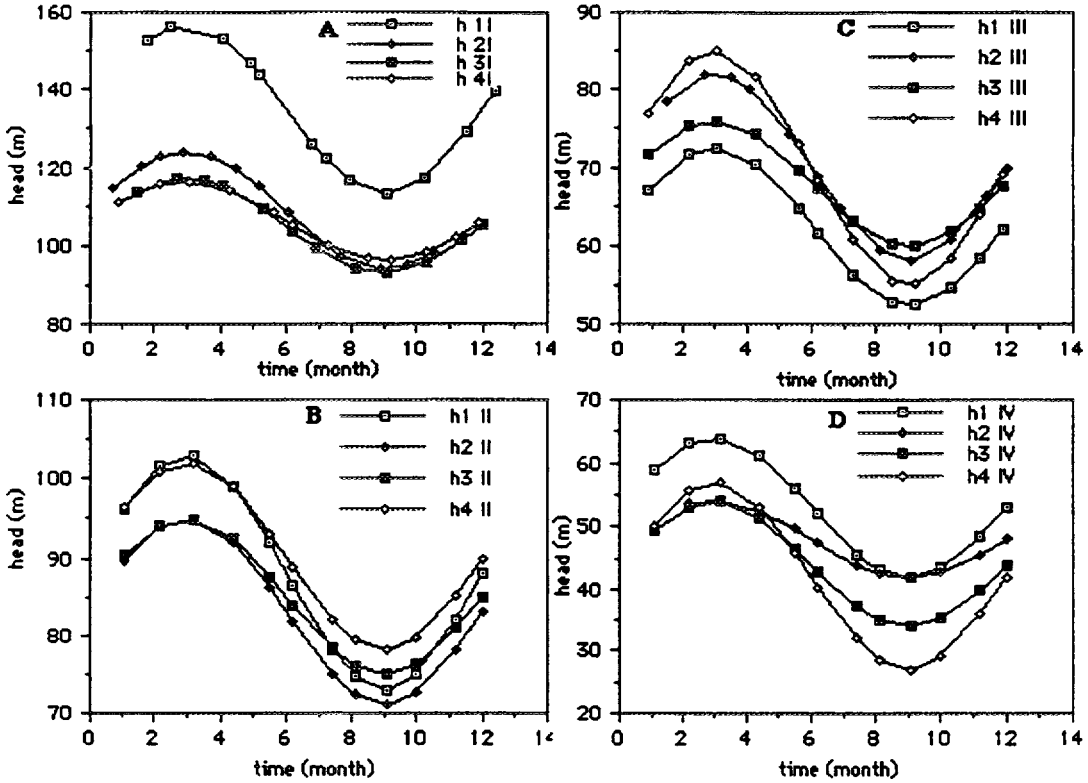

Figure 11: Arbitrary periodic distribution of hydraulic heads across active boundaries in Test 2.

Table 7 shows the results of estimated transmissivities across internal and external boundaries for an oscillating piezometric head regime and for a specific geometry of cells. The test shows that, as long as the data are precise and the number of mass-balance expressions exceeds the number of unknowns, the proposed algorithm is able to estimate correctly transmissivities and storage coefficients across permeable boundaries.

Table 7: Estimated transmissivity values between cells and across external flow boundaries.

Flow From Cell	to Cell	Distance Between Centers (m)	Width of Boundary (m)	Calculated Head Differences (m	Calculated Transmissivities (m^2/t)	Estimated Transmissivities (m^2/t)
I	II	1000.0	255.0	19.9	10.98	10.916
II	III	1500.0	385.0	19.9	12.97	12.983
III	IV	750.0	410.0	20.0	7.96	7.883

Table 7: Continued
Estimated transmissivity values between cells and across external flow boundaries.

Cell	Number of Active Boundaries	Distance Between Centers (m)	Width of Boundary (m)	Head Difference (m)	Calculated Transmissivities (m^2/t)	Estimated Transmissivities (m^2/t)
I	1	2000.0	375.0	35.0	6.86	6.792
I	2	1500.0	625.0	8.7	2.00	2.029
I	3	1750.0	250.0	5.1	3.50	3.418
I	4	2350.0	200.0	6.4	2.80	2.689
II	5	3300.0	330.0	8.1	5.00	4.898
II	6	2800.0	800.0	3.2	1.75	1.588
II	7	900.0	180.0	5.0	4.00	4.288
II	8	1200.0	360.0	10.2	2.00	1.972
III	9	1550.0	750.0	2.5	6.20	6.382
III	10	2250.0	300.0	9.9	3.00	3.020
III	11	1750.0	175.0	8.0	5.00	4.628
III	12	3000.0	360.0	9.8	5.00	4.800
IV	13	4200.0	480.0	13.1	1.75	1.856
IV	14	3600.0	1200.0	8.2	3.00	2.984
IV	15	1800.0	600.0	4.1	1.50	1.565
IV	16	4000.0	600.0	2.1	5.00	5.051

6. SENSITIVITY ANALYSIS: EFFECT OF ERRORS IN THE DATA

In real field situations the input data associated with each cell such as concentrations, piezometric head, and the dimensions of the flowing boundaries, are not known with the appropriate precision. Also, it might be that not all sources of recharge and the flow components have been properly identified. Therefore, the basic assumptions behind the model are not fully satisfied. To examine the effect of erroneous input data on the quality of such estimates, a schematic flow pattern for a simple longitudinal flow system, as illustrated in Figure 12, is repeatedly solved after corrupting the synthetic input data with various levels of non correlated Gaussian noise.

The rationale for the particular method used to generate our noise stems from the assumption that laboratory errors are a major cause of error in isotopic and hydrochemical analysis. The first step was to generate normal errors of zero mean and unit variance $N_{(0,1)}$ by means of the formula (Box and Muller, 1958, as cited in Bard, 1974):

$$N_{(0,1)} = (-2 \log_{10} U_1)^{0.5} \cos(2\pi U_2) \qquad (35)$$

where U_1 and U_2 are independent random variables drawn from uniform distribution. Next, each "true" C_k value entering into the model was transformed into a noisy concentration C_k^* according to:

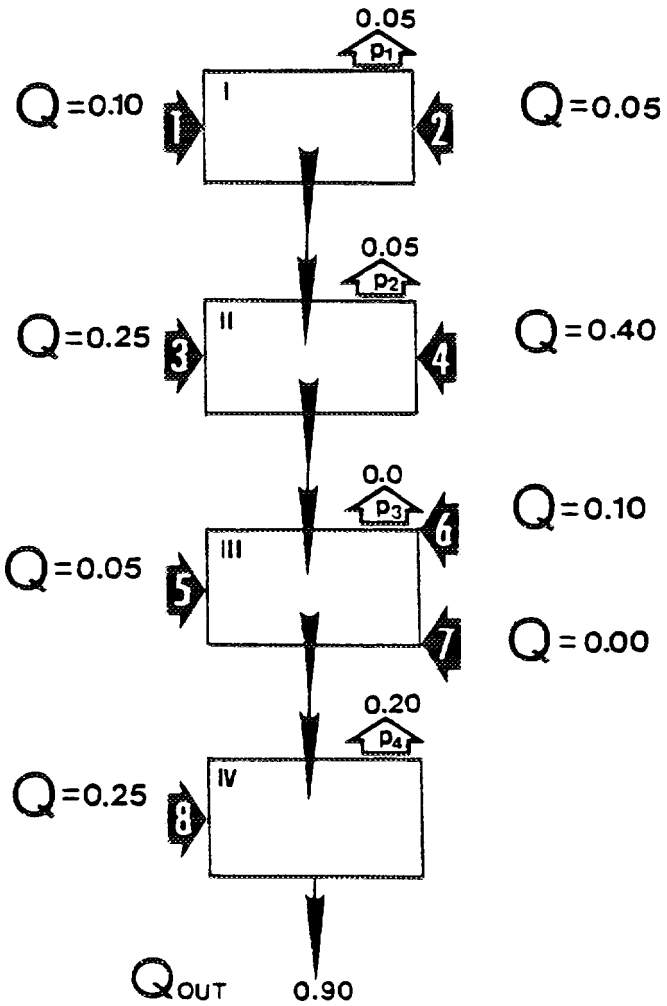

Figure 12: Schematic flow configuration used for sensitivity analyses
Q - rate of inflow; P - rate of pumping or discharge (Vol./time)

$$C_k^* = C_k\left[1+\beta_k N_{(0,1)}\right] \tag{36}$$

where β_k is a weighting parameter controlling the magnitude of the corrupted concentration C_k^* relative to that of the "true" concentration C_k. This causes the error to increase linearly with concentration, which seems to be realistic for laboratory data. When the noise was made independent of concentration, the Wolf algorithm at times failed to converge. In the case of a single river reach, Woolhiser, et al. (1982), found that errors in C are more important than errors in sink or sources when the number of flow rate equations in the model is less than the number of chemical balance equations.

A test was conducted with 100 noisy C data sets for β value equals to 0.05. In this particular test, only concentrations of the dissolved constituents were perturbed as being the most sensitive parameters to laboratory and field analyses. Results are illustrated in Figure 13 A. The Monte Carlo simulation was performed with perturbed concentrations restricted to an ionic balance of 4 %, electrical conductivity (EC) to TDI ratios between 35 and 55, and D to ^{18}O ratios between 6.5 and 8.5. For each appropriately perturbed set of data, the quadratic program was used to obtain an estimate of the unknown **Q** values. Figure 13A reveals that the mean **Q** values converge to stable values after about 20-40 realizations. Adar et al. 1988 found that it converged almost at the same level regardless of the magnitude of β, but within the framework of the above-mentioned constraints. However, the magnitudes of the estimated average fluxes (**Q**) depend heavily on the magnitude of β. When β = 0.2, these averages (with the exception of Q_7 which is zero) differ from the true values of 30-140%. When β = 0.01, this difference is reduced to 0.2-4%. Though the larger β is, the greater the error of estimation, the rate at which the estimation error increases with β, is decreased as the amplitude of the noise goes up.

Table 8. Statistics and Coefficient of conservancy w_k for 14 isotopic and ionic species from repeated laboratory standards (Analytical Laboratory, University of Arizona, 1984).

Species	Expected value	No. of repeated analyses	Average μ	Standard deviation σ	Coefficient of variation $\sigma / \bar{\mu}$	w_k
EC**	420.0	150	422.0	13.99	0.0316	0.90
Mg	56.5	17	57.6	3.13	0.0543	0.70
Ca	141.0	20	136.3	14.09	0.1030	0.60
Na	207.0	27	202.7	20.84	0.1030	0.60
K					0.0540*	0.45
HCO_3	724.0	27	761.5	87.53	0.1150	0.30
Cl	251.0	30	229.9	37.86	0.1650	1.00
NO_3	558.0	30	573.3	76.32	0.1330	0.10
SO_4	223.0	29	232.2	14.23	0.0613	0.30
F					0.0900*	0.20
Li					0.0600*	0.20
Si					0.1500*	0.20
^2H	-58.0	122	-58.1	3.71	0.0639	1.00
^{18}O	-8.6	78	-8.56	0.198	0.0230	1.00

* Estimated values obtained from UOA Analytical Center, Tucson, Ariz.
** Electrical conductivity.

A second test was performed in which different β_k values were assigned to the various isotopic and chemical species k according to:

$$\beta_k = \frac{\sigma_k}{\mu_k}. \tag{37}$$

Here μ_k is the mean of a large number of concentrations determined for laboratory standards of the **k** species, and σ_k is the associated standard deviation as given in Table 8. In this manner β_k becomes the coefficient of variation of the error in determining the laboratory standard for the **k** species. Two hundred and fifty realizations were performed to examine the stability and the rate of convergence of the calculated fluxes. Results are illustrated in Figure 13B. Results indicate that in spite of the general increase in the magnitude of β (Table 8), the system remains stable though it seems to converge after 40 to 80 realizations with greater deviations from the "true" assigned values.

The stricter the constraints, the closer is the average **Q** to the true flow rates. Adar et al. (1988) found that for data perturbed far beyond the aforementioned constraints, the solver failed to converge, reaching an unbounded solution. In fact, results of chemical composition from analytical laboratories are always checked for maintaining ionic balance. The same data is also examined for the linear correlation between EC and TDS. Similarly, a local constant slope is known to exist between deuterium and oxygen - 18. Detailed results for other combinations of constraints are given in Adar (1984), and the importance of ion balance for a single cell model was demonstrated for laboratory mixtures by Woolhiser, et al. (1985).

7. SUMMARY

This study demonstrates the use of hydrochemistry and environmental isotopes in an arid basin, such as the Aravaipa Valley and the southern Arava basin, where information about hydraulic gradients and aquifer parameters is relatively limited. The available data do not allow one to compute recharge from above, vertical leakage between aquifers, lateral recharge from tributaries or recharge from the surrounding mountain aquifers. This mathematical model can extract quantitative hydraulic information from spatial distribution of dissolved chemicals and stable isotopes. The latter information is often more easily accessible. The proposed model computes these flow components (and others) on the basis of the known or estimated total outflow from the basin and on the basis that the dissolved ions and environmental isotopes can be obtained for all outflows and potential inflow components. A qualitative assessment of the spatial distribution of potential recharge sources, sinks and local sources, and the subsurface flow pattern must be known. These data were obtained qualitatively on the basis of all the available geologic, hydrologic, and hydrochemical information.

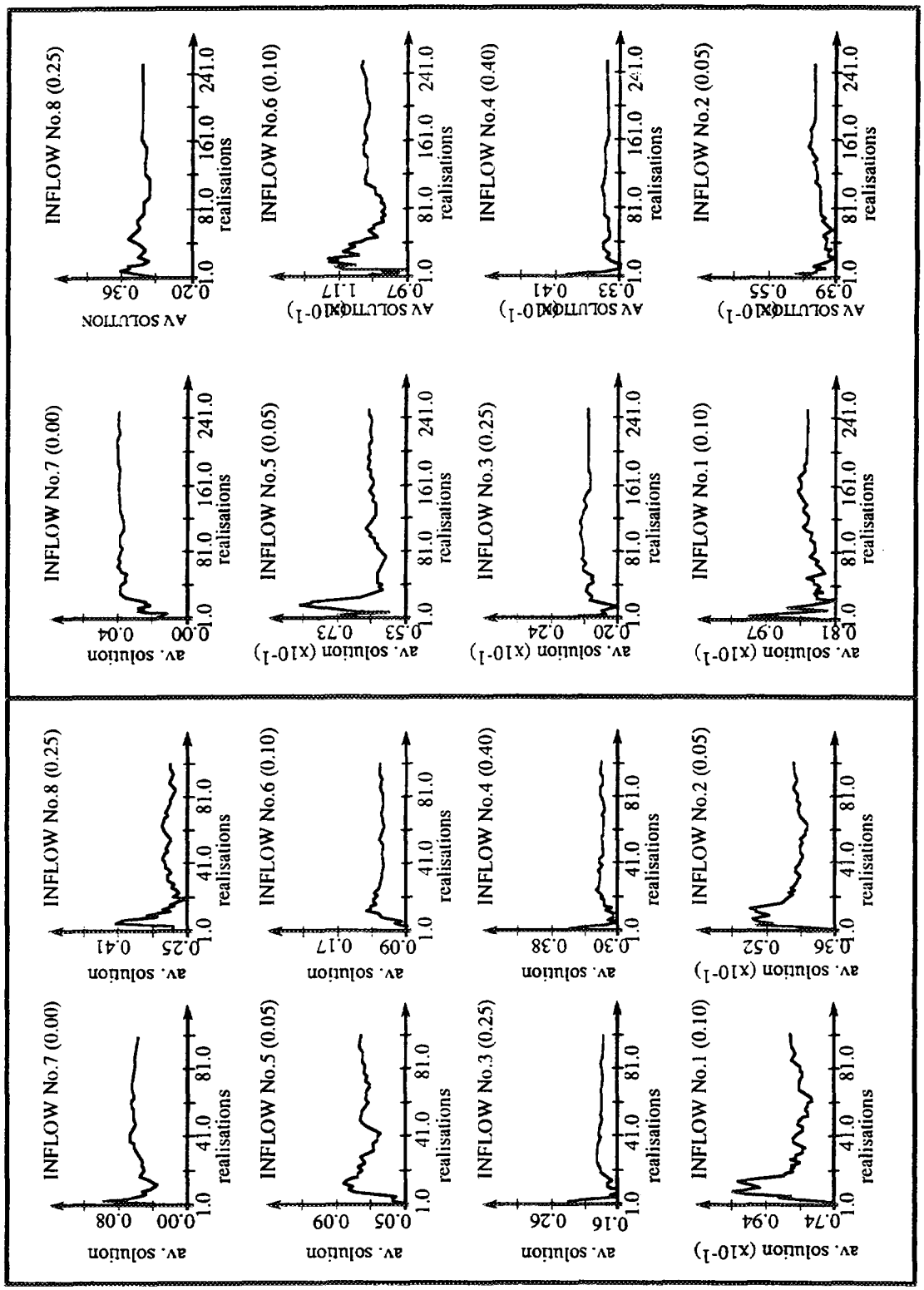

Figure 13: Results of Monte Carlo simulations with β_k values equal to 0.05 (A) and to the coefficient of variation determined from laboratory standards (B).

In a comparison between an analytical solution of the flow equation in one dimension and a solution provided by the mixing cell approach, Van Ommen (1985) deduced that the mixing cell model properly describes the spatial distribution of conservative and reactive tracers.

This model can also assess the spatial distribution of transmissivities providing that piezometric heads can be assigned to every cell and across the flowing boundaries. The results from the southern Arava basin are in a fairly good agreement with transmissivity values obtained by various types of pumping tests. The calculated transmissivities obtained from the aforementioned model are a sort of spatial average values span over the region across every flowing boundary between adjacent cells. This eliminates the vast variability caused by local (usually unknown) non homogeneous geological structures that heavily affects the results obtained by pumping tests.

The fact that the model yields good results when noisy data satisfy constraints similar to those that real data usually satisfy, suggests that the model should be able to deal with real hydrologic conditions. While errors in measured concentrations affect the estimation of fluxes, inaccurate information on the configuration and dimensions of cells, and on the hydraulic head temporal and spatial distribution has extreme influence on the evaluated transmissivities. With the above-mentioned limitations, the model seems to be very sensitive to the quality of the collected data. Deviations from the chemical and isotopic constraints yield an unbounded solution indicating either errors in input data or misunderstandings of the groundwater flow pattern, sources, and processes of aquifer recharge (Adar, 1984).

REFERENCES

Adar, E., 1984. Quantification of aquifer recharge distribution using environmental isotopes and regional hydrochemistry. Dissertation, University of Arizona, Tucson, Arizona, 251 pp.

Adar, E.M. and S.P. Neuman (1986). "The use of environmental tracers (isotopes and hydrochemistry) for quantification of natural recharge and flow components in arid basins". The 5th International Symposium on Underground Tracing, Athens, Greece, pp. 235-253.

Adar, E.M., Neuman, S.P. and Woolhiser, D.A., 1988. Estimation of spatial recharge distribution using environmental isotopes and hydrochemical data. I. Mathematical model and application to synthetic data. Journal of Hydrology, 97, pp. 251-277.

Adar, E.M. and Neuman, S.P., 1988. Estimation of spatial recharge distribution isotopes and hydrochemical data. II. Application to Aravaipa Valley in Southern Arizona, USA. Journal of Hydrology, 97, pp. 297-302.

Adar, E. and S. Sorek (1989). "Multi-compartmental modelling for aquifer parameter estimation using natural tracers in non-steady flow." Advances in Water Resources, Vol. 12, pp 84-89.

Adar, E.M., and S. Sorek (1990). " Numerical method for aquifer parameter estimation utilizing environmental tracers in a transient flow system". MODELCARE 90, International Conference on Calibration and Reliability in Groundwater Modelling, The Hague, Holland, K. Kovar, Ed. IAHS Pub. No. 195, pp 135-148.

Adar, E., E. Rosenthal, A.S. Issar and O. Batelaan. (1992) "Quantitative assessment of flow pattern in the southern Arava Valley (Israel) by environmental tracers in a mixing cell model." Journal of Hydrology Vol. 136, PP 333-354.

Bard, Y., 1974. Nonlinear Parameter Estimation (Appendix D). Academic Press, 332 pp.

Belan, R.A., 1972. Hydrogeology of a portion of the Santa Catalina mountains. M.S. Thesis, University of Arizona, 68 pp.

Besbes, M., Delhomme, J.P. and DeMarsily, G., 1978. Estimating recharge from ephemeral streams in arid regions: A case study at Kariouan, Tunisia. Water Resour. Res., 14(2), pp. 281-290.

Blake, G., Schlichting, E. and Zimmerman, M., 1973. Water recharge in a soil with shrinkage cracks. Soil Science Society of America Proceedings, 37, pp. 669-672.

Bos, M.G. and Nugteren, J., 1974. On irrigation efficiencies. International Institute for Land Reclamation and Improvement, Publication 19. Wageningen, The Netherlands, 89 pp.

Box, G.E.P. and E. Muller, E., 1974. A note on the generation of random normal deviates. Ann. Math. Statist., 29, pp. 610-611.

Bredenkamp, D.B., Schulte, J.M. and Du Toit, G.J., 1974. Recharge of a dolomite aquifer as determined from tritium profiles. Proc., IAEA, Vienna, pp. 73-94.

Briggs, P.C. and Werho, L.L., 1966. Infiltration and recharge from the flow of April 1965 in the Salt river near Phoenix, Arizona. Arizona State Land Department, Water Resources Report No. 29, 12 pp.

Burkham, D.E., 1970. Depletion of stream flow by infiltration in the main channels of the Tucson Basin, Southeastern Arizona. U.S. Geological Survey, Water Supply Paper 1939-B, 36 pp.

Campana, M.F. and Simpson, E.S., 1984. Groundwater residence times and discharge rates using discrete-state compartment model and ^{14}C data. J. Hydrol. 72, pp. 171-185.

Campana, M.F. and Mahin, D.A., 1985. Model - derived estimates of groundwater mean ages, recharge rates, effective porosities and storage in limestone aquifer. Journal of Hydrology, pp. 247-264.

Carrera, J. and Neuman, S.P., 1986a. Estimation of aquifer parameters under transient and steady-state conditions. I. Maximum likelihood method incorporating prior information. Water Resour. Res., 22(2), pp. 201-211.

Carrera, J. and Neuman, S.P., 1986b. Estimation of aquifer parameters under transient and steady-state conditions. II. Uniqueness, stability and solution algorithms. Water Resour. Res., 22(2), pp. 211-227.

Carrera, J. and Neuman, S.P., 1986c. Estimation of aquifer parameters under transient and steady-state conditions. III. Application to synthetic and field data. Water Resour. Res., 22(2), pp. 228-242.

Dincer, T., Al-Mugrin, A. and Zimmerman, M., 1974. Study of the infiltration and recharge through the sand dunes in arid zones with special reference to the stable isotopes and thermonuclear tritium. J. Hydrol., 23, pp. 79-109.

Duffy, C.J., Gelhar, L.W. and Gross, G.W., 1978. Recharge and groundwater conditions in the western region of the Roswell Basin. Partial technical completion report, Proj. No. A-005-NMEX, New Mexico Water Resources Research Institute, Las Cruces, New Mexico.

Eakin, T.E., 1966. A regional interbasin groundwater system in the White River area, Southern Nevada. Water Resour. Res. 2(2), pp. 251-272.

Flug, M., Abi-Ghanem, G.V. and Duckstein, L., 1980. An event-based model of recharge from an ephemeral stream. Water Resour. Res., 16(4), pp. 685-690.

Feth, J.H., Barker, D.A., Morre, L.B. Brown, R.J., and Veirs, C.E., 1966. Lake Bonneville: Geology and hydrology of the Weber Delta District, including Ogden, Utah. U.S. Geological Survey, Professional Paper 518, 76 pp.

Gat, J.R., and Dansgaard, W., 1972. Stable isotope survey of the fresh water occurrence in Israel and the Jordan rift Valley. J. Hydrol., 16, 177-211.

Gelhar, L.W., 1974. Stochastic analysis of phreatic aquifers. Water Resour. Res., 10(3), pp. 539-545.

Gorelick, S.M., Evans, B. and Remson, I., 1983. Identifying sources of groundwater pollution: An optimization approach. Water Resour. Res., 19(3), pp. 779-790.

Heerman, D.F. and Kincaid, D.C., 1974. Scheduling irrigation with a programmable calculator. Agricultural Research Service, ARS-NC-12.

Howard, K.W.F. and Lloyd, J.W., 1979. The sensitivity of parameters in the Penman evaporation equations and direct recharge balance. J. Hydrol., 41, pp. 329-344.

Issar, A., 1983. On the source of water from the thermomineral springs of Lake Kinneret (Israel). J. Hydrol., 60, 175-183.

Issar, A. and Gat, J., 1981. Environmental isotopes as a tool in hydrogeological research in arid basin. Ground Water, 19(5), pp. 490-494.

Issar, A. and Gilad, D., 1982. Groundwater flow systems in the arid crystalline province of southern Sinai. Hydrol. Sci. J., 27, pp. 309-325.

Jacob, C.E., 1943. Correlation of groundwater levels and precipitation on Long Island, New York, I. Trans. Amer. Geophys. Union, 24, pp. 564-573.

Jacob, C.E., 1944. Correlation of groundwater levels and precipitation on Long Island, New York, II. Trans. Amer. Geophys. Union, 25, pp. 928-939.

Kafri, U. and Ben-Asher, J., 1978. Computer estimates of natural recharge through soils in southern Arizona, U.S.A. J. Hydrol., 38, pp. 125-138.

Karmeli, D., Salazar, L.J. and Walker, W., 1978. Assessing the spatial variability of irrigation water applications. U.S. Environmental Protection Agency, EPA-6000/2-78-041, 201 pp.

Keith, S.J., 1981. Stream channel recharge in the Tucson Basin and its implications for ground water management. M.S. Thesis, Tucson, Arizona, University of Arizona.

King, T.G. and Lambert, J.R., 1976. Simulation of deep seepage to a water table. Trans. Amer. Soc. Agr. Eng., 19, pp. 50-54.

Lawrence, F.W. and Upchurch, S.B., 1982. Identification of recharge areas using geochemical factors analysis. Ground Water, 20(6), pp. 260-287.

Levin, M., Gat, J.R. and Issar, A., 1980. Precipitation, flood- and groundwaters of the Negev highlands: An isotopic study of desert hydrology. Proc., IAEA, Vienna, pp. 3-22.

Leggette, R.M., 1936. Note in Trans. Amer. Geophys. Union, 17, pp. 341-344.

Marsh, J.A., 1968. The effect of suspended sediment and discharge on natural infiltration of ephemeral streams. M.S. Thesis, University of Arizona, Tucson, Arizona, 42 pp.

Matlock, W.G., 1965. The effect of silt-laden water on infiltration in alluvial channels. Ph.D. dissertation, University of Arizona, Tucson, Arizona, 102 pp.

Matlock, W.G., 1970. Mathematical analysis of ground water recharge. Trans. Amer. Soc. Civil Eng., 13(6), pp. 785-791.

Matlock, W.G. and Davis, P.R., 1972. Groundwater in the Santa Cruz Valley, Arizona. Technical Bull. 194, University of Arizona, Agricultural Experiment Station, Tucson, Arizona, 37 pp.

Mazor, E., 1982. Rain recharge in the Kalahari - A note on some approaches to the problem. J. Hydrol., 55, pp. 137-144.

Mazor, E., Verhagen, B.T., Senschop, J.P.F., Robins, N.S. and Hutton, L.G., 1974. Kalahari groundwaters: Their hydrogen, carbon and oxygen isotopes. In: Isotope Techniques in Groundwater Hydrology, Proc., IAEA, Vienna, pp. 203-223.

Mero, F., 1963. Application of the groundwater depletion curves in analyzing and forecasting spring discharges influenced by well fields. Intern. Assoc. Sci. Hydrol. Publication No. 63, pp. 107-117.

Moench, A.F. and Kisiel, C.C., 1970. Application of the convolution relation to estimating recharge from an ephemeral stream. Water Resour. Res., 6(4), pp. 1087-1094.

Olmstead, F.H., Loeltz, D.J. and Irelan, B., 1973. Water resources of Lower Colorado River-Salton Sea area. U.S. Geological Survey, Prof. Paper 486-H.

Plummer, L.N., Jones, B.F., and Truesdell, A.H., 1976. WATEQF - A fortran IV version of WATEQ, a program for calculating chemical equilibrium of natural waters. U.S. geological Survey, Nat. Tech. Info. Serv., PB 261027, 61 pp.

Plummer, L.N., Prestemon, E.C., and Parkhurst, D.L., 1991. An interactive code (NETPATH) for modeling net geochemical reactions along a flow path. U.S. Geological Survey, Water Resources Investigations Report 91-4078, Reston, Virginia, 93 pp.

Rasmussen, T.C., 1982. Solute transport in saturated fractured media. M.Sc. Thesis, University of Arizona, Tucson, Arizona.

Rantz, S.E. and Eakin, T.E., 1971. A summary of methods for the collection and analysis of basic hydrologic data for arid regions. Open File Report, U.S. Geological Survey Water Resources Division, Menlo Park, California, 125 pp.

Rosenthal, E., Adar, E. Issar, A.S., and Batelaan, O. 1990. Definition of groundwater flow pattern by environmental tracers in the multiple aquifer system of southern Arava valley, Israel. Journal of Hydrology, Vol. 117, PP 339-368..

Shampine, W.J., Dincer, T. and Noory, M., 1979. An evaluation of isotope concentrations in the groundwater of Saudi Arabia. Proc. Isotope Hydrology, 1978. IAEA, Vienna, 2, pp. 443-463.

Simpson, S.E., 1975. Finite state mixing cell models. Bilateral United States - Yugoslavian Seminar in Karst Hydrology and Water Resources, Dubrovnik, 1975.

Simpson, E.S. and Duckstein, L., 1976. Finite state mixing-cell models. In: Karst Hydrology and Water Resources, V. Yevjevish, (ed.), Ft. Collins, Colorado. Water Resour. Publications, 2, pp. 489-508,

Tanji, K., 1977. A conceptual hydrosalinity model for predicting salt load in irrigation return flows. In: Managing Saline Water for Irrigation, H.E. Dregne (ed.). Proceedings of the International Conference on Managing Saline Water for Irrigation, Planning for the Future, Center for Arid and Semi-Arid Land Studies, Texas Tech. University, pp. 49-72.

Thornwaite, C.W. and Mather, J.R., 1957. Instruction and tables for computing potential evapotranspiration and the water balance. In: Publication in Climatology, 10(3), 311 pp.

Van Ommen, H.C., 1985. The "mixing cell" concept applied to transport of non-reactive and reactive components in soils and groundwater. Journal of Hydrology, 78, pp. 201-213.

Venetis, C., 1971. Estimating infiltration and/or the parameters of unconfined aquifers from ground water level observations. J. Hydrol., 12(2), pp. 161-169.

Verhagen, B.Th., Sellschop, J.P.F. and Jennings, C.M.H., 1970. Contribution of environmental tritium measurements to some geohydrological problems in Southern Africa. Proc., IAEA, Vienna, pp. 289-313.

Verhagen, B.Th., Dziembowski, Z. and Oosthuizen, J.H., 1978. An environmental isotope study of a major dewatering operation at Sishen mine, Northern Cape Province. Proc., IAEA, Vienna, pp. 65-81.

Vogel, J.C., Thilo, L. and Van Dijken, M., 1974. Determination of groundwater recharge with tritium. J. Hydrol., pp. 23: 131-140.

Wagner, B.J. and Gorelick, S.M., 1986. A statistical methodology for estimating transport parameters: Theory and applications to one-dimensional advective dispersive systems. Water Resources Research, 22, pp. 1303-1315.

Wagner, B.J. and Gorelick, S., 1986. Optimal groundwater quality management under parameter uncertainty. Water Resources Research, 23, pp. 1162-1174.

Walker, W.R., 1970. Hydrosalinity model of the Grand Valley. M.S. Thesis, Colorado State University, Ft. Collins, Colorado, 75 pp.

Wilmot, C.J., 1977. WATBUG: A FORTRAN IV algorithm for calculating the climatic water budget. Water Resour. Center, University of Delaware, Newark, Delaware, 55 pp.

Wilson, L.G. and DeCook, K.J., 1968. Field observations on changes in the subsurface water regime during influent seepage in the Santa Cruz River. Water Resour. Res., 4(6), pp. 1219-1234.

Wind, G.P. and Van Doorne, W., 1975. A numerical model for the simulation of unsaturated vertical flow of moisture in soil. J. Hydrol., 24, pp. 1-20.

Wolf, P., 1967. Methods of non-linear programming. Chap. 6. In: Interscience, J. Wiley, New York,pp. pp. 97-131.

Woolhiser, D.A., Emmerich, W.E. and Shirley, E.D., 1985. Identification of water sources using normalized chemical ion balances: A laboratory test. J. Hydrol., 76, pp. 205-231.

Woolhiser, D.A., Gardner, H.R. and Olsen, S.R., 1982. Estimation of multiple inflows to a stream reach using water chemistry data. Trans., ASAE, 25(3), pp. 616-622.

Yurtsever, Y. and Payne, B.R., 1978 a. Application of environmental isotopes to groundwater investigation in Qatar. Proc., IAEA, Vienna, pp. 465-490.

Yurtsever, Y. and Payne, B.R., 1978 b. A digital simulation approach for a tracer case in hydrological system (multi-compartmental mathematical model). Int. Conference on Finite Elements in Water Resources, London, 1978.

Yurtsever, Y. and Payne, B.R., 1985., Time-variant linear compartmental model approach to study flow dynamics of a karstic groundwater system by the aid of environmental tritium (a case study of south-eastern karst area in Turkey). Symposium of Karst Water Resources, Ankara-Antalya, July 1985, IAHS Publ. no. 161, pp. 545-561.

Zimmerman, U., Ehhalt, D., and Munnich, K.O., 1967. Soil water movement and evapotranspiration: Changes in the isotopic composition of the water. Isotope in Hydrology, IAEA, Vienna, pp. 567-585.

Zimmerman, U. Munnich, K.O., and Roether, W., 1966. Tracers determine movement of soil moisture and evapotranspiration, Science, 152 (3720), pp. 346-347.

BASIC CONCEPTS AND FORMULATIONS FOR ISOTOPE GEOCHEMICAL MODELLING OF GROUNDWATER SYSTEMS

R.M. KALIN
Department of Civil Engineering,
The Queen's University,
Belfast, Northern Ireland,
United Kingdom

Abstract

This chapter describes the basic chemical principles and methodologies for geochemical models and their use in the field of isotope hydrology. Examples of calculation procedures are given on actual field data. Summary information on available PC software for geochemical modeling is included. The specific software, NETPATH, which can be used for chemical speciation, mass balance and isotope balance along a flow path in groundwater systems, is discussed at some length with an illustrative example of its application to field data.

4.1 Introduction

Geochemical modelling of hydrologic systems is an area of active research that has potential applications to many problems including those of environmental assessment, palaeohydrology, diagenesis of minerals and nuclear waste. The goal of research in this area is to interpret the details of evolutionary reaction paths in groundwater systems that result from both natural and anthropogenic processes. The results of geochemical modelling can be used to use validate our conceptual understanding of hydrologic flow and geochemical processes. To facilitate this effort, computer codes have been written to simulate geochemical reactions by combining the theory of aqueous chemistry with extensive thermodynamic data.

Isotope hydrology has been widely applied as an integral part of hydrologic investigations for decades. This isotopic data has been used successfully by many to gain insight into the dynamics of groundwater flow or for the qualitative interpretation of groundwater systems. The isotopic composition of dissolved species can also be used to ascertain unique evolutionary reaction paths in groundwater systems. This coupled geochemical-isotopic modelling approach to hydrologic investigations can offer singular solutions to our interpretation of groundwater flow.

The concept of applying geochemical modelling to natural water systems was introduced by Garrels and Thompson in 1962 [1]. Their approach modelled water chemistry, decoupled from flow, and provided quantifiable information about geochemical processes in an aqueous system. This initial model described the distribution of 17 chemical species in seawater at 25°C and was able to quantify the predominant ion pair speciation. It was this approach of using rigorous

thermodynamic data to describe chemical speciation in water that set the framework for most of the geochemical models used in groundwater investigation.

Aqueous geochemistry includes reactions of inorganic and organic species in the aqueous phase and at the surface of clay or mineral grains. This chapter will focus on geochemical modelling of reactions that control the concentration and isotopic composition of dissolved inorganic species in groundwater. It is also intended to be an introduction to the basic concepts and formulations for isotope-geochemical process investigations, procedures and methodologies for geochemical modelling of groundwater systems.

The results we seek with geochemical modelling of groundwater systems are; 1) identification of those minerals or gasses that are dissolving and/or precipitation along a hypothetical flow path; 2) determination of the spatial variation in the mass of each chemical species entering or leaving the groundwater system; and 3) potentially, the prediction of water chemistry along flow paths or systems not yet studied. To attain these results we must interpret chemical reactions in a groundwater system based on a sound understanding of its geology and hydrogeology, and we must base our prediction of geochemical reactions on a solid foundation of chemical knowledge. For this, we have many geochemical models to choose from for our specific needs and applications.

Table I. Geochemical models, applications and concerns for groundwater investigations.

Models	Concerns
Chemical speciation	Model sensitivity
Ion Interaction	Sample analysis errors
Applications	Computational errors
Mass transfer	Thermodynamic data availability
Isotope fractionation	Kinetic controls on reactions
Redox	Coupled flow/reactions
Coupled reactions	

4.2 Hydrologic considerations: the conceptual model

The previous three chapters in this book have described the basic concepts and formulations for mathematical models which increase our understanding of groundwater flow and solute transport. Prior to the development of a geochemical model of groundwater, a detailed knowledge of the flow of water in the system is required. This knowledge includes a conceptual understanding of groundwater flow ie: geologic framework, piezometric surface map and flow net, but geochemical modelling does not require a working mathematical model of groundwater flow as a prerequisite.

The generation of the hydrologic flow and geochemical models can be concurrent and independent. However, it is not meaningful to model the geochemical evolution of groundwater between two water samples that are unrelated ie: between two wells that are not on the same flow path or water from

two separate aquifer systems. Once developed, the geochemical model can be used to refine or validate aspects of the hydrologic flow model through estimation of regional hydrologic parameters using calculations of flow velocities using age dating techniques or via interpretation of mixing of water from different sources.

The boundary conditions applied to geochemical modelling are based on the questions asked and the availability of geochemical data. If our goal is to use geochemical modelling to understand recharge processes and potential groundwater contamination, we must begin by collecting data on rainfall, runoff/river water, and minerals and gasses in the soil/unsaturated zone. If our goal is to age-date water in deeper saturated aquifers, we would choose groundwater near the recharge zone as our starting point. In each case, we attempt to reconstruct the geochemical evolution of water along its flow path.

There are hydrologic limitations that affect our ability to geochemically model groundwater systems. It is presently accepted that hydrodynamic dispersion can be neglected when geochemically modelling regional groundwater systems [2], but some systems on smaller scales might not be suitable for geochemical modelling if dispersion is not included in the interpretation. Groundwater systems dominated by fracture flow may contain waters of very different residence times and chemical composition at the same point down gradient [3]. Many wells are drilled to provide a water resource, and thus may be screened over a wide interval to maximize yield. Undefined hydrochemical mixing (either intrawell or interwell) between water from different hydrostratographic units can not be discerned without knowledge of the quantity and chemical composition of incoming water. Hence, it may not be possible to separate the effects of mixing from those of geochemical reactions along the flow path. Flow systems may be vertically stratified both chemically and as a function of age. Sufficient hydrochemical data is needed to select samples in the proper screened interval to intersect the conceptual hydrologic flow line. Groundwater withdrawal, recharge or contamination may alter the chemistry of water and affect which reactions are used to account for chemical changes down gradient. Finally, the palaeohydrology of the groundwater system may have changed due to natural climate change.

Given sufficient detail, these limitations can be overcome with geochemical modelling techniques. Too often, the availability of geochemical data is limited; but through a coupled knowledge of isotope hydrology and geochemical modelling we can ascertain a unique solution to the geochemical evolution of groundwater [4]. Before we study these methods in detail, we should consider the two methods of solving for chemical reactions and mass-transfer in groundwater systems, the forward solution and the inverse solution.

4.3 Forward solution

The forward solution to geochemical modelling is the prediction of water chemistry based on a knowledge of the mineral composition and the controlling geochemical reactions in the hydrologic system. Ultimately, it is the modeller who determines which geochemical reactions control water chemistry and at what point

the system has undergone mass-transfer and approach to equilibrium. The latter can often be controlled by kinetics (rate of reaction) and hydrologic flow velocity. To predict the chemistry of groundwater we assume; 1) the final (predicted) water is hydrologically related to the point chosen as representative of its initial water chemistry; 2) there are no changes in the geology and mineralogy between the initial and final points we represent with the model; 3) kinetic controls on water chemistry are insignificant, predicted or otherwise not controlling the chemistry of the final water; and 4) mixing of water is known and defined.

Table II. Forward modelling of groundwater

Initial Water	→	Applied Reactions	→	Final Water
known chemistry & isotopic composition (liquid and gas phase)		*known* stoichiometry, kinetics and mixing (liquid and gas phase)		**predicted** chemistry & isotopic composition

4.4 Inverse solution

The inverse solution to geochemical modelling is the determination of water-rock reactions along a hypothetical flow path based on change in chemistry between initial water and final water compositions. While the forward model relies on the selection of reactions that should occur, the inverse model relies on the choice of related initial and final water samples along the flow path. It is not possible to be assured that initial and final water samples are actually related. Consequently, it is important to interpret the results of the inverse solution with insight and knowledge of geochemistry and uncertainties in the conceptual understanding of groundwater flow in three dimensions. To solve for water-rock reactions we assume; 1) the initial and final water samples are hydrologically related; 2) balanced chemical reactions or mixing can be used to predict changes in the chemical composition of water; 3) all the major controlling reactions along the flow path are included; and 4) temporal changes in climate and hydrology have little effect on the model results or these effects can be accounted for. Generally, chemical speciation modelling is used in conjunction with the inverse solution to verify the controlling reactions along the flow path.

Table III. Inverse modelling of groundwater

Initial Water	→	*Inferred Reactions*	→	*Final Water*
known chemistry & isotopic composition (liquid and gas phase)		**predicted** stoichiometry, kinetics and mixing (liquid and gas phase)		*known* chemistry & isotopic composition (liquid and gas phase)

Table IV. Selected geochemical models

	NETPATH	EQ3/EQ6	MINTEQ	PHREEQE	SOILCHEM	WATEQ4F	1DREACT	SOLMINEQ
Reference*	[I]	[II]	[III]	[IV, V]	[VI]	[VII]	[VIII]	[IX]
Type (Speciation, Ion interaction, Inverse mass balance, Forward reac. path, Coupled flow/react.)	S, Imb	S, Frp	S	S,I,Frp	S	S	C,S,Frp	S,I
Number of elements	19	47	31	19	47	32	47	31
Number of minerals	175	713	328	175	250	321	713	214
Isotopes	C,N,O,H,S,Sr	-	-	-	-	-	-	-
Aqueous Species	132	686	373	120	1853	245	686	270
Organics	DOC	-	-	yes	889	12	-	80
Gasses	7	11	3	3	11	7	11	7
Sorption (Ion Exchange, Surface Complex)	no	no	6 models	IE	SC	no	no	IE
Redox elements	6	25	8	6	11	7	25	8
Activity coefficient (Debye-Hückel, Davies, Pitzer)	D-H, D	D-H, D, P	D-F, D	D-H, D, P	D-H, D	D-H, D	D-H, D, P	D-H, D, P
Temperature (°C)	0-100	0-300	0-50	0-100	0-50	0-100	0-300	0-350
Pressure (atm)	1	1+	1	1	1	1	1	1-1000

* See list of references at the end of this chapter.

Table IV presents an overview of selected geochemical models available for use in the interpretation of groundwater geochemistry. This is not a comprehensive list, but rather a general outline of a few models presently available for use.

4.5 Basic chemical principles for geochemical models

It is necessary to have some understanding of physical chemistry to understand the geochemistry of groundwater systems. The discussion in this section is not intended to be all inclusive, but a general overview of the basic terminology and principles required to understand the geochemical approach to groundwater modelling. There are many texts available that cover this topic if a more detailed discussion is needed.

A mole of a given substance is its formula weight expressed in grams eg: 1 mole of carbon is 12.011gm of carbon. In physical chemistry we express units of concentration in terms of *normality* (N), number of equivalent weights of solute per litre of solution; *molality* (m), moles of solute per kilogram of solvent; and *molarity* (M), moles of solute per litre of solution. Molarity and molality are nearly identical except at high concentrations (eg. brines) or at high temperatures where the density of water diverges from 1.0. A chemical *species* can be an ion, molecule, solid phase or gas phase, and so on, that takes part in geochemical reactions. Thus, in the chemical system NaCl and H_2O, some of the possible species include: $NaCl_{(s)}$, Na^+, Cl^-, $H_2O_{(l)}$, $H_2O_{(g)}$, OH^- and H^+. Speciation modelling is a method of calculating the activity and equilibrium state of species (either dissolved or solids) in an aqueous solution as determined by constraining thermodynamic data. In groundwater systems it is rare that actual equilibrium conditions exist, but the equilibrium approach is useful in that it can indicate the direction of a reaction (eg: precipitation or dissolution) and it can offer a good approximation of the real system.

Thermodynamic data consists generally of empirically derived constants that govern chemical reactions in aqueous solutions. Chemical reactions in natural water systems are often modelled using equilibrium expressions where the *solubility* of a given solute (mineral or gas) is defined as the amount that dissolves until the solution is *saturated* with respect to that mineral or gas.

A reversible chemical reaction can be represented by the *Law of Mass Action* equation:

$$a(A) + b(B) \rightleftharpoons c(C) + d(D) \qquad (4.1)$$

where a,b,c, and d are the stoichiometric coefficients of reactants (A),(B),(C),and (D). At equilibrium, the concentrations of the products and reactants are constant, thus there is a constant of proportionality for this reaction.

$$K_{eq} = \frac{(C)^c (D)^d}{(A)^a (B)^b} = K_{sp} \qquad (4.2)$$

This constant of proportionality (K_{eq}), is the familiar expression for the equilibrium constant of reaction 4.1, for dissolution of a solid it is also known as the solubility product (K_{sp}). A system at equilibrium is in a state of minimum energy. A system not in equilibrium can move toward equilibrium by releasing energy. The appropriate measure of the energy in a chemical system is the *Gibbs Free Energy* (G) which is related to enthalpy (heat content, H) and entropy (order, S). The change in energy that occurs during a geochemical reaction (ΔG°_r) can be calculated from the change in Gibbs Free Energy of the system:

$$\Delta G_r^o = \Delta H_r^o - T\Delta S_r^o \quad \therefore \qquad (4.3)$$

$$\Delta H_r^o = \Delta H_{products}^o - \Delta H_{reactants}^o \qquad (4.4)$$

$$\Delta S_r^o = \Delta S_{products}^o - \Delta S_{reactants}^o \qquad (4.5)$$

where T is temperature in °K. Values of ΔH°_r and ΔS°_r can be obtained from published tables of standard-state enthalpy and entropies of formation.

The equilibrium constant can be calculated directly from the free energy if the free energy of the reaction is known. In this way, geochemical reactions that are not represented in the thermodynamic database of a given geochemical model may be added to the system of chemical equations applied to a particular groundwater system.

Equation 4.6 governs the relationship between K_{eq} and ΔG°_r at a temperature of 25°C:

$$\Delta G_r^o = -RT \ln K_{eq} \qquad (4.6)$$

where R is the gas constant (8.3143 J mol^{-1} $°K^{-1}$; 1.98717 cal mol^{-1} $°K^{-1}$) and T is temperature on the kelvin scale.

Example I:

Geochemical analysis has determined the mineral anhydrite is present as one aquifer mineral, and due to high sulphate in the water we suspect that anhydrite takes part in mass-transfer reactions along a hydrologic flow path. There is no equilibrium constant for this species in our geochemical model and so we must calculate the equilibrium constant (solubility product) of anhydrite at 25°C. Given the balanced reaction:

$$CaSO_4 \rightleftharpoons Ca^{2+} + SO_4^{2-}$$

Thermodynamic data (source: Wagman *et al.* [5]):

Species	ΔG°(kJ/mol)	ΔH°(kJ/mol)	S°(J/mol•°K)
Ca^{2+}	-555.58	-542.83	-53.1
SO_4^{2-}	-744.53	-909.27	20.1
$CaSO_4$ (anhydrite)	-1321.79	-1434.11	105.2

ΔG°_r = (-555.58) + (-744.53) - (-1321.79) = 21.68 kJ/mol

Solving equation 4.6 for Log K_{eq} we obtain the relationship:

$$\log K_{eq} = \frac{-\Delta G_r^o}{R\,T}$$

or at 25°C where $\Delta G°_r$ is in kJ/mol:

$$\log K_{eq} = \frac{-\Delta G_r^o}{5.708}$$

The equilibrium constant (K_{eq}) or solubility product (K_{sp}) of anhydrite at 25°C is $10^{-3.8}$. This value is significantly different than the value of $10^{-4.36}$ used by NETPATH [6] or another calculated value of $10^{-4.31}$ using thermodynamic data from Faure [7]. The thermodynamic data chosen to calculate equilibrium values must be evaluated by the user, and its uncertainty should be considered a part of the uncertainty involved when geochemical modelling.

Most groundwater systems fall within ± 25°C of the standard state, but even within this range the affect of temperature on values of $\Delta H°_r$ and $\Delta S°_r$ can introduce errors in thermodynamic data. Many geochemical models contain heat capacity expressions [8] in the thermodynamic database that allow for extrapolation of the equilibrium constant to much different temperatures.

If the temperature extremes are not great, generally between 0°C and 50°C, the *van't Hoff expression* can be used to extrapolate the equilibrium expression to the new temperature:

$$\ln K_{T_2} - \ln K_{T_1} = \frac{\Delta H_r^o}{R}\left(\frac{1}{T_1} - \frac{1}{T_2}\right) \qquad (4.7)$$

For temperatures outside this range, it is up to the user to determine if the appropriate thermodynamic data is given by the model for valid extrapolation of equilibrium constants at the required temperature. Within this range, if the equilibrium constant is given for one temperature and the standard enthalpy of reaction is known, the equilibrium constant can be calculated for the temperature of each groundwater sample.

Example II.

Calculate the equilibrium constant of anhydrite (Example I) at 65°C using the van't Hoff expression. From the thermodynamic data given in Example I and Equation 4.4, the $\Delta H_r°$ can be calculated as follows:

$\Delta H_r° = \{ (-542.83) + (-909.27) \} - (-1434.11) = -17.99$ kJ/mol

Given R = 8.3143 J/mol = 0.0.0083143 kJ/mol we can solve for the equilibrium constant of anhydrite using Equation 4.7:

$$\ln K_{T_2} = \frac{-17.99}{0.0083143}\left[\frac{1}{298.15} - \frac{1}{333.15}\right] + \ln 10^{-3.8}$$

The equilibrium constant of anhydrite calculated from the thermodynamic data given in Example I extrapolated to 60°C is $10^{-4.13}$.

In very dilute solutions ions do not generally interfere with each other, but due to electrostatic interactions between ions and with the polar water molecule, oppositely charged ions in most groundwater samples surround one another. This effect reduces the free/available concentration of each constituent. We express this by saying the *activity* of the sample is not the same as the concentration.

The interaction between ions depends not only on the concentration of ions in solution but also on the charge of the ion and the size of the ion.

The activity of a species is the product of the concentration and the *activity coefficient* γ_i of each species (i):

$$[a_i] = \gamma_i \, (conc._i) \qquad (4.8)$$

The activity is calculated from equations that relate activity and concentration to the *ionic strength* of a solution. The concentration of ion charges in the water sample is expressed as the ionic strength of the solution:

$$I = \frac{1}{2} \sum m_i z_i \qquad (4.9)$$

In equation 4.9, m_i is the molar concentration of each ion species and z_i is the charge of each ion. Geochemical models may use different equations to calculate the activity of each species in solution.

The first of these is the extended *Debye-Hückel* equation that is generally used to calculate the activity of a species in solutions with I<0.1:

$$-\log \gamma_i = \frac{A z_i^2 \sqrt{I}}{1 + a_i B \sqrt{I}} \qquad (4.10)$$

For equation 4.10, z_i is the charge on the ion, A and B are constants that depend on the dielectric constant of the solvent and temperature, and a_i is the effective diameter of the ion in the solution in Angstroms. The effective diameter of the ion is often chosen as a best fit to the data rather than a measured value. Table

V lists the values for A and B as a function of temperature and Table VI lists a_i for several ions in aqueous solution.

A second equation developed by *Davies* is also used in some geochemical models. This equation includes the charge of the ion, z_i, the constant A from the Debye-Hückel equation (Table V) and is reliable up to ionic strengths of I = 0.5:

$$- \log \gamma = A z_i^2 \left[\frac{\sqrt{I}}{1 + \sqrt{I}} - 0.2 I \right] \qquad (4.11)$$

Figure 1 shows the variation of activity coefficient with ionic strength for both the Davies and Debye-Hückel equations. At higher ionic strengths the activity can dramatically change the effective concentration of chemical species in solution. As ionic strength increases, interaction between ions begins to dominate.

For high ionic strength solutions (eg. brines) the activity can be calculated with the ion interaction methods developed by Pitzer [9]. Geochemical models that account for the activity of solutions with high ionic strengths, $1 \geq I \leq 20$, are generally for specialized purposes. Most groundwater systems are orders of magnitude less than this and either the Davies or Debye-Hückel equations are reliable.

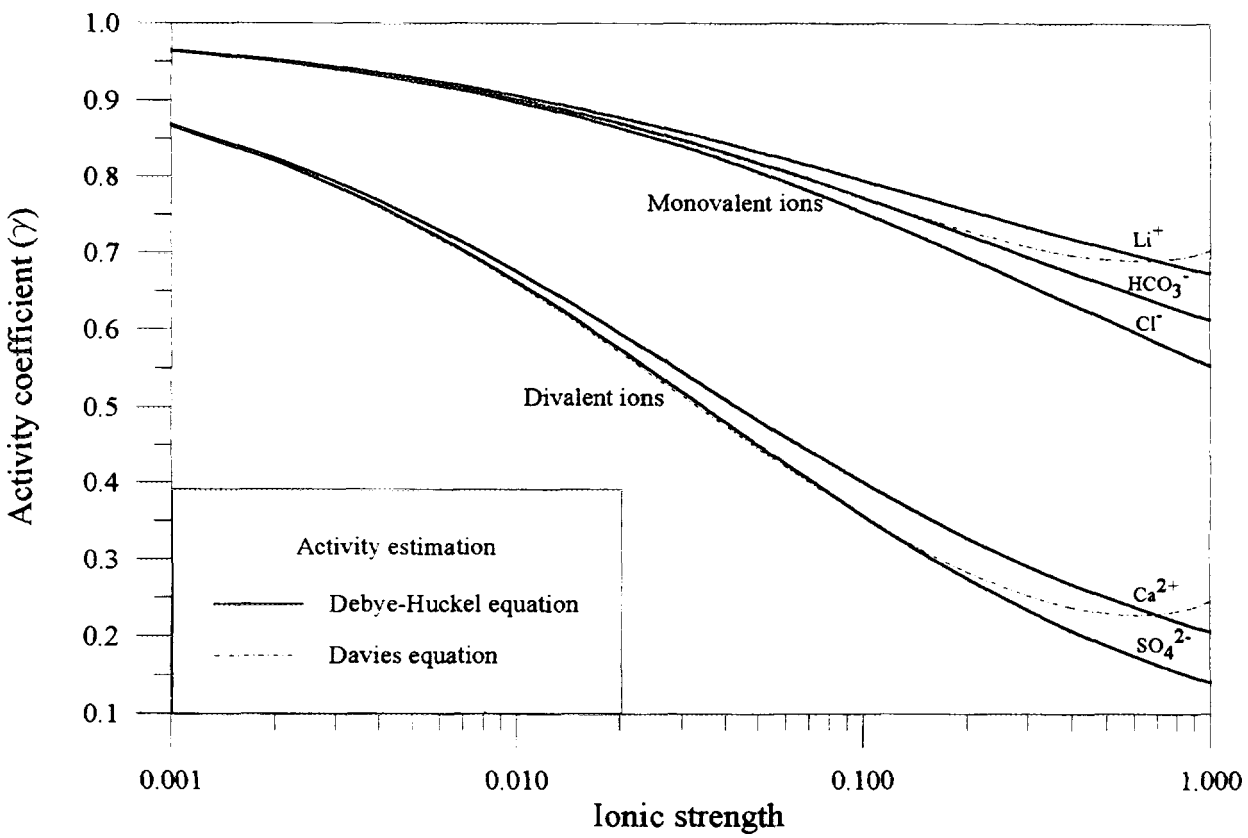

Figure 1. Change in the calculated activity coefficient as a function of the ionic strength of the solution.

The activity of water is generally near 1.0, but at higher ionic strengths this may not hold true. Chemical speciation models calculate the activity of water for a given solution. The activity of a solid phase is by generally assumed to be one unless the geochemical model considers chemical reactions at mineral surfaces. In this case the activity of the solid phase is determined.

Table V. List of constants used in the Debye-Hückel equation

Temperature, °C	A	$B(10^8)$
0	0.4883	0.3241
5	0.4921	0.3249
10	0.4960	0.3258
15	0.5000	0.3262
20	0.5042	0.3273
25	0.5085	0.3281
30	0.5130	0.3290
35	0.5175	0.3297
40	0.5221	0.3305
45	0.5271	0.3314
50	0.5319	0.3321

Table VI. List of a_i values used in the Debye-Hückel equation

a_i, Å (10^{-8})	ions
2.5	Rb^+ Cs^+ NH_4^+ Tl^+ Ag^+
3	K^+ Cl^- Br^- I^- NO_3^-
3.5	OH^- F^- HS^- BrO_3^- MnO_4^-
4.0/4.5	Na^+ HCO_3^- $H_2PO_4^-$ HSO^{3-}
	Hg_2^{2+} SO_4^{2-} PO_4^{2-} CrO_4^{2-}
5	Ba^{2+} Sr^{2+} S^{2-} Ra^{2+} Cd^{2+}
6	Li^+ Ca^{2+} Fe^{2+} Mn^{2+} Zn^{2+}
8	Mg^{2+} Be^{2+}
9	H^+ Al^{3+} Cr^{3+}
11	Th^{4+} Zr^{4+} Ce^{4+} Sn^{4+}

source: Garrels and Christ [10]

Example III:

Calculate the ionic strength of groundwater collected from Tucson basin Well B-83, and using the Debye-Hückel equation (4.10) calculate the activity of calcium, sulphate and bicarbonate ions in solution.

Chemical composition of Tucson basin Well B-83

Species	mg/l	GFW	mol/kg
Ca^{2+}	33.0	40.08	8.23×10^{-4}
Mg^{2+}	9.3	24.305	3.83×10^{-4}
Na^+	73.0	22.99	3.18×10^{-3}
K^+	3.0	39.10	7.67×10^{-5}
Cl^-	35.0	35.45	9.87×10^{-4}
SO_4^{2-}	110.0	96.06	1.14×10^{-3}
HCO_3^-	144.0	61.02	2.36×10^{-3}
SiO_2°	29.0	60.09	4.83×10^{-4}

pH = 7.8; Temperature = 26.5°C; dissolved O_2 = 6.9 mg/l; Eh = 0.32 mv

$$I = \tfrac{1}{2}[(8.23 \times 10^{-4})(+2_{Ca})^2 + (3.83 \times 10^{-4})(+2_{Mg})^2 + (3.18 \times 10^{-3})(+1_{Na})^2 + (7.67 \times 10^{-5})(+1_{K})^2 + (9.87 \times 10^{-4})(-1_{Cl})^2 + (1.14 \times 10^{-3})(-2_{SO4})^2 + (2.36 \times 10^{-3})(-1_{HCO3})^2 + (4.83 \times 10^{-4})(0_{SiO2})^2 + (1.58 \times 10^{-8})(+1_{H})^2]$$

$$= \mathbf{7.99 \times 10^{-3}}$$

Using the ionic strength of the groundwater sample from Well B-83 and the data in Tables V and VI (linear extrapolation to the temperature of the sample), the calculated activity coefficients (γ) for calcium, sulphate and bicarbonate using the Debye-Hückel equation (4.10) are:

$A = 0.5098 \quad B = 0.3284 \times 10^{8}$ and $a_{Ca} = 6.0 \times 10^{-8}$

$-\log \gamma_{Ca} = 0.15498$

$\gamma_{Ca} = 0.6999$

$A = 0.5098 \quad B = 0.3284 \times 10^{8}$ and $a_{SO4} = 4.5 \times 10^{-8}$

$-\log \gamma_{SO4} = 0.16101$

$\gamma_{SO4} = 0.6902$

$A = 0.5098 \quad B = 0.3284 \times 10^{8}$ and $a_{HCO3} = 4.0 \times 10^{-8}$

$-\log \gamma_{HCO3} = 0.040781$

$\gamma_{HCO3} = 0.9104$

The activity of each species is the product of the activity coefficient (γ) and the concentration.

$$[a_{Ca}] = \gamma_{Ca}(Ca^{2+}) = 0.6999 * 8.23 \times 10^{-4} = 5.76 \times 10^{-4}$$

$$[a_{SO4}] = \gamma_{SO4}(SO_4^{2-}) = 0.6902 * 1.14 \times 10^{-3} = 7.87 \times 10^{-4}$$

$$[a_{HCO3}] = \gamma_{HCO3}(HCO_3^{-}) = 0.9104 * 2.36 \times 10^{-3} = 2.14 \times 10^{-3}$$

The activities of some dissolved species are, in part, controlled by the activity of hydrogen ion (pH) and acid-base equilibrium. Acid-base chemical reactions can be expressed as the dissociation of an acid to hydrogen ion and the related base:

$$HA \leftrightarrows H^+ + A^- \qquad (4.12)$$

This reaction is governed by the law of mass action and the equilibrium constant for this reaction is often called the *dissociation constant* (K_A). The equilibrium expression for acid-base reactions describes the interaction of hydrogen ions with ions in solution. The pH of groundwater is usually controlled by equilibrium acid-base reactions involving dissolved carbonate species. During recharge, groundwater is brought into contact with elevated concentrations (above atmospheric) of carbon dioxide in the soil/vadose zone. Both root respiration and biologic activity are sources of CO_2.

The concentration of soil CO_2 establishes the initial groundwater CO_2 - H_2O system where carbonic acid is formed until equilibrium is reached:

$$CO_2 + H_2O \leftrightarrows H_2CO_3 \qquad (4.13)$$

Carbonic acid will dissociate into hydrogen ion and bicarbonate ions:

$$H_2CO_3 \leftrightarrows H^+ + HCO_3^- \qquad (4.14)$$

and bicarbonate will dissociate into hydrogen ion and carbonate ion.

$$HCO_3 \leftrightarrows H^+ + CO_3^{2-} \qquad (4.15)$$

These three reactions proceed concurrently such that any shift in the equilibrium of one reaction produces a change in the equilibrium of the other two reactions. In the CO_2 - H_2O system, the pH of water is a function of the equilibrium dissociation of both carbonic acid and bicarbonate, and the partial pressure of CO_2.
The equilibrium constant for these three reactions are.

$$K_{CO_2} = \frac{[a_{H_2CO_3}]}{[a_{CO_2}]\,[a_{H_2O}]} \qquad (4.16)$$

$$K_1 = \frac{[a_{HCO_3^-}]\,[a_{H^+}]}{[a_{H_2CO_3}]} \qquad (4.17)$$

$$K_2 = \frac{[a_{CO_3^{2-}}]\,[a_{H^+}]}{[a_{HCO_3^-}]} \qquad (4.18)$$

To reduce mathematical errors and for convenience, equilibrium constants are often presented as pK values where: $pK_{eq} = - \log K_{eq}$ (Table VII). The dissociation of carbonic acid is the major source of hydrogen ions in groundwater that are consumed in chemical weathering of minerals in the aquifer. If we assume the activity of water is 1.0 we can rearrange equations 4.16, 4.17 and 4.18 to calculate the pH of pure water as a function of pCO_2.

The hydrogen ion concentration from the dissociation of carbonic acid can be calculated as follows:

$$[H_2CO_3] = [CO_2]\,K_{CO_2} \qquad (4.19)$$

$$[H^+] = \frac{[H_2CO_3]\,K_1}{[HCO_3^-]} \qquad (4.20)$$

substitution of equation 4.19 into 4.20 results in:

$$[H^+] = \frac{[CO_2]\,K_{CO_2}K_1}{[HCO_3^-]} \qquad (4.21)$$

The hydrogen ion concentration from the dissociation of bicarbonate is:

$$[H^+] = \frac{[HCO_3^-]\,K_2}{[CO_3^{2-}]} \qquad (4.22)$$

The total hydrogen ion in solution is then the sum of equations 4.21 and 4.22:

$$[H^+]_{total} = \frac{[CO_2]\,K_{CO_2}K_1}{[HCO_3^-]} + \frac{[HCO_3^-]\,K_2}{[CO_3^{2-}]} \qquad (4.23)$$

The equilibrium constants for the carbonate system are listed as a function of temperature in Table VII. The pH of pure water is 7.0, and we know that dissociation of carbonic acid will reduce the pH of water to less than 7. We can use equation 4.22 and K_2 at 25°C from Table VII to estimate the ratio of $[HCO_3^-]$:$[CO_3^{2-}]$ at pH 7:

$$\frac{[H^+]}{K_2} = \frac{[CO_3^{2-}]}{[HCO_3^-]} = \frac{10^{-7}}{10^{-10.38}} = 10^{-3.38} \qquad (4.24)$$

Because the concentration of CO_3^{2-} is more that 1000 times less than the concentration of HCO_3^- at pH 7, the hydrogen ion contribution from the dissociation of bicarbonate will be negligible when compared to the contribution from the dissociation of carbonic acid. From equation 4.14 we know the dissociation of carbonic acid produces equal concentrations of $[H^+]$ and $[HCO_3^-]$.

If we assume that all of the hydrogen ion in solution is from the dissociation of carbonic acid, equation 4.23 simplifies to:

$$[H^+]^2_{total} = [CO_2]\,K_{CO_2}K_1 \qquad (4.25)$$

We calculate, using equation 4.25, that the pH of pure water at 25°C in contact with soil atmosphere having a 3% concentration of CO_2 is 4.7. The pH of recharging groundwater is generally not this low because carbonic acid is not the only dissolved species in water and some of the hydrogen ion produced from the dissociation of carbonic acid is continually consumed during chemical weathering of minerals.

In aqueous solutions, any number of chemical species may combine to form both neutral and charged species. The formation of *complex* species is controlled by equilibrium processes. An equilibrium constant can be applied to reactions that

form complex ions and species in solution. Formation of complex species affects the relationship between activity and concentration by distributing a chemical species among complexes. The concentration of a complexed ion pair is dependent not only on the concentration of each ion, but also on how the concentration of all the complexed species are affected by variations in pH, Eh (electrical potential of the solution) and other ions in solution. The solution to this convoluted problem is achieved through iterative calculations within chemical speciation models.

Table VII. Equilibrium constants for Equations 4.16, 4.17 and 4.18 as a function of temperature (after Plummer and Busenberg [11])

T(°C)	K_{CO2}	K_1	K_2	$K_{Calcite}$
0	1.11	6.58	10.63	8.38
5	1.19	6.52	10.55	8.39
10	1.27	6.46	10.49	8.41
15	1.34	6.42	10.43	8.43
20	1.41	6.38	10.38	8.45
25	1.47	6.35	10.33	8.48
30	1.52	6.33	10.29	8.51
45	1.67	6.29	10.20	8.62
60	1.78	6.29	10.14	8.76

For example, consider the distribution of carbon species in a solution containing CO_2 ,NaCl and H_2O. The total carbon in the solution will be the sum of carbon contained in different complex ion pairs:

$$m_{C_T} = m_{H_2CO_3^\circ} + m_{HCO_3^-} + m_{CO_3^{2-}} + m_{NaHCO_3^\circ} + m_{NaCO_3^-} \qquad (4.26)$$

The concentration of each complexed ion pair in Equation 4.26 depends on the concentration of carbon dioxide, sodium chloride and, due to the dissociation reactions of carbonic acid, is a function of pH. A complete chemical analysis of the major elements dissolved in groundwater include: Ca^{2+}, Mg^{2+}, K^+, Na^+, Cl^-, SO_4^{2-}, HCO_3^-, NO_3^-, pH and dissolved oxygen, and may also include: F^-, Br^-, $Fe^{2+/3+}$, PO_4^{3-}, and trace metals. A complete description of all the complex ions in solution becomes quite extensive. We can clearly see why it is more convenient to use a computer code to simultaneously solve for the concentration of each complex ion pair in this extensive system of equations. But to solve for each ion pair, the thermodynamic database of the geochemical model must contain the equilibrium constants for the dominant complexed species. Only then can the result accurately predict the activity of all species in solution.

The goal of geochemical modelling is identification of probable reactions that control the evolution of the groundwater and any chemical changes that occur within the aquifer resulting from these reactions. It is not possible to know the exact geochemical reactions occurring at every point in a groundwater system, but we can determine the average resulting chemical mass balance from our knowledge of the minerals that comprise the aquifer system and from changes in groundwater chemistry.

Evaluation of the geochemistry of groundwater must begin with study of the aquifer geology and the composition of *primary* minerals present in the geologic formation, and *secondary* minerals formed during geochemical water-rock reactions. The chemical composition of groundwater is determined by reactions of water with minerals present in the soil, vadose zone and aquifer hence knowledge of the chemical composition of these mineral phases is required.

Detailed mineralogic investigation on aquifer materials is lacking for most hydrologic investigations. Without this data it is not possible to conclude with certainty which geochemical reactions actually occur, only which water-rock interactions explain the observed data [12]. It is incumbent for the researcher to review geologic reports and collect samples of aquifer materials for geochemical analysis. This phase of the groundwater study should consider the points in Table VIII.

Geochemical reactions describe the chemical decomposition of sedimentary, igneous and metamorphic rocks and minerals that comprise the aquifer. Decomposition of each mineral phase depends on its stability in the presence of water and the rate of decomposition varies greatly between minerals.

Table VIII. Points to cover during evaluation of aquifer mineralogy.

Does regional geology control both water flow and mineralogy?
What minerals are present (including petrographic analysis)?
What is the abundance of each mineral (are trace minerals also important)?
Can you identify primary and secondary mineral phases?
What is the chemical composition of each mineral?
Does the mineralogy vary between water bearing zones?
What is the isotopic composition of minerals in the aquifer?
Does the isotopic composition vary between water bearing zones or spatially?

In general, this process of chemical weathering can occur either in the presence of reactive atmospheric gasses (O_2, CO_2) referred to as *open system* reactions, or as *closed system* reactions that are isolated from the atmosphere. Geochemical reactions occurring in regional groundwater systems begin as open system reactions at or near the recharge zone and move toward closed system reactions down gradient. The geology of the aquifer and diffusion through the vadose zone will determine the availability of atmospheric gasses. Any combination of open and closed conditions can occur along a flow path depending

on the geology and hydrology of the system. This consideration can affect interpretation of isotopic data especially when isotopic age dating water.

Before detailed geochemical modelling we should develop a conceptual geochemical model based on our knowledge of the geology, mineralogy and hydrology of the system. We consider the geochemical evolution of groundwater in parts. In the recharge zone(s), water-rock chemical reactions are controlled by the presence of atmospheric gasses. The dissolution of CO_2 provides a source of hydrogen ion for weathering and O_2 is available for reactions with organic material, metals and mineral phases. If carbonate species are available, dissolution likely dominates under open-system conditions and silicate minerals will incongruently weather to clays. Once water has moved down gradient, if no additional source of CO_2 is available, it will be consumed in the process of silicate weathering or carbonate dissolution. When available CO_2 is exhausted, the pH will rise changing the distribution of species in solution, potentially resulting in precipitation of minerals from solution (eg. calcite). Dissolved oxygen may be depleted down gradient through reactions with dissolved organic carbon and reduced species (eg. Fe^{2+}).

Geochemical models are used to infer water-rock reactions through evaluation of the water-mineral equilibrium state, but it is unlikely that groundwater exists in overall chemical equilibrium with the aquifer minerals. Often there are a small number of mineral phases that appear to be in equilibrium while reactions progress as a function of water flow, temperature and pressure changes. Therefore, the geochemical evolution of groundwater is controlled by a combination of reversible equilibrium reactions and one or more non-reversible reactions related through common ion effects or changes in activity coefficients, pH or Eh. The net effect is that geochemical reactions and mass-transfer continue along the flow path but the water appears everywhere to be in equilibrium with certain mineral phases.

To evaluate the equilibrium state of a groundwater with respect to mineral phases, the activity coefficients and concentrations are determined using a chemical speciation model. Using the solubility product equation (K_{sp}), the measured values are used to calculated the *ion activity product* (IAP).

For example, the IAP for anhydrite is calculated as the sum of the activity of calcium and the activity of sulphate:

$$CaSO_4 \leftrightarrows Ca^{2+} + SO_4^{2-}$$
$$IAP = [aCa^{2+}]\,[aSO_4^{2-}] \qquad (4.27)$$

The difference between the theoretical K_{sp} and the IAP indicates the saturation state of the water with respect to a given mineral phase. The saturation index (SI) is defined as:

$$SI = LOG\ \frac{IAP}{K_{sp}} \qquad (4.28)$$

If the SI is less than zero, the groundwater is undersaturated with respect to the mineral phase and there is potential for the mineral to dissolve. If the SI is

greater than zero, the groundwater is oversaturated with respect to the mineral phase and the mineral may precipitate from solution.

Other factors such as kinetic hinderance of reactions, or mineral stability in the presence of other minerals may also determine whether or not a mineral precipitates or dissolves. Example I showed three different values for the solubility product of anhydrite. Any uncertainty in the thermodynamic data will introduce errors when calculating the K_{sp} and thus affect the calculated SI.

Example IV.

Calculate the saturation index of calcite and anhydrite for the water chemistry of Tucson basin Well B-83 given in Example III. The K_{sp} for calcite as a function of temperature was given in Table VII. Extrapolation to the temperature of 26.5°C (for Well B-83), $pK_{calcite} = 8.39$. In Examples I and II we calculated the K_{sp} for anhydrite, which when extrapolated to 26.5°C, $pK_{anhydrite} = 3.81$.

In Example III, the activity of calcium, sulphate and bicarbonate species were calculated as:

$$[\, a_{Ca} \,] = \gamma_{Ca} (Ca^{2+}) = 0.6999 * 8.23 \times 10^{-4} = 5.76 \times 10^{-4}$$

$$[\, a_{SO4} \,] = \gamma_{SO4} (SO_4^{2-}) = 0.6902 * 1.14 \times 10^{-3} = 7.87 \times 10^{-4}$$

$$[\, a_{HCO3} \,] = \gamma_{HCO3} (HCO_3^{-}) = 0.9104 * 2.36 \times 10^{-3} = 2.14 \times 10^{-3}$$

The ion activity product, IAP, for anhydrite can be calculated from this data using equation 4.27:

$$IAP_{anhydrite} = [Ca^{2+}]\,[SO_4^{2-}] = [5.76 \times 10^{-4}]\,[7.87 \times 10^{-4}] = 10^{-6.34}$$

thus:

$$SI_{anhydrite} = Log \frac{10^{-6.34}}{10^{-3.18}} = -3.16$$

Groundwater from Well B-83 is undersaturated with respect to the mineral phase anhydrite. The negative saturation index indicates there is a thermodynamic potential for anhydrite to dissolve in this water. To calculate the saturation index of calcite, we first need the activity of carbonate ion $[CO_3^{2-}]$. We can use the calculated activity of bicarbonate, equation 4.18 and the data in Table VII to calculate the activity of carbonate ion as follows:

$$[a_{CO_3^{2-}}] = \frac{[a_{HCO_3^-}]\,K_2}{[a_{H^+}]} = \frac{10^{-2.67}\ 10^{-10.32}}{10^{-7.8}} = 10^{-5.19}$$

The IAP for calcite is given by the equation:

$$CaCO_3 \rightleftharpoons Ca^{2+} + CO_2^{2-}$$
$$IAP = [Ca^{2+}]\ [CO_3^{2-}]$$

and can be calculated as follows:

$$IAP_{calcite} = [5.76 \times 10^{-4}]\ [6.45 \times 10^{-6}] = 10^{-8.43}$$

thus:

$$SI_{calcite} = Log\ \frac{10^{-8.43}}{10^{-8.39}} = 0.04$$

Groundwater from Well B-83 is saturated with respect to the mineral phase calcite. We can infer from this result that groundwater in this region of the Tucson basin is in apparent equilibrium with calcite.

It is important to consider apparent equilibrium conditions where the SI is near zero or remains constant down gradient along a flow path. If water-rock reactions continue at apparent equilibrium, mass-transfer may not be zero along the flow path. Evidence for continuation of mass-transfer reactions include geochemical evidence for mineral abundance, evaluation of additional chemical data, isotopic results for minerals and/or dissolved species and from mass-balance modelling of groundwater chemistry. Only when a mineral phase is in chemical equilibrium and there is no mass-transfer along the flow path can a mineral present in the system be considered in equilibrium.

Minerals that reach equilibrium and undergo mass-transfer react *congruently* where dissolution and precipitation of the mineral phase can occur during geochemical reactions. A common congruent geochemical reaction is the dissolution and precipitation of calcite:

$$CaCO_{3\ (calcite)} \rightleftharpoons Ca^{2+} + CO_3^{2-} \qquad (4.29)$$

At low pH values or where the SI is less than zero, ie: in recharge zones, reaction 4.29 proceeds as written and calcite dissolves. As geochemical reactions continue and hydrogen ion (H^+) is consumed during weathering of silicate minerals, the concentration of carbonate ion (CO_3) will increase concurrently with increasing pH and reaction 4.29 reverses and precipitates calcite. In both of these cases, the calculated saturation index of calcite will equal zero. It would be a mistake to think that because the SI = 0 that calcite no longer takes part in geochemical reactions when the mineral phase is dissolving at equilibrium in the first case and precipitating at equilibrium in the second.

Incongruent reactions occur when minerals undergo irreversible mass-transfer reactions along a flow path and do not reach equilibrium. In this case, dissolution of the mineral proceeds in a forward step to products that can undergo additional geochemical reactions.

One example of an incongruent reaction is the dissolution of anorthite and the formation of kaolinite:

$$CaAl_2Si_2O_8\ _{(anorthite)} + H_2O + 2H^+ \rightarrow Al_2SI_2O_5(OH)_4\ _{(kaolinite)} + Ca^{2+} \quad (4.30)$$

Reaction 4.30 can only proceed as written from geochemical reactions in groundwater systems and the SI of anorthite will be a function, not of this reaction, but of other geochemical reactions that are controlling the activity of hydrogen ion, calcium ion and water. We can infer that reaction 4.30 occurs during geochemical evolution of groundwater by petrographic identification of anorthite and kaolinite in aquifer materials in combination with supporting mass-balance modelling. The researcher must consider which of the minerals present in aquifer materials dominate geochemical reactions and which minerals undergo little or no reactions.

Mineral stability diagrams can be used to infer what geochemical conditions are necessary for minerals to coexist at equilibrium or to determine which minerals are stable or unstable in the groundwater system. The interpretation of data with mineral stability diagrams can be misleading due to uncertainties in thermodynamic data for minerals controlling hydrogeochemical reactions. Example V shows the how the basic chemical principles from section 4.5 can be used to construct a mineral stability diagram.

Example V

Geologic investigation showed the minerals oligoclase, montmorillonite and some kaolinite occur in the Tucson basin aquifer [13] in Arizona, USA. The balanced chemical reaction representing the phase boundary between Na-montmorillonite and kaolinite is:

$$3Al_2Si_{3.67}Al_{0.33}O_{10}(OH)_2Na_{0.33} + 11.5H_2O + H^+ \Rightarrow 3.5Al_2Si_2O_5(OH)_4 + 4H_4SiO_4 + Na^+$$

To represent this reaction on the mineral stability for the Na_2O-CaO-SiO_2-H_2O system shown in Figure 2 we must first determine the equilibrium constant for this reaction.

$$K_{sp} = \frac{[Na^+]\ [H_4SiO_4]^4}{[H^+]}$$

The ΔG_f° of Na-montmorillonite is determined using the estimation technique of Tardy and Garrels [14,15]:

Component Moles	G_f Component	kcal/mol
1.65 Al_2O_3	-382.4	-630.96
2.67 SiO_2	-204.6	-546.282
1 H_2O	-59.2	-59.2
0.33 Na_2O	-175.4	-57.882
		Σ= -1284.81 kcal/mol

The gibbs free energy and equilibrium constant of the reaction can be calculated from the stoichiometrically balanced reaction.

ΔG_{rxn}= 19.08 kcal/mol; $K_{sp} = 10^{-13.99}$

The equilibrium of this reaction is represented as a line drawn on Figure 2. Linearization of the equilibrium equation in log form yields the equation of the line separating the stability field of Na-montmorillonite and kaolinite.

$\log K_{sp} = 4 \log [H_4SiO_4] + \log [Na]/[H]$ or
$\log [Na]/[H] = -4 \log [H_4SiO_4] - 13.99$

The line representing the stability of oligoclase is determined using published thermodynamic data [7] as follows:

$$(NaAlSi_3O_8)_4 \bullet CaAl_2Si_2O_8 + 19H_2O + 6H^+ \Rightarrow 3Al_2Si_2O_5(OH)_4 + Ca^{+2} + 4Na^+ + 8H_4SiO_4$$

ΔG_f = -20.6 kcal/mol; $K_{sp} = 10^{+31.55}$
$\log [Na]/[H] = -2\log [H_4SiO_4] + 7.89 - 0.25\log[Ca]/[H]^2$

The equilibrium constants and lines in Figure 2 that represent the stability of the silica phases: amorphous silica (a), chalcedony (c) and quartz (q) are represented by the reaction:

$$SiO_{2\,(a,\,c\ or\ q)} + 2H_2O \rightleftharpoons H_4SiO_4$$

ΔG_f = 3.60 kcal/mol;	$K_{sp} = 10^{-2.64}$	$\log [H_4SiO_4] = -2.64$
ΔG_f = 4.57 kcal/mol;	$K_{sp} = 10^{-3.35}$	$\log [H_4SiO_4] = -3.35$
ΔG_f = 5.59 kcal/mol;	$K_{sp} = 10^{-4.01}$	$\log [H_4SiO_4] = -4.01$

Similar calculations were made to create the mineral stability diagram for the CaO-Na_2O-SiO_2-CO_2-H_2O system shown as Figure 3 with the addition of two lines that represent equilibrium of calcite:

$$CaCO_3 + 2H^+ \rightleftharpoons Ca^{2+} + CO_2 + H_2O$$

$\log [Ca]/[H]^2 = 11.35$ at $[CO2] = 10^{-1.5}$ $\log [Ca]/[H]^2 = 12.84$ at $[CO_2] = 10^{-3.0}$

The activity of groundwater samples collected from the Tucson basin aquifer [13] are plotted on Figures 2 and 3. The interpretation of these diagrams is potentially misleading unless they are considered together and possibly with other mineral stability diagrams that include $[K^+]$ and $[Mg^{2+}]$. When plotted on Figure 2, Tucson basin groundwater plots within the montmorillonite stability field constrained by the solubility of the silica phase chalcedony. One inference from this figure could be that chalcedony is a controlling mineral phase. However, from petrographic and x-ray investigation show that it is not a dominant mineral in the aquifer material. We also know that on the time scales of most groundwater flow, silica phases are very slow to react .

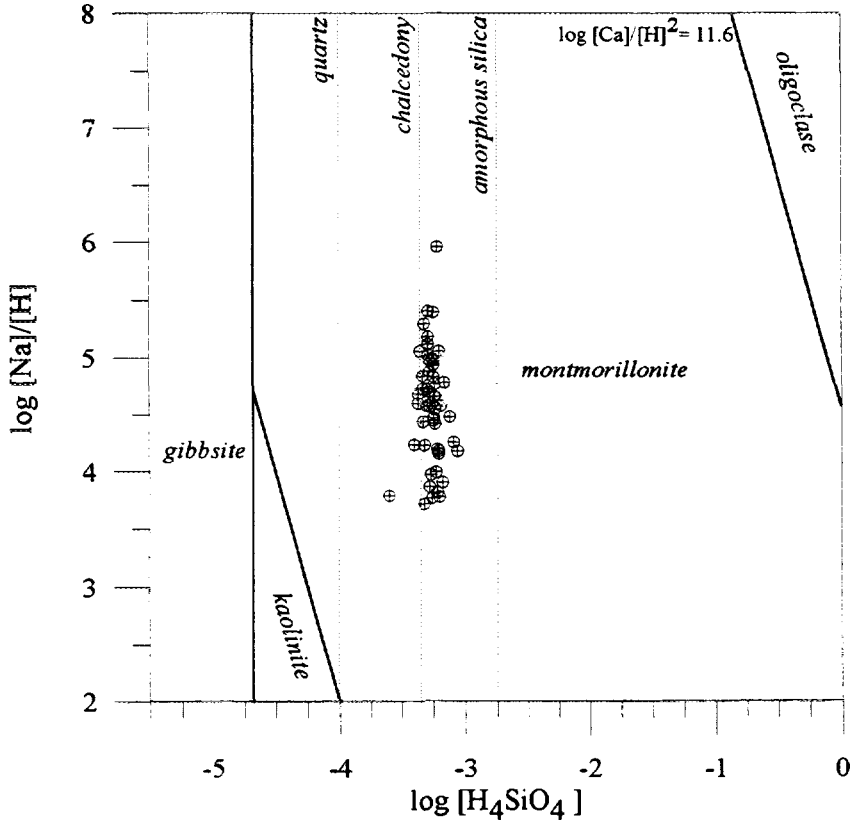

Figure 2. Mineral stability diagram representing thermodynamic constraints on sodium, hydrogen and silica activities for equilibrium reactions between oligoclase, montmorillonite, kaolinite and gibbsite.

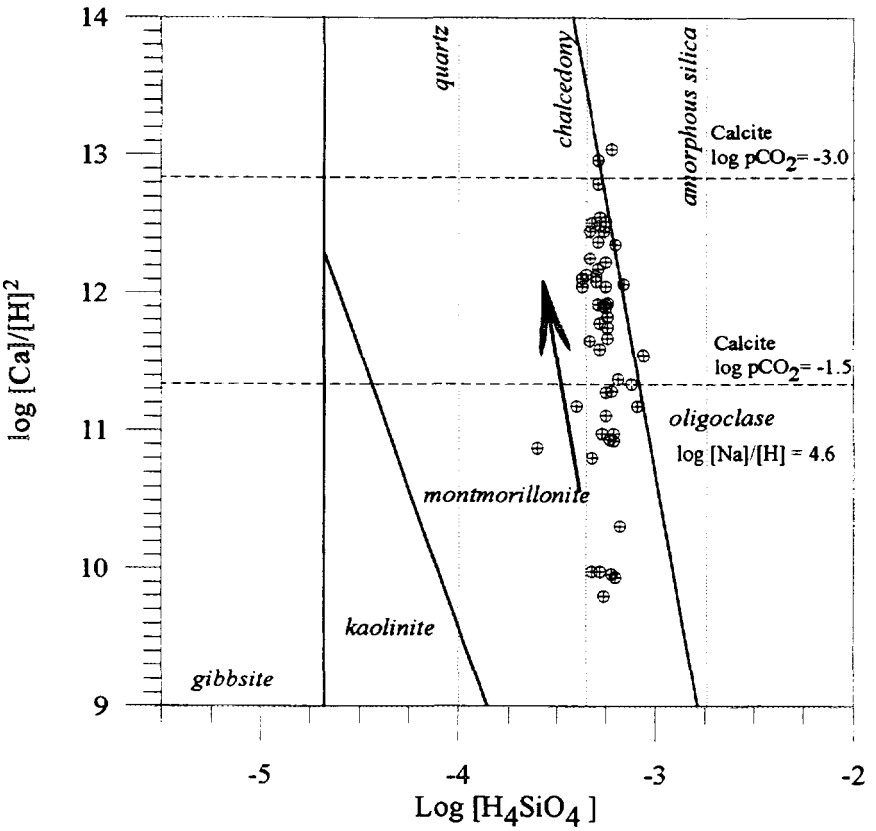

Figure 3. Mineral stability diagram representing thermodynamic constraints on calcium, hydrogen and silica activities for equilibrium reactions between oligoclase, montmorillonite, kaolinite and gibbsite.

Reexamination of the same data plotted on Figure 3 shows there is a trend in the chemistry data along the flow path (arrow shows direction of down gradient geochemical evolution). Interpretation of Figure 3 suggests geochemical evolution of the Tucson basin groundwater is controlled by the incongruent dissolution of oligoclase to montmorillonite, not by chalcedony. The data plot along the plagioclase-montmorillonite phase boundary in Figure 3. The recharge water incongruently reacts with plagioclase precipitating montmorillonite. Down gradient waters plot along a trend upward (arrow Figure 3) as geochemical reactions continue under closed conditions when pCO_2 is consumed as a source of hydrogen ion and the groundwater reaches an apparent equilibrium with the mineral calcite. To verify this inference, mass-balance and mass-transfer modelling of these groundwater samples must support this assumption without violating any mineral phase boundaries.

4.7 Chemical speciation modelling

The previous sections of this chapter have shown that much of geochemical modelling is conceptually based, dependent on our understanding of chemical processes. To assist this process, computer codes are available that perform complex chemical and mass-balance calculations. Chemical speciation models are based on the concept of ion pairs and equilibrium chemistry presented in section 4.5. Our interpretation of results when using these models relies on the accuracy and reliability of thermodynamic data and analytical results for groundwater chemistry.

The data required for chemical speciation modelling of groundwater are the concentrations of the major elements in solution (field determination of alkalinity is needed for accurate calculation of pCO_2), the concentration of any minor or trace elements in solution that are of interest to the study, accurate pH and temperature (at time of collection), Eh and/or dissolved O_2 (if oxidation state of groundwater and metals is of interest), and relevant thermodynamic data. A guide to reliable chemical data for each groundwater sample is the *charge imbalance* calculation (equation 4.31).

In general, the charge imbalance for good analytical data is within 1 percent. The use of chemical data for geochemical modelling of groundwater having a charge imbalance of more than 5 percent can propagate errors and should be considered carefully.

$$\%charge\,imbalance = \frac{\sum_{i=1}^{I} (M_i, Z_i)_{cations} - \sum_{i=1}^{I} (M_i, Z_i)_{anions}}{\sum_{i=1}^{I} (M_i, Z_i)_{cations} + \sum_{i=1}^{I} (M_i, Z_i)_{anions}} * 100 \qquad (4.31)$$

Assessing the validity of thermodynamic data used in a chemical speciation model can be difficult. Many of the codes listed in Table IV were developed to solve a specific class of problems in aqueous geochemistry. Users of these codes

should consider the valid application of each model and the source of thermodynamic data used by the model.

It is acceptable to supplement or change thermodynamic data for a given model if the use carefully evaluates calculated saturation constants (from the literature or laboratory studies). The user of chemical speciation models should consider adding minerals or species that are of interest for each groundwater system to the thermodynamic data base.

For example, if the mineral fluorphlogopite ($KMg_3(AlSI_3O_{10})F_2$ is present in a hydrostratographic unit of interest and high fluoride concentrations have been measured in groundwater and are suspected to have resulted from the decomposition of this mineral, the solubility constant (K_{sp}) can be calculated from the ΔG_f° (-1461.63 kcal/mol) [15]. This thermodynamic data can be added in the format specified by the model and used to calculate the saturation index of fluorphlogopite for all groundwater samples that have total chemical analyses including [K], [Mg], [Al], [Si] and [F].

Ongoing efforts to question the reliability of thermodynamic data and to add new species of interest to geochemical models will reduce internal inconsistencies between mineral-water equilibrium constants and observed groundwater geochemical systems.

Mass balance for each element, charge balance for the solution and equilibrium expressions for complex ion pairs are used to constrain the speciation of ions in solution. The mass balance expression is used to balance the analytical concentration of an element with the distribution of the element between ion pairs in solution.

$$(m_I)_t = \sum_{I}^{I} (m_i)_{ion\ pairs} \qquad (4.32)$$

where I is the total number of species in solution, m_i is the molality of each species or ion pair that contains element m in solution, and $(m_I)_t$ is the total analytical concentration.

The charge balance equation requires that the sum of the charges for all positive and negative species in solution combine to zero [16].

$$\sum_{i=1}^{I} (m_i, z_i)_{cations} = \sum_{i=1}^{I} (m_i, z_i)_{anions} \qquad (4.33)$$

For equation 4.33, include all ions of elements m in solution where z_i is the charge on the ion or ion pair in solution. Let us again consider the system including CO_2, NaCl and H_2O. The mass balance expressions used to determine the total carbon, sodium and chloride in solution are:

$$m_{C_T} = m_{H_2CO_3^\circ} + m_{HCO_3^-} + m_{CO_3^{2-}} + m_{NaHCO_3^\circ} + m_{NaCO_3^-} \quad (4.34)$$

$$m_{Na_T} = m_{Na^+} + m_{NaHCO_3^\circ} + m_{NaCO_3^-} + m_{NaCl^\circ} \quad (4.35)$$

$$m_{Cl_T} = m_{Cl^-} + m_{NaCl^\circ} + m_{HCL^\circ} \quad (4.36)$$

The charge balance equation (4.33) would balance all of the positive and negative charges from equations 4.34, 4.35 and 4.36. This system of equations is used to determine the activity of a master species for each element and solves for the distribution of complex ions in solution using mass action expressions and the known thermodynamic data for ion association equilibrium expressions.

Computers are ideal to handle the repetitive iterations required to converge on a solution for speciation modelling and resulting in calculation of concentration and activity for each species and ion pair in solution, calculation of the partial pressure of gas phases and the saturation indices of mineral phases.

Oxidation-reduction reactions may also be of interest when studying geochemical water-rock reactions. The dissolution of reduced minerals, eg: iron sulphide, often occurs through reactions with dissolved oxygen. The stability of many trace elements in groundwater is dependent on the oxidation potential of the water. These include distribution of sulphur between hydrogen sulphide and sulphate, the speciation of nitrogen between the reduced and various oxidized states and the oxidation of dissolved organic carbon (DOC).

Dissolved organic matter (DOM) can be derived from naturally occurring organic matter in aquifer materials, DOC in recharge water, organic matter washed into karstic systems or from waste disposal and mining activities. The oxidation of organic matter may deplete dissolved oxygen down gradient.

Some trace metals are much more toxic in the reduced state than in oxidized states, eg: Cr^{6+} is much more toxic than other more oxidized states. To provide insight into the redox chemistry of groundwater and the presence and oxidation state of metals in a groundwater system, we can apply the same approach of equilibrium modelling.

We can write a balanced oxidation-reduction reaction between element A and electrons.

$$A_{oxidized} + ne^- = A_{reduced} \quad (4.37)$$

Given equation 4.37 we can calculated the Gibbs free energy, ΔG_r°, and the equilibrium constant for the reaction.

$$K_{redox} = \frac{[A_{reduced}]}{[A_{oxidized}]\,[e^-]^n} \quad (4.38)$$

The activity of the electron is easily measured in a groundwater system or can be estimated from the concentration of dissolved oxygen. Therefore, equation 4.38 is usually expressed as a function of the activity of the electron.

$$pe = -Log[e^-] = \frac{1}{n}\left[LogK - Log\frac{[A_{reduced}]}{[A_{oxidized}]}\right] \quad (4.39)$$

and:

$$Eh = \frac{2.303RT}{\mathcal{F}} \frac{1}{n} \left[LogK - Log \frac{[A_{reduced}]}{[A_{oxidized}]} \right] \qquad (4.40)$$

where $\mathcal{F}$ is the Faraday constant. Eh is generally measured in volts and pe is a dimensionless value like pH. If study of trace metal geochemistry is important for a given groundwater system, it is important to measure the Eh and dissolved oxygen during sampling in the field.

Balance oxidation-reduction reactions are by convention written to represent the transfer of only one electron to simplify electron balance calculations. A detailed discussion of electrochemical reactions and associated phase diagrams is beyond the scope of this chapter, but a detailed discussion can be found in a number of the suggested readings.

The redox state of the groundwater can be used to balance electron transfer in mass-transfer models. Geochemical modelling and isotope hydrology can offer insight into chemical reactions for groundwater systems that undergo redox reactions (ie: methanogenisis, oxidation of dissolved organic matter, oxidation of sulphides).

Redox state is defined by Plummer et al. [17] as:

$$RS = \sum_{i=1}^{I} (v_i, m_i) \qquad (4.41)$$

where v_i is the operation valence of species m_i. To use mass balance models to determine the transfer of electrons in a groundwater system, accurate measurements of oxidized and reduced species are needed, ie: for balancing sulphide oxidation reactions measurement of H_2S, HS^-, SO_4^{2-}, pH, Eh and O_2 are needed in addition to the normal chemical analysis. The concentration of dissolved organic matter should also be measured when electrochemical reactions are of interest. It is more difficult to accurately define balanced electrochemical reactions due to uncertainties in thermodynamic data and measurement errors.

Propagation of errors, including those in analytical data, thermodynamic data and computation add to uncertainty in the computed saturation indices for mineral phases. It is important for those using geochemical models to evaluate these uncertainties and how they affect the interpretation of water-mineral reactions in groundwater systems.

Uncertainty in the calculated SI will vary between mineral phases depending on analytical data and thermodynamic data. For instance, uncertainties in the calculated saturation index of calcite depend on errors in calculating the activity of calcium ion, carbonate ion and the K_{sp} of calcite. Given good analytical data, this uncertainty is generally better than ± 0.1. The SI of dolomite ($CaMg(CO_3)_2$) includes additional uncertainties in calculating the activity of magnesium. The SI of siderite ($FeCO_3$) includes uncertainty in the activity of Fe^{2+} including the distribution of iron species between oxidation states calculated from Eh or dissolved O_2 when ferric ion is not specifically measured.

For complex alumina-silicate minerals the propagation of errors can increase uncertainty in the calculated saturation index to more than $\pm$ 0.5. Uncertainty in the calculated saturation index for complex silicate minerals could potentially result in unreliable results. It is important to critically examine these questions to reduce potential over-interpretation of chemical speciation results.

4.8 Mass balance - mass transfer

The inverse modelling technique uses mass balance calculations to ascertain the amount of mineral phases dissolving or precipitating along a defined flow path between the representative recharge well and each down gradient well. At this step we combine the conceptual model of water-mineral reactions with the measured chemical composition of mineral phases, and the concentration of dissolved elements in initial groundwater (recharge source) and final groundwater (down gradient well). This method is based on the conservation of mass and electrons during geochemical evolution of groundwater and was represented by Plummer *et al.* [17] with the equations:

$$\sum_{p=1}^{P} \alpha_p b_{p,k} = \prod_{k=1}^{K} \Delta m_{t,k} \qquad (4.42)$$

$$\sum_{i=1}^{I} v_i m_{i_{final}} - \sum_{i=1}^{I} v_i m_{i_{initial}} = \Delta RS \qquad (4.43)$$

Equation 4.42 represents a reaction where the net moles of each element entering or leaving the solution through processes of dissolution, precipitation, biological activity, gas transfer or isotopic exchange is summed for all mineral phases, P, where α_p is the mass transfer coefficient representing the number of moles of p^{th} mineral phase dissolving (positive) or precipitating (negative) from the solution; $b_{p,k}$ is the stoichiometric coefficient of the k^{th} element in the p^{th} mineral phase; $\Delta m_{t,k}$ is the total change in mass (final water minus initial water) of the k^{th} element in solution. Mass balance of the electron is calculated from the change in redox state from between initial and final waters.

The solution of the mass balance equation defines a balanced chemical reaction and the change in mass for each mineral phase:

$$Groundwater_{initial} + primary\ minerals \rightarrow Groundwater_{final} + secondary\ minerals$$

There may not be a unique solution for this balanced chemical reaction. In this case, we must combine the results of mass balance calculations with the results of chemical speciation modelling, mineralogic investigation, and our conceptual understanding of groundwater flow and geochemical evolution to identify solutions that are inconsistent.

Results from mass balance calculations are not constrained by thermodynamics and thus can result in thermodynamically invalid mass transfer. The saturation state of a mineral gives us an indication of the thermodynamic

potential for dissolution or precipitation and we would expect the mass balance results to be consistent with the saturation index. A given mass balance result would be suspect if the solution predicts precipitation of a mineral phase between the initial and final samples, yet the saturation index indicates that both groundwater samples are undersaturated with respect to the same mineral phase. Interpretation of the saturation index of various minerals calculated for groundwater in the Tucson basin system is described in the following example.

Example VI

The conceptual model of geochemical evolution of groundwater in the Tucson basin [13] begins with water-rock interactions in the recharge zones that are driven by high pCO_2 values. The CO_2 is a source of hydrogen ions for incongruent weathering reactions of primary silicate minerals and the dissolution of carbonate phases. As groundwater flows down gradient, the system is closed to CO_2 and the calculated pCO_2 should decline as carbon dioxide is consumed as a source of hydrogen ion for silicate weathering. Reactions with ubiquitous calcite should results in down gradient water in apparent equilibrium with carbonate phases.

Figures 4 and 5 show the change in pCO_2 and the saturation index of calcite as a function of distance from recharge down gradient. The results of mass balance modelling should be consistent with thermodynamic constraints on CO_2 (dissolution) and calcite. From Figure 5 it is not possible to predict if mass transfer (precipitation or dissolution) of calcite continues after the groundwater has reached saturation, but mass transfer can be predicted with mass balance results. Note error bars were calculated for the saturation index for each sample.

Figures 6 and 7 show the saturation index for selected silicate minerals as a function of distance from recharge zone. The SI for silicate minerals have greater uncertainty due to compounding of analytical errors.

The saturation index of chalcedony is essentially constant down gradient suggesting an apparent equilibrium of this mineral phase, and geochemical reactions in the Tucson basin probably do not include chalcedony. Results of mass balance modelling should not predict dissolution or precipitation of chalcedony (SiO_2) during geochemical evolution of groundwater.

The saturation index of plagioclase is highly variable and shows a general trend toward equilibrium along the flow path. Plagioclase is undersaturated everywhere in the Tucson basin and mass balance reactions should only predict dissolution of plagioclase.

Both mineral phases kaolinite and montmorillonite are over saturated along the flow path and show declining trends toward equilibrium from recharge to down gradient wells. Kaolinite and montmorillonite were found during petrographic and XRD investigation of aquifer materials and were suspected products of the incongruent weathering of orthoclase and plagioclase respectively. Results of mass balance calculations should predict the precipitation of clay mineral phases during reaction path modelling.

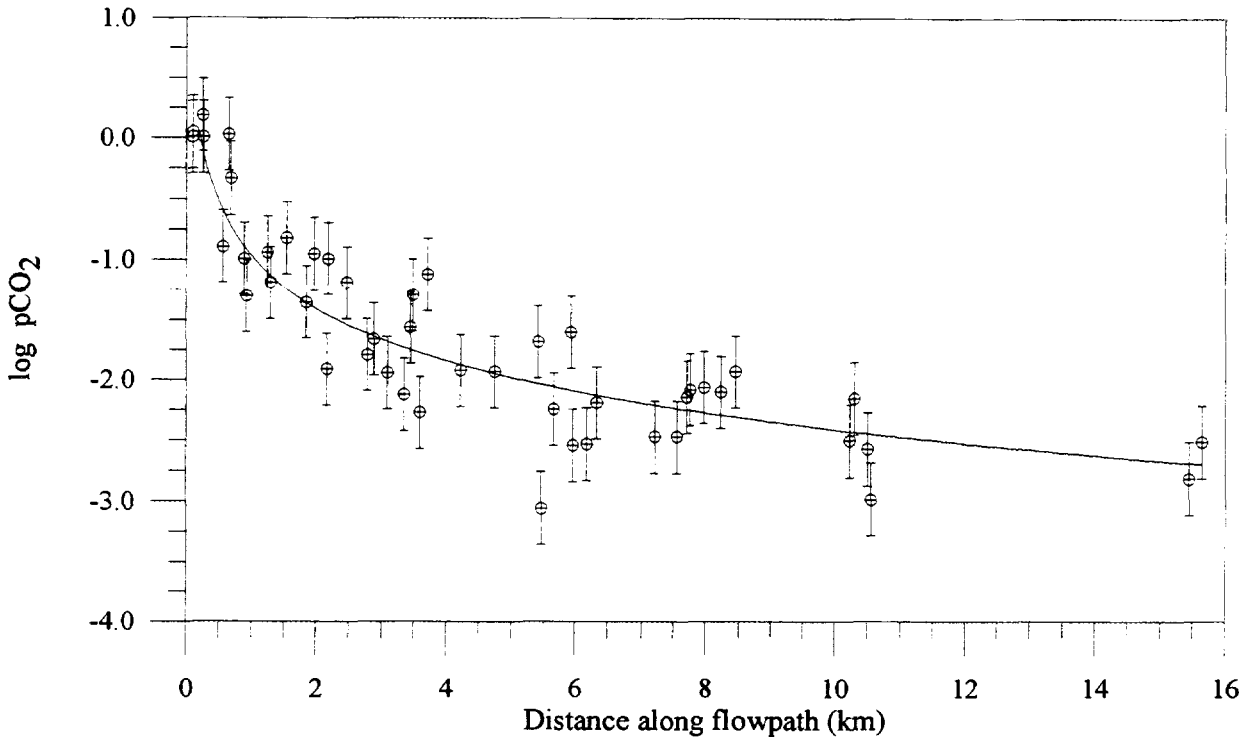

Figure 4. Calculated partial pressure of carbon dioxide for Tucson basin groundwater as a function of distance from recharge source.

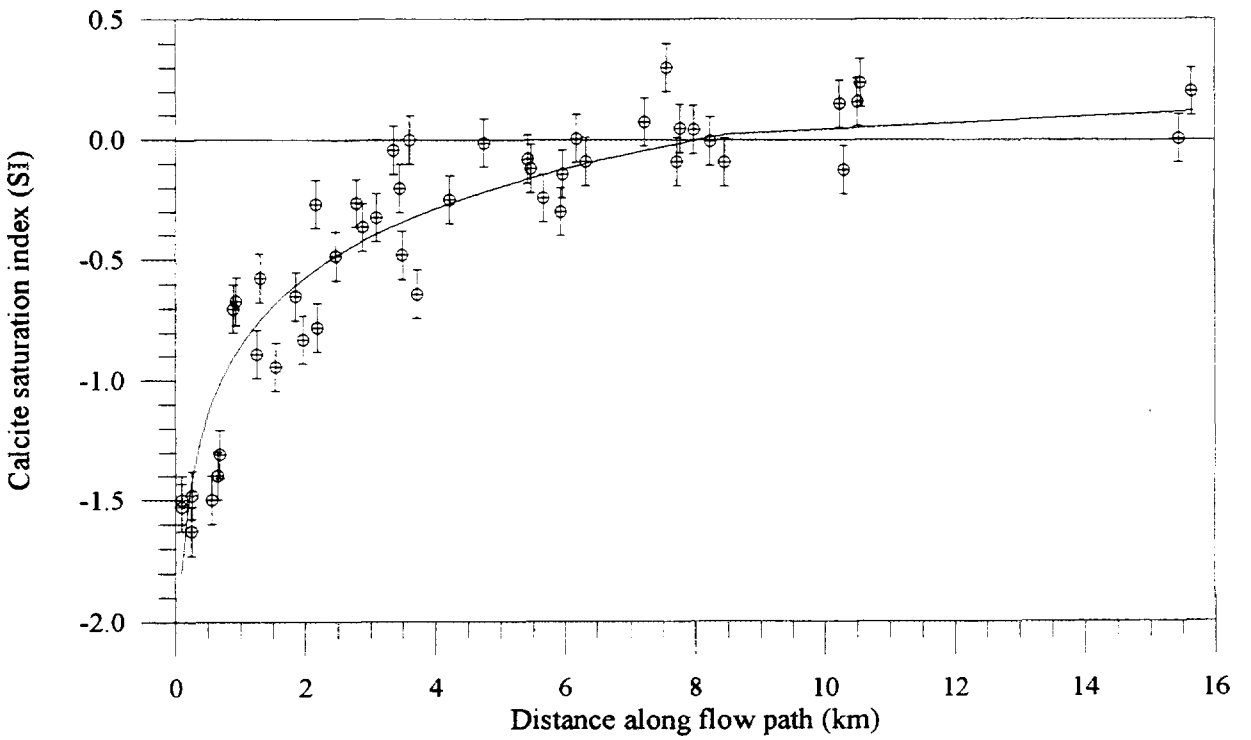

Figure 5. Calculated saturation index of calcite for groundwater in the Tucson basin as a function of distance from recharge source.

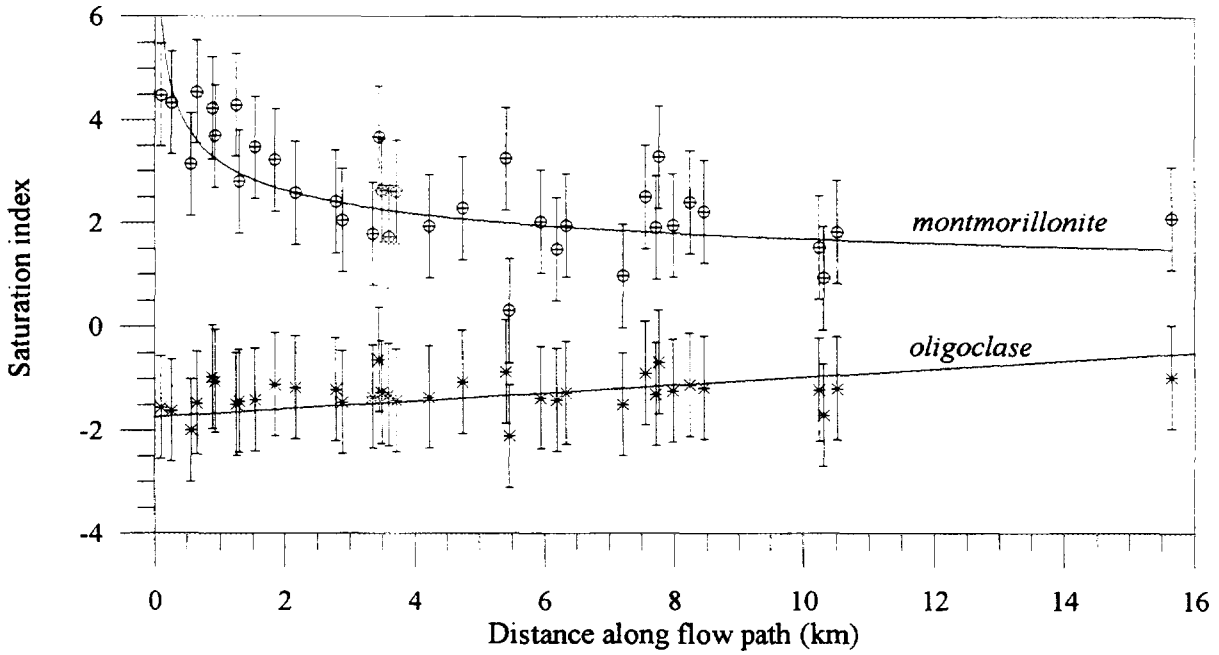

Figure 6. Calculated saturation index of oligoclase and montmorillonite for groundwater in the Tucson basin as a function of distance from recharge source.

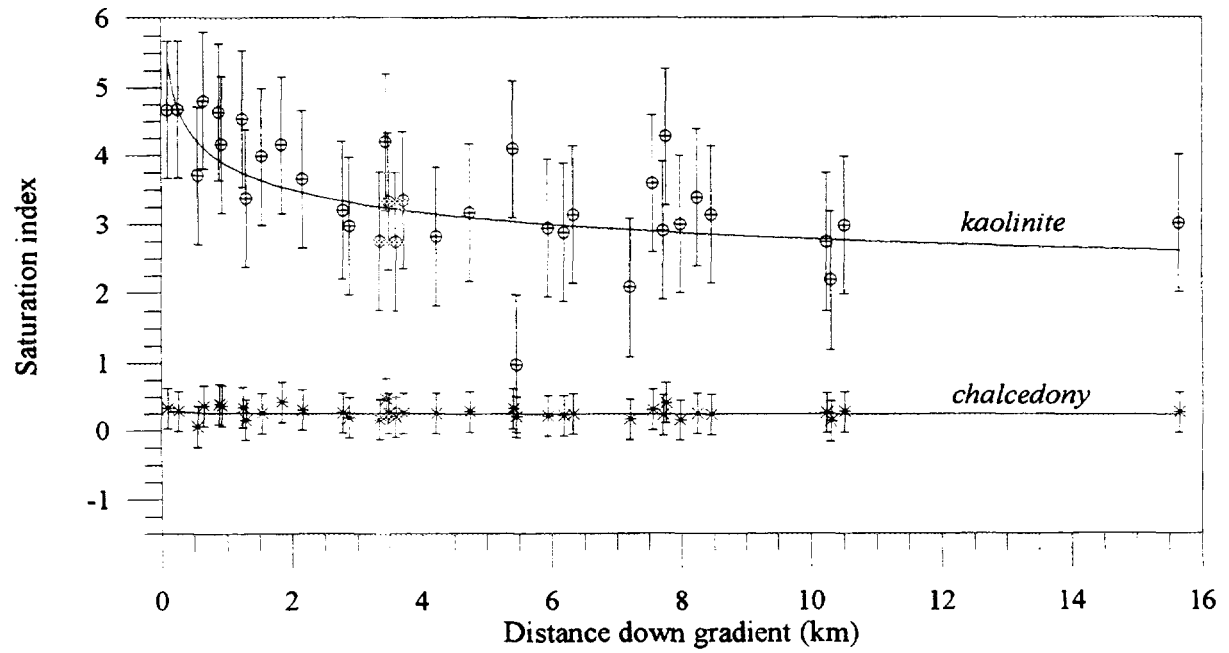

Figure 7. Calculated saturation index of kaolinite and chalcedony for groundwater in the Tucson basin as a function of distance from recharge source.

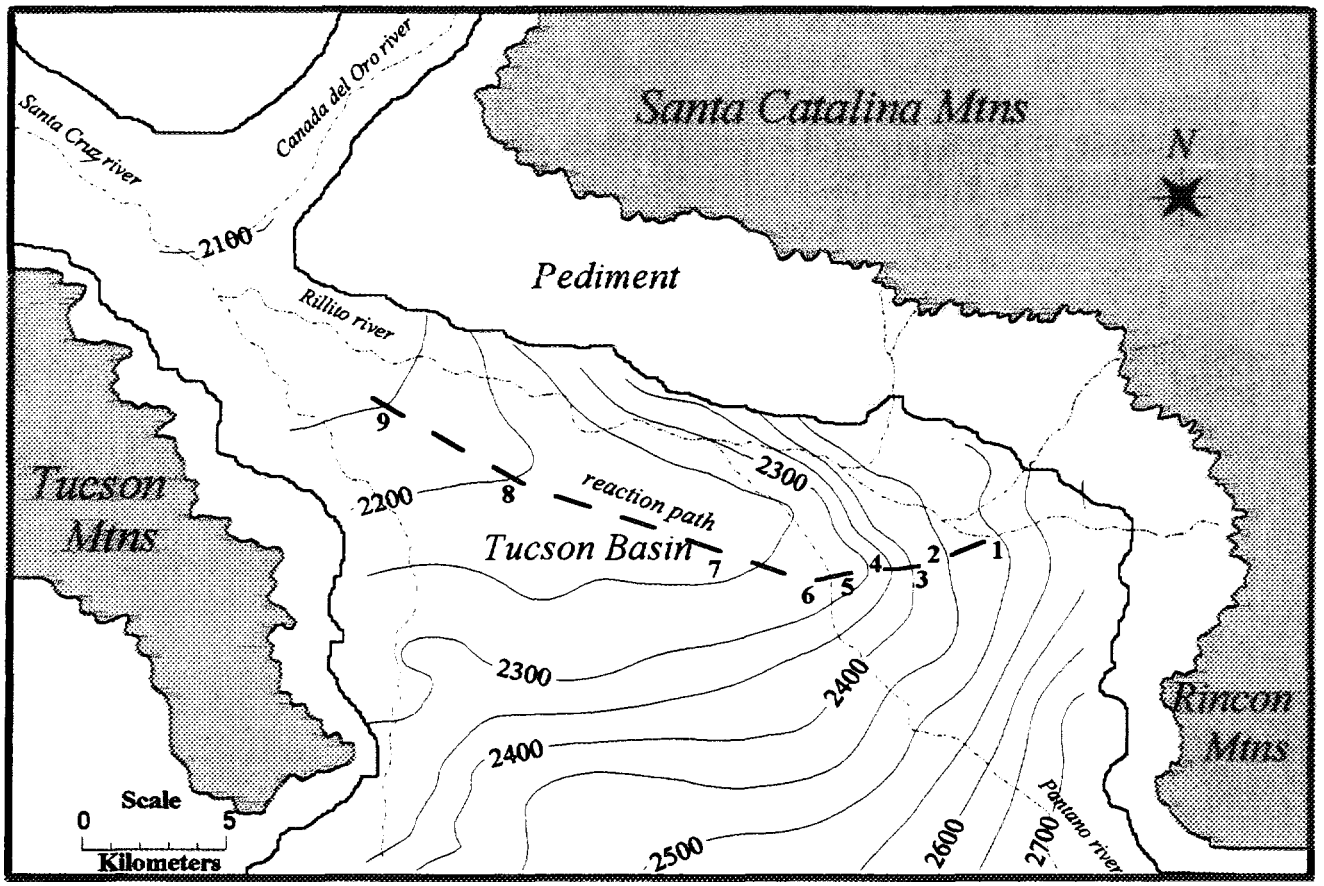

Figure 8. Location of 9 groundwater samples that are hydrologically related along the same flow path as defined by the piezometric surface of groundwater in Tucson basin aquifer (1988).

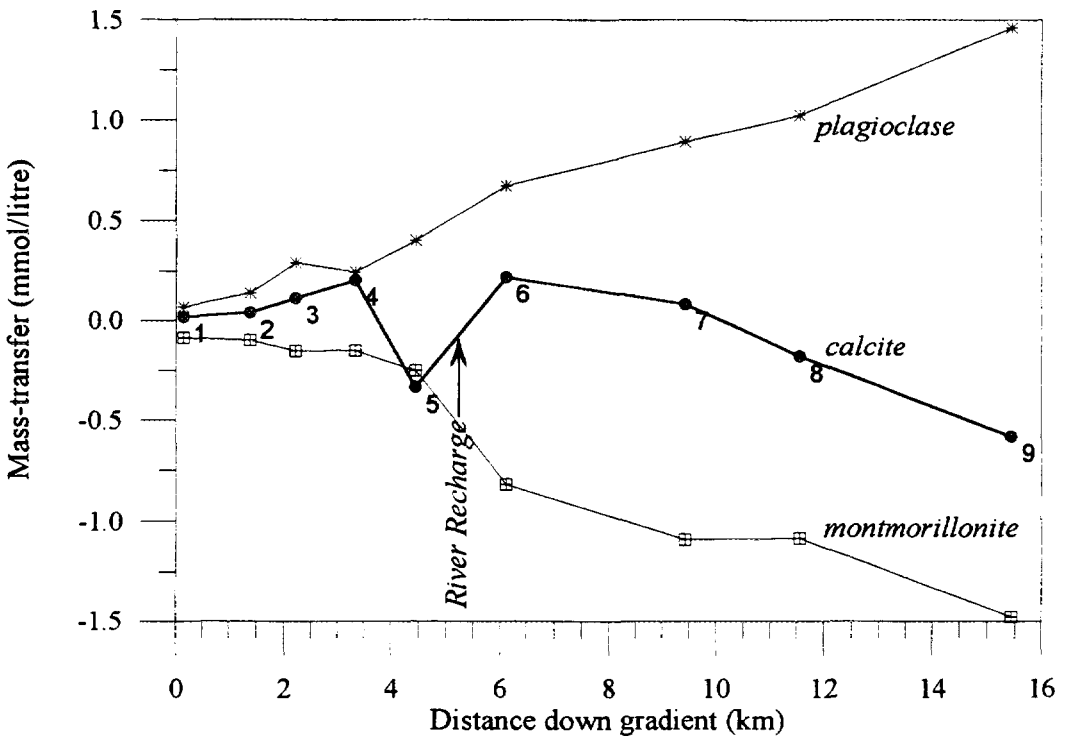

Figure 9. Calculated mass transfer of calcite, oligoclase and montmorillonite along the reaction path defined in Figure 8.

Petrographic and XRF/XRD identification of secondary mineral phases are used to confirm mass balance results that suggest precipitation of minerals (ie: the presence of secondary calcite is evidence of calcite precipitation). We expect that mass transfer will continue in the same direction along the flow path unless there is a change in the hydrology (ie: additional recharge or discharge) or a change in controlling geochemical conditions (ie: moving from open to closed conditions). In these cases, mass transfer may change sign as geochemical evolution of groundwater continues. Some mineral phases will dissolve near the recharge source and, due to subsequent geochemical reactions, will precipitate further down gradient. Again, evaluation of the saturation index will confirm the potential for this behaviour. Inconsistent results may occur when the initial and final groundwater samples are not hydrologically related along the same flow path. It is important to critically review the hydrologic controls for initial and final groundwater samples used for mass transfer calculations. The following example shows how mass transfer results confirm our understanding of the geochemical processes dominating a groundwater system.

Example VII.

Here we will examine how geohydrology affects the calculated mass transfer along one flow path in the Tucson basin [13]. The potentiometric surface of groundwater was determined from water elevations measurements (Figure 8). Nine wells that are hydrologically related were chosen to define a reaction path the followed from recharge in the eastern basin to discharge in the north-central basin. The chemistry of these waters were analyzed with chemical speciation modelling. The results of geologic investigation were used to determine the controlling geochemical water-rock reactions [13].

The calculated mass transfer (Figure 9) shows the incongruent dissolution of plagioclase to montmorillonite continues along the flow path. This result confirmed our hypothesized interpretation of mineral stability diagrams and calculated change in saturation index. The mass transfer of calcite varies from; dissolution - precipitation - dissolution - precipitation. The interpretation of the calculated mass transfer of calcite is initially problematic because the saturation index for down gradient water suggests equilibrium with calcite.

This flow path is an example of how mass transfer of calcite occurs as both dissolution and precipitation at equilibrium. Initially, calcite dissolves as a result of geochemical reactions in the recharge zone and approaches equilibrium (Figure 8,9 point 1). Once under closed geochemical conditions, pCO_2 is consumed as weathering of plagioclase continues (points 2-5). The subsequent rise in pH increases the activity of $[CO_3^{2-}]$ and calcite precipitates under equilibrium conditions.

Recharge from the Pantano river in the east-central basin brings in aggressive, undersaturated water and the geochemical system is again open to pCO_2 (point 6). At this point calcite dissolution occurs at equilibrium. Finally, silicate weathering again forces the precipitation of calcite as closed geochemical conditions prevail down gradient (points 7-9). Isotopic validation of this hypothetical set of reactions is one way to assure us they are valid.

In regional groundwater systems, large jumps or changes in mass balance calculations are unusual and may signify either misinterpretation of the relationship between initial and final groundwater samples, or possibly important unknown hydrologic or geologic changes (ie: introduction of contaminants or change in lithology).

If detailed study of an aquifer is required, the density of sampling points used in mass balance calculations can be increased. When increasing sampling density, the calculated mass transfer can more closely relate to actual mass transfer in the aquifer, but the affects of aquifer heterogeneity and the screened sampling interval become more important. At large scales, hydrodynamic dispersion along a flow path between widely spaced sampling points is incorporated in the results of mass balance calculations. But for closely spaced sampling points, separation of dispersive and reactive controls on groundwater chemistry are not possible.

Mineral stability diagrams and chemical speciation can be used to infer thermodynamic control of water-rock reactions in the absence of forward modelling. However, when possible, the forward solution can be used to compute changes in distribution of species in response to changes in the chemical composition of water, temperature and pressure, mineral dissolution or precipitation and irreversible reactions. The geochemical models PHREEQE [18] and EQ3/6 [19] are two of the commonly used forward models. The use of the model PHREEQE is discussed in depth by Plummer *et. al* [17]. Application of forward modelling requires, from the user, a solid background in geochemistry of groundwaters and a good understanding of water-rock chemical reactions.

Forward modelling is constrained by the thermodynamics of water-rock chemical reactions and can be used to validate the results of mass balance calculations and eliminate solutions that violate thermodynamic constraints of water-rock geochemical reactions. Forward modelling is not required to confirm geochemical evolution of groundwater, but is another tool for interpretation and validation of mass balance results.

Each of the plausible results from mass balance calculations can be checked with forward modelling. If, after forward modelling, the number of plausible models is reduced to one then a unique solution has been found that defines geochemical evolution of the groundwater, but this is often not the case. To find a unique solution for the geochemical evolution of a groundwater system new information, such as isotopic data, should be used to reduce the number of plausible reactions.

4.9 Isotopic validation of geochemical modelling

Isotopic data is potentially a key component for interpretation of geochemical reactions occurring in groundwater systems. The isotopic composition of various elements contains a record of the initial isotopic composition of water during recharge and of subsequent chemical reactions or mixing that occurred down gradient. Isotopic results are independent of the process of speciation modelling and mass balance calculations and therefore, it can provide a valuable check on the

computed mass transfer. Isotopically balanced reactions are easily combined with balanced chemical reactions, and are used to compare the isotopic composition of elements measured in the final water with calculated values.

$$Ca^{\frac{13}{12}}CO_3 + {}^{\frac{13}{12}}CO_2 + H_2O \rightleftharpoons Ca^{2+} + 2H^{\frac{13}{12}}CO_3^- \qquad (4.44)$$

Equation 4.44 represents the dissolution of carbon dioxide and calcite in a groundwater system. The carbon isotopic composition *must be known for each phase* if it is to be used to validate the stoichiometric mass balance of equation 4.44. The confidence we apply to the results of isotopic mass balance is related to confidence in the measured values. Extrapolating equation 4.44 to include all carbon phases that take part in a balanced geochemical equation might include some or all of the following; CO_2, $CaCO_3$, $CaMg(CO_3)_2$, CH_4, HCO_3^-, $FeCO_3$ and DOC. Only when the isotopic composition of all these species is known can an accurate mass balance of the stable isotopes of carbon be realized.

It is important to recognize which phases have significantly affect on the final isotopic composition of water, and which phases have secondary affects. Many geochemical study have assumed isotopic values for one or more of the controlling phases, thus introducing errors in the final result. The geochemical modeller must consider which species are dominating the geochemical evolution of a given groundwater system and measure the isotopic composition of each. This involves measurements to insure that spatial variation in the isotopic composition along the flow path are accounted for.

There are a large number of isotopes that indicate hydrogeochemical information such as mineral dissolution, recharge sources, mixing of waters, hydrostratographic facies, temporal movement of water and contamination from anthropogenic sources. Isotopes that can be used to validate mass balance reactions include: $^{13/12}C$, $^{14/12}C$, $^{15/14}N$, $^{18/16}O$ $_{(H2O\ and\ SO4)}$, $^{2/1}H$, ^{3}H, $^{4/3}He$, $^{34/32}S$, $^{37/35}Cl$, ^{36}Cl, $^{6/7}Li$, and $^{87/86}Sr$.

When choosing which elements to use for isotopic study and validation of mass balance, it is important to first consider the potential information that each isotope might provide and how the results of the isotopic measurement will be used to constrain the mass balance reaction. For instance, $^{18/16}O$ of water is useful for determining the source of recharge and can be used to calculate a mixing ratio between two sources of water, but if the isotopic difference between the two sources approaches the errors in measurement, it is then meaningless to spend time and resources on these measurements.

$$R_{MB} = \frac{I_{e1} - I_{e2}}{\sqrt{\sigma_{e1}^2 + \sigma_{e2}^2}} \qquad (4.45)$$

R_{MB} is the resolution of mass balance calculated from the difference between two end member isotopic measurements, I_{e1} and I_{e2} having errors of σ_{e1} and σ_{e2} respectively. A few initial measurements can determine the worth of applying isotopic data for validation of mass balance.

Table IX. Resolution of mass balance for hypothetical isotopic measurements. Error and difference in isotopic ratio affect the resolution of potential mass balance and mixing calculations.

Isotope	End member 1	End member 2	Resolution of mass balance	
$\delta^{34}S$	-14.0 ± 0.2	+14.0 ± 0.2	1:100 (1σ)	1:50 (2σ)
^{3}H	< 1.0	40±0.5	1:80 (1σ)	1:40 (2σ)
$\delta^{15}N$	+3.0±0.2	+8.0±0.2	1:25 (1σ)	1:12.5 (2σ)
$\delta^{37}Cl$	+1.0±0.1	-1.0±0.1	1:20 (1σ)	1:10 (2σ)

Uncertainty in the initial isotopic composition of each phase ultimately accounts for much of the error assigned to results of isotope mass balance validation of geochemical reactions. Uncertainties of various carbon species in the carbonate system can have a large affect on the mass balance corrected radiocarbon age of groundwater. We can examine uncertainties in mass balance and isotope balance modelling by studying the affect of uncertainty on our calculations.

The equation that describes the isotopic balance of carbon based on the mass balance of carbon species entering or leaving the groundwater system as a result of geochemical reactions (after Wigley *et al.* [20]) is:

$$d(R_2 C_{tot}) = \sum_{i=1}^{N} d(R_{E_i} C_{E_i}) - \sum_{j=1}^{M} d(R_{L_j} C_{L_j}) \qquad (4.46)$$

where C_{tot} is the total dissolved carbonate in the groundwater; R is the isotopic ratio of dissolved carbon (S), the carbon entering the groundwater (E_i) from phase i, and leaving the groundwater (L_j) to phase j; C_{ei} is carbon entering the groundwater from source i, and C_{Lj} is carbon leaving the groundwater to phase j. The solution of equation 4.46 is derived from results of mass balance calculations and isotopic measurements. This solution does not include uncertainty in the data. Example VIII shows how this uncertainty can affect the modelled radiocarbon age of groundwater.

Example VIII.

The data in Table X was collected for study of the spatial variation in isotopic composition of carbon dioxide in recharge zones for a number of groundwater systems in Arizona [13,21]. Results of geochemistry and isotope hydrology were used to determine mass transfer and age dating of groundwater in the Tucson basin as part of collaborative research with the USGS and the IAEA Coordinated research programme on mathematical models and their applications to isotope studies in groundwater hydrology.

The measured isotopic composition of soil carbon dioxide is required to fix the initial carbon isotopic composition of CO_2 dissolving in groundwater at recharge. This value influences the initial carbon isotopic composition of groundwater to be used to solve the isotope mass balance of chemical reactions and for correction of radiocarbon age determination.

The variance of real data is much greater than analytical error. Pearson [22] addressed this problem by examining the affect of measurement errors, both chemical and isotopic, to the solution of equation 4.46. If the variance of the initial carbon isotopic composition is applied to equation 4.46, we can identify how uncertainty will affect mass balance results.

Monte-Carlo simulation of the variance in measured stable isotopic composition of initial sources of carbon has been applied to the mass balance result for Tucson basin Well A-3. Even though there appeared to be a unique solution for the result of mass balance calculations, we find that when uncertainty in the data is added, there is no longer a unique solution. The corrected radiocarbon age of groundwater no longer has a single value but a distribution (Figure 10) of corrected ages. Therefore, the geochemical modeller should balance the results of modelling with knowledge of uncertainties in data.

Table X. Soil CO_2 samples from recharge zones of Arizona groundwater systems [21].

Site Name	Winter $\delta^{13}C$ (‰)	Summer $\delta^{13}C$ (‰)
Stone Cabin*	-20.1/-20.1	-19.7
Sol Rhea*	-21.1/-21.0	-19.4
Sheep Canyon	-19.3	-18.4
Camp Mohave	-22.5	-22.7
Miller's		-21.1
Huachuca Spring*	-22.0/-21.8	-21.0
McClure's	-20.0	-21.4
Dragoon	-20.4	-19.3
South Pass	-17.0	-17.5
Road Cut		-21.3
Tule*	-20.1/-20.1	-16.7
Big Bend*	-20.6/-20.4	-19.5
Carr Canyon		-21.6
Millers		-19.1
Cochise	-19.9	-20.1
Rucker Cottonwood	-20.5	-21.9
Peppersauce*	-22.1/-22.0	-21.2
Copper Creek	-18.1	-19.2
Muskhog	-17.5	-18.0
Cave*	-19.8	-23.1/-23.3
LWC	-23.1	-19.0
Carr Canyon	-18.9	-21.6
Marijilda Wash	-18.0	-20.4
E Turkey Creek	-20.4	-20.4
Iron Spring*	-19.5/-19.5	-20.9
Mud Springs	-19.8	
Average Value	-20.01	20.18
Variance (‰)	1.56	1.55

* Two samples were taken for a quality assurance check of vacuum line techniques and mass spectrometric results. All ^{13}C values have a standard deviation of +/- 0.1 permil PDB.

Inclusion of more than one isotope in mass balance calculations is often an effective means of limiting the propagation of errors and the number of potential solutions. The geochemical modeller must weigh the potential benefit of each isotopic measurement with the need to find a unique solution for the mass balance results. This evaluation should also consider the overall goals and study objectives.

If tritium measurements for a particular groundwater system show no evidence of palaeowaters, then stable carbon and radiocarbon measurements will not reveal additional information about the age of the water. However, if the groundwater system lies within a karstic terrain and the question of water-rock reactions and isotopic exchange with carbonate minerals along the flow path are of interest, then a combination of stable carbon and radiocarbon measurements can be used to validate these reactions.

As the complexity of the groundwater system increases, or there is an increased need to refine our understanding of groundwater geochemical evolution, the conceptual and mass balance models can evolve to include additional information.

Let us briefly consider how chemical reactions and isotopic exchange can affect the stable carbon and radiocarbon isotopic composition of groundwater and minerals. The age dating of groundwater with radiocarbon depends on how we interpret the following questions; 1) what proportion of the TDIC in groundwater is derived from atmospheric CO_2 at time of recharge; and 2) how does isotopic exchange alter the radiocarbon content of TDIC?

Uncertainties in answering the first question are compounded by our lack of understanding of recharge mechanisms. This includes realization of what non-atmospheric sources of carbon exist in the vadose zone and their apparent contribution and radiocarbon age (ie: old soil carbon). Radioactive decay of carbon-14 in the soil zone is generally assumed negligible, but if recharge occurs through geologically old soils, biologic respiration may dilute the carbon-14 of atmospheric CO_2. We must also consider the validity of extrapolating present hydrologic conditions into the past without considering climatic change.

Under normal geochemical conditions, the main source of carbon in recharging groundwater comes from soil CO_2. As pointed out before, measurements of the isotopic composition of carbon in the soil zone are needed to properly model carbon mass balance. The reaction of carbonic acid with carbonate minerals dilute the initial carbon isotopic composition. If carbonate minerals occur in the recharge zone, the initial isotopic composition of groundwater will be a mixture of these two sources.

In the open systems, isotopic exchange between the gas and liquid phases may occur [23].

$$^{14}CO_2 + H^{12}CO_3^- \leftrightarrows {}^{12}CO_2 + H^{14}CO_3^- \qquad (4.47)$$

To account for the concurrent dilution and isotopic exchange, a value of 85±5 % is used as an empirical value assigned to the concentration of carbon-14 in

recharge water [23]. Inclusion of isotopic exchange reactions into mass balance modelling can calculate the expected carbon isotopic composition of recharge water if isotopic enrichment factors and the isotopic composition of all phases are known. The mass and isotope balance model NETPATH [6] allows the user to choose enrichment factors of either Mook *et al.* [24] or Deines *et al.* [25] for calculation of mass balance and isotopic exchange.

The oxidation of dissolved organic matter will add carbon to the groundwater TDIC. Even in semi-arid regions, DOC may approach 10 mg/l in recharge waters [21]. Aquifer materials may contain kerogen and other organic matter. Where organic matter comprises a significant input of carbon to a groundwater system, the isotopic composition of the organic matter should be investigated and the mass balance and isotope balance of DOC should be included in the modelling effort.

Down gradient dissolution of carbonates are generally described under open or closed geochemical conditions. There is not a sharp boundary between the two cases so the geochemical modeller must set limits that define open and closed states. In practice, results of speciation modelling can be used to set the boundary between open and closed conditions at the point down gradient where pCO_2 begins to decline along the flow path.

Isotopic exchange is not limited to interaction between CO_2 and water but may occur between the liquid and solid phase as well.

$$Ca^{12}CO_3 + H^{14}CO_3^- \leftrightarrows Ca^{14}CO_3 + H^{12}CO_3^- \qquad (4.48)$$

Where this reaction occurs, it is assumed to be surface reactions resulting in localized microscopic dissolution/precipitation. Though not well defined, the isotopic fractionation between the liquid and solid phase is probably very small [26, 27]. For closed system reactions, the affect on the ^{13}C and ^{14}C of TDIC from isotopic exchange with the solid phase will vary depending on the difference between the isotopic composition of both.

The interpretation of geochemical reactions during groundwater recharge at steady state depends on which temporal resolution is chosen. Dissolution of secondary calcite phases may occur as pulses of undersaturated recharge water moving rapidly through the recharge zone and along a given flow path. Precipitation of calcite may occur at the same point when flow rates are lower and kinetically slower silicate weathering reactions begin to dominate. It is important to consider the temporal variations in the groundwater system and collect samples at appropriate times.

In an open system, the $\delta^{13}C$ and ^{14}C of secondary calcite would be similar to the isotopic composition of groundwater TDIC (Equations 4.47 and 4.48). Identification of exchange reactions in groundwater systems is difficult. For some groundwater systems the water is in apparent equilibrium with respect to calcite but mass transfer reactions still continues. Confirmation of mass transfer and isotopic exchange reactions require collection and isotopic analysis of carbonate mineral from aquifer materials at points down gradient. The following example shows how

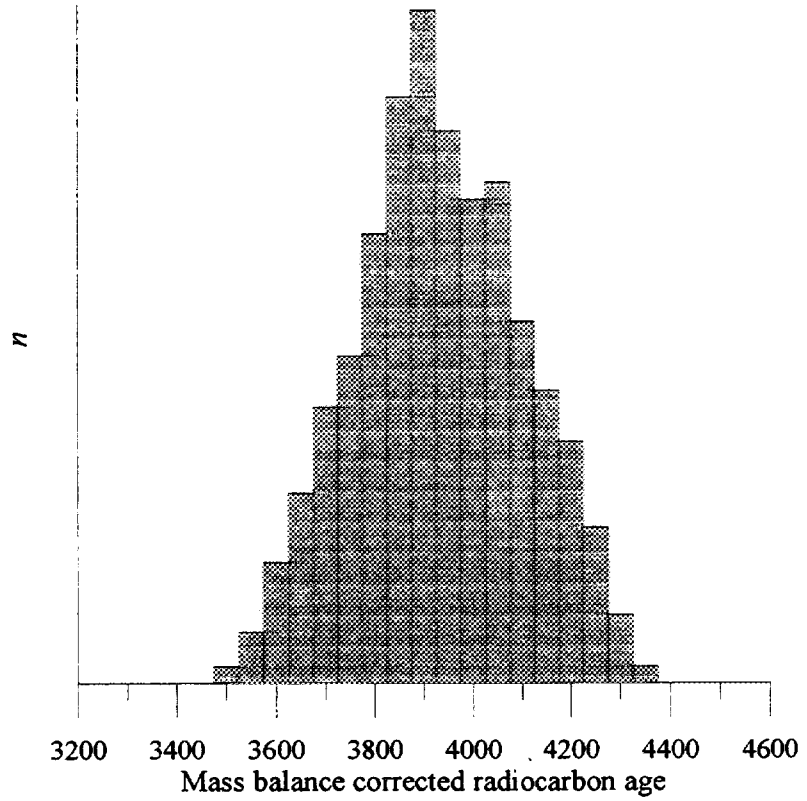

Figure 10. Distribution of mass balance corrected radiocarbon ages of groundwater after Monte-Carlo simulation of uncertainty in isotopic and analytical data.

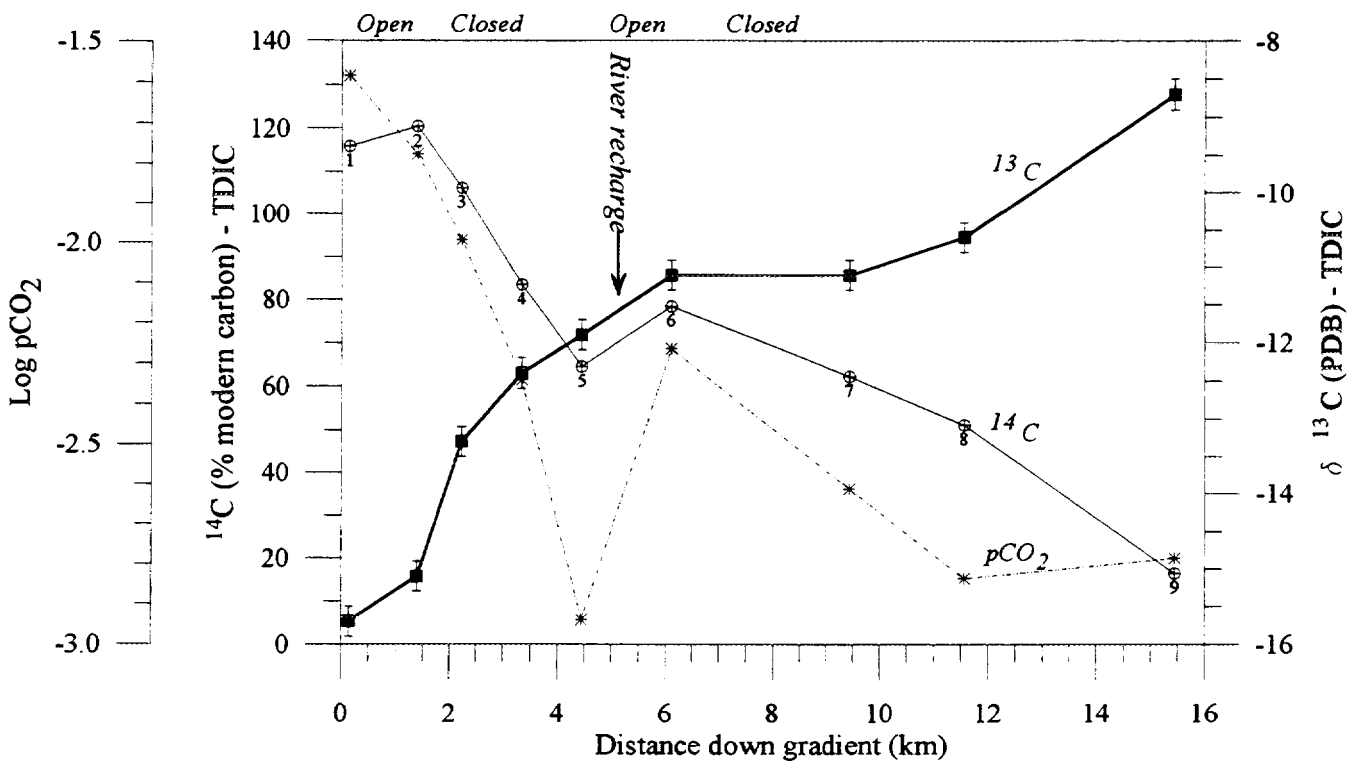

Figure 11. Variation in carbon isotopic composition along reaction path defined in Figure 8.

carbon isotopes were used to interpret hypothesized geochemical reactions for the Tucson basin flow path described in Example VII.

Example IX.

Isotopic validation was required for the flow path defined in the Tucson basin for Example VII. Along this flow path, we hypothesized that recharge waters dissolve calcite due to dissolution of pCO_2 and then during closed geochemical conditions, pCO_2 is consumed for weathering of plagioclase and calcite precipitates under equilibrium conditions. However, additional recharge from the Pantano river added aggressive water and open geochemical conditions are suspected before geochemical evolution continues under closed conditions down gradient.

Carbon isotopic measurements were made on calcite in the recharge zone to verify open system dissolution and isotopic exchange reactions, and to determine the appropriate isotopic composition of calcite for mass balance modelling (Table XI). The ^{13}C and ^{14}C isotopic composition of carbonates show that both processes occur as expected. Mass transfer results (Figure 9) predict calcite precipitation down gradient. Carbon-14 is ubiquitous in Tucson basin groundwater, and we would suspect that calcite at depth should have a finite radiocarbon activity. Results of stable and radiocarbon analysis of secondary calcite collected from three cores at *ca.* 180 metres depth in the central basin have measurable ^{14}C activity.

Table XI. Carbon isotopic measurements made on mineral phases and recharge water in the Tucson basin [21].

Sample	$\delta^{13}C$ (PDB)	^{14}C (pMC)
Calcrete in river bed (collected 1966)	-14.3 ± 0.1	151.3 ± 3.3
Soil carbonate near surface of recharge zone	- 6.1 ± 0.1	66.0 ± 2.0
Avg. - 7 carbonates beneath surface of recharge zone	- 3.4 ± 0.5	21.5 ± 8.5
Avg. - 3 carbonates from well cuttings (180 metres depth)	- 2.7 ± 0.2	1.0 ± 0.4
Avg. - 5 groundwater at recharge zone	-15.1 ± 0.3	113.5 ± 4.2
Soil CO_2	-20.1 ± 1.5	Modern

The calculated pCO_2 and change in carbon isotopic composition of TDIC along the modelled Tucson basin flow path are shown in Figure 11. High pCO_2 in the recharge zone is confirmed and, as the water moves down gradient, closed conditions occur. At the Pantano river, the pCO_2 increases confirming expectations that open geochemical conditions occur at this point along the flow path. Finally, decreased pCO_2 down gradient confirm closed conditions again.

Mass transfer calculations predict carbonate dissolution for samples 1-4 and 6. Isotopic measurements of these waters show evidence of ^{13}C enrichment resulting from dissolution of calcite. Precipitation of calcite is predicted by mass transfer modelling for samples 5 and 7-9. As expected, isotopic exchange with the solid phase these waters produce little enrichment of ^{13}C from previous water up gradient.

Radiocarbon concentrations for samples 1-3 define the bomb pulse of post-1964 recharge water in the Tucson basin (diluted as a result of dissolution reactions with calcite). Carbon input to the groundwater system at the Pantano river is confirmed from the increase in ^{14}C for TDIC between points 5 and 6 where modern pCO_2 is introduced.

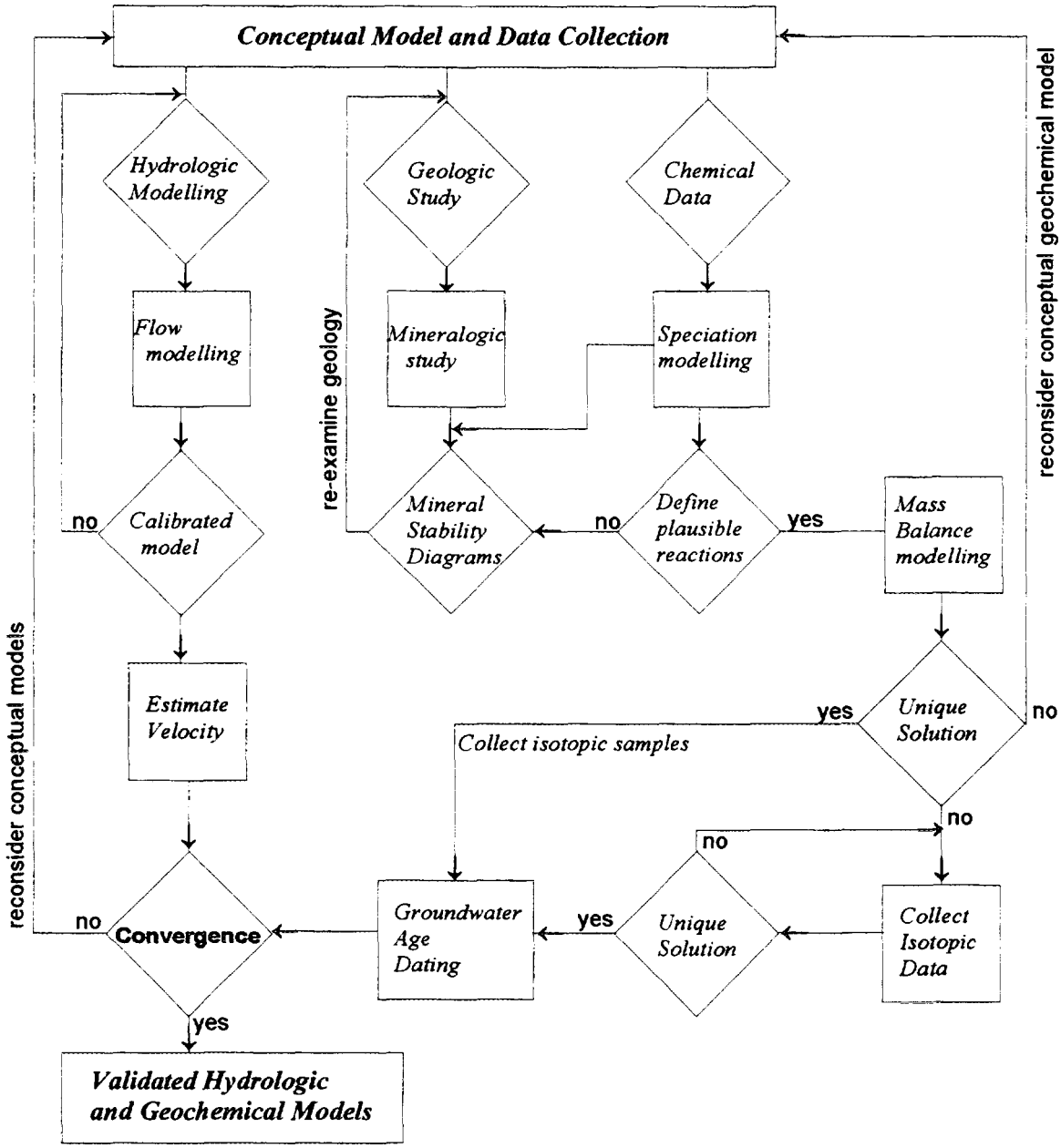

Figure 12. Schematic of the logical approach to the combined use of hydrologic, geochemical and isotopic investigation of groundwater systems.

Radioactive decay and closed geochemical reactions change the ^{14}C activity in down gradient groundwater between points 4-5 and after point 6.

The observed variations in carbon isotopic composition for groundwater along this flow path have supported geochemical reactions inferred from results of mass balance calculations. This has increased our confidence in the conceptual model of geochemical reactions and we are justified in using the results of mass transfer calculations to calculate corrected radiocarbon ages of groundwater along this flow path.

Table XII. Water chemistry, isotopic composition and mineral saturation indices of two wells, one representing recharge at the mountain-pediment interface and the other, palaeowater down gradient [21].

Species	Recharge Well	Down Gradient Well
Temp. (°C)	25.4	43.3
pH	6.9	8.1
Ca^{2+} (mg/l)	24.3	13.6
Mg^{2+} (mg/l)	12.6	2.6
Na^{+} (mg/l)	42.6	155
K^{+} (mg/l)	4.3	7.5
HCO_3^{-} (mg/l)	200	146
SO_4^{2-} (mg/l)	40.4	317
Cl^{-} (mg/l)	40	34
Si (mg/l)	22.8	29.8
Al (mg/l)	0.08	0.08
^{3}H (TU)	8.0 ± 2.0	< 1.0
^{13}C (‰ PDB)	-12.0 ± 0.1	-10.7 ± 0.1
^{14}C (% Mod)	99.6 ± 0.6	16.5 ± 0.6
^{18}O (‰ SMOW)	-9.1 ± 0.1	-10.7 ± 0.1
D/H (‰ SMOW)	-66 ± 2	-80 ± 2.0
^{34}S (‰ CDT)	+6.7 ± 0.5*	+12.4 ± 1.3*
Molality Ratios		
Ca/Na	0.33	0.05
Mg/Na	0.28	0.02
SO_4/Cl	0.45	4.13
Calculated Saturation Index		
SI Calcite (^{13}C = -2.4 ‰)	-0.86	0.02
SI Gypsum (est ^{34}S = 14.0 ‰)	-2.38	-1.89
SI Plagioclase	-0.67	-0.87
SI Montmorillonite	4.98	0.52
SI Orthoclase	0.68	-0.06
SI Kaolinite	5.98	1.81

* average values for ^{34}S of groundwater in recharge zones and groundwater from deep stratigraphic units

Geochemical modelling and hydrologic modelling should be considered an evolutive process. Validation of our understanding of groundwater flow with geochemistry is dependent on our confidence in both modelling efforts. The global hydrologic system is dynamic and is scale dependent, both spatially and temporally.

Variations in the physical controls of water movement in groundwater systems occur on scales ranging from hours to centuries. It is therefore important

for the modeller to appreciate the scale to which the models, geochemical, hydrologic and isotopic, are appropriate as well as the underlying assumptions and uncertainties in their efforts. To summarize this, Figure 12 presents a schematic for the general logic of coupling hydrologic modelling, geochemical modelling and isotopic validation. The combination of these efforts will hopefully realize the goal of coupling flow and mass transfer, but this will only result from a sound understanding of all three.

4.10 Using NETPATH: speciation, mass balance and isotope balance modelling of groundwater systems

There are a large number of models that can be used to interpret the geochemical evolution of groundwater systems. Mangold and Tsang [28] have reviewed many of the numerical codes available for groundwater investigation. In this section we will consider the model NETPATH [6] which combines three elements, a groundwater database, a chemical speciation model and a mass balance / isotope balance model. *NETPATH* is an abbrieviation for: an interactive code for modelling NET geochemical reactions along a flow PATH. The demonstration of NETPATH here is not intended to exclude the useful nature of many other geochemical models. NETPATH is the only model that combines isotopic results with the approach that has been discussed in this chapter on basic concepts and formulations for isotope-geochemical process investigation. In this last section, we will examine how NETPATH results can be used to interpret the geochemical and isotopic mass balance of geochemical reactions between two groundwaters.

Table XII gives the measured chemical and isotopic data for two wells from the Tucson basin [21], one representing recharge at the mountain-pediment interface and the other, palaeowater down gradient. The down gradient water is geochemically interesting and potentially very old. The area around this well contains active, high-sulphate warm springs that occur along low-angle faults that dip from the surrounding mountains toward the basin. The measured temperature of the groundwater averages 43.3°C. Groundwater at the mountain-pediment interface was used to define the chemistry of initial recharge water for geochemical modelling.

The data was entered into NETPATH's database program, DB. During the process of saving the data, DB runs the chemical speciation model WATEQF calculating chemical speciation and mineral saturation indices for each groundwater sample entered in the database. The calculated saturation indices for dominant mineral phases in the Tucson basin aquifer are given in Table XII.

The change in molal ratios (Table XII) indicate that ion exchange (Ca/Na and Mg/Na) has occurred. This would be expected if montmorillonite is the dominant clay mineral produced during incongruent weathering of plagioclase. There is no substantial change in chloride concentrations along the flow path. The large change in SO_4/Cl is probably from dissolution of gypsum. Gypsum does not reach equilibrium (SI < 0) because of the common ion effect with ion exchange of Ca for Na.

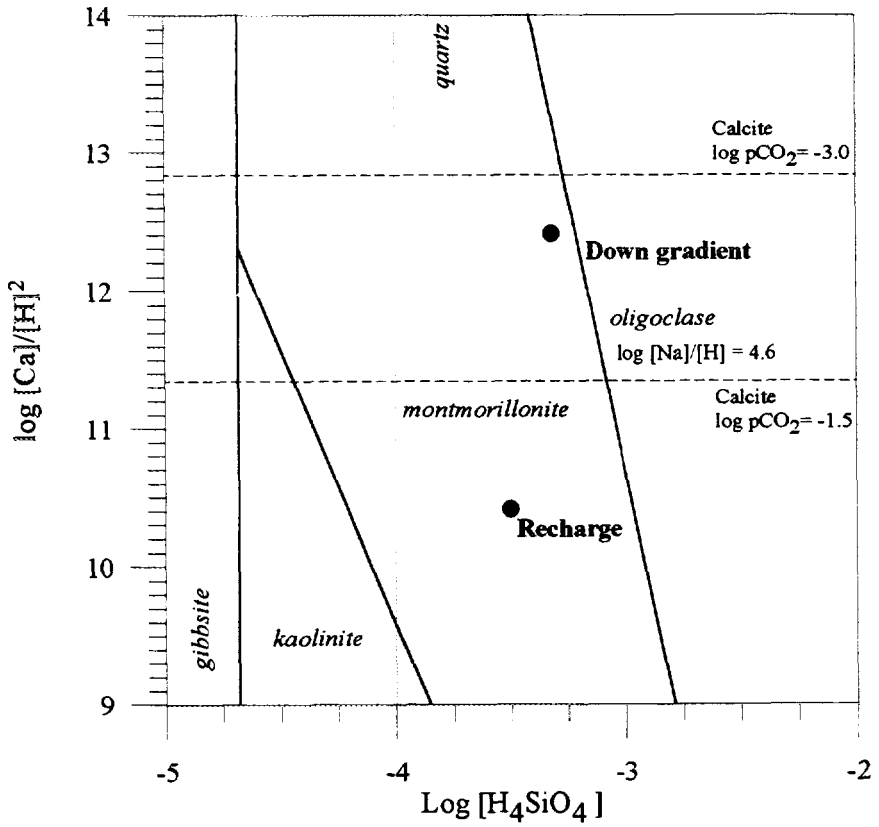

Figure 13. Recharge and down gradient water from Table XII plotted on a mineral stability diagram representing thermodynamic constraints on potassium, hydrogen and silica activities for equilibrium reactions between orthoclase, kaolinite, muscovite and gibbsite.

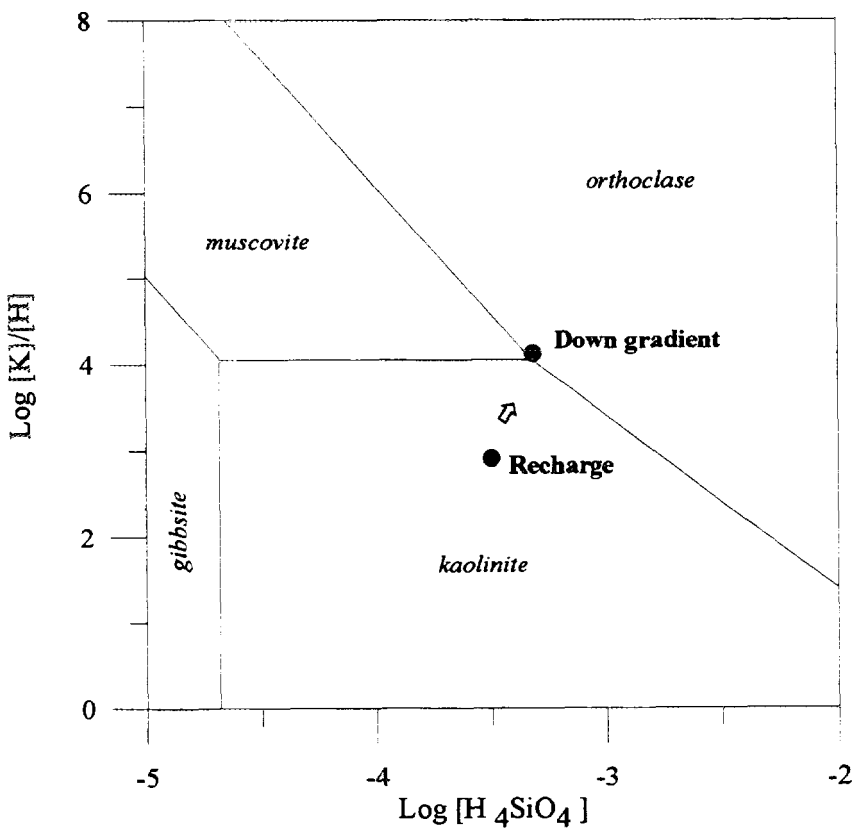

Figure 14. Recharge and down gradient water from Table XII plotted on a mineral stability diagram representing thermodynamic constraints on calcium, hydrogen and silica activities for equilibrium reactions between oligoclase, montmorillonite, kaolinite, and gibbsite.

The down gradient water has reached equilibrium with calcite and orthoclase. Plagioclase shows little change in saturation index possibly due to the common ion effects of Ca/Na exchange on clays and calcite equilibrium. Both clay minerals montmorillonite and kaolinite are very oversaturated up gradient and are near equilibrium (given uncertainties in thermodynamic data) down gradient.

We can interpret saturation indices by plotting these two samples on mineral stability diagrams (Figures 13 and 14) Recharge water plots in the kaolinite field indicating there is thermodynamic potential for kaolinite precipitation. Figure 13 confirms that orthoclase trends from undersaturation to final chemical equilibrium between muscovite, orthoclase and the clay mineral kaolinite. Figure 14 verifies the thermodynamic potential of montmorillonite precipitation for the initial water and the trend toward equilibrium incongruent reactions between plagioclase and montmorillonite.

The elements used in NETPATH to constrain the mass-balance solution included carbon, sulphur, calcium, aluminum (assumed conservative in the solid phase), magnesium, potassium, sodium, iron (assumed conservative in the solid phase), silicon and stable carbon isotopic ratios (Table XIII). Conservation of aluminum during the incongruent dissolution of silicate phases dictates that all aluminum in plagioclase and orthoclase is used in the precipitation of clay minerals. This results in no change in the dissolved aluminum between initial and final water. Similarly, conservation of iron in the solid phase leads to no change of dissolved

Table XIII. Constraints and mineral phases used in NETPATH to model the geochemical evolution of down gradient groundwater from Table XII.

Constraints: 9	Phases: 11*	Parameters
Carbon	- Montmorillonite	Mixing: No
Calcium	Calcite	Evaporation: No
Magnesium	+ Orthoclase	Isotope Calc: Yes
Potassium	SiO_2	Exchange: Ca/Na
Iron	+ Gypsum	Init C-14: Mass -
Sulphur	- Goethite	
Balance		
Aluminum	- Kaolinite	
Sodium	+ Ilmenite	
Silica	+ Oligoclase	
	Exchange Mg/Na	
	Exchange (default)	

* Positive indicates that only dissolution of the mineral phase is allowed to solve the mass balance; Negative sign indicates that only precipitation of the mineral phase is allowed. No sign indicates that both precipitation and dissolution of the mineral can be modelled.

Table XIV. NETPATH input for the stoichiometric and isotopic composition of mineral phases determined from geologic investigation of Tucson basin sediments.

Mineral	Elemental composition				
Montmorillonite					
0.17 Ca	0.13 K	0.47 Mg	0.3 Fe	1.47 Al	3.8 Si
Calcite					
1.0 Ca	1.0 C	-2.4 $\delta^{13}C$	1.0 ^{14}C		
Oligoclase					
0.2 Ca	0.8 Na	1.2 Al	2.2 Si		
Gypsum					
1.0 Ca	1.0 S	14.0 $\delta^{34}S$ (est)			
Orthoclase					
1.0 K	1.0 Al	3.0 Si			
Kaolinite					
2.0 Al	2.0 Si				
Exchange Ca/Na					
-1.0 Ca	2.0 Na				
Exchange Mg/Na					
-1.0 Mg	2.0 Na				
Goethite					
1.0 Fe					
SiO_2					
1.0 Si					
Ilmenite					
1.0 Fe	1.0 Ti				

Fe^{+2} and Fe^{+3} in groundwater. The ubiquitous presence of dissolved oxygen in the Tucson basin groundwater suggests that any iron will reside either as goethite or as substitution in montmorillonite.

Chloride is not used as a constraint for two reasons; 1) because there is no significant change in chloride concentration during geochemical evolution of the water; and 2) the presence of minerals that contain chloride could not be identified in the aquifer sediments.

The reactant phases used in NETPATH for determining mass-transfer were determined through mineralogic analysis of basin sediments and gas phases (Table XIII and XIV). These phases included calcite, montmorillonite (chemical composition analyzed), goethite, orthoclase, oligoclase (calcium/sodium ratio was determined), gypsum, kaolinite, ilmenite and quartz. Further, ion exchange of Ca/Na and Mg/Na on clays were allowed because the clay minerals in the sediments are known to have ion exchange potential.

To accurately determine the balanced chemical reactions, the measured stoichiometric composition of each mineral phase is listed in Table XIV. There are options available within NETPATH to change the chemical composition of mineral

phases. We will have more confidence in the mass balance results if the model is given the accurate chemical composition of mineral phases rather than estimated compositions.

NETPATH permits the user to dictate whether precipitation or dissolution of mineral phases will be allowed. In this way, reactions that we know are not permitted due to thermodynamic constraints can be excluded from analysis. For instance, the calculated saturation index of gypsum is less than zero for both water samples. From this we know that thermodynamic constraints do not permit precipitation of gypsum along the flow path between these two points. Therefore, only the mass balance solutions calculated by NETPATH for which the mineral phase gypsum dissolved are considered .

Only the isotopic results for carbon and sulphur were used to validate the mass balance results with this data. The mass balance solution for chemical data is expected to correspond with mass balance of isotopes. Of the isotopic data for the initial and final groundwater samples (Table XII), only carbon and sulphur have potential for validating mass-transfer chemical reactions between the initial and final water. It is assumed that no isotopic enrichment occurs between the liquid and solid phase.

Table XV. Results of four successful NETPATH mass balance models for geochemical reactions defining the chemistry of down gradient Tucson basin groundwater (in mmol/litre).

Mineral Phase	Model 1	Model 2	Model 3	Model 4
Montmorillonite	-0.8754	-0.0000	-22.602	-1.1044
Calcite	-1.7509	-1.7509	-1.7509	-1.7509
Orthoclase	+0.1949	+0.0812	+3.0194	+0.2247
SiO_2	-0.2297	-1.1081	+21.569	
Gypsum	+2.8816	+2.8816	+2.8816	+2.8816
Kaolinite	-0.6518	-0.6781		-0.6449
Ilmenite	+0.2626		+6.7805	+0.3313
Oligoclase	+ 1.9962	+1.0625	+25.171	+2.2405
Ca/Na Exchange	1.6481			1.6580
Mg/Na Exchange		1.0635	-10.211	0.1076
Isotopic Exchange	0.750	0.750	0.750	0.750
$\delta^{13}C$ (-10.7 ‰ measured)	-10.75	-10.75	-10.75	-10.75
Init ^{14}C (16.5 pMC measured)	72.06	72.06	72.06	72.06
$\delta^{34}S$ (12.5 $\pm$ 1.3 ‰ CDT)	13.07	13.07	13.07	13.07
$\delta^{87}Sr$ (not measured)	na	na	na	na
$\delta^{15}N$ (not measured)	na	na	na	na
Radiocarbon age (A/A_o = 16.5 / 72.1)	11,400	11,400	11,400	11,400

The tritium content of down gradient water is below detection and the content in recharge water is low. The lack of tritium in the down gradient well is important hydrologic information because it indicates that no 'young' water is mixing in the down gradient well. Calculation of a mixing ratio is the only mass balance parameter that tritium would be useful for in this situation. Given the lack of evidence for mixing, tritium was ignored for inclusion in NETPATH modelling.

The stable isotopic composition of H_2O is distinctly different between the initial and final groundwater samples. The low radiocarbon content of water from the down gradient well suggests the difference in isotopic composition may be due to climate change and palaeowater. We do not have confidence that climatic conditions of recharge for the palaeowater are the same as the recharge water. $\delta^{18}O$ and δD may be useful for palaeohydrologic interpretation, but can not constrain the mass balance of chemical reactions between the initial and final water.

Forty-five potential mass balance solutions exists given the constraints and phases in Table XIII. Even when constrained with carbon and sulphur isotopic balance, there are four potential solutions for balanced chemical reactions between the initial and final water as modelled with NETPATH (Table XV). These results must be compared with thermodynamic constraints and geochemical knowledge of the system to choose the one reaction that best describes the geochemical evolution of groundwater between these points.

The mass balance result number 1 predicts the precipitation of quartz or another silica phase. The precipitation of silica phases is not thermodynamically allowed when coprecipitation of clay mineral phases occurs. The same applies to model number three. This model also required a very large mass transfer coefficients to balance the result. Therefore, the results of model number one and number three are suspect.

Model result number two predicts precipitation of silica and no precipitation of montmorillonite along the flow path. From the mineral stability diagrams we know that thermodynamics favour the precipitation of montmorillonite over kaolinite. Petrographic investigation of secondary minerals also show a predominance of montmorillonite over kaolinite. Therefore, the result of model two is suspect.

The result of model four is the only balanced reaction that does not violate thermodynamic constraints. There is a unique solution for the mass balance between the initial and final groundwater samples. We can then write the balanced chemical equation for this reaction:

$$\text{Initial water chemistry} + 2.24\underset{\text{(Tucson oligoclase)}}{Ca_{0.05}Na_{0.9}Al_1Si_3O_8} + 0.33\underset{\text{(ilmenite)}}{FeTiO_3} + 1.65\text{Ca/Na exchange}$$

$$+ \ 0.11\text{Mg/Na Exchange} + 2.88\underset{\text{(gypsum)}}{CaSO_4} + \ 0.22\underset{\text{(orthoclase)}}{KAlSi_3O_8} \ \rightarrow$$

Final water chemistry + 0.77 $Ca_{0.167}K_{0.13}Mg_{0.47}Fe_{0.3}Al_{1.47}Si_{3.77}O_{10}(OH)_2$
(Tucson basin montmorillonite)

+ 0.32$Al_4Si_4O_{10}(OH)_8$ + 0.78$CaCO_3$
(kaolinite) (calcite 0.75 isotopic exchange)

With a unique solution for mass balance, we are confident in the correction of the radiocarbon age of the water, and indeed the sample represents palaeowater. The coupled geochemical-isotopic modelling approach to hydrologic investigations provided a singular solutions to our interpretation of the geochemical evolution of water between these two points.

4.11 Summary

The goal of isotope-geochemical modelling is to identify probable chemical reactions that control the evolution of groundwater chemistry and isotopic composition. We can determine the mass balance and mass transfer in a groundwater system from knowledge of the minerals and reactive phases in the aquifer system and changes in groundwater chemistry. For most hydrologic studies in the past, detailed mineralogic and isotopic investigation on aquifer materials has been lacking. Without this data it is not possible to conclude with certainty which geochemical reactions dominate a groundwater system.

The forward and inverse solutions to geochemical modelling offer advantages and disadvantages. The inverse solution can provide the most reaction information given detailed mineralogic, isotopic, chemical and hydrologic data on a groundwater system. Inverse modelling requires that initial and final groundwater samples are related hydrologically and care must be taken to collect water along defined flow paths. The results of inverse modelling provide the net mass transfer between initial and final points. Mass transfer coefficients are easily applied to isotopic mass balance resulting in isotopic validation of inverse model results and corrections for age dating groundwater. However, inverse model results can be adversely affected by errors in analytical data and invalid assumptions. Inverse model results are also not constrained by thermodynamics.

When chemical and mineralogic data are limited, forward modelling can be used to compute changes in groundwater chemistry in response to user defined changes in chemical composition, temperature, pressure, mineral dissolution and precipitation and irreversible reactions. Forward modelling is constrained by the thermodynamics of water-rock interactions but is highly dependent on the accuracy of the thermodynamic data available. Mineral stability diagrams and saturation indices can be used to investigate thermodynamic constraints on geochemical reactions in the absence of forward modelling.

The examples used in this chapter were intended to give the reader an overview of the isotope-geochemical approach to modelling geochemistry of groundwater systems. The reader is strongly urged to apply these techniques to their particular hydrologic study. It is important that uncertainties in analytical data, hydrologic information, geologic understanding and computational methods

should always be identified. Care should be taken not to over-interpret isotope-geochemical data or the results of geochemical modelling.

Geochemical modelling of groundwater systems and the coupling of geochemical and isotopic data can offer independent interpretation of the dynamics of groundwater flow. The isotopic composition of dissolved species can be used to ascertain unique chemical reaction paths in groundwater systems. This coupled geochemical-isotopic modelling approach to hydrologic investigations can provide singular solutions to our interpretation of groundwater flow.

REFERENCES

SELECTED GEOCHEMICAL MODELS

[I] NETPATH - Plummer, L.N., E.C. Prestemon, and Parkhurst, D.L. 1991, *NETPATH - USGS Water Resource Investigations Report 91-4078*, Reston Va. USA

[II] EQ3/6 - Worley, T.J. 1979, 1983, *UCRL-52658 and UCRL-53414, Lawrence Livermore National Laboratory*, Livermore CA, USA

[III] MINTEQ - Felmy, A.R., D. Girven and A.E. Jenne 1983, *MINTEQ, US-EPA*, Washington DC. USA and *Report PNL-4921, Pacific Northwest Labs*, Richland Washington USA

[IV] PHREEQE - Parkhurst, D.L., D.C. Thorstenson and L.N. Plummer 1980, *PHREEQE - USGS Water Resour. Invest. 80-96, NTIS Tech Reprot PB 81-16780*, Springfield Va USA

[V] PHRQPITZ - Plummer, L.N., D.L. Parkhurst, G.W. Flemming and S.A. Dunkel 1988, *PHRQPITZ - USGA Water Resources Investigation*, Springfield Va USA

[VI] SOILCHEM - Sposito, G. and J. Coves, *SOILCHEM - Kearney Foundation, University of California, Riverside and Berkeley*, Los Angeles, CA USA

[VII] WATEQ4F - Ball, J.W. and D.K. Nordstrom 1990, *WATEQ4F - USGS Open File Report 87-50*, USA

[VIII] 1DREACT - Steefel, C.I. 1993, *1DREACT - Battelle, Pacific Northwest Labs. Richland WA, USA*

[IX] SOLMINEQ - Kharaka, Y.K, W.D. Gunter, P.K. Aggarwal, E.H. Perkins and J.D. DeBraal 1988, *SOLMINEQ88 - USGS Water Resources Invest. Reprot 88-4227*, Menlo Park Ca. USA

BIBLIOGRAPHY

[i] Garrels, R.M. and C.L. Christ 1965, *Solutions, Minerals and Equilibria*, Harper & Row, New York, USA

[ii] Stumm, W. and J.J. Morgan 1981, *Aquatic Chemistry*, Wiley-Interscience, New York, USA

[iii] Butler, J.N. 1982, *Carbon Dioxide Equilibria and Their Applications*, Addison-Wesley, Reading Ma. USA

[iv] Thurman, E.M. 1985, *Organic Geochemistry of Natural Waters*, Martinus Nijhoff/Dr. W. Junk, Dordrecht (Netherlands)

[v] Hem, J.D. 1985, *Study and interpretation of the chemical characteristics of natural water*, 3rd ed. USGS Water Supply Paper 2254

[vi] *Standard Methods for the Examination of Water and Wastewater,* American Public Health Association, Washington DC
[vii] *Methods for Chemical Analysis of Water and Wastes*, Document EPA-600 4-79-020, US Environmental Protection Agency, Office of Research and Development, Cincinnati Ohio
[vii] Garrels, G.M. and F.T. Mackenzie, 1971, *Evolution of Sedimentary Rocks*, W.W. Norton, New York, USA
[ix] Nordstrom, D.K. and J. Munoz 1985, *Geochemical Thermodynamics*, Benjamin/Cummings, Menlo Park California
[x] *Interpretation of Environmental Isotope and Hydrochemical Data in Groundwater Hydrology*, IAEA, Vienna
[xi] Drever, J.I. 1988, *Geochemistry of Natural Waters*, Prentice Hall, New Jersy USA
[xii] Pankow, J.F.1991, *Aquatic Chemistry Concepts*, Lewis Publishers, Michigan, USA
[xiii] Freiser, H. and Q. Fernando 1979, *Ionic Equilibria in Analytical Chemistry*, R.E. Kreigler Publishing, Florida, USA
[xiv] Morel, F.M.M. 1983, *Principles of Aquatic Chemistry*, Wiley and Sons, New York, USA
[xv] Snoeyink, V.L. and Jenkins, D. 1980, *Water Chemistry*, Wiley and Sons, New York USA
[xvi] Richardson, S.M. and H.Y. McSween Jr. 1989, *Geochemistry: Pathways and Processes*, Prentice-Hall, New Jersey, USA
[xvii] Faure, G. 1986, *Principles of Isotope Geology*, Wiley and Sons, New York, USA
[xviii] Hoefs, J. 1980, *Stable Isotope Geochemistry*, Springer Verlag, New York USA
[xix] Brookins, D.G. 1988, *Eh-pH Diagrams for Geochemistry*, Springer-Verlag, New York, USA

REFERENCES

[1] Garrels, R.M. and M.E. Thompson 1962, *Am. J. Sci.* **260** pp57-66
[2] Wigley, T.M.L., L.N. Plummer and F.J. Pearson 1978, *Geochim. Cosmochim. Acta* **42** pp 1117-1139
[3] Winograd, I.J. and F.J. Pearson Jr. 1976, *Water Resour. Res.* **12** pp1125-1143
[4] Plummer, L.N., J.F. Busby, R.W. Lee and B.B. Hanshaw, 1990, *Water Resour. Res,* **26**(9) pp1981-2014
[5] Wagman, D.D., W.H. Evans, V.B. Parker, R.H. Schumm, I. Harlow, S.M. Bailey, K.L. Churney and R.L. Nuttall 1982, *J. Phys. Chem. Ref. Data* **11**(supp 2) pp1-392
[6] Plummer, L.N., E.C. Prestemon, and Parkhurst, D.L., 1991, *NETPATH - USGS Water Resource Investigations Report 91-4078*
[7] Faure, G. 1991, *Principles and Applications of Inorganic Geochemistry*, MacMillan, New York 626pp
[8] Nordstrom, D.K. and J.L Munoz 1985, *Geochemical Thermodynamics.* Benjamin/Cummings, Menlo Park, California, 477 pp.
[9] Pitzer, K.S. 1973, *J. Phys. Chem.* 77 pp268-277
[10] Garrels, R.M. and C.L. Christ 1965, *Solutions, Minerals and Equilibria*, Harper and Row, New York 450 pp.
[11] Plummer, L.N. and E. Busenberg 1982, *Geochim. Cosmochim Acta,* **46** pp1011-1040
[12] Robertson, F.N. 1991, *USGS Professional Paper 1406-C*, United States Government Printing Office, Washington DC, 90 pp
[13] Kalin, R.M. and A. Long, 1994, *IAEA TechDoc-777* Vienna, Austria , pp209-254
[14] Tardy, Y. and R.M Garrels 1976, *Geochim. Cosmochim Acta,* **40**, pp 1051-1056

[15] Tardy, Y. and R.M. Garrels 1977 *Geochim. Cosmochim Acta*, **41**, pp 87 - 92
[16] Lindsay, W.L 1979, *Chemical Equilibrium in Soils*, Wiley, New York 449pp
[17] Plummer, L.N., D.L. Parkhurst and D.C. Thorstenson 1983, *Geochim. Cosmochim. Acta*, **47** pp665-686
[18] Parkhurst, D.L., D.C. Thorstenson and L.N. Plummer 1980, *PHREEQE - USGS Water Resour. Invest. 80-96, NTIS Tech Reprot PB 81-16780*, Springfield Va 210pp
[19] Worley, T.J. 1983, *EQ3/6 - UCRL-53414* Lawrence Livermore National Laboratory, Livermore Ca.
[20] Wigley, T.M.L., L.N. Plummer and F.J. Pearson, 1978, *Geochim. Cosmochim. Acta.* **42**, pp1117-1139
[21] Kalin, R.M. 1994, *PhD. Dissertation*, The University of Arizona, 510pp
[22] Pearson, F.J. 1992, *in: Radiocarbon After Four Decades: An Interdisciplinary Perspective*, Springer-Verlag, pp261-275
[23] Vogel, J.C. and D. Ehhart 1963, *Radioisotopes in Hydrology*, IAEA Vienna, pp385-395
[24] Mook, W.G., J.C. Bommerson and W.H. Staverman 1974, *Earth and Planet. Sci. Lett.* **22**, pp169-176
[25] Deines, P., D. Langmiur and R.S. Harmon 1974, *Geochim. Cosmochim. Acta.* **38**, pp1174-1164
[26] Fontes, J.C. and J.M. Garnier 1979, *Water Resources Research*, **15**, pp399-413
[27] Mook, W.G. 1980, in P.Fritz and J.C. Fontes eds: *Handbook of Environmental Isotope Geochemistry*, Elsevier, Amsterdam
[28] Mangold, D.C. and C. Tsang 1991, *Reviews of Geophyscs*, **29**(1) pp51-79

LIST OF RELATED IAEA PUBLICATIONS

1983 Guidebook on Nuclear Techniques in Hydrology,
Chapter-25: Models for Tracer Data Analysis,
Technical Report, Series No. 91

1986 Mathematical Models for Interpretation of Tracer Data in Groundwater Hydrology,
IAEA-TECDOC-381

1993 Nuclear Techniques in the Study of Pollutant Transport in the Environment,
(Interaction of Solutes with Geological Media: Methodological Aspects),
IAEA-TECDOC-713

1994 Mathematical Models and Their Applications to Isotope Studies in Groundwater Hydrology,
IAEA-TECDOC-777